5-1997

An Investigation of Unsteady Vortex Flow Over A Maneuvering Delta Wing

Harry James Kowal
University of Tennessee - Knoxville

To the Graduate Council:

I am submitting herewith a dissertation written by Harry James Kowal entitled "An Investigation of Unsteady Vortex Flow Over A Maneuvering Delta Wing." I have examined the final electronic copy of this dissertation for form and content and recommend that it be accepted in partial fulfillment of the requirements for the degree of Doctor of Philosophy, with a major in Aerospace Engineering.

Ahmad D. Vakili, Major Professor

We have read this dissertation and recommend its acceptance:

Roger Crawford, Jimmy Wu, John Caruthers, Ralph Kimberlin, Frank Collins

Accepted for the Council:

Carolyn R. Hodges

Vice Provost and Dean of the Graduate School

(Original signatures are on file with official student records.)

To the Graduate Council:

I am submitting herewith a dissertation written by Harry James Kowal entitled "An Investigation of Unsteady Vortex Flow Over A Maneuvering Delta Wing." I have examined the final copy of this dissertation for form and content and recommend that it be accepted in partial fulfilment of the requirements for the degree of Doctor of Philosophy, with a major in Aerospace Engineering.

Ahmad D. Vakili, Major Professor

We have read this dissertation
and recommend its acceptance:

Accepted for the Council:

Vice Provost
And Dean of The Graduate School

AN INVESTIGATION OF UNSTEADY VORTEX FLOW OVER A MANEUVERING DELTA WING

A Dissertation

Presented for the

Doctor of Philosophy

Degree

The University of Tennessee, Knoxville

Harry James Kowal

May 1997

DEDICATION

To my wife, Cheryl, for endless support and motivation.

In the memory of my brother, Michael, who showed me what it was like to have the courage to realise my dreams.

ACKNOWLEDGEMENTS

I learned very early in my PhD program that you can never really do it alone. In fact, for me, if it were not for the help and support of many people, I know I would not have been able to successfully complete this dissertation.

First and foremost, I would like to thank my family for their understanding and steadfast support. Seven years is a long time to hold on to a dream and you continuously gave me the energy and motivation to see it through. You believed in me. To merely say thank you is an understatement; I owe you all so much.

I wish to thank my advisor and good friend Dr. Ahmad Vakili who gave me the inspiration to pursue a doctorate and who continuously gave me direction when needed. To Dr. Roger Crawford who convinced me that I was capable of anything as long as I was willing to do the work: thank you very much. I wish to thank all the members of my committee: Dr. 'Jimmy' Wu, Dr. John Caruthers, Dr. Ralph Kimberlin; and Dr Frank Collins, for all their help and for the kindness they showed to me and to my family throughout the years.

I would like to thank LCol Doug Tudor of the Aerospace Engineering Test Establishment at the time and Dr. Ben Lee of the National Research Council, Ottawa who helped me set up a collaborative program that enabled me the benefit of gaining state of the art CF-18 research experience. A special thanks to Perry Luchia and Mike Brush who dedicated their personal time to fly me to Tennessee from Cold Lake so that I could complete my comprehensive exams.

I would like to thank all the members of the Mechanical Engineering Department at RMC for making it possible for me to do experimental research. A very special thanks to Dr. Mike Bardon and Dr. Donald Gauthier for their endless support. It seemed that every time I ran into a brick wall both of you were there to help me over it whether it was in the form of funding or re-assigning technical support to give my research priority. Thank you both very much. A special thanks to Aaron MaCluskie, Jason Randall, Chris Saunders, and John Waugh who, through the completion of their fourth year projcct, challenged me and continuously provided me with renewed energy to move forward. In addition, I would like to thank Marie-Pierre Delorme and Marc Labreche for their support and for the motivation they provided me to succeed.

Finally, I would like to thank the technical staff in the Mechanical Engineering Department of RMC. It seems that almost every person had their hands in some aspect of my work. A special thanks to Gerald Black who used his meticulous craftsmanship to build my delta wing model to exact specifications. Also, a special thanks to Wendy Libbey who helped out throughout my research program with in a variety of computer and instrumentation difficulties.

ABSTRACT

An investigation of the vortex breakdown phenomenon using flow visualization qualitatively and quantitatively was conducted with a 70° delta wing under conditions of steady and unsteady pitch, roll and combinations of pitch and roll. Testing was carried out in the water tunnel located in the Mechanical Engineering Department of the Royal Military College of Canada, Kingston, Ontario.

Steady state roll experiments with the delta wing pitched at 30° showed that the behaviour of vortex breakdown as a function of roll angle could be considered linear over the front half of the delta wing; however, the behaviour beyond a certain critical roll angle was nonlinear. The steady state coupling effect for simultaneous variations in pitch and roll appeared to be a superposition of the individual effects of pure pitch and pure roll.

For the unsteady analysis, the 70° delta wing was oscillated in pitch about the centre chord at a mean angle of attack of 30° with an amplitude of oscillation of ±5°. The study was conducted at four values of reduced frequencies ranging from $k_{pitch} = 0.12$ and $k_{pitch} = 0.52$. The observations showed that the unsteady behaviour of the vortex core angle as a function of angle of attack was independent of reduced pitch frequency. Unsteady roll experiments were carried out with the 70° delta wing fixed at a pitch angle of 30° with roll oscillations of ±18° about the wing's level position. Tests were conducted at the same pitch frequencies as for the unsteady pitch analysis which corresponded to reduced frequencies that varied from $k_{roll} = 0.05$ to $k_{roll} = 0.19$. Unsteady maneuvering

experiments were carried out with the 70° delta wing oscillating in pitch about a mean angle of attack of 30° with an amplitude of ±5° while undergoing a corresponding roll oscillation about the centerline with an amplitude of ±18°. The unsteady maneuvering experiments were conducted at the same pitch frequencies as for pure pitch and pure roll and the reduced frequencies were also kept consistent. The results showed that, for all unsteady motions, a hysteresis effect existed that increased with reduced frequency. The results showed that the coupling effect of pitch and roll for the right wing was a reduction in hysteresis; however, the coupling effect for the left wing was an increase in hysteresis.

For all motions investigated, the results of this study showed that an increase in reduced frequency also resulted in an increase in the amount of phase lag. For pure pitching and rolling motion, there was a notable increase in phase lag when the delta wing transitioned from the downstroke to the upstroke as compared to the transition from the upstroke to the downstroke. The coupling effects of unsteady pitch and roll was an apparent superposition of the phase lag.

Empirical prediction equations for steady state conditions were examined under modification for leading edge geometry. Limited success was obtained in predicting the location of the vortex breakdown for conditions of pure pitch and pure roll; however, neither equation accurately predicted the effects of the coupled variations of pitch and roll.

TABLE OF CONTENTS

LIST OF TABLES

LIST OF FIGURES

NOMENCLATURE

Symbols

b	wing trailing edge span, in.
c	wing root chord length, in.
C_L	coefficient of lift.
$C_{L,P}$	coefficient of lift derived from potential flow theory.
$C_{L,V}$	vortex flow coefficient of lift based on vortex flow.
f	pitching frequency, Hz.
k_{pitch}	reduced frequency based on oscillations in pitch, $k_{pitch} = 2\pi fc/U$.
k_{roll}	reduced frequency based on oscillations in roll, $k_{roll} = 2\pi fb/2U$.
K_P	aspect ratio constant approximated by lift coefficient slope at zero angle of attack.
K_V	aspect ratio constant for sharp edged delta wings.
q	freestream dynamic pressure, $q = \frac{1}{2}\rho U^2$.
Re	Reynolds number, $Re = Uc/\nu$.
S	wing planform area, in^2.
t	time, sec.
t^*	nondimensional, time.
u	propagation velocity of the breakdown location, ft/sec.
U	freestream velocity, ft/sec.
x	distance from the apex of the model parallel to the wing root chord, in.
z	perpendicular distance from the surface of the model, in.

Greek Symbols

α angle of attack, deg.

$\dot{\alpha}$ pitch rate, rad/sec.

γ leading edge incidence angle, deg.

θ angle vortex core makes with wing surface, deg.

K reduced pitch rate, $K = \dot{\alpha}_{max} c/2U$.

Λ sweep angle, deg.

μ reduced propagation velocity, $\mu = u/cf$.

ν kinematic viscosity, ft^2/sec.

ρ density, lb_f/ft^3.

σ model pitch angle, deg.

τ convective time unit.

ϕ roll angle, deg

$\dot{\Phi}$ reduced roll rate, $= (b/2U)(\delta\phi/\delta t)$.

ω angular velocity in rad/sec, $\omega = 2\pi f$.

ψ angle the vortex core makes with the projected root chord line (measured from top surface view of delta wing).

CHAPTER I

INTRODUCTION

In an effort to better appreciate the applications of aerodynamics, Wu[1] provides an interesting perspective on the evolution of lift offering that the application of unsteady aerodynamics or time dependant flows is the key to obtaining ultimate lift. He classifies the pursuit of ultimate lift into three distinct generations. The first generation of lift is based upon bound vorticity where optimum lift depends on a smooth external flow field and the minimizing of flow separation. The resultant lift relationship is the classical lift curve slope. The associated requirements for wing design depends on a sharp trailing edge and the wing camber and thickness are critical design components. The result is a moderate C_{Lmax} at low angles of attack. The second generation of lift is identified as vortex lift. In this generation, the methodology is to use the flow qualities of a detached vortex to enhance the lift contributions of the wing. The associated design criteria is a highly swept slender wing planform with a sharp leading edge. The result is a higher C_{Lmax} at higher angles of attack. Optimization of lift in this generation depends highly on the use of flow control methods. The aim of the third generation of lift is to exploit that which has been developed in the second generation by using the energy in the wake of separated flow and the unsteadiness that results from flow at high angles of attack to enhance the lifting qualities of the flow. For subsonic flow this requires unsteady excitation of organized or controlled vorticity through physical oscillation of wing surfaces as well as

articulated or deformable surfaces.

In my opinion, we are at the brink of the third generation of lift and I firmly believe that there are significant contributions yet to be made. This study is, therefore, focused on the extension of the second generation of lift into the third generation and is an effort aimed at furthering the knowledge and understanding of unsteady vortex flow. The application revolves around modern fighter aircraft which operate in high alpha flight regimes. Common design methods make use of highly swept wing planforms and, in some cases, leading edge extensions (LEXs). These configurations allow for the formation of an intense rolled-up vortex which provides for a significant nonlinear lift contribution called vortex lift. The unfortunate limitation to vortex lift is a phenomenon known as vortex breakdown which provokes highly turbulent flow downstream of the vortex breakdown location. As a result, modern fighter aircraft, in particular, twin tailed aircraft structures which make use of vortex lift are subjected to random aerodynamic interactions. These interactions translate into tail buffet loads that result from pressure fluctuations due to flow separation or impact forces from vortical flows themselves.

For the F/A-18 aircraft, tail buffet loads have been alleviated somewhat through the addition of a LEX fence modification which was developed to reposition the vortex away from the vertical tail. The problem of random interactions causing tail buffeting with the vertical fins, however, is still a major concern because of the significant structural implications on the fatigue life of the aircraft. Even after the implementation of the LEX fence, cracks have been discovered on the vertical fins. A fleet modification which reinforced the structure surrounding the affected area has been carried out, but cracks

were since discovered at the base of the tail itself indicating that the problem was not resolved but merely relocated.

A better understanding of the aerodynamics surrounding vortex lift and the vortex breakdown phenomenon is instrumental to extending the life of high performance aircraft like the F/A-18 and is paramount to addressing problems like tail buffet on any twin tailed aircraft. A large amount of work on vortex breakdown has been conducted to date. Fundamental studies have usually been carried out on delta wing configurations. Recent research has concentrated on time dependant flows and their effects on the position of vortex breakdown. Experimentation has been carried out for delta wings oscillating in a pure pitching motion and those oscillating in a pure rolling motion. The research in this study examines the behaviour of the vortex breakdown location as a 70° swept delta wing maneuvers simultaneously in pitch and a roll. In addition, available experimental results for pure pitch and pure roll investigations has been expanded through the use of the 70° swept delta wing. It is anticipated that the Computational Fluid Dynamics (CFD) community would benefit from the observations made and the information gathered in this investigation. Experimentation for this study has been performed using the water tunnel at the Royal Military College (RMC) of Canada, Kingston, Ontario.

CHAPTER II

BACKGROUND

Fundamentals of Vortex Lift

Highly swept wing planforms like those of a delta wing are being thoroughly investigated in the pursuit of achieving lift at high angles of attack. As Polhamus[2] states, these wings exhibit flow in which a highly stable vortex forms along the leading edge resulting in the production of large increases in lift known as vortex lift. Vortex lift is the result of a low pressure region created by the vortical flow near the wing surface which, in essence, creates suction over the wing surface. This behaviour can add substantial nonlinear components to the lift force of the wing. The location of lowest pressure for a wing planform coincides with the centre of the leading edge vortex. A wing designed for vortex lift allows for controlled flow separation at the leading edge. The concept of vortex lift deviates dramatically from conventional attached flow theory. Instead of postponing the inevitable separation for somewhat limited gains, vortex lift uses the properties of separated vortical flow to enhance lift.

Polhamus[3] introduced a definition of total lift for a delta wing as the sum of potential lift and a vortex lift increment. He based his concept for calculating vortex lift on an analogy between the vortex lift and the leading edge suction associated with the potential flow about the leading edge. This concept is referred to as the leading edge

suction analogy and with it, Polhamus[3] developed the following relationship for the vortex lift coefficient:

$$C_{L,V} = K_V \cos\alpha \sin^2\alpha \quad \textbf{(1)}$$

where $C_{L,V}$ is the vortex flow lift coefficient and K_V is a function of aspect ratio for sharp edged delta wings. Polhamus[3] also provided that the relationship between the potential flow lift coefficient and angle of attack (for zero suction, attached flow lift) can be expressed by:

$$C_{L,p} = K_p \sin\alpha \cos^2\alpha \quad \textbf{(2)}$$

where $C_{L,p}$ is the potential flow lift coefficient for the condition of zero leading edge suction and K_p varies with aspect ratio and is approximated by the slope of the lift coefficient at zero angle of attack. Note that for small angles of attack, $C_{L,p}$ reduces to:

$$C_{L,p} = K_p \alpha \quad \textbf{(3)}$$

which is a linear relationship between the coefficient of lift and the angle of attack. The

expression for total lift becomes:

$$C_L = K_p \sin\alpha \cos^2\alpha + K_V \sin^2\alpha \cos\alpha \quad \textbf{(4)}$$

Hemsch[4] makes the distinction between vortex lift and non-linear lift. As illustrated in Figure 2.1, nonlinear lift is the difference between the actual lift at a given α and that given by the linearly approximated $K_p\alpha$. Vortex lift is the increment above the attached flow lift with zero leading edge suction and is due to the presence of the leading edge vortex. It has been shown that separation vortices appear at smaller angles of attack for sharp leading edges than for rounded leading edges. Polhamus[2] reported on NASA Langley's study of the Lippisch highly swept delta wing DM-1 test glider modified with a sharp leading edge. The results shown in Figure 2.2 demonstrated large vortex lift increments. As well, the analysis with a variation of leading edge profiles, presented by Peake[5], demonstrated a marked increase in lift coefficient for a bevelled leading edge as compared to a rounded or elliptic leading edge. This is illustrated in Figure 2.3.

As a result of the foundation provided by previous work, current studies concentrate on the vortex behaviour over slender sharp leading edged delta wings. As shown in Figure 2.4, leading edge vortices are formed over a delta wing when the boundary layer or shear layer detaches from a surface rolling up into a well organized vortical shape and leaving a long swept separation line. This process is referred to as the roll-up of a vortex sheet. As the sheet rolls up, its intersection with the plane normal to

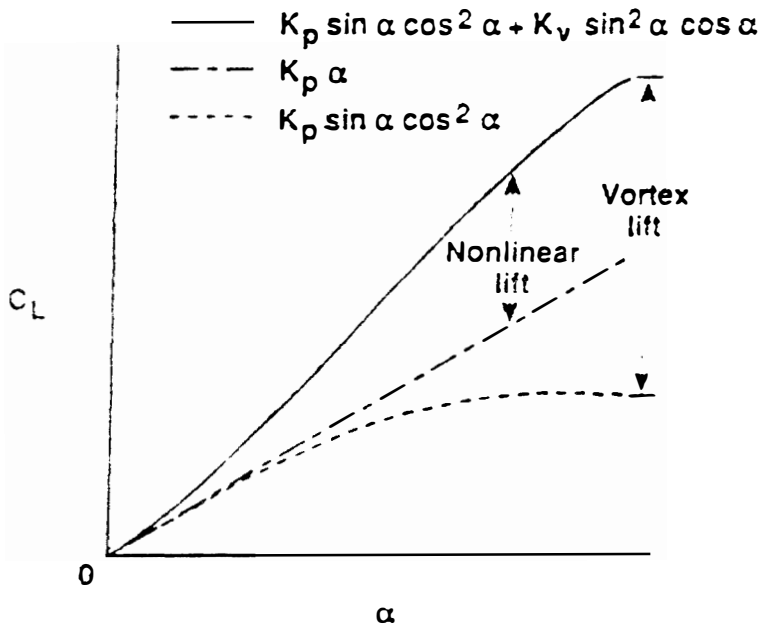

Figure 2.1. Vortex Lift Versus Nonlinear Lift. [4]

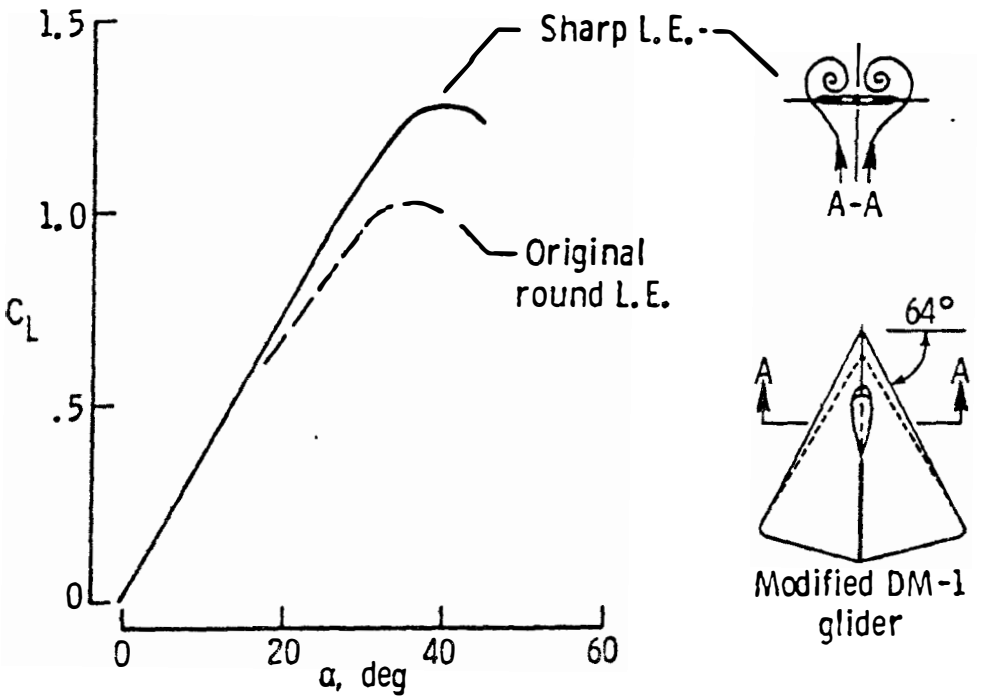

Figure 2.2. Modified Lippisch DM-1 Test Glider Result. NASA Langley 1946. [2]

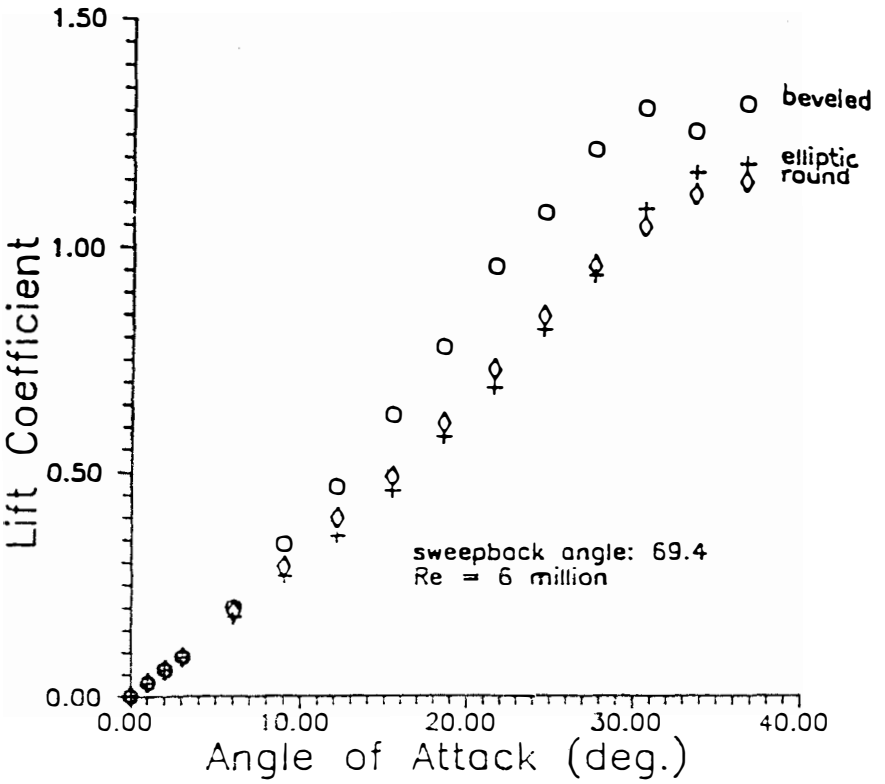

Figure 2.3. Effect of Leading Edge Profile on Lift Coefficient. Barlet, 1955. [2]

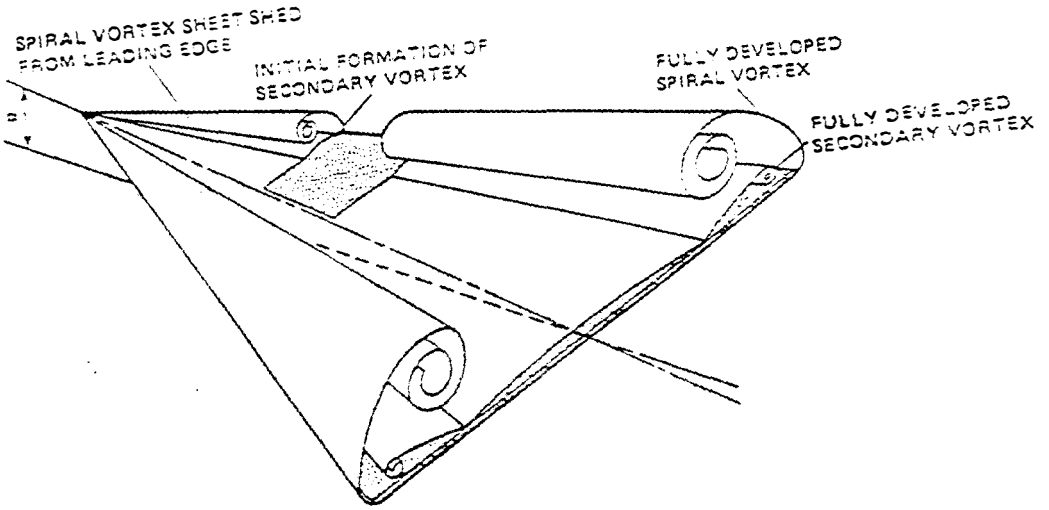

Figure 2.4. Sharp Leading Edge Induced Vortical Flow. [6]

the lifting surface forms a spiral, and the velocity profile in the inner portion or core of the spiral is nearly axisymmetric. The core size increases as the flow progresses downstream. The circulation about the core increases with distance along the axis as well as axial speed along the centerline due to the continuous drop in centerline pressure as the core vorticity increases. The definition of the core, however, is somewhat arbitrary. The main purpose in isolating a core has been to define the region that contains most of the vorticity. This definition has been used as a simplifying assumption in theoretical analyses. In the ideal case, the centre of the leading edge vortex is designed to be located on the order of a core diameter above the lifting surface and along the leading edge. Should the characteristics of vortex core change dramatically, as in the case of vortex breakdown, the aerodynamic qualities of the flow are destroyed.

Research has shown that the size of the vortical core formed by the roll-up of a vortex sheet is independent of Reynolds number[6,7]. Reynolds number is defined as:

$$Re = \frac{Uc}{\nu} \tag{5}$$

where: c is the wing centerline or root chord length;

U is the velocity of the fluid flow; and

ν is the kinematic viscosity of the fluid.

Wedemeyer[6] generalizes that the overall lift of slender, sharp leading edge, delta wings

is relatively insensitive to Reynolds number. Lee and Ho[7] further distinguishes that this insensitivity only applies to surfaces with sharp leading edges since surfaces with rounded leading edges are affected by the laminar/turbulent transition in the boundary layer and thus affected by a change in Reynolds number. The flow details associated with the state of the boundary layer on the wing upper surface can cause very large variations in local pressure distribution through their effect on the location of secondary separation lines. These secondary separations occur when the flow under the primary vortex is swept toward the wing leading edge, by the action of the vortex and encounters the adverse spanwise pressure gradient near the leading edge. As illustrated in Figure 2.4, this results in a secondary vortex having vorticity of the opposite sign. Secondary effects are highly dependant upon the local state of the boundary layer and therefore on Reynolds number and the longitudinal station.

Gad-el-Hak and Blackwelder[8] examined the structure of the shear layer that separated from the leading edge of a 60° swept delta wing. Their results showed that the classical large vortex shed from the sharp leading edge of a delta wing originates as a series of smaller discrete vortices which rotate around each other and pair to form larger vortices while simultaneously moving downstream. These discrete vortices are depicted in Figure 2.5. This phenomenon was more apparent in the angle of attack range of 10° to 15°. For lower angles of attack, it was felt that the pairing process was inhibited by the boundary layer and for higher angles of attack, the flow was more turbulent which seemed to mask the phenomenon. Gad-el-Hak and Blackwelder[8] concluded that discrete vortex shedding and the pairing process in an important aspect in the dynamics of the larger

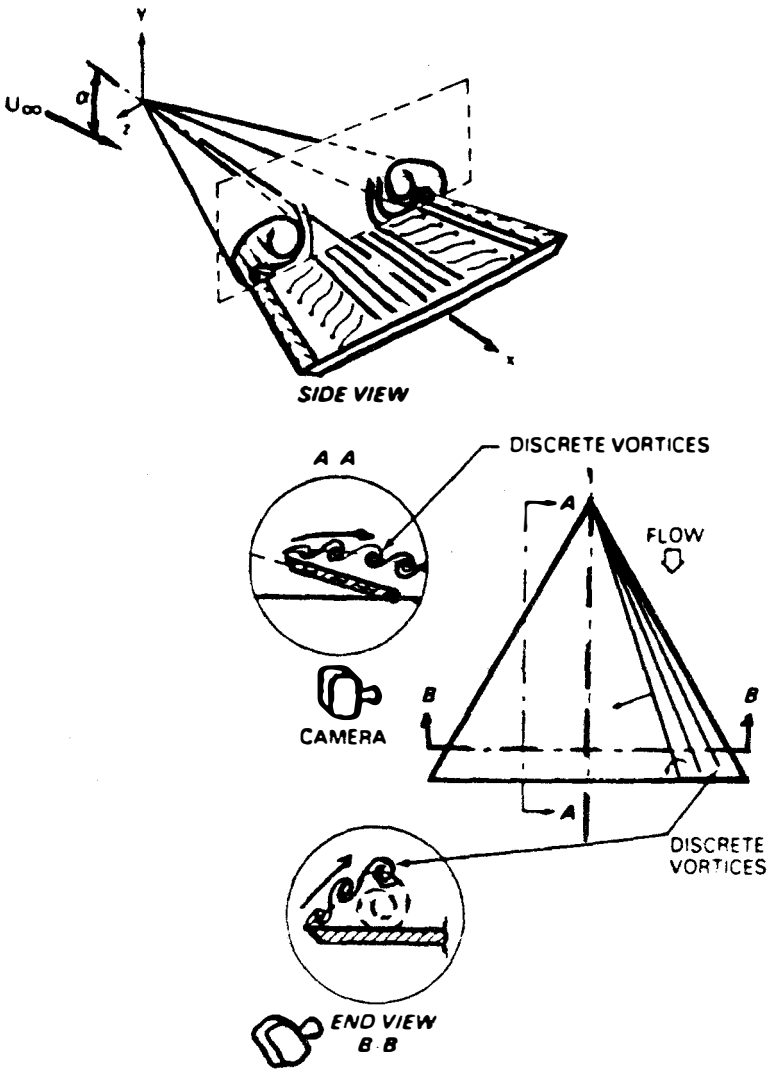

Figure 2.5. Discrete Vortices. [8]

primary vortex structure.

Lee and Ho[7] reviewed the concept of vorticity balance based on the assumption that the flow conditions are governed by a concentrated vortex. Vorticity is generated on the surface and diffused into the boundary layer. In the case of attached flow, the vorticity is removed continuously by free stream convection. However, in the case of separated flow, a local shear layer has been formed and rolled up into a concentrated vortex which is convected downstream with the velocity of the freestream. The balance of vorticity refers to the relationship between surface vorticity flux and that transported in the freestream. This relationship dictates whether there will be an accumulation or depletion of vorticity above the solid surface. The surface flux is governed mainly by the local pressure gradient and the motion of the surface. For the delta wing, the vorticity flux is further governed by the condition of the boundary layer at the leading edge prior to flow separation. Lee and Ho[7] commented that a stationary leading edge vortex is only established when a balance of vorticity exist. When there is an imbalance of vorticity, the result is vortex breakdown.

Vortex Breakdown

Generally, the term "vortex breakdown" or similarly "vortex burst" describes an abrupt change of the flow field structure. Some of the earlier works on the phenomenon of vortex breakdown were carried out by Peckham & Atkinson[9] in 1957, Elle[10] in 1960 and Lambourne and Bryer[11] in 1962. The breakdown of leading edge vortices over wings with highly swept leading edges has been observed when the angle of attack

exceeded a critical value. Vortex breakdown is often the limiting factor in achieving optimum lift through leading edge vortices. An example of the vortex breakdown phenomenon in the flow over a delta wing is shown in Figure 2.6. Flow visualization in the form of dye injection introduced by the tip of each of the leading edge vortices has been employed.

The illustration in Figure 2.7 shows the dramatic change in lift coefficient due to vortex breakdown for a variety of delta wing planforms at a given angle of attack. Peake[5] has compared the phenomenon of vortex breakdown to that of a normal shock wave. The shock wave separates supersonic flow which is insensitive to downstream conditions from subsonic flow which is influenced by all of its surroundings. Similarly, upstream of the vortex breakdown location, the presence of the breakdown is not visibly evident nor detectable through velocity measurements. Also, as Peake[5] discusses, experiments have revealed that flow downstream of the burst is always less stable than that upstream of the burst. Vortex breakdown causes significant modification to the vortex structure. It acts like a switch from laminar flow to turbulent flow or from less turbulent flow to more turbulent flow. Similar to the shock wave, vortex breakdown appears to be a discontinuous transition between two distinct flows. In that respect, vortex breakdown has also been compared to the hydraulic jump phenomenon observed in fluid flows.

Although there have been many forms of the vortex breakdown phenomenon reported, they generally have been divided into two primary characteristic forms; the bubble (axisymmetric) form which is referred to as the B-type and the spiral form which is

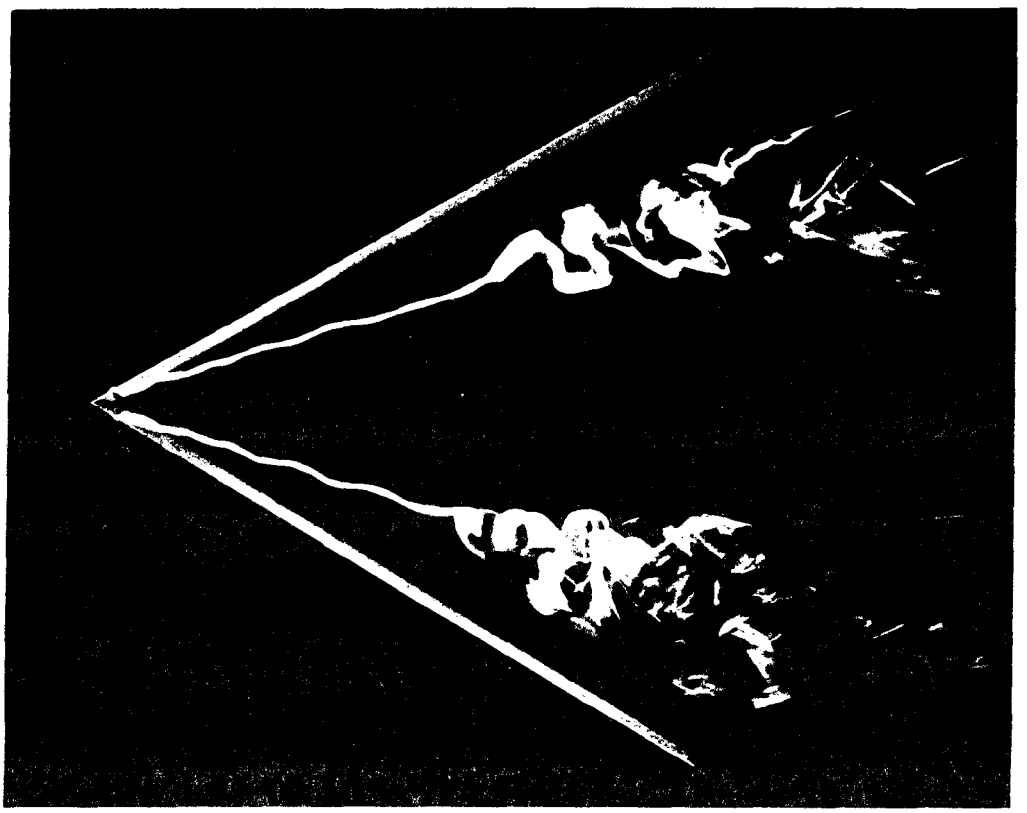

Figure 2.6. Vortex Breakdown Above a Delta Wing. ONERA Werle, 1963. [12]

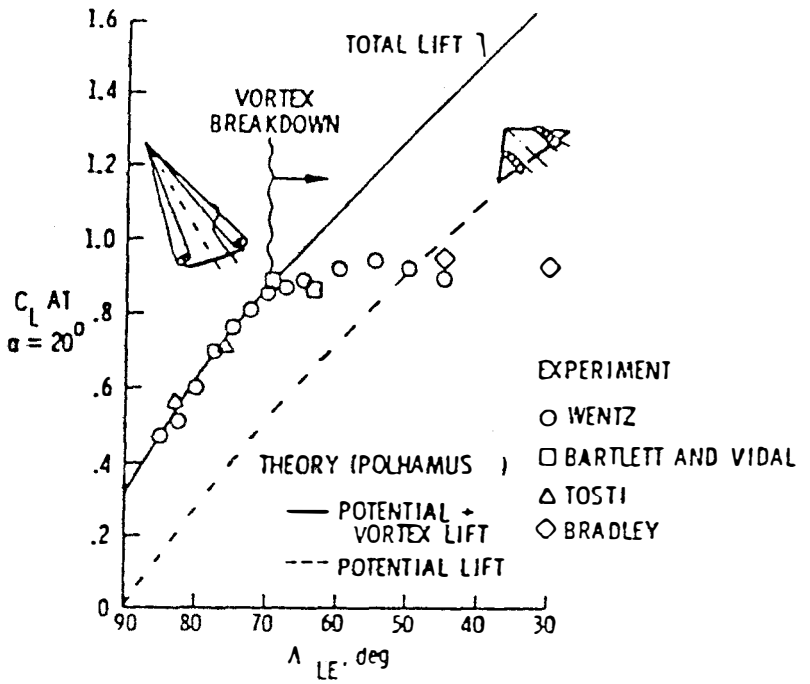

Lift capability of delta wings at $\alpha = 20°$.

Figure 2.7. Effect of Vortex Breakdown on Lift Coefficient. [6]

referred to as the S-type. These two breakdown forms are illustrated in Figure 2.8. In either form, a stagnation point on the vortex axis is followed by a limited region of reversed axial flow near the vortex centerline. In the S-type, streamlines originally near the vortex axis change direction and assume a spiral or corkscrew shape about an expanded body of stagnant fluid until finally the filament breaks up into large scale turbulence. In the B-type, however, the central filament reaches a free stagnation point from which it expands in a nearly axisymmetrical flow about a body of recirculating fluid similar to a body of revolution.

There is evidence to support the idea that the two breakdown types are distinctly different. Peake[5] provides measured values of core expansion ratios (wake core diameter/approach flow core diameter) that show that expansions associated with the B-type are quite different than those associated with the S-type. As well, support for the distinction between the two types comes from vortex tube analyses which focussed on swirl angles (defined as the angle between the tangential and axial velocity components of the vortex). For low values of swirl, the flow exhibits no unusual behaviour. When swirling exceeds a critical value, a large amplitude disturbance is initiated. Peake[5] demonstrated that, for a Reynolds number of approximately 3.0×10^4 or more, based on the length scale of tube diameter, the first form of breakdown observed was the S-type. As the swirl level was increased, the breakdown moved upstream. This behaviour continued until a second critical value of swirl was reached and the S-type transformed to a B-type. The position of the breakdown moved rapidly upstream from where it was when it was an S-type. There were ranges in which S-type and the B-type transformed

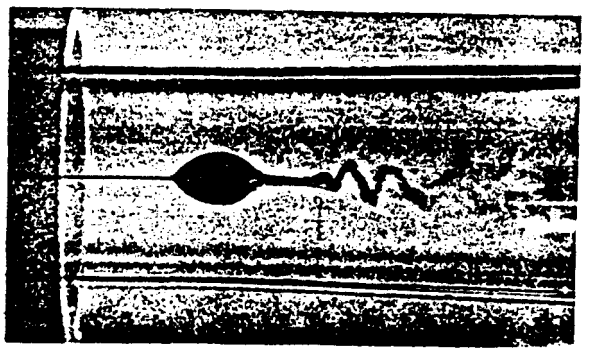

(a)

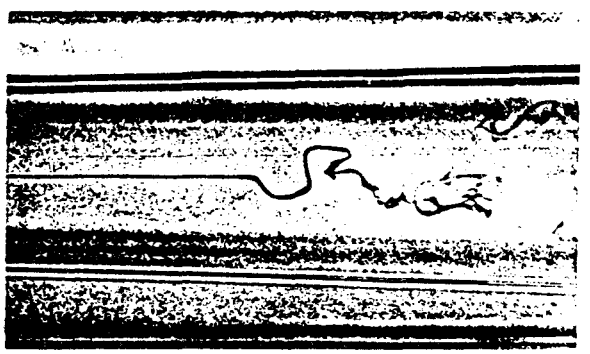

(b)

Figure 2.8. Vortex Breakdown Forms: (a) B-type; and (b) S-type. [13]

back and forth between one another. The position of the breakdown also oscillated between the location appropriate to its type.

Although the interest in vortex breakdown originally arose from its application to leading edge vortices, a large amount of experimental work has been conducted in circular ducts or vortex tubes. This is partially due to the fact that flow in vortex tubes can be easily controlled and that the flow is axisymmetric. Lee and Ho[7], however, point out that there is a fundamental difference between vortices generated in a tube and those generated over a delta wing. In the vortex tube experiments, Reynolds number is a dominating parameter where the flow over a delta wing is not. Liebovich[13] explains that, for vortex tube experiments, vorticity is shed into the centre of the tube by a vane generator thus producing a vortex of relatively constant vorticity. On the other hand, in the flow over a delta wing vorticity is being constantly fed into the core of the vortex resulting in an almost linear increase in vorticity along the vortex core.

Physically speaking it has been observed that an essential feature for the occurrence of vortex breakdown, whether the flow is axisymmetric or non-axisymmetric, is a region of low total pressure near the axis of the vortex. Vortex breakdown results from a stagnation in the flow in the presence of an adverse pressure gradient. Small changes in the external flow are sufficient to produce a large pressure gradient along the axis because the pressure gradient is magnified towards the axis of the vortex. A quantitative description of vortex breakdown, however, can only be obtained by solving the full non-linear equations of motion.

For reasons of simplifying the governing equations all theories of vortex

breakdown assume that the flow upstream from the breakdown is axisymmetric. Some theories ignore the asymmetric features of breakdown assuming they are only secondary effects. The main commonality in all theories pertaining to axisymmetry is the concept of critical flow. In all experiments with vortex tubes reported by Peake[5], it was found that vortex breakdown occurs when the swirl component of the flow was sufficiently large. The swirl angle was thought of as a critical parameter. The increasing swirl reduced the necessary pressure gradient required for the onset of vortex breakdown. Further increasing the swirl angle past the critical value caused the breakdown position to move upstream.

Peake[5] provides two main categories of explanation that are used when analysing the vortex breakdown phenomenon. These are theories that relate breakdown to flow instability and theories that do not. All theories are reported to predict vortex breakdown to occur generally within the experimentally observed range of swirl angles. They also accurately predict the sensitivity of breakdown to the severity of axial pressure gradients. No theory, however, gives an accurate prediction of the location of breakdown as compared to experimental results nor does any theory give the flow detail inside the breakdown region. Furthermore, none of the theories have found general acceptance. An interesting comment made by Peake[5] quotes Ludwig (1970) stating that it cannot be expected that all sudden changes of vortex structure which is called vortex breakdown can be explained by one theory alone. This statement has gained recognition since it has been discovered that there are so many mechanisms that are involved in the vortex breakdown phenomenon.

Steady State Analyses

There has been much research performed to date investigating the factors affecting the location of vortex breakdown under steady state conditions. These factors can be grouped into areas involving flow conditions and those involving the specifics of delta wing geometry.

A change in wing orientation is the most apparent factor which affects the location of the vortex breakdown. As the of angle of attack increases, for example, the location of vortex breakdown moves forward toward the apex of the delta wing. Conversely, as the angle of attack decreases, the position of the vortex breakdown moves back toward the trailing edge. In fact, the position of vortex breakdown can move past the trailing edge and propagate downstream a considerable distance. Lowson and Riley[14] have reported on many investigations that have been conducted on the behaviour of vortex breakdown over delta wings of various sweep angles as a function of angle of attack and have demonstrated that, although there are similar trends reported, there is no universally agreed location for vortex breakdown on a delta wing as a function of angle of attack and leading edge sweep. A compilation of steady state delta wing data for various sweep angles as a function of angle of attack was published by Wentz and Kohlman[15] and is provided in Figure 2.9.

Lee and Ho[16] have shown that the location of vortex breakdown for a slender delta wing of a given sweep angle is uniquely related to the leading edge incident angle. Huang and Hanff[17] presented the following static prediction model which correlated the

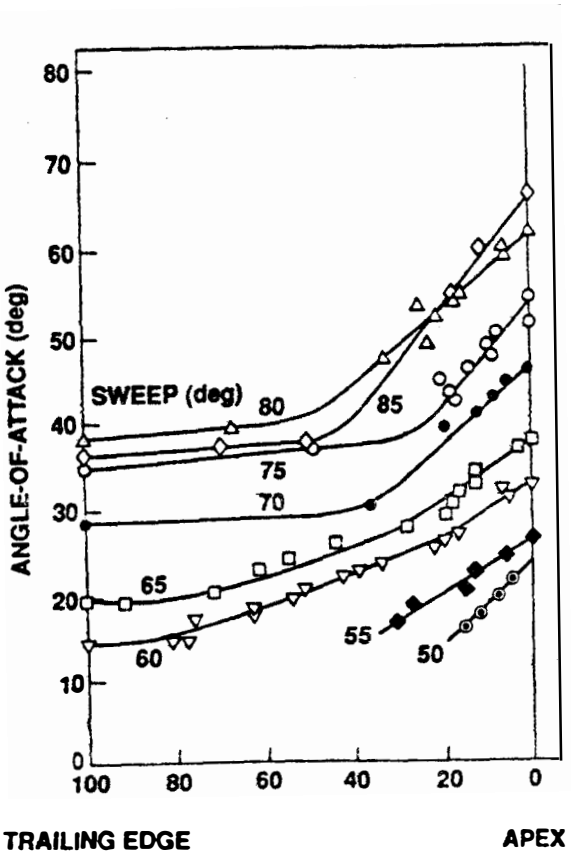

Figure 2.9. Vortex Breakdown Position on Sharp Edged Delta Wings. [15]

location of vortex breakdown for a slender delta wing of a given sweep angle as it related to the leading edge incidence angle, γ:

$$\frac{x}{c} = \frac{N}{\tan\gamma - 0.32} - A \qquad \textbf{(6)}$$

where:

$$\gamma = \cos^{-1}(\cos\alpha \sin\Lambda)$$
$$N = 0.4 + 0.1 \cot\Lambda$$
$$A = 0.17 + 0.38\cot\Lambda + \cot^2\Lambda$$
$$\tan\gamma \sim U_\phi / U_\infty$$

A review of published data as it compares to Huang and Hanff's[17] prediction model is shown in Figure 2.10.

When the delta wing is oriented with a pitch angle and a non-zero roll angle, the angle of attack and sweep angle seen by the flow is modified. For a given roll angle, the effective angle of attack and effective sweep angle change can be expressed as follows:

$$\alpha(\phi) = \tan^{-1}(\tan\sigma\cos\phi)$$
$$\Lambda(\phi) = \Lambda \pm \tan^{-1}(\tan\sigma\sin\phi) \qquad \textbf{(7)}$$

For the 70° delta wing, Figure 2.11 illustrates these effective changes for a given roll angle. Hanff and Ericsson[17] explain that, from these equations and for a given roll

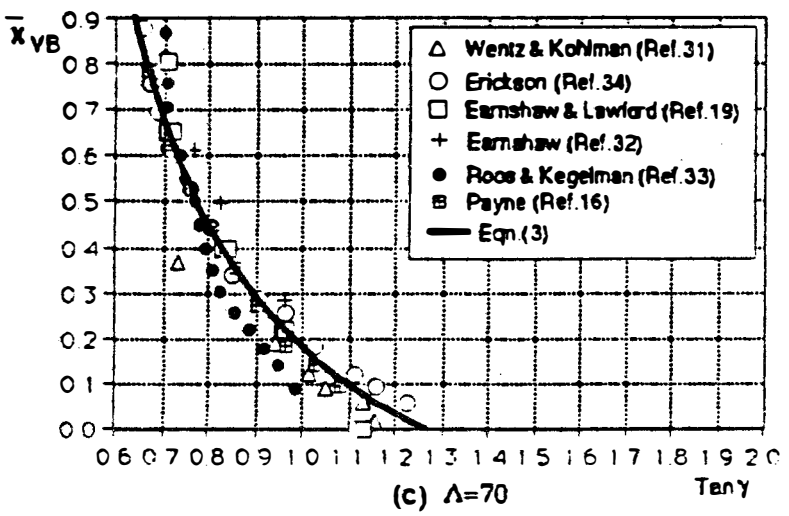

Figure 2.10. Steady State Vortex Breakdown Data for a 70° Swept Delta Wing. [17]

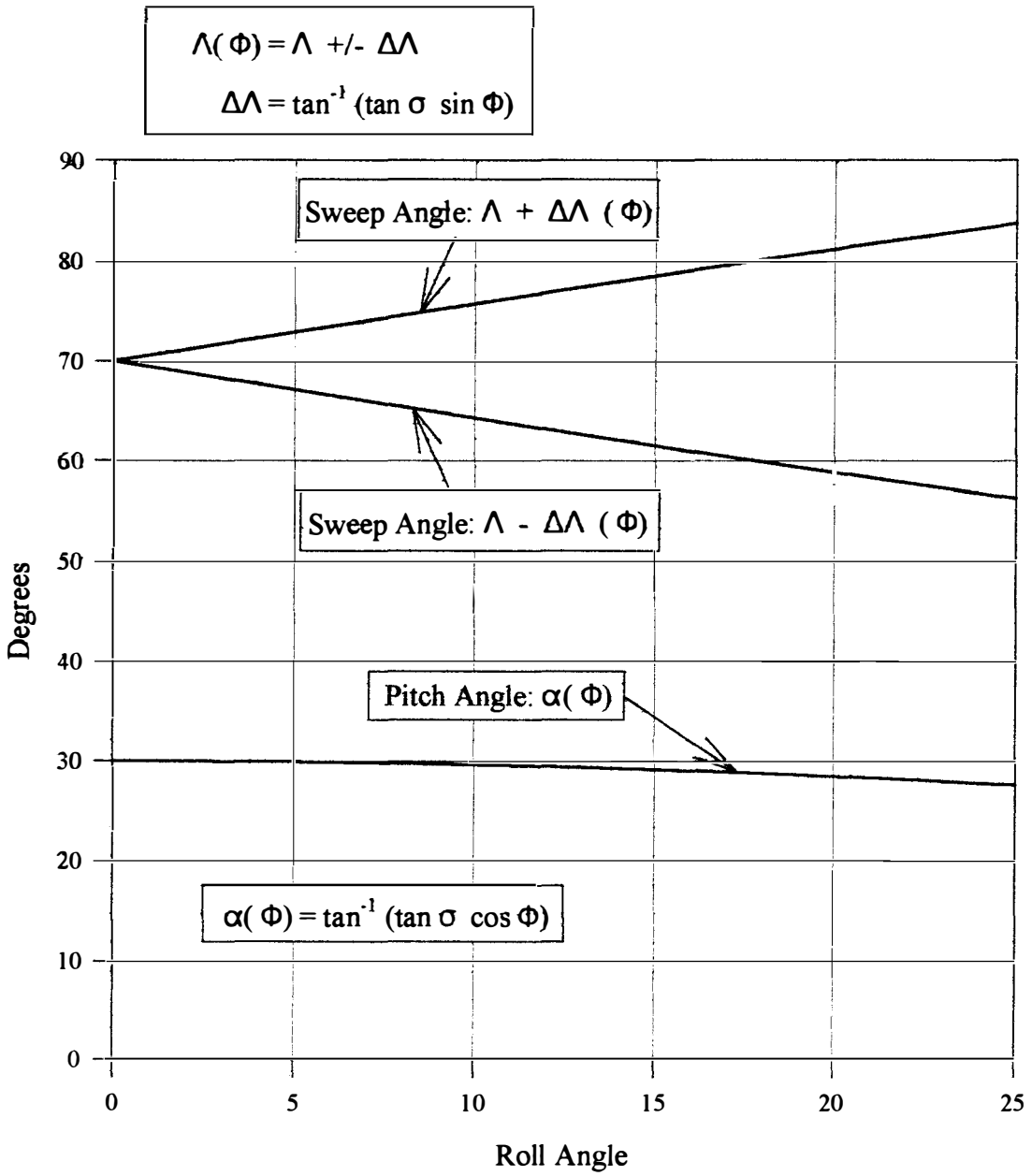

Figure 2.11. Effect of Roll Angle on Effective Leading Edge Sweep and Effective Angle of Attack.

angle, the leeward half of the wing (the half that rolled up) experiences a decrease in angle of attack and an increase in sweep angle. Both factors cause a lowering of the swirl parameter and lead to an aft displacement of the location of the vortex breakdown. The wing that rolls down also experiences a decrease in angle of attack, but sees a decrease in sweep angle. The decrease in sweep angle dominates to augment the swirl parameter and lead to a forward motion of the breakdown point location. Because the effects of the change in angle of attack and change in sweep angle operate in the same direction on the leeward half of the wing (the half that rolled up) and the changes operate in opposite directions on the windward half of the wing (the half that rolled down), the displacement of the breakdown location is usually larger on the leeward half of the wing.

Huang and Hanff[18] showed very good correlation between experimental data and the following expression for the prediction of the vortex breakdown location which was modified after extensive review of empirical data:

$$\frac{x}{c} = \frac{N}{\tan\gamma - B} - A \qquad \textbf{(8)}$$

where:

$$\gamma = \cos^{-1}(\cos\alpha(\phi)\ \sin\Lambda(\phi))$$
$$N = 0.33 + 0.3/\tan^2\Lambda(\phi)$$
$$A = 0.20 + 1.6/\tan^2\Lambda(\phi)$$
$$B = 0.43 - 0.1/\tan\Lambda(\phi)$$
$$\tan\gamma \sim U_\phi / U_\infty$$

An example the data published by Huang and Hanff[18] is shown in Figure 2.12.

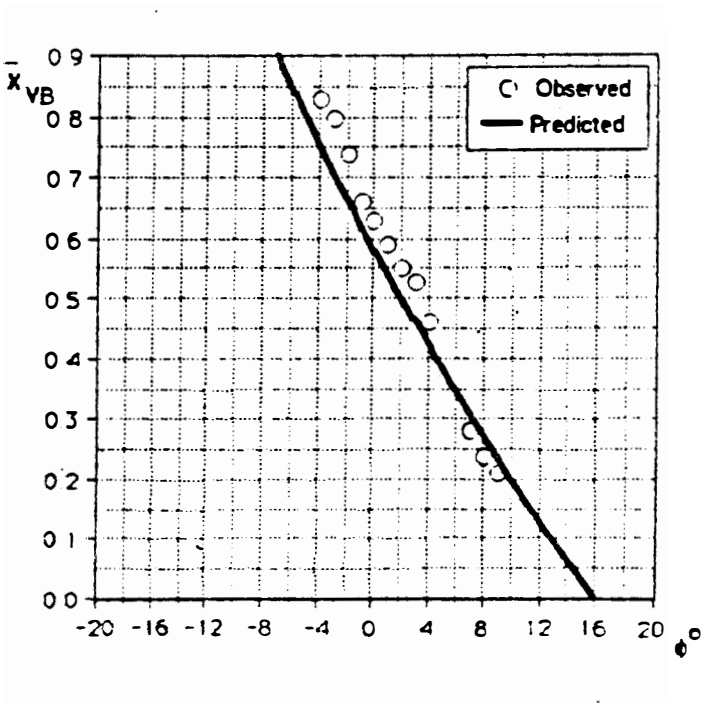

Figure 2.12. Static Breakdown Location for Rolled Model. [18]

The roll data is consistent with that which has been published for a delta wings experiencing changes in yaw as well as for analyses of delta wings of varying sweep angles. Fundamentally, vortex breakdown occurs first at the side of the delta wing which is turned into the flow direction. Erickson[19], in his work on slender delta wing vortices, has shown this relationship as well as the tendency for vortex breakdown to increase as sweepback angle is decreased. Also, Jarrah[20] showed that, as sweep angle increases, the slope of the lift curve increases due to the increased strength of the leading edge vortices.

Other studies involving the change of flow conditions have shown that if the flow downstream of the breakdown is blocked, the location of the vortex breakdown tends to move forward. For example, Gursul and Yang[21] used a control cylinder situated in the flow during their data collection which caused the position of the vortex breakdown to move upstream.

One relationship which has been investigated at length involves the relationship of vortex breakdown and Reynolds number. It has been demonstrated and accepted in all the published data that there is no significant influence of Reynolds number on the position of vortex breakdown. Atta and Rockwell's [22] reported that the location of vortex breakdown for a stationary delta wing at a given angle of attack and at a low Reynolds number of 5.8×10^4 was in good agreement with the study of Wedemeyer[6] which was carried out at much higher Reynolds numbers. Jarrah[20] investigated the aerodynamic forces and moments of the flow over three delta wings of different sweep angles. He concluded that the influence of Reynolds number had a negligible effect on the flow over

sharp edge models. He did comment, however, that the Reynolds number could have an effect on the fine scales in the vortex structure.

In addition to the influence of the sweep angle, other geometric features have a significant influence on the position of the vortex breakdown. Recently, Lowson[14] conducted a study to examine the reasons for the variations in published results of the location of vortex breakdown on delta wings of similar sweep angle. He reviewed a number of studies and found similar trends in the data existed as long as the wing leading edge was kept sharp; however, he also found that serious anomalies existed when he focussed on the details of similar model geometry which included thickness ratio, leading edge chamfer and leading edge radius. Lowson[14] tested for repeatability by examining several delta wings with geometries identical to those used in some published studies and was successful in reproducing previously published data using models of exact geometry used in prior investigations. He concluded that the variation from various investigations of the vortex breakdown position at the same sweep and angle of attack was due primarily to the detailed model geometry, particularly the geometry of the apex. He also concluded that the effects of vortex breakdown position due to variations in geometry far outweigh those due to support interference, methods of flow visualization, wind tunnel factor and changes in Reynolds number. Other researchers have made similar conclusions. Thompson[23], for example, conducted a comparative analysis of the differences between data obtained from various researchers who carried out essentially the same experimentation. He noted that even for two studies that were performed on essentially the same model design, differences in breakdown location were noted as high as 25% for a

fixed angle of attack. He generalized that the differences apparent in the data could be attributed to leading edge geometry, thickness ratio, measurement technique / researcher defined breakdown point, blockage, wing support interference, or the direction of quasi-steady motion (increasing or decreasing incidence).

Unsteady Wing Motions

In general, researchers have described unsteady wing motions as being transient or oscillating. Typically, a transient motion is an impulse motion that has a start point and a stop point. The cycle is defined either by an increasing or by a decreasing angle of attack which starts from rest. For an increase in angle of attack, the motion is sometimes referred to simply as pitching. For a decrease in angle of attack, the term often used is plunging. The oscillating motion has been defined using the form of a sawtooth but more often that of a sine wave.

As noted earlier, it is generally accepted throughout studies involving vortex flow that vortex flow over a delta wing at high angle of attack is relatively independent of Reynolds number. To quantify the unsteadiness in an unsteady flow, nondimensional parameters have already been developed. For wings undergoing harmonic oscillations, the term used is reduced frequency, k. For oscillations in pitch, reduced frequency is defined by:

$$k_{pitch} = \frac{2\pi fc}{U} \tag{9}$$

where: c is the wing chord length;

f is the oscillation frequency; and

U is the freestream velocity.

This dimensionless frequency represents the ratio of the wing chord length, c, to the wavelength, U/f, of the forced motion. Reduced frequency is used as a comparison parameter with which data from different studies can be correlated. Some studies define reduced pitch frequency without the two in the numerator, so care must be taken when making comparisons of data with other studies. In this study, the values for reduced pitch frequency were calculated using the above definition. In addition, for unsteady pitch motions, the axis of pitch rotation is an important parameter in affecting the resultant behaviour of the location of vortex breakdown. Studies have been carried out using various locations as the axis of rotation; however, the axis of pitch rotation for this investigation was the centre chord location.

The non-dimensional parameters for unsteady roll motions have been developed similar to those for unsteady pitch motions. For wings undergoing harmonic roll oscillations, reduced frequency is defined by:

$$k_{roll} = \frac{2\pi f b}{2U} \tag{10}$$

where: b/2 is the wing trailing edge half span length.

For impulse pitch motions, the nondimensional term used for comparison of data is reduced pitch rate defined as:

$$\mathrm{K} = \frac{\dot{\alpha}_{max}\, c}{2U} \tag{11}$$

where: $\dot{\alpha}_{max}$ is the pitch rate in radians per second.

For impulse roll motions, the non-dimensional term is reduced roll rate defined as:

$$\dot{\Phi} = \frac{b}{2U}\,\frac{\delta\phi}{\delta t} \tag{12}$$

where $\delta\phi/\delta t$ is the roll rate in radians per second.

It is not certain which motion best relates to actual flight conditions, although some comparisons have been presented in support that certain types of motion and

combinations thereof can relate directly to actual flight conditions. It is more important to recognize, however, that the only clear way of exploiting the advantages of vortex lift is to investigate its behaviour completely.

Delta Wing Aerodynamics Involving Unsteady Pitching Motions

Thompson[23] commented that the unsteady response of vortex flow over a delta wing undergoing pitching motion can be divided into two categories: low angle of attack motion; and high angle of attack motion. For low angle of attack motion, the unsteady flowfield response is quasi-steady, but for high angle of attack motion, the unsteady flowfield response is characterised by the occurrence of vortex breakdown and a hysteresis effect in terms of the breakdown location. Ashly et al.[24] explained that when a delta wing oscillates in pitch, the flowfield over the wing is incapable of instantaneously adjusting to the angle of attack. The flowfield takes a finite period of time to make the adjustment and, meanwhile, for unsteady motion, the unsteady maneuver continues to change. The result is that the flowfield is continually adjusting to new flow conditions. LeMay[25] also provided that, at low angles of attack, a time delay can mean the delay of vortex formation, whereas, at high angles of attack, it could mean the delay in formation or movement of vortex breakdown.

A large amount of work on delta wings undergoing unsteady pitching motions has been conducted to date that investigated the delay in flowfield response at high angles of attack. The observations made by Atta and Rockwell[22] indicate that there is a drastic

phase shift in the vortex breakdown location with respect to the wing motion. Their study concluded that this phase shift of the vortex core development with respect to the wing motion is essential to the occurrence of hysteresis in the overall flow structure. LeMay[25] examined the phase-angle relationship between the location of vortex breakdown and angle of attack for small ranges of angle of attack and for larger amplitude oscillations. He found a strong dependence on reduced frequency. He also found that Reynolds number had little effect on the phase lag over the range he investigated. Thompson[23] suggested that the delay in the formation or the delay in motion of vortex breakdown was not typically a result of convective properties of the flow, but rather the unsteady effects in the aerodynamic loads. For example, Ashly et al.[10] showed that, when delta wing is given a sudden increase in angle of attack, the vortex breakdown location moves aft of its steady state location. The result is a coherent vortex structure formed over a greater part of the wing thus enhancing lift. Similarly, when a delta wing is given a sudden decrease in angle of attack, the vortex breakdown location moves further upstream of its steady state location. The vortex covers less of the wing resulting in less lift.

Researchers have generally observed that both transient or impulse pitching motion as well as oscillatory pitching motion result in an unsteady hysteretic behaviour. Hysteresis effects can be regarded as overshoots or undershoots in relation to the behaviour during steady state conditions. The overshoots and undershoots are sometimes termed hysteresis "loops" Gad-el-Hak and Ho[26] observed that when the frequency of oscillation was decreased to a very low value, the hysteresis tends to diminish and the flow

reaches a quasi-steady state. Even at the lowest value of reduced frequency he tested, LeMay[25] observed a hysteresis loop in the location of the vortex breakdown. An example of LeMay's[25] data is presented in Figure 2.13.

Referring to Figure 2.13, it can be seen that as reduced frequency increased, the hysteresis loops became greater at a given angle of attack. The movement of the vortex breakdown location was restricted accordingly. At the higher reduced frequencies, the wing would begin its pitch-up portion of the cycle before the breakdown location could reach its aftmost static location. Hysteresis effects as a result of unsteady motion have been well documented for several characteristics which include vortex breakdown location, surface pressure, lift, drag, pitching moment and normal force. In addition, the study of transient motion, provides for information about the flowfield in terms of the length of time it requires to return to the steady state conditions upon completion of the maneuver. This data is typically measured in terms of convection time units which Reynolds[27] define as the time it takes the freestream flow to travel the length of the wing.

Magness[28] has shown that it is possible to subject a wing to a transient motion that is a portion of an oscillating motion; however, the flow field behaviour will not necessarily be the same for the two cases. In addition, Thompson[23] commented that the unsteady response of the leading edge vortex flow field is very sensitive to the initial conditions of the flow and that the magnitude of both the overshoot and the undershoot can change. In fact, Wolffelt[29] and Brandon and Shah[30] have shown that differences can result for initial angles varying by less than five degrees. Thompson[23] concluded

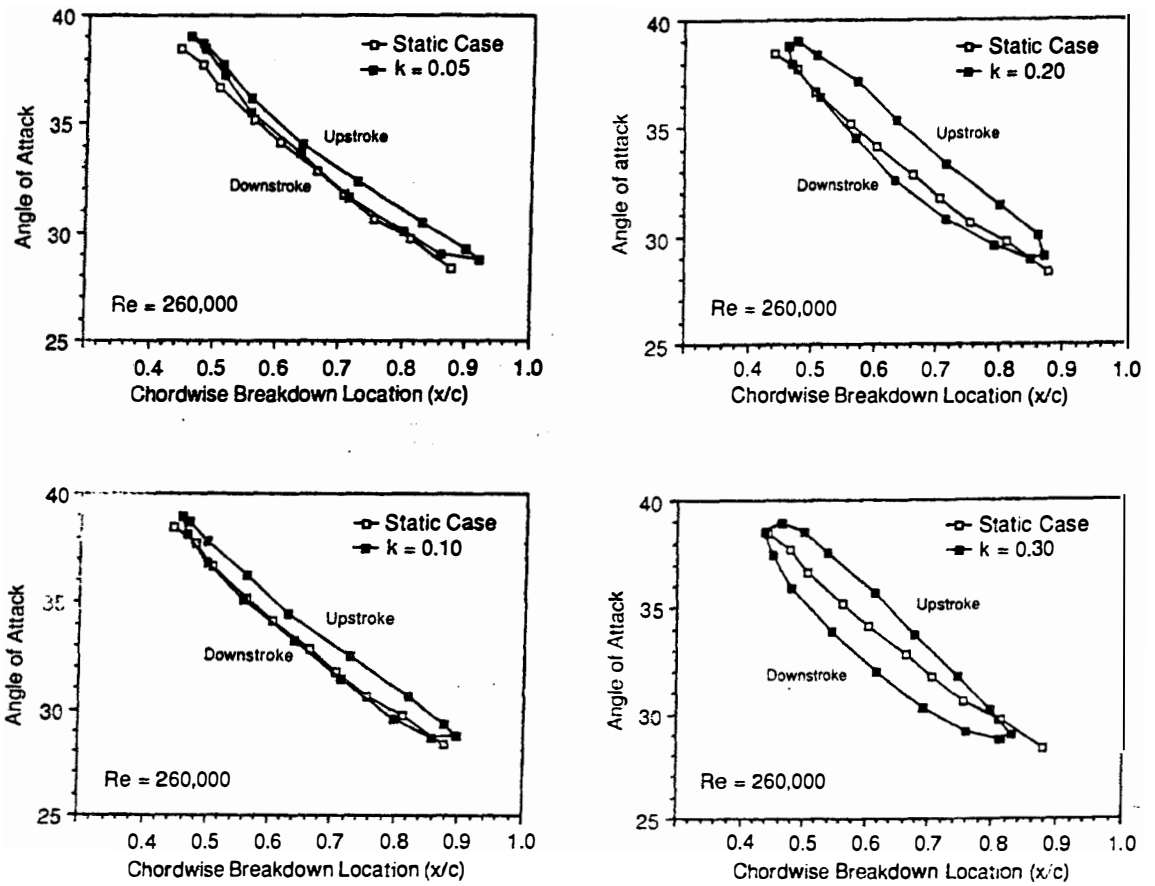

Figure 2.13. Chordwise Location of Vortex Breakdown. [25]

that all these phenomenon demonstrates that the leading edge vortices and their aerodynamic effects have a strong dependence on the exact motion history. LeMay[25], for example, collected data for large amplitude motion during which he pitched a 70° delta wing from 0° to 45° at reduced frequencies of $k_{pitch} = 0.05$ and $k_{pitch} = 0.30$ with a root-chord Reynolds number of 2.6×10^5. He reported a similar hysteresis effect as compared to the steady data and he also noted that the hysteresis was greater for an increased reduced frequency. LeMay[25] compared the data from motion with a small range of angle of attack to larger amplitude motion and concluded that for the same Reynolds number and reduced frequency, the hysteresis effect was more pronounced with the large amplitude motions. This is more evidence to support the premise that the motion history has a profound effect on the behaviour of the location of vortex breakdown.

LeMay[25] also examined the phase-angle relationship between the location of vortex breakdown and angle of attack. LeMay's[25] study found a strong dependence on reduced frequency. He also found that a change in Reynolds number had little effect on the phase lag over the range he investigated.

Past Delta Wing Research Involving Unsteady Pitching Motion

Unsteady delta wing research was started as early as the 1950s. Investigators at that time focussed their studies on motions at small angles of attack since the objective at the time was to assess classical linearized theory for finite wings in simple harmonic motion. In 1954, W.R. Laidlaw[31] studied the unsteady aerodynamic loads on a

rectangular wing, a swept wing, and a delta wing. Since only small angles of attack were studied, the formation of leading edge vortices was not commented upon. In 1963, L. Woodgate[32] examined the pitching moment derivatives on a 70° swept wing delta wing undergoing small amplitude pitching oscillations in a wind tunnel. The angle of attack only varied from 0.5° to 1.5° with mean angle of attack from 0° to 15°. Woodgate[32] found a Reynolds number effect to exist between the range of 1.28×10^6 and 2.56×10^6 which he attributed to the state of the secondary flow. Woodgate[32] also found that there were no significant differences due to changing angle of attack. Thompson[23] felt that this was to be expected considering the low angles of attack and the small deviations.

Experiments investigating the hysteretic behaviour of vortex breakdown were carried out in the 1960s. In 1960 and 1962, Lambourne and Bryer[11],[33] studied the vortex flow generated by a sharp leading edge, 65° swept delta wing. As well, in 1964, Lowson[34] conducted experiments with vortex breakdown. It was not until the 1980s, however, that a significant amount of work was carried out which involved the unsteady vortex flow over delta wings.

In 1981, Erickson[35] conducted a series of water tunnel studies investigating the behaviour of leading edge vortices. Tests were conducted at a freestream velocity of 0.33 ft/sec. The Reynolds number was approximately 3.0×10^4. Vortex core trajectories and core stability characteristics were obtained for a variety of wing planforms ranging from 60° to 80° sweep. Erickson[35] concluded that the water tunnel results of flow over thin, sharp edged delta wings provided reasonable estimates of leading edge vortex behaviour which would be expected at higher Reynolds numbers in air. Erickson[35] showed that,

for high angles of attack, the location of vortex breakdown measured in the water tunnel were consistent with those measured in wind tunnel as well as those observed in flight tests. Erickson[35] also qualitatively assessed the effects of deflected leading and trailing edge flaps as well as the leading edge contouring of the vortex characteristics of simple wing planforms and scale models of fighter configurations.

In 1984, Gad-el-Hak and Ho[26] investigated the behaviour of dynamically pitching delta wings in a towing tank at a root-chord Reynolds numbers up to 3.5×10^5. Testing included a delta wing with a leading edge sweep angle of 45° and with a NACA 0012 profile at each spanwise location as well as a flat plate delta wing with a leading edge sweep angle of 60°. The delta wings were oscillated sinusoidally about the quarter-chord location and about a given mean angle of attack. The amplitudes of the oscillations were varied from ± 5° to ± 10° and ± 15°. Gad-el-Hak and Ho[26] reported a substantial hysteresis in the vortex flow relative to the static case. Their study concluded that this hysteretic behaviour was a strong function of reduced frequency and that a distinct change in the flowfield was documented for a reduced frequency of $k_{pitch} \approx \pi$.

In 1986, Wolffelt[29] investigated the movement of the location of vortex breakdown by oscillating a sharp leading edge, 60° swept delta wing. The studies were conducted in a water tunnel with a root chord Reynolds number of 1.0×10^5. The delta wing was oscillated with a pitch frequency of f = 0.58 Hz which translated to a reduced frequency of $k_{pitch} = 0.18$. Wolffelt[29] reported a distinct difference in the hysteretic behaviour of the vortex breakdown location for angle of attack ranges of 0° to 20°, 5° to 25°, and 10° to 30°. As well, he demonstrated that the hysteresis loops did not always

encompass the steady data but rather were displaced.

In 1987, Atta and Rockwell[22] studied the hysteresis of vortex development and breakdown on an oscillating delta wing. Their delta wing had a sweep angle of 52° and was oscillated about its trailing edge with a reduced frequency of $k_{pitch} = 0.76$. The mean angle of attack was 10° and the amplitudes of oscillations were ±10°. Atta and Rockwell[22] observed a phase shift of the vortex core development with respect to the wing motion and linked this behaviour to the occurrence of hysteresis in the overall flow structure. In 1990, Atta and Rockwell[36] examined the flow structure of a pitching delta wing at various Reynolds numbers. Several models were used that were geometrically similar each having the same 52° sweep angle. The range of Reynolds number investigated were $2.9 \times 10^3 \leq R_e \leq 5.8 \times 10^3$ and $2.9 \times 10^3 \leq R_e \leq 1.34 \times 10^4$. The wing was oscillated about the trailing edge and about a mean angle of attack of 10° with amplitudes of ±10° and the reduced frequency was varied from $k_{pitch} = 0.0125$ to $k_{pitch} = 0.97$. Atta and Rockwell[36] observed two fundamental types of vortex development when analysing a complete oscillation cycle: one that occurred during low reduced frequencies and the other at higher reduced frequencies. They identified that there exists a threshold value of excitation frequency above which the core of the leading edge vortex is aggressively shifted downstream from the apex. Below the threshold, the origin of the vortex core gradually moves upstream towards the apex until the vortex core is fully developed. Atta and Rockwell[36] also examined the structure of the vortex breakdown and its strong dependence on reduced frequency reporting that low value of reduced frequency generally produced the classical spiral type vortex breakdown mode, but at

higher reduced frequencies there were a number of other modes that competed with and often superseded the spiral type breakdown mode. Atta and Rockwell[36] reported on the existence of two secondary vortices adjacent to the primary vortex: one adjacent to the leading edge which is fed by vorticity shed from the leading edge and the other, inboard and between the first and the primary vortex, which is fed by vorticity from the wall boundary layer. The secondary vortex immediately adjacent to the leading edge undergoes a development and breakdown process similar to the primary vortex but out of phase from the primary vortex; in fact, the hysteretic behaviour of this secondary was seen to be quite similar to that of the primary vortex. Because the breakdown of this secondary vortex always lead that of the primary vortex, Atta and Rockwell[36] concluded that the resulting region of reverse flow along the leading edge of the wing just prior to the onset of breakdown of the primary vortex was a key element in the primary vortex breakdown process. Atta and Rockwell[36] make some interesting comments about the unsteady flow phenomenon about a pitching delta wing; however, since their model was oscillated about the trailing edge as opposed to the centre chord it is difficult to compare with their data.

In 1988, Brandon and Shaw[30] investigated the effect of large amplitude pitching motion on the aerodynamic force and stability characteristics of flat plate wings with sharp leading edges. The models tested included a rectangular wing as well as a 70° and a 45° swept delta wing. The models were oscillated about the 40% chord position with amplitudes of ±18° at various mean angles of attack and at reduced frequencies varying from $k_{pitch} = 0.009$ to $k_{pitch} = 0.0376$. The studies were carried out in a wind tunnel using

smoke injection and a laser flow visualization technique. Results showed that there were substantial overshoot and hysteresis in the normal force coefficient and that the magnitude of the overshoot and the size of the hysteresis loops were a strong function of the mean angle of oscillation and of reduced frequency. Brandon and Shaw[37] continued their research in 1990 studying the aerodynamic behaviour of a fighter model undergoing large amplitude pitching motions. The data collected for oscillatory motion compared well with their delta wing data presented in 1988. Additionally, constant pitch rate ramp motions from 0° to 75° were used to investigate the effects of pitch rate on aerodynamic characteristics. Brandon and Shaw[37] reported substantial increments in lift, drag and pitching moment as a result of the ramp pitching motions which were highly dependent on the reduced pitch rate and the wing motion time history. These effects were attributed to the lags in the flowfield formation as well as in the location of the vortex breakdown. Lift increments persisting to as high as 50 convective time units were measured.

1989 Jarrah[38] conducted a test program with the objective of producing an standard set accurate aerodynamic data for simple delta wing models undergoing sinusoidal and ramp variations in angle of attack. The three models tested had sweep angles of approximately 76°, 70° and 64°, each with a sharp leading edge with a bevel angle of 30°. The range of reduced frequency and reduced pitch rate varied from 0.01 to 0.08. Jarrah's[38] study was divided into three portions which investigated a low to moderate angle of attack range which was defined by angle of attack excursions from 0° to 30°, a low to high angle of attack range which was defined by angle of attack excursions from 0° to 60°, and a low to extreme angle of attack range which was defined

by angle of attack excursions from 0° to 90°. Jarrah[38] concluded that, for all sweep angles tested, unsteady effects of the flowfield and its response to a variation of reduced frequency and pitch rate were negligible in the low to moderate angle of attack range . He surmised that the flow had sufficient time to adjust itself to the changing angle of attack and, consequently, the flow could be considered quasi-steady. For the high to extreme angle of attack excursions, however, Jarrah[38] reported large hysteresis in aerodynamic loads and in the position of the vortex breakdown. The magnitude of the hysteresis was seen to increase with increasing reduced frequency and pitch rate, but was reduced with increasing sweep angle for a given reduced frequency or pitch rate. Jarrah[38] also noted that decreasing the sweep angle reduced the asymmetry observed in the flowfield fluctuations. Jarrah[38] also concluded that there was no significant qualitative difference between the sinusoidal and the ramp type motions. Jarrah noted that for a given reduced frequency or pitch rate and a set final angle of attack, an increase in the initial angle of attack increased the hysteresis effects. Similarly, for a fixed reduced frequency or pitch rate and a set initial angle of attack, an increase in the final angle of attack also increased the hysteresis effects.

In 1990, Jarrah[39] reported on a test program that studied ramp and oscillatory motion from 0° to 90° angle of attack. He used the model with the 76° sweep angle and a 30° bevel on the leading edge. Tests were conducted at a Reynolds number of 4.5 x 10^5. The delta wing was rotated about the 75% chord position at reduced frequencies ranging from $k_{pitch} = 0.01$ to $k_{pitch} = 0.08$. The results showed little hysteresis at low values of reduced frequencies, however; significant hysteresis was seen for higher values.

Jarrah[39] noted that during the upstroke, the core of the vortex reached a maximum height not exceeding the steady state value and the vortex breakdown position continued to move upstream. For the pitch-up motion, Jarrah[39] reported that the time constant associated with the burst lag was quite large in comparison with the convective time scale, τ, defined as c/U. Based on flow visualization data with K = 0.02, the time lag was estimated at 7 convective time lengths. During the downstroke motion, Jarrah[39] noted that the wing was initially stalled and that the leading edge vortices were slow to reform. Jarrah attributed the extended lag in the vortex breakdown during the pitchdown motion to the persistence of a wake-like flow that existed at the end of the upstroke motion. In both sinusoidal and ramp maneuvers, the vortex breakdown point crossed the trailing edge at higher angles of attack than the corresponding steady state. Flow visualization measurements suggested that the breakdown position during pitch-up was highly asymmetric, however; the data also showed that the variation between sinusoidal and ramp maneuvers were small.

In 1990, LeMay[25] studied the response of vortex flow and vortex breakdown location on a 70° swept delta wing with sharp leading edges that was oscillated sinusoidally about the centre chord. The effects of reduced frequency and Reynolds number were investigated. In one study, the reduced frequency was varied from k_{pitch} = 0.5 to 0.30 when the root chord Reynolds number was 2.6×10^5. In the other study, the Reynolds number was varied between 9×10^4 and 3.5×10^6 and the reduced frequency was held at $k_{pitch} = 0.20$. LeMay[25] selected two ranges of angle of attack. He varied the oscillations from 29° to 39° in order that the position of the vortex breakdown was

restricted within the bounds of the wing surface. Throughout this range of angle of attack, the vortex breakdown position varied from approximately x/c = 0.4 to x/c = 0.9. LeMay[25] also examined the angle of attack ranging from 0° to 45° to provide information through the range of angle of attack and to higher angles of attack.

At the lowest value of reduced frequency tested, LeMay[25] observed a hysteresis loop in the location of the vortex breakdown location. As reduced frequency increased, the hysteresis effect became greater at a given angle of attack. This was seen by the restriction in the movement of the vortex breakdown location. At the higher reduced frequencies, the wing would begin its pitch-up portion of the cycle before the breakdown location could reach its aftmost static location.

LeMay[25] observed that as the reduced frequency was increased, the hysteresis loops became more symmetrical about the static case. At reduced frequencies of k_{pitch} = 0.05 and k_{pitch} = 0.10, the breakdown location lagged the static case on the upstroke but was comparable to the static case on the downstroke. As the reduced frequency was increased to k_{pitch} = 0.20, the amount the breakdown location lagged increased and a similar lag developed on the downstroke. At a reduced frequency of k_{pitch} = 0.30, the hysteresis loop was symmetric about the static data and the lag in the breakdown location was about equal for the upstroke and the downstroke of the pitching cycle.

LeMay[25] also examined the phase-angle difference between the chordwise breakdown location and the model position. Two trials were conducted for the 70° swept delta wing. In the first trial, the Reynolds number was held constant at 2.6 x 10^6 and the reduced frequency was varied from k_{pitch} = 0.05 and k_{pitch} = 0.30. In the second trial, the

reduced frequency was held constant at $k_{pitch} = 0.20$ and the Reynolds number was varied between 9.0×10^4 and 3.5×10^5. Phase lag values were found by plotting the breakdown location and the model angle position against time for a cycle. The phase angle was determined graphically by determining the time difference between the relative breakdown location peaks. LeMay[25] found that as reduced frequency increased so did the phase lag. He also found that a change in Reynolds number had little effect on the phase lag over the range he investigated.

LeMay[25] also studied the dependence of Reynolds number and reduced frequency on the propagation velocity (u_x) of the breakdown location. The propagation velocity was computed by numerically differentiating the chordwise breakdown location for a cycle of motion varying the angle of attack from 29° to 39°. The normal component of the propagation velocity was considered small in comparison to the axial component and, therefore, was neglected. LeMay[25] observed that the increase in breakdown point velocity seemed more dependent on pitching frequency than Reynolds number or reduced frequency and, therefore, defined a reduced propagation velocity (μ) where $\mu = u_x / (cf)$. LeMay[25] showed that the effect of reduced frequency on the reduced propagation velocity was minimal throughout most of the pitching cycle. He reported a slight dependence on reduced frequency at the beginning of the upstroke where the angle of attack started increasing. In terms of variation of Reynolds number, there were no distinct changes apparent for $k_{pitch} = 0.20$ and the Reynolds number between 9.0×10^4 and 3.5×10^5.

LeMay[25] collected data for large amplitude motion during which he pitched the

70° delta wing from 0° to 45° at reduced frequencies of $k_{pitch} = 0.05$ and $k_{pitch} = 0.30$ with a root chord Reynolds number of 2.6×10^5. He reported a similar hysteresis and also noted that the hysteresis was greater for an increased reduced frequency. LeMay[25] compared the data from the small range of angle of attack motion to larger amplitude motion and concluded that for the same Reynolds number and reduced frequency, the hysteresis effect was more pronounced with the large amplitude motions. This is more evidence to support the premise that the motion history has a profound effect on the behaviour of the location of vortex breakdown. LeMay[25] went on to examine the phase lag relationship between the large and the small motion. He found the behaviour to be similar. For large amplitude motion at $k_{pitch} = 0.05$, the phase lag was 5° and at $k_{pitch} = 0.30$, the phase lag was 20°. For the small amplitude motion at $k_{pitch} = 0.05$, the phase lag was 5° and at $k_{pitch} = 0.30$, the phase lag was 22°.

In 1992, Thompson[23] studied the unsteady aerodynamics of 70° swept delta wings undergoing large-amplitude pitching motions. The study was comparison in nature and so the thickness to chord ratio was varied from 3.1 to 4.6. As well, the difference between a single bevelled and double bevelled leading edge was examined. For the steady case, Thompson[23] found that the effect due to thickness consisted in an upstream shift in the breakdown location with an increased thickness and the effect due to leading edge shape was a downstream shift in the breakdown location due to the addition of an upper surface bevel which effectively increased the wing's camber. Thompson[23] reports that the effect due to thickness increase was not consistent with other published data. For oscillatory motion from 0° to 60°, the results pertaining to the unsteady location of the

vortex breakdown were similar for the single bevel and the double bevel delta wing. Thompson[23] noticed that as the reduced frequency was increased, the location of the vortex breakdown moved on to the delta wing at a lower angle of attack and with a smaller propagation velocity. Thompson[23] observed that during the downstroke portion of the oscillation, the breakdown would reform near the apex, but it would remain stationary while the delta wing moved through several degrees of pitch and then the breakdown would continue to move aft. Jarrah[89] also noted that the effect of increased reduced frequency was greater during the downstroke of a sinusoidal oscillation and he attributed this to the lag in the reformation of the leading edge vortex. Thompson[23] correlated the position at which the breakdown remained steady with the maximum angular velocity of the delta wing which occurred near the mean angle of attack. Throughout the pitching oscillations, the location of the breakdown was consistently forward of the position it would otherwise have been if the delta wing was stationary. Thompson[23] analysed the vortex breakdown propagation velocity, but could not determine any relationship that was consistent with reduced frequency. He did note that the vortex breakdown propagation velocity was consistently greater during the upstroke than the downstroke part of the oscillatory motion.

In 1993, Hebbar, Sheshagiri, and Platzer[40] carried out a study focussed on the development and breakdown of the vortex over a rapidly maneuvering model X-31 aircraft. Static and dynamic tests were conducted at angles of attack from 0° to 50° using dye injection as a flow visualization technique. The flow velocity of the water tunnel was 0.25 ft/sec which corresponded to a Reynolds number of 1.02×10^4. Dynamic tests were

carried out with ramp maneuvers which pitched from 0° to 50° and also plunged from 50° to 0° at reduced pitch rates of $k_{pitch} = 0.12$ and $k_{pitch} = 0.34$. The dynamic tests showed that the location of the vortex breakdown point relative to the static case moved rearward with increasing pitch-up motion and forward with increasing pitch-down motion.

In 1993, Rediiotis, Stapountzis, and Telionis[41] investigated the nature the vortex shed from a delta wing. Five geometrically similar wings with sweep angles of 76° were tested in three test facilities which a included two separate wind tunnels and a water tunnel. Their investigation showed that vortex shedding was induced over the wing at angles of attack over 35°. In this region, the leading edge vortices remained attached to the wing all the way from the apex to the trailing edge of the wing. Above 35°, the portion of the vortex above the aft part of the wing was seen to detach from the wing surface and shed. In the range of angle of attack from 35° to 70°, the vortices on each side of the apex were shed simultaneously while, for angles of attack greater than 70°, the leading edge vortices were shed alternatively. In all cases the shedding frequency was nonlinearly dependent on angle of attack.

In 1994, Rediniotis, Klute, Hoang, Telionis[42] investigated the transient flowfield over a delta wing during pitching motions to very high angles of attack. Two delta wings each with a sweep angle of 75° were tested. One had a thickness to chord ratio of 2% with a leading edge bevel angle of 29° and the other had a thickness to chord ratio of 4.6% with a leading edge bevel of 45°. The models were mounted on a strut and pitched about their apex from 28° to 68° with a reduced pitch rate of 0.0089. Their study re-confirmed the inherent hysteresis in the flowfield as a result of the pitching motion,

however, evidence was presented stating that during the dynamic pitch-up, vortex breakdown does not creep up from downstream; but, instead it appears almost simultaneously along the entire chord of the wing and then spreads radially outward.

In 1994, Gursul and Yang[21] studied a pitching delta wing to determine the effects the pressure gradient over the wing had on the phase lag between the motion of the wing and the movement of the location of the vortex breakdown. The model tested was a 70° swept delta wing with a thickness-to-chord ratio of 5.3% and a leading edge bevel of 45°. Reynolds number was varied from 1.27×10^5 to 2.54×10^5. The model was pitched sinusoidally about the centre chord with reduced frequencies up to 0.53. Angle of attack ranges investigated were 29° to 39°, to compare with the data from LeMay[25], and 10° to 15°, for which breakdown was absent over the wing. Gursul and Yang[21] showed that, as angle of attack increased, the pressure fluctuations due to the signature of the vortex breakdown also increased since the circulation of the leading edge vortex also increased with angle of attack. It was concluded that the pressure fluctuations induced by the helical mode instability of vortex breakdown could be used to quantify the phase lag between the wing motion and the breakdown location. For both ranges of angle of attack, it was shown that the phase delay between the wing motion and the pressure field increased with increasing reduced frequency and that the phase delay was not sensitive to Reynolds number variations.

In 1995, Lin and Rockwell[43] studied the onset and development of vortex breakdown within the vortex shed from the leading edge of a delta wing pitching to high angles of attack. Lin and Rockwell[43] noted that the onset of large phase lags of the

flow pattern relative to the motion of the wing in a given consequence of not only pitching motions but also rolling motions. The objective of their work was to quantitatively describe the relaxation of the vortex following a sudden pitch-up motion to a high angle of attack. Experimentation was carried out in a water channel using a delta wing with a sweep angle of 75° and a thickness to chord ratio of 0.053 with a chord length of 0.79 ft. The Reynolds number of the flow was 9.2×10^3 and the wing was pitched from an initial angle of attack of 25° to a final angle of attack of 50° at a reduced pitch rate of 0.30. Lin and Rockwell[43] analysed the location of the vortex breakdown as it varied with time. Immediately following the cessation of the pitching maneuvre and at low values of dimensionless time, t^*, the vortex breakdown moved upstream toward the apex of the wing at a constant propagation speed, m = -0.72 (where $m = c_v / U$). After this period of constant speed, the vortex breakdown location accelerated abruptly to a propagation speed, m = -1.12 and then slowed to a constant speed of m = -0.04. Lin and Rockwell[43] concluded that this transformation from a relatively fast to a slow speed of the upstream movement of the vortex breakdown location was related to an abrupt transformation in the vortex breakdown structure and has consequences in terms of phase lag during a maneuvre. Lin and Rockwell[43] speculated that if a means of control could be found to hasten the abrupt transformation of the vortex structure, the time delay could be maximized and an overshoot relative to static lift characteristics could be realized. Lin and Rockwell[43] also showed that immediately following the sudden pitch-up of the wing, the location of the vortex breakdown also moved abruptly toward the surface of the wing.

Delta Wing Aerodynamics Involving Unsteady Roll Motions

Similar to studies involving unsteady pitching motions, investigations involving unsteady roll motions have typically focussed on oscillatory and transient (or impulse) motion. In addition, however, free-to-roll experiments have been conducted to gain a better insight into problems like wing rock. Hanff and Jenkins[44], for example, conducted a test program which focussed on free-to-roll experiments where the model was rotated to an initial angle of attack and was allowed to adjust itself freely to the freestream conditions. The dynamics involved in the rolling delta wing change the behaviour of the flow characteristics dramatically. Ericsson and Hanff[45] reported on the large time delay in the movement of the vortex breakdown location as the delta wing was oscillated which is evidence of an inherent hysteretic behaviour. Ericsson and Hanff[45] suggested that a more extensive analysis with an increased data base is needed to determine how the effect of past time history depends on change in roll angle and reduced frequency.

Ericsson and Hanff[45], however, reported that applying a time-lag effect to the static results was not sufficient for predicting flow characteristics under dynamic conditions. The characteristics of the flow under dynamic roll conditions, were seen to be similar in nature to those experienced during unsteady pitching conditions due to the hysteresis effect. In the case of the pitching motion, a change in the effective geometry of the wing occurs through a pitch rate induced accelerated flow. A similar roll rate induced change in effective geometry was reported to be present for values of lift and associated

roll moment for a 65° delta wing under dynamic roll conditions. The effect of longitudinal camber on the location of vortex breakdown has been investigated by Lambourne and Bryer[11]. For the same angle of attack, a delta wing with positive camber caused the location of the vortex breakdown to be downstream of the trailing edge, whereas the delta wing with the negative camber cause the breakdown to occur close to the apex. It was then argued that the roll rate induced camber effect would be similar to the pitch rate induced camber effect. Huang and Hanff[18] performed static tests with models deformed to produce a roll rate induced camber and the results were consistent. The half of the wing which was twisted up experienced a delay in vortex breakdown as compared to the half of the wing which was twisted down. This compared well with a flat delta wing undergoing a positive roll rate where the roll rate induced camber caused a delay in the vortex breakdown on the downstroking half of the wing but promoted it on the upstroking half of the wing. This relationship is illustrated in Figure 2.14.

To assist in the prediction of normal forces on rolling delta wings at high incidence angles, Huang and Hanff[18] developed an expression for predicting the location of the leading edge vortex breakdown based on empirical results. The predicted normal force coefficients calculated by Huang and Hanff[18] compared reasonably well with experimental data which gave credibility to the accuracy of the method used to predict the location of the vortex breakdown. An example of the data presented by Huang and Hanff[18] is provided in Figure 2.15.

In 1996, Ericsson[47] published a report that described the difficulties associated with predicting the behaviour and associated effects of vortex breakdown over a rolling

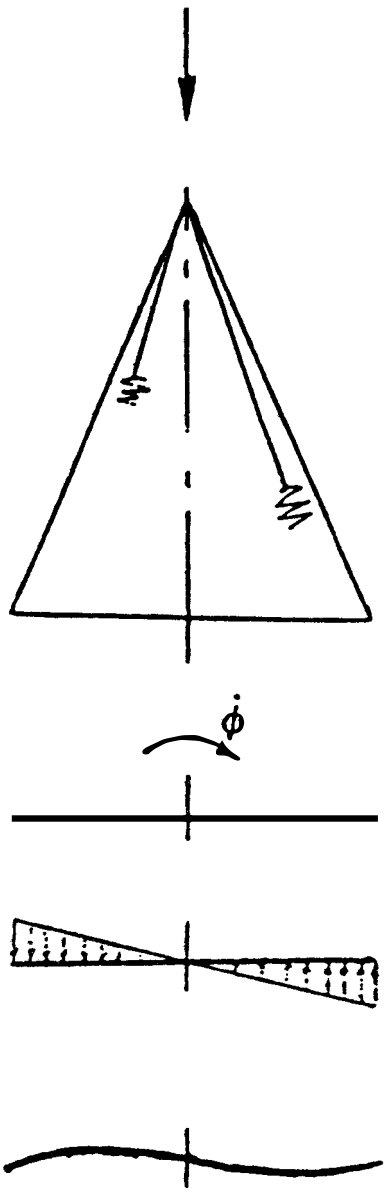

Figure 2.14. Roll Rate Induced Camber. [45]

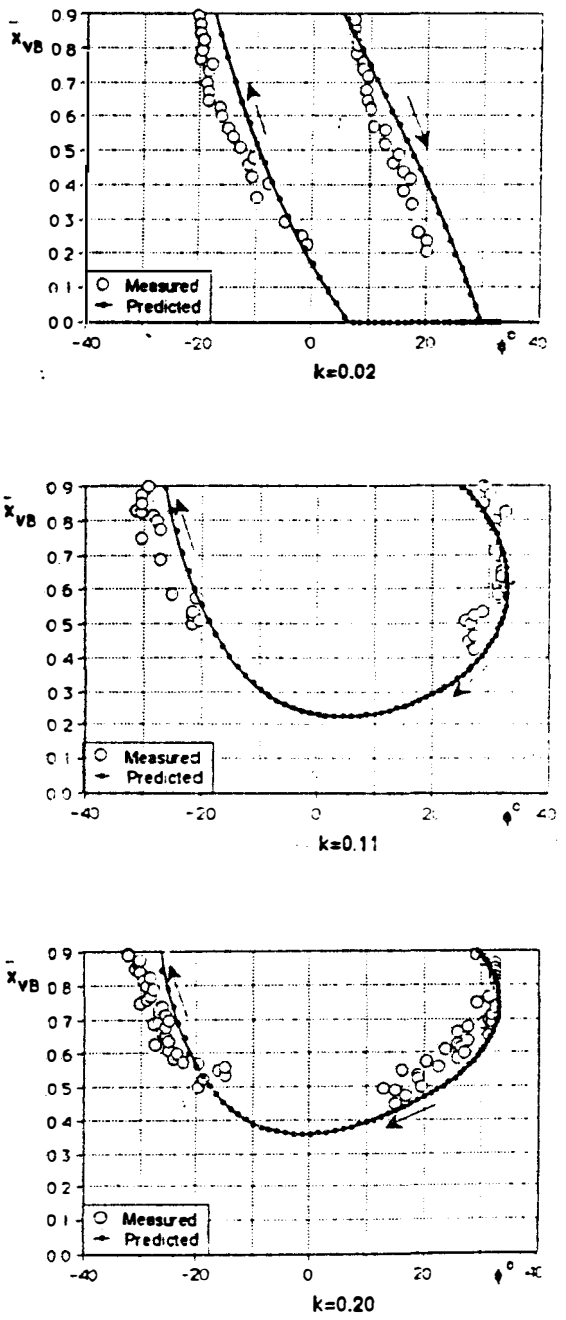

Figure 2.15. Breakdown Location Under Roll Oscillation Conditions (Right Wing). [18]

delta wing. He discussed two attempts that have been made and the successes of each. The first attempt, which has already been discussed in the work, was carried out by Huang and Hanff[18] who used an analytical method. The second was by Chaderjian[48] who used a numerical method. Ericsson[47] concluded that neither method appeared to have provided an adequate simulation of the experimental results and suggested that the difficulty was presented by the fact that the large effect of roll rate induced camber was highly nonlinear due to the existence of critical states and that the behaviour of the flow was associated with significant time history effects. The existence of critical states, which were related to effective leading edge sweep angle and effective angle of attack, was shown by a dramatic and nonlinear change in the relationship between location of vortex breakdown and roll angle for steady and unsteady conditions. Ericsson[47] argued that in the absence of accounting for these critical states, empirical prediction equations could not accurately predict the location of vortex breakdown. Ericsson[47] also concluded that, although the computation method developed by Chaderjian[48] did show an effect of the critical states, the agreement with experimental data needs to be better before the prediction of dynamic characteristics can be possible.

Past Delta Wing Research Involving Unsteady Roll Motion

In 1990, Hanff and Jenkins[44] reported on their investigation of a 65° delta and a 80°/65° double delta wing undergoing rolling motions. Static and dynamic tests were conducted up to an angle of attack of 40° and concentrated on force measurements. A

large base of data was collected, but the results presented were for the case of 30° angle of attack. In the dynamic tests, the model was oscillated sinusoidally in roll about mean roll angles of 0°, 14°, 28°, and 42° and with amplitudes varying from ±5° to ±40°. The maximum reduced frequency tested was $k_{roll} = 0.2$ and the maximum reduced roll rate was 0.15. The test program focussed on free-to-roll experiments where the model was rotated to an initial angle of attack and allowed to adjust itself freely to the freestream conditions. From their data, Hanff and Jenkins[44] determined that there were multiple trim angles, termed roll attractors, at which the model would settle once released and that the trim angle depended on the angular rate achieved during the motion.

In 1991, Hanff and Ericsson[49] continued their work on multiple roll attractors with the principle objectives to obtain a better insight of the vortex dynamics associated with large amplitude and high rate roll oscillations. The 65° delta wing model was examined under static and dynamic conditions. In addition, further free-to-roll tests were analysed. As previously discussed, for static changes in roll angle, the effective sweep of the leeward half of the wing (the half that rolls up) increases and causes the location of the vortex breakdown to move aft from the apex. Similarly, the effective sweep of the windward half of the wing (the half that rolls down) decreases and causes the location of the vortex breakdown to move toward the apex. This asymmetric movement of the location of the two vortex breakdown locations causes a stabilizing rolling moment; however, the increase in sweep of the leeward half of the wing causes an increase in vortex induced lift and the decrease in sweep of the windward half of the wing causes a decrease in vortex induce lift which has a destabilizing result on the rolling moment. The

net balance between these two effects determines whether there is an overall stabilizing or destabilizing rolling moment. Hanff and Ericsson[49] have shown that if $\phi < 3.5°$ for a sweep angle of 65° and a pitch angle of 30°, the statically destabilizing effect, which results from relatively small changes in the vortex breakdown location (< 10%), is insignificant compared to the increase in roll stability which is produced by the increase in vortex lift generated by the leading edge vortices upstream of the breakdown location. As the roll angle is increased further but not more than 7°, Hanff and Ericsson[49] have noted that a large shift in the position of vortex breakdown occurs which significantly effects the vortex induced lift and results in an overall destabilizing effect on the roll stability. With the large asymmetry in breakdown location, the dominant effect becomes the roll moment produced by the leeward half of the wing. Although the leeward half of the wing produces less vortex lift than before because the vortex breakdown location has moved aft, it now produces more than the windward half of the wing since the windward half of the wing has less of a leading edge vortex upstream of the breakdown location because the breakdown location has moved forward by so much. This analysis supports the off-zero trim angles that Hanff and Ericsson[49] have observed in experimentation.

Hanff and Ericsson[49] also reported on the large time delay in the movement of the vortex breakdown location as the delta wing was oscillated. This behaviour was attributed to flow inertia effects which limited the propagation speed of the breakdown location to values lower than the freestream velocity. Hanff and Ericsson[49] suggested that the rolling moments as a function of roll angle would be affected considerably under dynamic conditions involving large angular rates such as those encountered in the free-to-

roll tests.

In 1992, Huang and Hanff[17] presented their work on a method for the prediction of leading edge vortex breakdown on a 65° delta wing at high incidence. Static and dynamic tests were conducted at a chord Reynolds number of 2.4×10^6 and the model inclined at a pitch angle of 30°. The test rig was designed to oscillate at an amplitude of 40° of roll and a reduced frequency of 0.2. The static prediction model used has been discussed earlier. Huang and Hanff[17] showed very good correlation between experimental data and an expression for the prediction of the vortex breakdown location based on a steady value modified by a quasi-steady value and unsteady perturbations.

In 1993, Huang and Hanff[18] continued their research on rolling delta wings to include the prediction of normal forces at high incidence angles which included a prediction technique to estimate breakdown locations. The predicted normal force coefficients compared reasonably well with experimental data which gives good credibility to the accuracy of the method used to predict the location of the vortex breakdown. Of interest is their observation of the variation of the vortex breakdown location as the delta wing was dynamically oscillated. Huang and Hanff[18] report that in the presence of small offset roll angles and high amplitudes, both vortex breakdown points moved between the apex and past the trailing edge. At higher frequencies and small amplitudes, the vortex breakdown points did not progress past the confines of the wing. For large offset angles and small amplitudes, the vortex on the windward half of the wing remained burst at the apex while the leeward one remained in the confines of the wing. In addition, Huang and Hanff[18] reported that there were cases where the vortex on the windward half of the

wing broke down at the apex and the other vortex moved onto the leeward half of the wing during a portion of the roll oscillation cycle.

In 1994, Ericsson and Hanff[45] reported on experiments conducted involving the high angle of attack roll dynamics of a sharp leading edged 65° swept delta wing. Their objective, in part, was to obtain a better insight associated with large amplitude and high rate roll oscillations. Their investigation focussed on roll oscillations around a mean roll angle of 0° with the delta wing pitched at an angle of 30°. The results showed that both static and dynamic roll characteristics were dominated by the effect of vortex breakdown. Ericsson and Hanff[45] showed that the dynamic effect of vortex breakdown is largely controlled by the roll rate induced conical camber. Static tests were performed with models deformed to produce a roll-rate induced camber and the results showed that the half of the wing which was twisted up experienced a delay in vortex breakdown as compared to the half of the wing which was twisted down. This compared well with a flat delta wing undergoing a positive roll rate where the roll rate induced camber caused a delay in the vortex breakdown on the downstroking half of the wing and promoted it on the upstroking half of the wing.

In 1995, Ericsson[50] studied the effects of roll rate induced camber and of time lag on a 65° swept delta wing with a sharp leading edge. He analysed the effect of the roll rate induced camber on the leeward and the windward side leading edge vortices for the static (undeformed) and dynamic (instantaneously deformed) delta wings and noted that as the roll rate was decreased, the roll rate induced camber effect was reduced and the deviation of the static to the dynamic data was reduced as well. In addition, Ericsson[50]

showed the effects of time lag through the displacement of the dynamic curves as compared to the static curve is an indication of the time lag effect.

Focus of Current Research

The focus of the current research was the water tunnel testing of a model delta wing statically and undergoing unsteady motions. The model was sized for the water tunnel to minimize the effects of blockage and optimize the quality of the flow visualization. The model geometry was designed to ensure maximum comparison of available data. An apparatus was devised so that the delta wing could be maneuvered in both pitch and roll, separately and simultaneously.

In the analysis of the delta wing undergoing steady and unsteady pitching maneuvers, data was collected and compared with existing data to ensure validity of test results and the integrity of the experimental setup and procedure. Further analysis was carried out for steady and unsteady roll conditions which demonstrated the symmetry of the flow phenomenon. Although there exists roll data for other delta wing designs, this research provided an additional data base of information for a 70° swept delta wing. In addition, most delta wing experiments undergoing unsteady roll motion have concentrated on free-to-roll tests and not the force maneuvers that were studied in this research.

Experimentation was also carried out with the delta wing maneuvering in pitch and roll. This is one of the first studies that examined the steady and unsteady vortex flow over a delta wing that is maneuvering in pitch and roll simultaneously. The data collected

were analysed with an emphasis placed on the position of the vortex breakdown as it related to the motion of the delta wing as well as an examination of lag time characteristics and vortex breakdown propagation velocities. A comparison of the three types of motion enabled an estimate of the pitch and roll coupling effects of a delta wing undergoing unsteady pitching motion that is simultaneously maneuvering in roll.

CHAPTER III

EQUIPMENT

RMC Water Tunnel

Experimentation was carried out using the water tunnel located at the Royal Military College (RMC) of Canada, Kingston, Ontario, Canada. A schematic diagram of the RMC water tunnel is illustrated in Figure 3.1. The water tunnel is a closed, non-pressurized system constructed from aluminum and can hold up to 150 imperial gallons. The tunnel test section is made from clear plexiglass on the sides and the bottom but is open on the top. It measures 8 inches high by 8 inches wide by 24 inches long. The flow velocity can be varied from 0 ft/sec to a maximum tunnel velocity of 2.5 ft/sec. The qualities of the flow in the water tunnel were investigated by Randall and Waugh[51] who determine that the average turbulence in the flow was less than 2%. The decision to use the water tunnel for this experimental research was based on availability of the facility and the fact that the focus of this research centred on flow visualization. In addition, Erickson[35] commented that, because vortex flow over a thin flat plate, sharp leading edge delta wing is insensitive to Reynolds number, water tunnels make good facilities in which to visualize the vortex flow phenomenon. As well, water tunnel flow visualization can be carried out in much detail because of the low testing speeds.

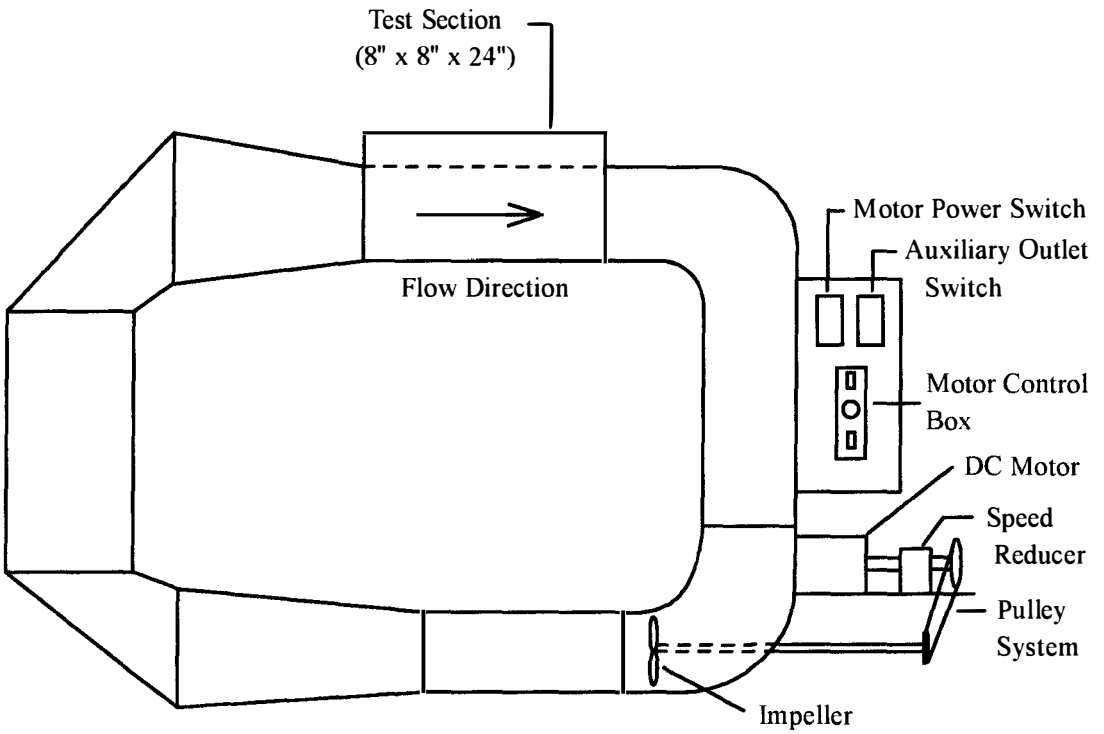

Figure 3.1. Water Tunnel at The Royal Military College of Canada

Model Delta Wing Design

The delta wing model used in this study was designed with the specific requirement to reproduce vortex breakdown; however, to ensure maximum comparison of available data for experiment validation, the design specifications were based on one of the models used in the studies of Thompson[23]. A schematic diagram of the delta wing model is provided in Figure 3.2. Constructed from aluminum, the model was designed as a flat plate with a sweep angle of 70° and an aspect ratio of 1.46. The root chord length was 4.8125 inches and the base measured 3.5 inches. The thickens of the model was 0.22 inches for a thickness-to-chord ratio of 4.6%. Dimensions of the delta wing model were accurate to within 1/32 inches. To ensure a sharp leading edge, the windward side of the model was bevelled at a 45° angle. Two dye injection ports were positioned symmetrically about the apex and as close to the apex as possible. A small channel was cut along the centerline of the model to house the plastic tubing that carried the dye from a dye reservoir to the dye ports. Once the tubing was in place, the channel was filled and covered over. The surface was then smoothed and painted.

The size of the delta wing model was restricted to the constraints of the water tunnel to keep the amount of geometric blockage to a minimum. As a result, the model size was a lot smaller than that used in Thompson[23]. However, Thompson[23] conducted a comparison study of the unsteady location of vortex breakdown using three different model sizes. The Reynolds number was 1.5×10^4 and the reduced frequency was $k_{pitch} = 0.03$ corresponding to dimensional pitch frequencies of 0.314, 0.707, and 1.26 Hz

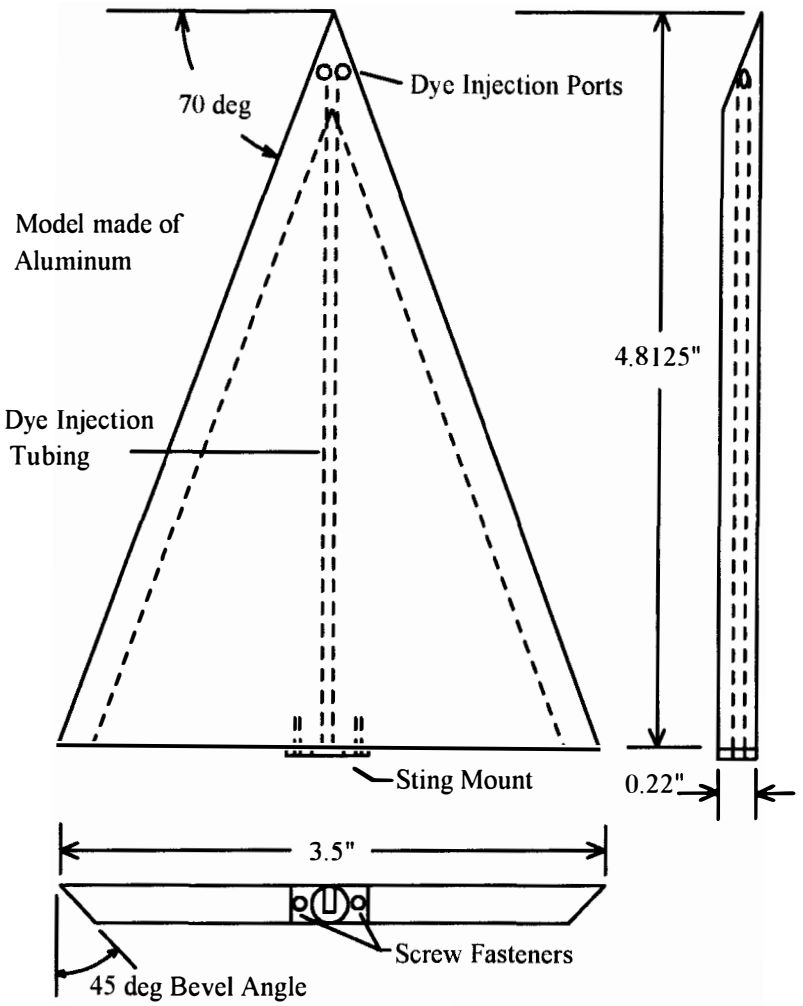

Figure 3.2. Delta Wing Model

for a full scale, two-thirds scale and one-half scale, respectively. The data was collected while oscillating the wing from 0° to 60° in sinusoidal motion. The data shown in Figure 3.3 shows that the unsteady characteristics of the breakdown location are independent of model size and therefore insensitive to Reynolds number. Thompson[23] also showed similar behaviour for a reduced frequency of $k_{pitch} = 0.09$.

Maneuvering Apparatus

An apparatus was designed so that the delta wing could maneuver in pitch and roll, separately and simultaneously. The design concept was similar to the one used in experiments carried out by Hebber and Platzer[40] specifically because their experiments were also conducted using a water tunnel. The maneuvering apparatus was designed within the constraints of the size of the RMC water tunnel test section and with the goal of inducing the least amount of interference into the flow. The maneuvering apparatus was also required to reproduce test conditions of other studies so that comparison could be made with available data. The maneuvering apparatus was designed to rotate the delta wing model in pitch about the centre chord location and in roll along the root chord and about the model's geometric centre. LeMay[25], in his study of a pitching delta wing, conducted tests to examine the influence the change in pitching axis had on the location of vortex breakdown. Tests were performed with the pitching axis located at the one-quarter, one-half and three-quarters chord locations with a reduced frequency of $k = 0.30$ and a root chord Reynolds number of 2.6×10^5. LeMay[25] observed that as the location

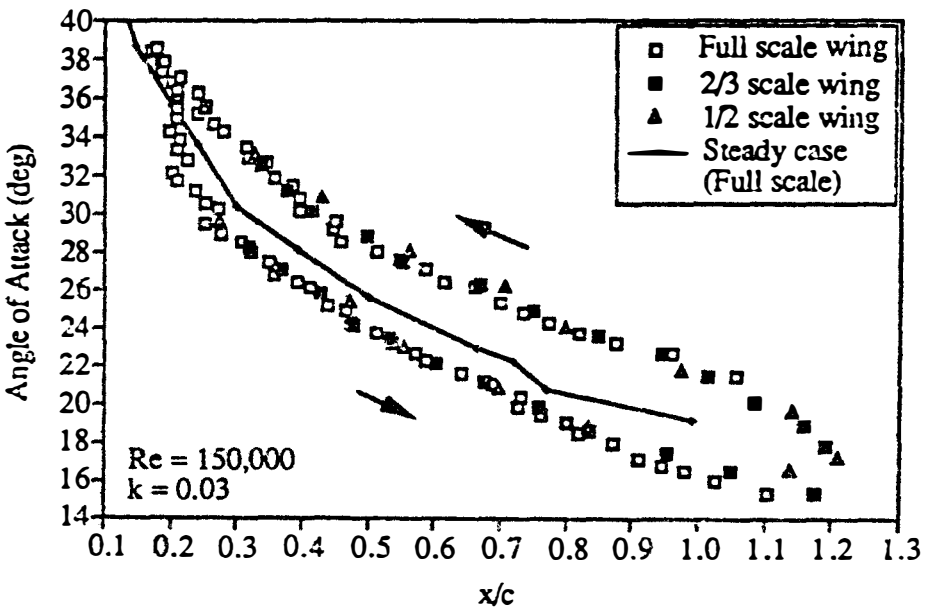

Figure 3.3. Unsteady Location of Vortex Breakdown for Full Scale and Sub-scale Wings. Thompson[23]

of the pitching axis was moved toward the trailing edge, the average location of the vortex breakdown also moved aft. LeMay's[25] study demonstrated that it is critical to know the location of the pitching axis in order to compare data.

A side view of the delta wing model connected to the maneuvering apparatus is shown in Figure 3.4. As shown is Figure 3.4, the delta wing model was held upside down in the water tunnel. The model was situated so that the top surface of the delta wing faced the bottom of the test section and the direction of the flow caused the formation of the vortices on the top surface of the model. The model was held in place by a cylindrical sting of radius 0.22 inches. The sting was connected to the Primary C-Beam. The Primary C-Beam was a constant radius resting on a set of two rollers so that the model could be rotated in pitch about its geometric centre. In addition, the design of the maneuvering apparatus ensured that the model was situated in the centre the test section. The Primary C-Beam was driven by the Primary Drive Cam which was connected to a Drive Rod. The Drive Rod was driven by a drive mechanism which provided a sinusoidal input motion.

Figure 3.5 shows a three dimensional schematic view of the delta wing and the maneuvering apparatus as they were situated in the water tunnel. As shown in Figure 3.5, a Secondary C-Beam of exact design specifications was off-set from the Primary C-Beam by a distance of 3.49 inches to allow for the variations in roll when the two C-Beams were connected by a connecting rod. A Secondary Drive Cam was used to drive the Secondary C-Beam.

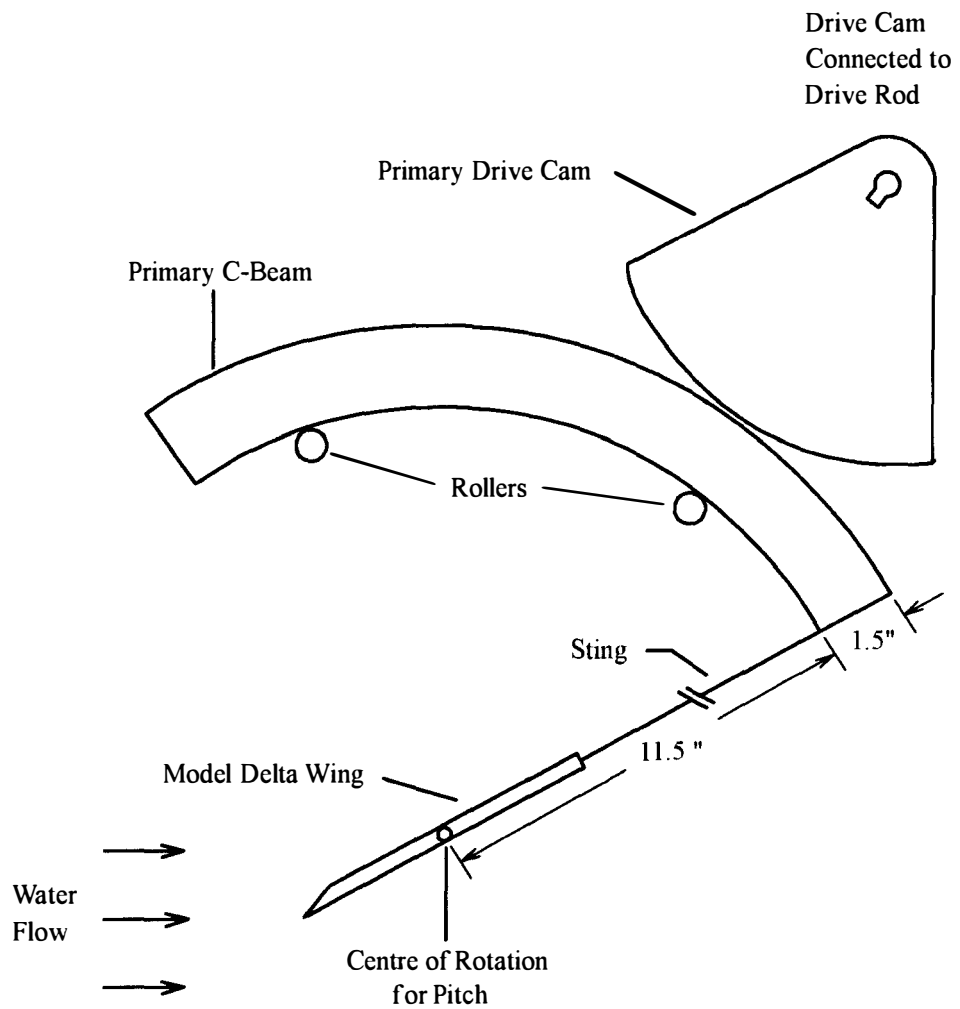

Figure 3.4. Side View of Delta Wing Situated in the Test Section

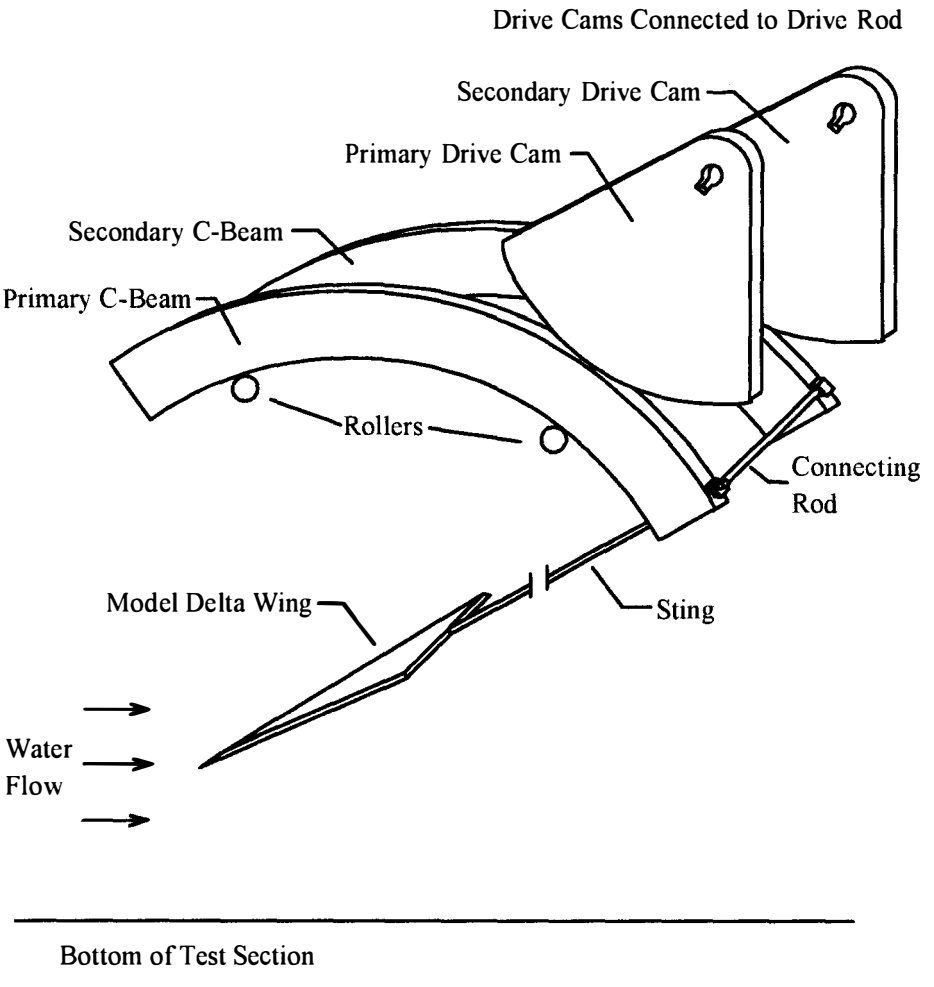

Figure 3.5. Delta Wing and Maneuvering Apparatus in the Test Section of the Water Tunnel

A Schematic diagram of the Drive Mechanism used to provide motion to the model is shown in Figure 3.6. As shown in Figure 3.6, the Drive Rod which connected to the Primary and Secondary Drive Cams was connected by a series of linking rods to a Drive Wheel which provided a continual sinusoidal motion. The Drive Wheel was attached to a gear box which was connected to a variable speed DC motor. The DC motor was a Motomatic®Motor Generator, Model No. E6BOMC, manufactured by the Electro-Craft Corporation. The benefit of using the gear box was that a higher motor speed could be used which resulted overall in a smooth operation of the Drive Mechanism. The speed of the motor was controlled by a Servodyne Controller, Catalogue No. 4445-30, which was manufactured by Cole-Parmer. The motor controller enabled the variation in the speed of the motor. The limitations of the Drive Mechanism to provide smooth motion at the lower reduced frequencies defined the lower limits of reduced frequency used in the study.

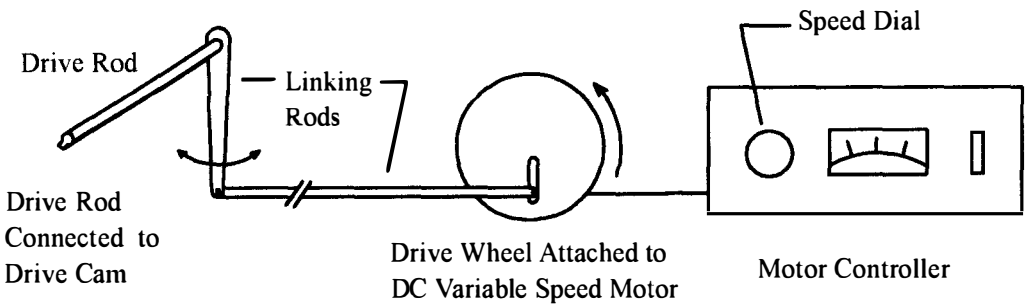

Figure 3.6. Drive Mechanism

The Primary and secondary Drive Cams connected to the same Drive Rod of the drive Mechanism; however, the two Drive Cams were never connected or driven simultaneously. Referring to Figure 3.5, the following is an explanation of the various motions provided by the maneuvering apparatus. For variations in pure pitch, the Connecting Rod and the Secondary Cam were disconnected. The Primary C-Beam was driven alone by the Drive Mechanism through the Primary Drive Cam and the model was rotated in pitch about the centre chord location. For variations in pure roll, the Primary Drive Cam was disconnected and the Primary C-Beam was fixed in place at a desired angle of attack. With the Connecting Rod connected, the Secondary C-Beam was driven alone by the Driven Mechanism through the Secondary Drive Cam and the model was rotated in roll along the root chord about the model's geometric centre. For variations in pitch and roll simultaneously, the Secondary Drive Cam was disconnected and the Secondary C-Beam was fixed in place. With the Connecting Rod in place, the Primary C-Beam was driven alone by the Drive Mechanism through the Primary Drive Cam. The model was simultaneously rotated in pitch about the centre chord location and in roll along the chord line about the model's geometric centre. It should be noted that because the different C-Beams were used for roll and roll while pitching, these two movements were 180° out of phase with each other. The tunnel speed was kept constant and the pitch frequency provided by the drive mechanism was varied to keep the similarity of reduced frequencies consistent with published data.

Flow Visualization

There are an increasingly large number of fluid problems that can be solved analytically; however, even simple fluid flow problems can be inherently complex. The need for quality experimental results therefore is paramount to furthering understanding. In terms of studying the vortex breakdown phenomenon, the nature of the vortex flow is too sensitive for direct probing. Therefore, the ideal method for gathering information is the use of a non-intrusive technique. The importance of visualizing a flow field cannot be overstated. Flow visualization techniques generally offer a useful tool to gain an overall appreciation of a flow field before the investigator embarks on detailed quantitative measurements. In certain applications, such as this research, flow visualization and data analysis techniques have become quite sophisticated such that quantitative measurements can be made from the flow phenomenon being visualized. Furthermore, in this day of CFD where accurate solutions can be generated, flow visualization becomes an essential part of verifying computational test results.

There are a vast number of techniques available for studying fluid flow. The concept of unsteady aerodynamics makes it even more difficult when analysing a given flow with classical methods. For steady flow, a streamline, a streakline and a pathline have all the same appearance, but for unsteady flow, the three are distinctly different. A streamline is a curve everywhere tangent to the instantaneous velocity vectors (or parallel to the direction) of the flow. A streakline is the locus of all fluid particles that have passed through a prescribed fixed point during a specified period of time. A pathline is the curve

traversed by a particular fluid particle during a specified interval of time. Typically, a continuous tracer introduced into the flow field at a point visualizes streaklines, hence, at any instant the visualization provides the time history of the tracer but not the local event.

Another difficulty associated with unsteady flows is the additional time scale imposed by the unsteadiness of the motion. In experimental studies, accurate simulation of true flow field conditions depends on the correlation of dimensionless physical parameters. These parameters must express the geometric, kinematic and dynamic similarities of the laboratory modelling with the actual flow field. It is usually not difficult to satisfy geometric and kinematic similarities by scaling up or down dimensions and velocities. As well, the dynamic similarity is obtained by satisfying the appropriate ratio of forces such as keeping Reynolds Number constant or providing the same Mach Number. For the unsteady flow, there is an additional requirement to satisfy similar time scales which in some flows can be the dominating part of the flow. In terms of an oscillating delta wing, the results of different studies can be compared by ensuring a common reduced frequency. Fortunately, many flow visualization techniques that were developed for observing steady flows can be easily adopted to unsteady flow.

There are a number of flow visualization techniques available for studying high angle of attack separated vortical flows and which are readily adaptable to studying unsteady aerodynamics in a water tunnel. The possibility of using Particle Imagery Velocimetry (PIV) was examined and it was all too apparent that PIV was the ideal method to use for water tunnel experiments. Unfortunately, it quickly became apparent that the cost of the equipment required to be purchased was well beyond what was

allocated. Therefore, the method chosen for visualizing the flow in this study was the classical dye injection technique because it was simple to employ and cost effective.

The type of dye used was 1% Ferrous Phenanthrolien. During experimentation, dye was introduced into the flow field from an external source through small dye ports situated asymmetrically and close to the apex of the model as shown in Figure 3.2 Care was taken to introduce the dye into the flow at a rate that did not adversely affect the fluid flow being observed. A dye reservoir that fed the dye injection tubes with dye was lowered and raised to provide the required amount of dye into the flow. A schematic illustration of the dye being introduced into the flow field as the model is viewed from the top and the bottom is provided in Figure 3.7.

Video Equipment

To record the experimentation, the data was recorded on video with SuperVHS format using a Panasonic SuperVHS video camera, model AG-450. A tripod was set up next to the water tunnel at an appropriate distance away and the camera was positioned perpendicular to the flow direction. When experiments were carried out with pure variations in pitch, the camera was focussed on the centre of the tunnel and a side view of the delta wing was obtained. For experiments involving any variations in roll, the camera was focussed on the image in a mirror situated beneath the tunnel and set at an angle of 45°. Since the bottom of the water tunnel was clear plexi-glass, this camera view provided a clear view of the top surface of the model.

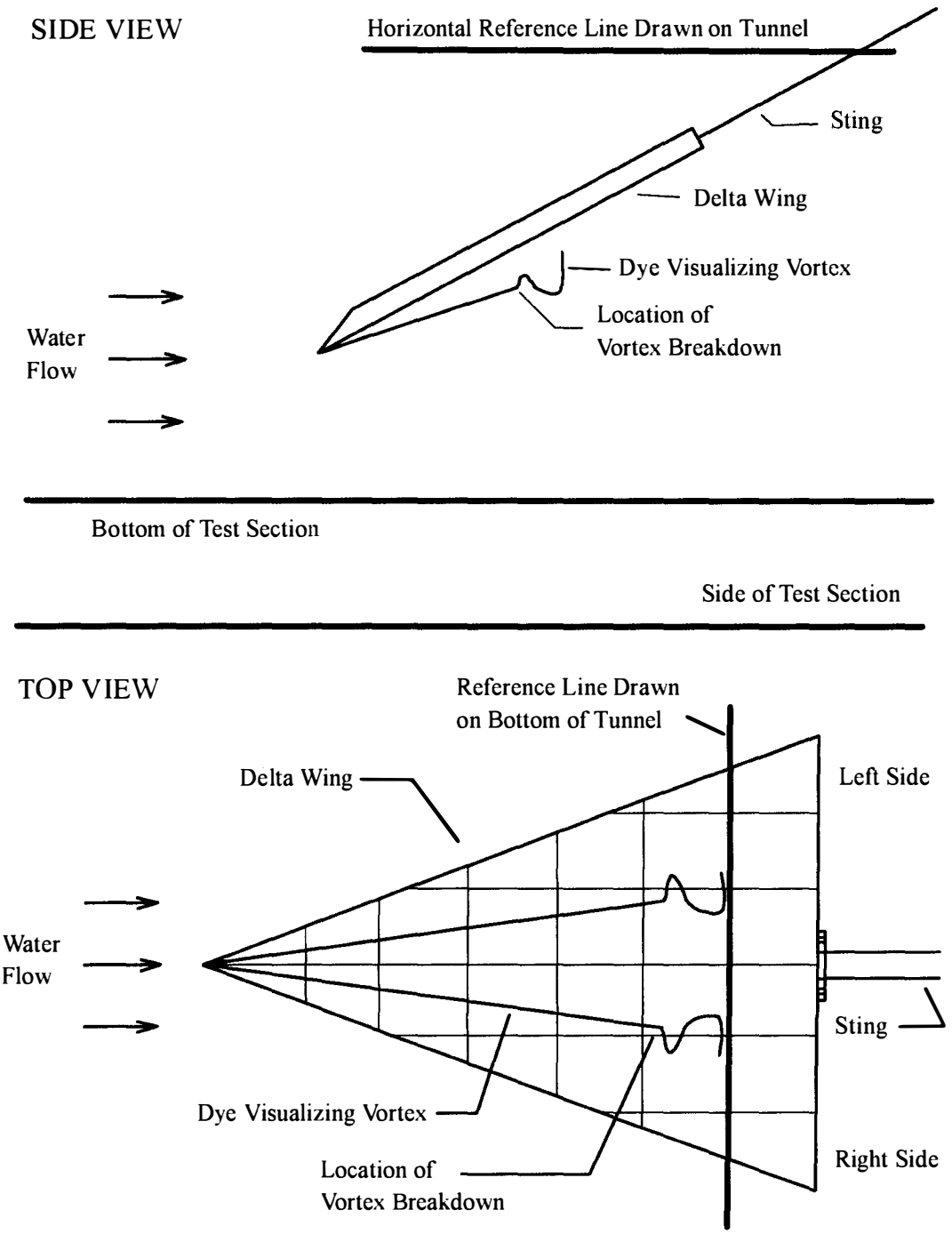

Note: Delta Wing View is a Mirror Image Through Bottom Of Test Section

Figure 3.7. Schematic Illustration of Top and Bottom View of Delta Wing

CHAPTER IV

EXPERIMENTAL METHOD AND PROCEDURE

Data Acquisition

To analyse the vortex breakdown phenomenon and make quantitative measurements, the video data was transferred to a personal computer using a VCR in the SuperVHS mode connected to a Video Blaster™ card installed in the computer. A software program called Adobe Premiere™ LE was used in conjunction with the video card to digitally capture a series of video frames. Because of the hardware constraints of the computer and the limitations of the software program, the data was captured at a resolution of 320 pixels by 240 pixels. The zoom capability of the analysis program provided the necessary detail to allow for accurate measurements. The amount of video imaging that could be digitized was dependant on the size of the hard drive in the computer. Some of the longer run times at the lower reduced frequencies took up as much as 130 Mega Bytes of hard disk space.

The video segments were recorded at a rate of 30 frames per second. The software program, Adobe Premiere, allowed the video segments to be viewed frame by frame. In addition, each frame could be exported as an individual bitmap file. The bitmap files were imported into an analysis software called Sigma Scan/Image™ where each frame was analysed individually and quantitative measurements were made.

Water Tunnel Calibration

The velocity of the flow in the water tunnel could be varied from 0-2.5 ft/sec. An early attempt was made to establish a calibration curve for the water tunnel so that a known relationship between the tunnel dial setting and the tunnel velocity could be used. Two experimental techniques were employed and the procedures were repeated many times and over a number of months as a check on data repeatability. It was determined that constant updating of the calibration curve was necessary to keep the calibration curve current. Therefore, for each experiment conducted, the flow velocity in the tunnel was determined by means of a dye injection technique. With the model in the tunnel, the dye was introduced into the flow field at a specific height just upstream of the test section and allowed to travel through the test section. The injector used was similar in shape to a Pitot tube that was oriented so that the dye was introduced into the oncoming flow. Once entrained by the flow, the dye was carried downstream through the test section. Vertical lines were painted on the side of the test section that were precisely 6 inches apart. The dye, as it travelled trough the test section and across the two lines, was captured on SuperVHS video tape. Data reduction was carried out once the video was digitized. Analysing the flow frame by frame gave an accurate assessment of the time taken for the dye to travel the measured distance. Since the flow velocity was kept quite slow, the time for the dye to travel could be estimated to within ±1 frame. For a flow velocity of 0.469 ft/sec, this represented an error of 3.1%. Ten samples of dye were analysed each time and the flow velocity was calculated as an average of the data. The maximum uncertainty,

calculated as a percentage of the maximum deviation divided by the averaged value, was less than 2%. This was within the error estimated. To ensure that the flow velocity had remained constant throughout testing, the velocity of the flow was always calculated prior to and immediately after each test run. When the flow velocity calculated before and after each test run compared extremely well, the invariance of the flow velocity during testing was confirmed. If the flow velocity before and after testing did not correspond, the test results were rejected and the test points were repeated.

Pitch Experiments (With Zero Roll)

Figure 4.1 is a digitized image and the associated schematic diagram of the side view of the delta wing as it was situated in the water tunnel. A horizontal reference line was drawn on the side of the water tunnel parallel to the flow direction to enable measurement of angle of attack. With the use of Sigma Scan and its zoom feature, quantitative measurements of the vortex breakdown location and the angle of attack were carried out for each bitmap file analysed. To do this, the measurement feature of the program was used to place a point at the location of vortex breakdown as it is illustrated in the schematic diagram of Figure 4.1. Another point was then placed at the apex of the delta wing and still another at the base of the delta wing. Based on the pixel location of the points that were placed, the distance, d, and the chord length, c, were calculated in terms of pixels. The vortex angle , θ, was similarly calculated. A similar approach was used to find the angle of attack, α. Because the resulting information required was a ratio,

there was no need to calibrate each bitmap file to a specific distance. The following equation was used to find the non-dimensionalized vortex breakdown position:

$$\frac{x}{c} = \frac{d\cos\theta}{c} \tag{13}$$

Experiments Involving Roll

When experimentation involved any non-zero roll angle, the view from the bottom of the test section was used. This approach provided better visualization of the pair of vortices shed from the leading edge. As well, it became essential for conditions where the delta wing was rotated through large roll angles since, when the delta wing was rotated through large roll angles and the model was viewed from the side, part of the delta wing model would physically block out one of the vortices. Regardless of the camera view used, it was difficult to measure directly the steady state roll angle. The analysis provided in Annex A shows how the roll angle was determine. For the test conditions analysed, the roll angle was varied from -18° to 18°.

Figure 4.2 provides a schematic and digitized view of the top of the delta wing as viewed through the bottom of the tunnel. Because the location of the vortex core was located a distance away from the surface of the model and the model was rotated at an angle away from the viewing plane, an analysis of the projected distances was conducted. This analysis is included as Annex B to this report.

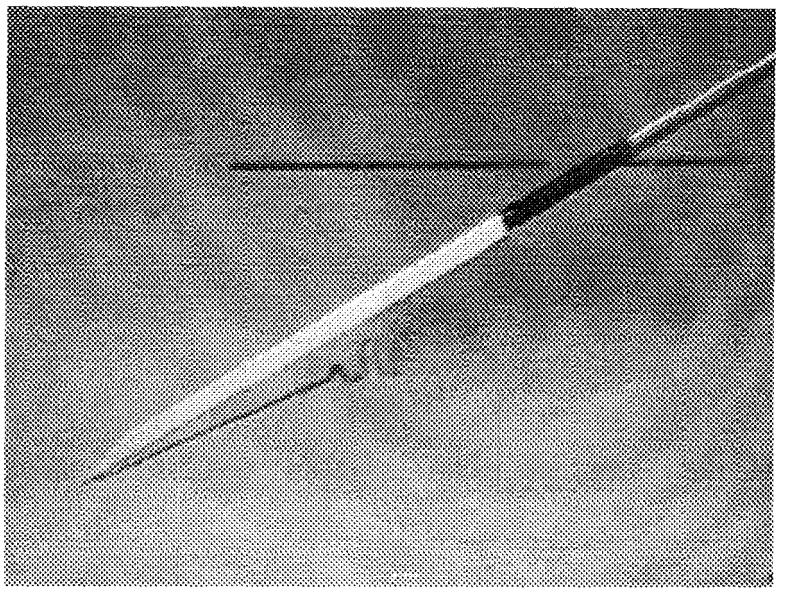

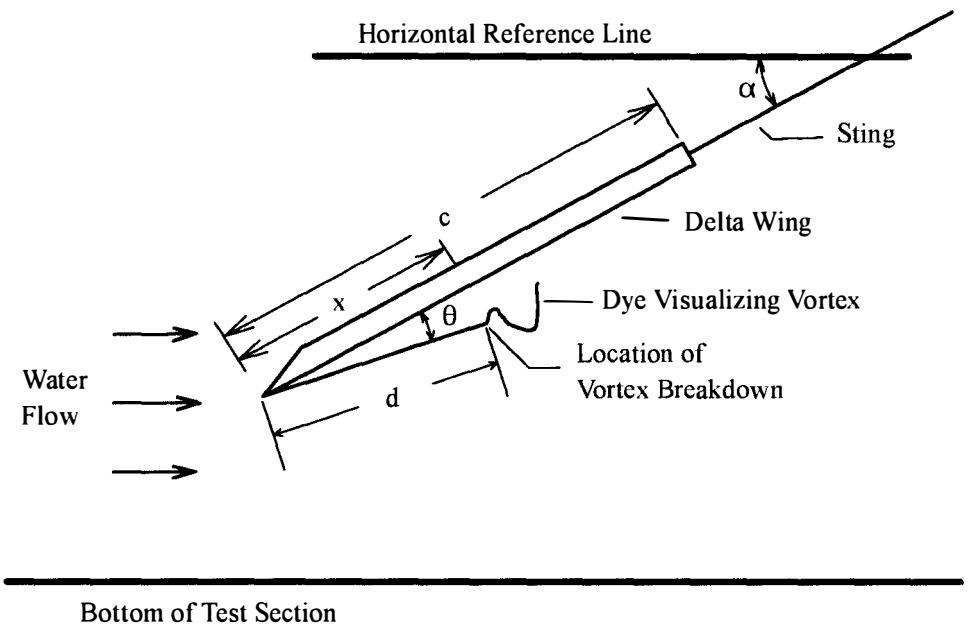

Figure 4.1. Schematic and Digitized Side View of the Delta Wing in the Water Tunnel

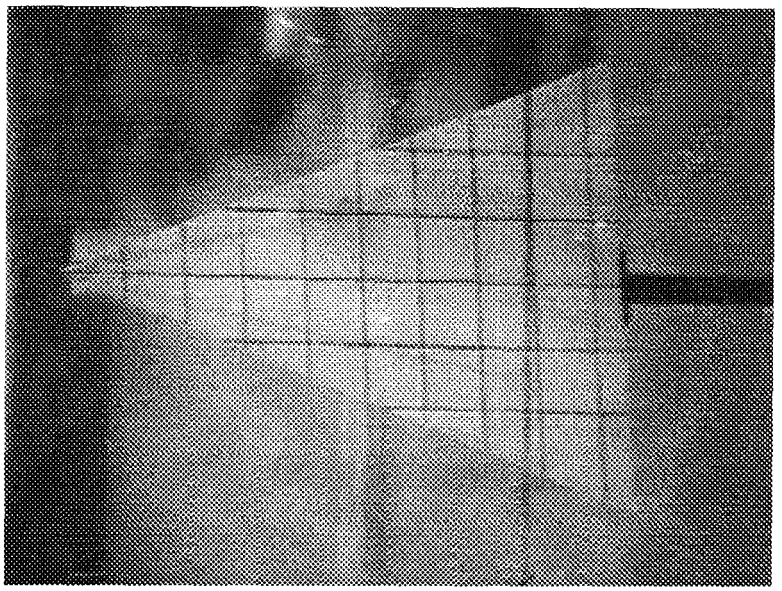

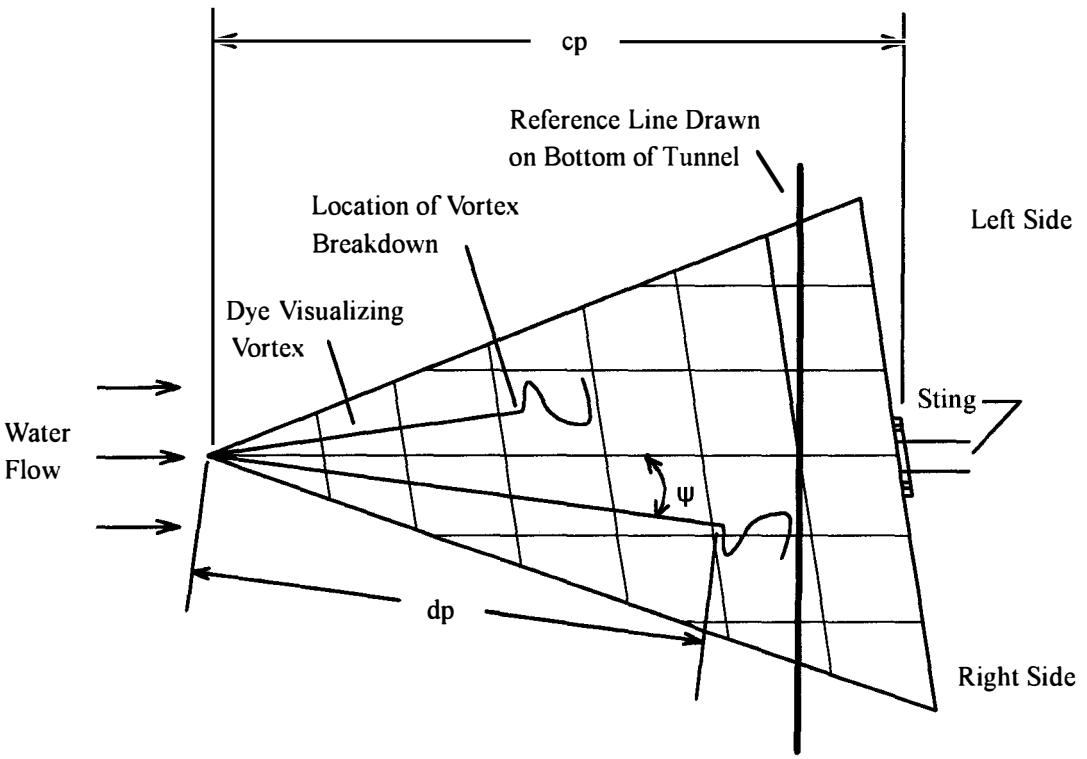

Figure 4.2. Schematic and Digitized Top View of The Delta Wing as Seen Through The Bottom of The Water Tunnel (Note that Image is a Mirror Image)

The analysis in Annex B was based on experimental research conducted by Huang and Hanff[18] who showed that the height of the vortex breakdown above the wing surface was independent of roll angle. With this information, a coordinate transformation could be carried out and the following equation was derived for use in data reduction:

$$\frac{x}{c} = \frac{d_p \cos\psi}{\cos\sigma + \sin\sigma\left[\dfrac{\dfrac{\tan\theta'}{\cos\phi} - \cos\sigma\tan\psi\tan\phi}{1 + \sin\sigma\tan\psi\tan\phi}\right]} \cdot \frac{\cos\sigma}{c_p} \qquad \textbf{(14)}$$

where: d_p is the project distance from the location of vortex breakdown to the apex;

ψ is the angle the vortex core makes with the projected root chord line;

σ is the model pitch angle;

θ' is the vortex core angle for zero roll angle; and

c_p is the projected root chord length where $c_p = c\cos\sigma$.

To determine the information necessary in the above equation, a similar measurement technique as previously described for pitch data was used with the aid of the Sigma Scan software. Referring to Figure 4.2, a point was placed at the location of vortex breakdown, at the delta wing apex and at the centre of the base. The centerline painted on the model helped pinpoint the centre of the base. The distances, in pixels, of the projected location of the vortex breakdown from the apex, d_p, and the projected distance of the root chord length, c_p, were measured. The projected angle the vortex core made with the root

chord line, ψ, was also measured. The above correction was applied to all the data involving non-zero roll angles.

Identification of Vortex Breakdown Location

Some subjectivity that existed when analysing the data could be attributed, in part, to the quality of the flow visualization and for the cases where the flow visualization quality was really poor, a repeat of the test point was carried out. The main source for subjectivity, however, was in the determination of the precise location of vortex breakdown. Various researchers[23][25][34] have identified this as being a contributing factor for discrepancies in published data. Although the vortex breakdown phenomenon has been recorded as having two main breakdown forms: the bubble and the spiral, there are numerous minor deviations to these main forms which leave the researchers open to interpretation. In this study, for example, there were some cases where the vortex core would gradually increase and in others, the vortex core would bend slightly before totally breaking down. An example of how the location was identified as the specific vortex breakdown location is shown in Figure 4.3. This was consistent with other studies of comparable nature.

Uncertainty Analysis

An estimate of error incurred through data processing was conducted in this study

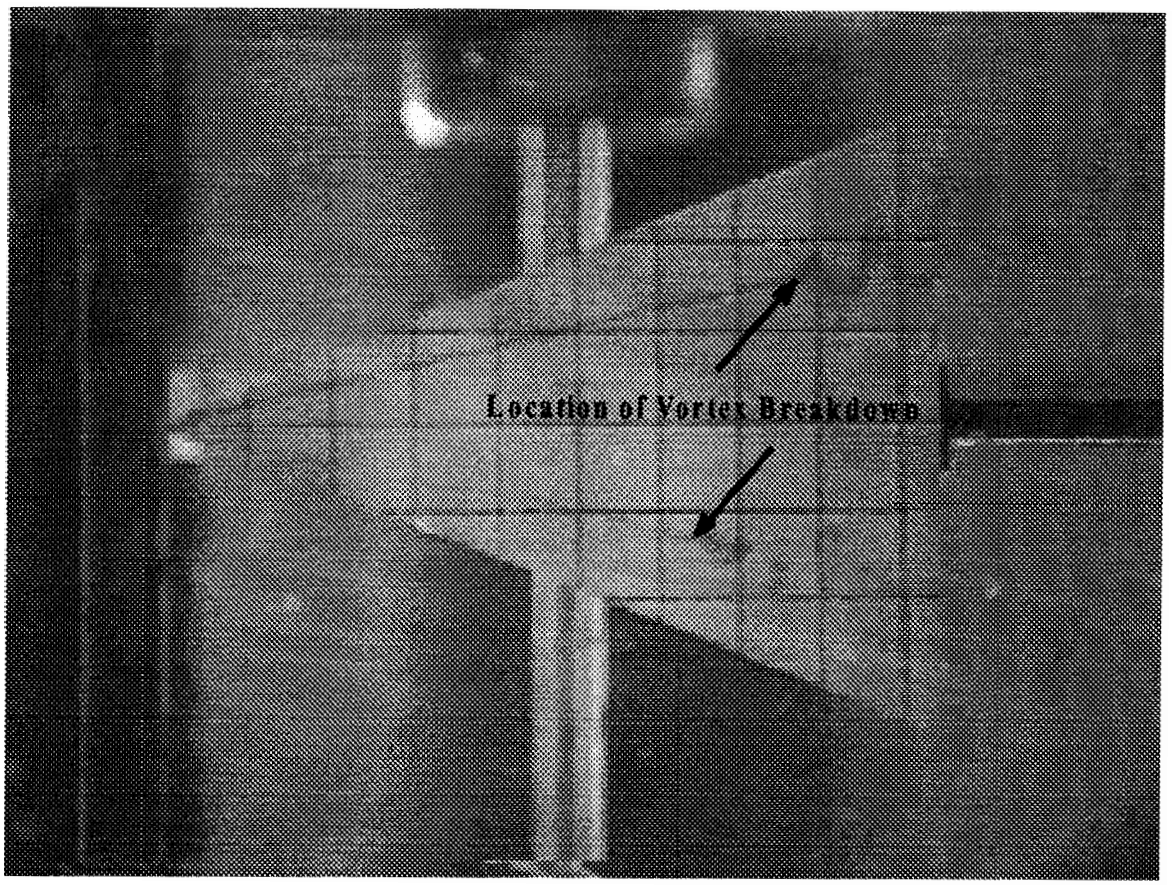

Figure 4.3. Identification of Precise Vortex Breakdown Location

by digitizing the same video frame 20 times and exporting it as a bitmap file. Each of the 20 bitmap files were analysed separately. The process was repeated a number of times. The resultant data showed that the angle of attack measurements could be repeated with an accuracy of 0.5% (based on an angle of attack of 40°) and that the distance measurements could be repeated with an accuracy of 0.3% (based on a maximum distance measurement of 1.5 x c). This meant that maximum angle of attack measurements (40°) were repeatable to within ±0.2° and maximum distance measurements (1.5 x c) were repeatable to within x/c = ±0.02. The method used to evaluate roll angles is presented in Annex A. The uncertainty associated with the evaluation of steady state roll and was ±0.446°. The uncertainty associated with the evaluation of the unsteady roll angle was that which existed for the measurement of pitch angle plus that which was associated with the measurement of the distance between C-Beams. The overall the evaluation of the unsteady roll angles were repeatable to within 0.6% which gave an uncertainty of ±0.108° for $\phi = \pm 18°$.

These results compared well with other researchers. Jarrah[39], for example, estimated his uncertainty in angle of attack to be ±1° and his uncertainty in measuring distance to be ±0.05 inches. LeMay[25] estimated that his measurements were repeatable to within ±0.3° for the angle of attack and to within x/c = ±0.01 for the breakdown location. As well, Thompson[23], who also digitized the same frame several times and repeated the process several times, found the breakdown location could be measured repeatably within an accuracy of 0.4% of the chord length while the angle of attack could be measured within an accuracy of 0.2%. Thompson[23] was later able to refine these

errors to 0.2% and 0.15% respectively with an upgrade of image analysis hardware.

Vortex breakdown is an unsteady flow phenomenon that exhibits unsteady behaviour. Even in the case of steady state analyses, researchers have observed fluctuations in the longitudinal direction and have had to use their judgement in estimating the position of the vortex breakdown for a given angle of attack. LeMay[25] commented on these fluctuations in the vortex breakdown location, and, to account for them, he gathered statistical information on the fluctuations. For the minimum and maximum angles of attack, he recorded breakdown locations at a sampling rate of 64 Hz for 128 samples. He used a Discrete Fourier transform (DFT) on the vortex breakdown position and computed an rms variation in breakdown location at each angle of attack. He reported that the average rms fluctuations about the mean was 1.3% of the root chord and concluded that there was no apparent dominant frequency in the breakdown point fluctuations in the range 0 to 32 Hz. Lowson's[34] approach was much simpler. He averaged the chordwise location where the dark core first began to expand with the location where the dark core first appeared in the turbulent wake. He concluded that for wings of 75° of sweep or less, the longitudinal oscillations covered no more than 6% of the chord. Thompson[23] also commented on the inherent unsteadiness in the location of the vortex breakdown and reported on fluctuations of up to ±4% of the root chord from its mean position.

The data presented in Figure 4.4 provides an example of typical fluctuations inherent to the location of vortex breakdown for steady state conditions. The delta wing was fixed at a pitch angle of 28° and a roll angle of -8.3°. The vortex breakdown location

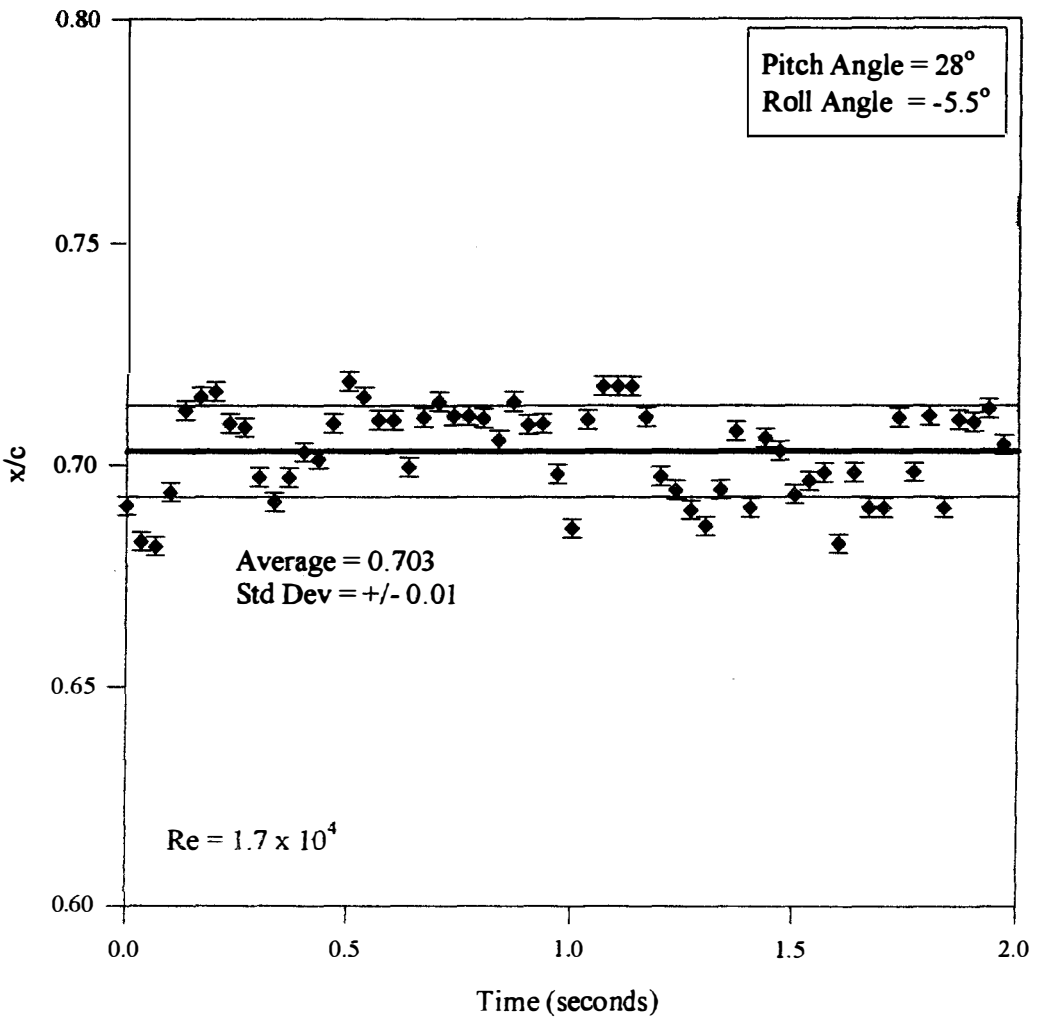

Figure 4.4. Steady Vortex Breakdown Location as Function of Time

is shown as a function of time. Sixty consecutive frames were analysed which provided 2 seconds of data. The mean location was calculated as x/c = 0.70 using the following:

$$\bar{x} = \frac{1}{n} \sum_{i=1}^{n} x_i \qquad \textbf{(15)}$$

where: n - represents the sample size; and I - identifies the individual sample.

The actual vortex breakdown location, however, varied from 0.68 to 0.72. This represented a fluctuation in the location of vortex breakdown of 5.7% which is consistent with existing data. Included in Figure 4.4 are the error bands associated with each data point. These were calculated as being 0.3% of the measured value as previously discussed. Also included in Figure 4.4, is the error band of the mean location which was calculated as the sample standard deviation as follows:

$$s_x = \sqrt{\frac{1}{n-1} \sum (x - \bar{x})^2} \qquad \textbf{(16)}$$

To minimize the amount of uncertainty in the location of vortex breakdown for steady state conditions, 20 consecutive video frames were converted to bitmap files and analysed individually. The results were presented as the mean and the error bars shown on the graphs were expressed as the sample standard deviation. For the unsteady analyses

where the delta wing was in motion, there was observed to be less of a fluctuation in the location of vortex breakdown. Accordingly, it was only necessary to analysed 6 - 10 cycles of motion. The results were also presented as the mean and the error bars as the sample standard deviation.

As previously discussed for experiments involving roll, data acquisition was carried out by viewing the model through the bottom of the tunnel to provided a record of the visualization of the flow phenomenon over the top surface of the delta wing. Because the location of the vortex breakdown was located a distance away from the wing's surface and the model was rotated at an angle away from the viewing plane, an analysis was carried out that provided a correction factor. This correction factor applied to the data collected from test points involving non-zero roll angles and was similar to that which would account for a parallax error. To gather an appreciation for the sensitivity of the correction factor, a comparison of uncorrected (measured) roll data with corrected roll data was carried out with the steady state roll data that was collected at a pitch angle of 30°. The results are presented in Figure 4.5 where the data show that the corrections applied were within the error bands of the data collected. The roll correction would have a greater effect on the data at higher pitch angles, and so, the roll correction factor was applied to all the data in this study that involved non-zero roll angles.

For experiments involving unsteady motion, a drive mechanism was selected that could provide a constant sinusoidal input that could be varied in frequency. This oscillatory motion was chosen so that maximum comparison of available data could be made. Based on the limitation of the maneuvering apparatus and those associated with

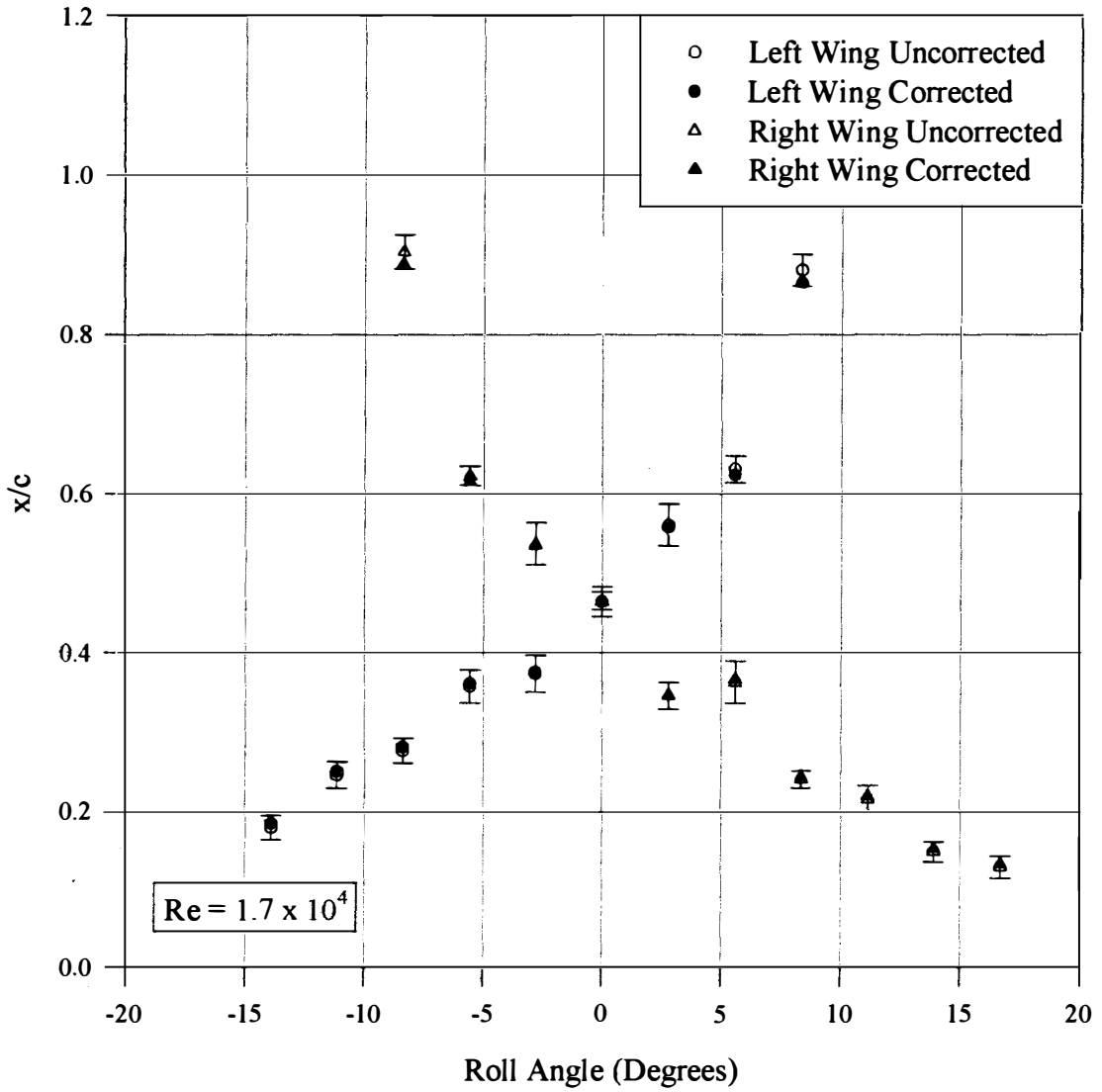

Figure 4.5. Comparison of Uncorrected (Measured) Roll Data With Corrected Roll Data

causing disturbances in the water tunnel, large amplitude pitch oscillations were not conducted. Instead, the approach taken was similar to LeMay[25] who varied the pitch oscillations from 29° to 39° in order that the position of the vortex breakdown was restricted within the bounds of the wing surface. The model used in this study had a single bevel where the model used in LeMay's[25] had a double bevelled leading edge. In order that the location of vortex breakdown was restricted within the bounds of the delta wing in this study, pitch oscillation from 25° to 35° were carried out.

For data comparison, however, it was also necessary to examine the behaviour of the flow phenomenon in terms of an upstroke and a downstroke. The upstroke represented an increase in angle of attack or roll angle from the minimum value to a maximum value and the downstroke represented an decrease in angle of attack or roll angle from the maximum value to a minimum value. Accordingly, a cosine function was used to better represented the desired input.

For the experiments involving unsteady pitch motions only, the side view of the experimental set-up made it quite simple to measure the angle of attack. To evaluate the accuracy of data acquisition with that represented by the input function, a comparison of the measured angle of attack versus time was made with data generated using a cosine function. The following cosine function was used:

$$\alpha = \alpha_0 + A_P \cos \omega t \qquad \textbf{(17)}$$

where: α_o - is the mean angle of attack;

A_p - is the oscillation amplitude;

t - is the time; and

ω - is the angular velocity.

The data presented in Figure 4.6 was collected for four different values of reduced frequency. For each value reduced frequency, six cycles of unsteady pitch oscillations were analysed and the results were averaged. The function that best fit all the data was created with $\alpha_0 = 29.8^\circ$ and $A_p = 5.0$; however, because of the error inherent to the evaluation of the pitch angle, the unsteady pitch motion was nominally referred to as oscillations in pitch angle of $30^\circ \pm 5^\circ$.

The roll angle was not easily measured and so a calculated roll angle was used throughout the study. As previously presented, the maximum roll angle was shown to be 18°. The roll oscillations were carried out about a zero roll angle. The cosine function used for roll angle was:

$$\phi = 18.0 \cos \omega t \qquad \textbf{(18)}$$

The unsteady roll motion was referred to as oscillations in roll of $\pm 18^\circ$. To identify the position of zero roll angle, a line was drawn on the bottom of the tunnel perpendicular to the flow. A check of accuracy was conducted by verifying that the two shedding vortices were broken down symmetrically from the apex of the wing. As shown in previous figures, lines were also drawn on the model itself. When the lines on the model were

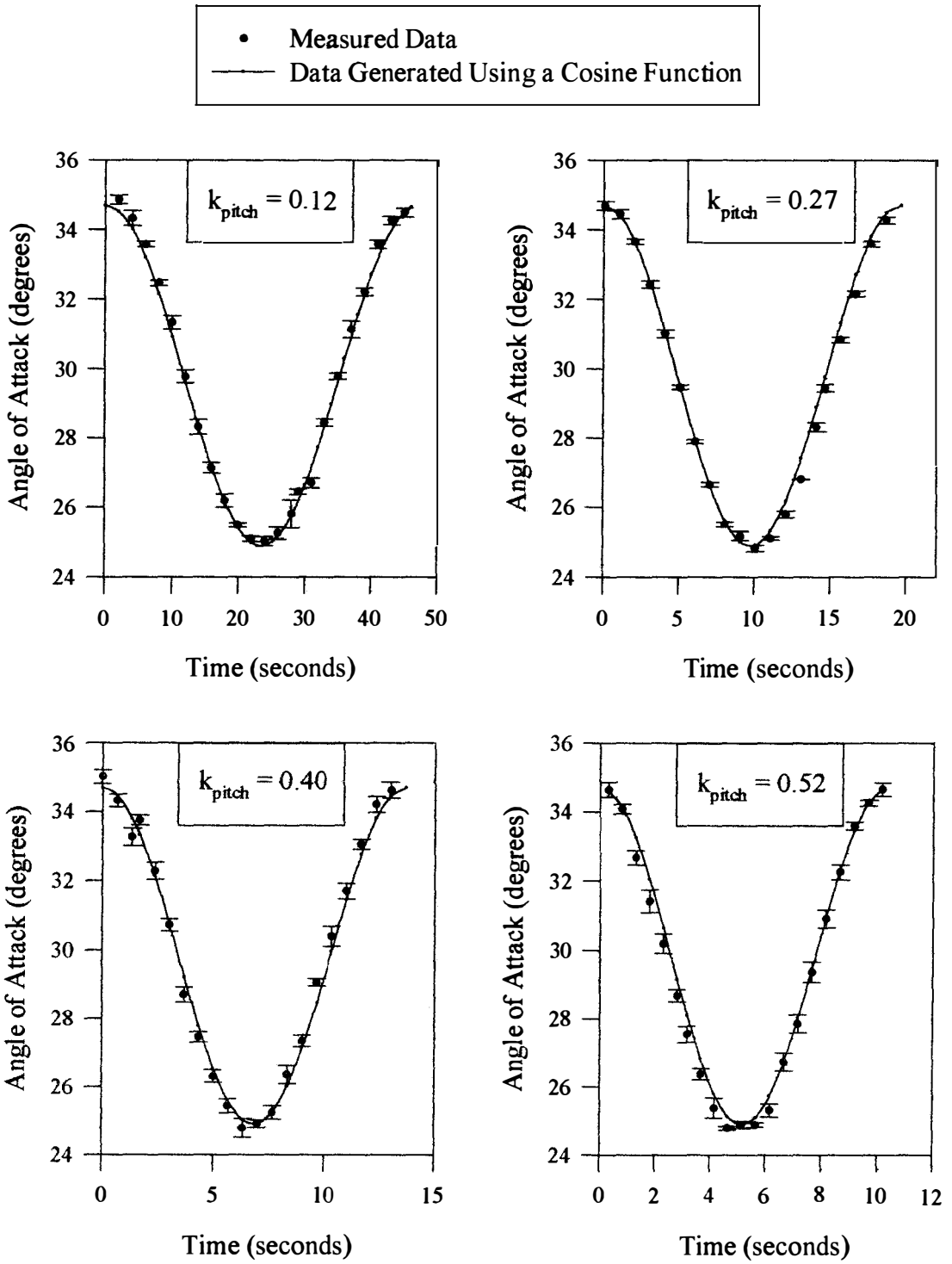

Figure 4.6. Uncertainty Analysis of Measured Angle of Attack

parallel with the reference line on the tunnel, the model was assumed to be at zero roll angle. With the roll frequency known, the roll angle could be calculated at any time by analysing a video sequence frame by frame.

Throughout the testing, the Reynolds number that has been specified was calculated using the standard equation as follows:

$$Re = \frac{Uc}{\nu} \tag{5}$$

The errors associated with the calculation of Reynolds number were a direct result of the errors associated with the flow velocity, U, the root chord length, c, and the kinematic viscosity, ν. The errors associated with the flow velocity has been determined as being 3.1%. The dimensions of the model were accurate to within 1/32 inches which added another 0.6%. Finally, changes in the temp of the water in the tunnel caused changes in ν which contributed another 3.7%. The accuracy of the Reynolds number calculation, therefore, was within 7.4%. This was consistent with the study of Thompson[23] who reported an accuracy for Reynolds number of within 11%.

The unsteady motion analysed in this research was characterized in terms of reduced frequency. Reduced frequency has been defined for pitch oscillations as well as for roll oscillations. Recall, for pitch oscillations, k_{pitch} has been defined as:

$$k_{pitch} = \frac{2\pi fc}{U} \quad \textbf{(9)}$$

and for roll oscillations, k_{roll} has been defined as:

$$k_{roll} = \frac{2\pi fb}{2U} \quad \textbf{(10)}$$

To maintain a given reduced frequency, the flow velocity was held constant at 0.467 ft/sec throughout the tests. The variations in reduced frequency were carried out by varying the frequency of oscillation provided by the drive mechanism. Accordingly, the lower limit of reduced frequency analysed was limited by the ability of the motor controller and the drive mechanism to provide a smooth input to the maneuvering apparatus. Frequency of oscillation was calculated by capturing the motion on video and analysing a series of digitized video frames. Six consecutive cycles of data were analysed. The maximum uncertainty associated with frequency of oscillation was estimated to be within 0.9%. This was estimated for the fastest frequency of oscillation which took the least amount of time for one cycle completion and consequently provided fewer frames to analyse.

The overall uncertainty associated with reduced frequency was due as well to the errors associated with the flow velocity and the characteristic length, c or b, which have already been estimated to be within 3.1% and 0.6% respectively. Therefore, the uncertainty associated with reduced frequency was within 4.6%.

Blockage Effects

The size of the delta wing model was restricted to the constraints of the water tunnel and designed specifically to keep the amount of geometric blockage to a minimum. The information presented in Figure 4.7 shows the percent blockage ratio for a given angle of attack. The blockage ratio was calculated as a ratio of the projection of the cross sectional area of the model and sting with the cross sectional area of the test section. It should be noted that the maximum frontal area presented by the model occurred when the model roll angle was zero and so the data presented represents the maximum blockage. As well, except for the steady state data collected for variations in pitch, the model pitch angle was oscillated from 25° to 35°. Accordingly, the maximum tunnel blockage for the majority of the data was 8.5% (corresponding to a model pitch angle of 35°). For the steady state data collected for variations in pitch, the angle of attack was increased to as high as 40° and; therefore, the maximum tunnel blockage was calculated as 9.3%. These results are consistent with existing data: Peckham and Atkinson[9]: 8.0%; Thompson[23]: 9.8%. Some researchers have been able to considerably reduce the amount of blockage in their studies: Brandon and Shah[30]: 0.3%; Manor, Millar and Wentz Jr[52]: 2.3%; and Gad-el-Hak and Ho[26], 5.8%. Other have accepted higher amounts of blockage: LeMay[25]: 26%, and have had to apply correction factors to their data. Thompson[23] commented that the accepted upper limit for which blockage corrections need not be applied is 10%. Accordingly, there were no blockage corrections applied to the data in this study.

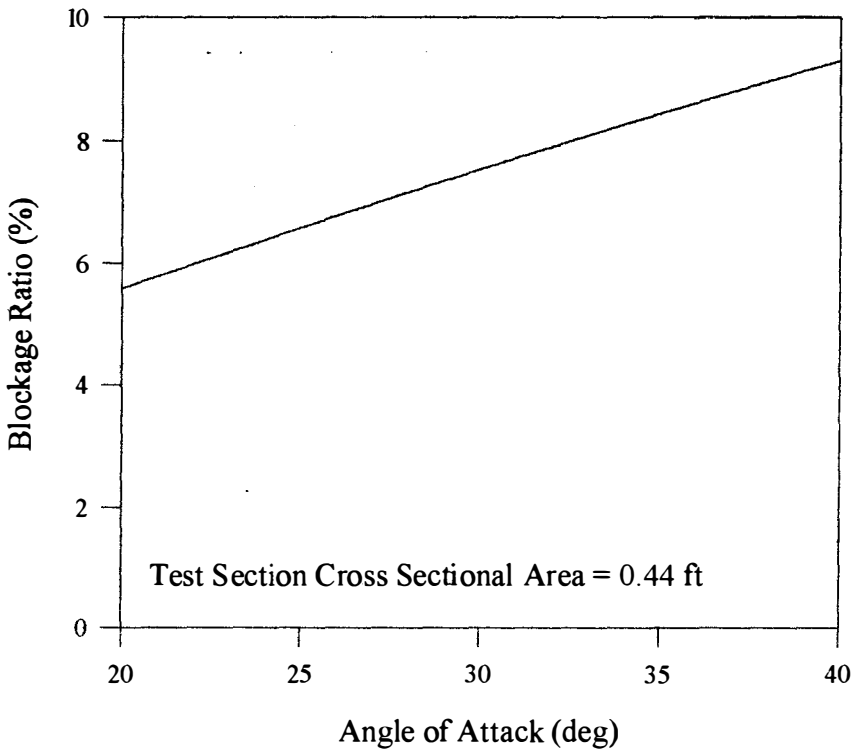

Figure 4.7. Percent Test Section Blockage Versus Angle of Attack

Test Matrix

Experimental testing was conducted in stages. Initially, steady state testing was carried out for variations in pitch. The model angle of attack was varied from 22° to almost 40° at various static intervals. Next, experimentation involving the delta wing maneuvering with unsteady pitch oscillations was conducted. Four distinct values of reduced frequency were tested. The testing continued with an analysis of steady state variations in roll angle at a given pitch angle. The pitch angle was fixed at 30° which was selected to be consistent with existing studies. The investigation of unsteady roll oscillations for the same fixed pitch was then carried out. The four frequencies of oscillations that were used in the investigation of unsteady pitching motion were also used for unsteady roll motion. Because of the difference in definition of reduced frequency for pitch and roll, however, this led to a different set of four reduced frequencies. In the final series of tests, steady state and unsteady investigations were carried out for the delta wing that was maneuvered in pitch as well as roll. For the unsteady investigations, the same drive mechanism provided the pitch and rolling motion and so the pitching and rolling frequencies were the same. For comparison, the frequencies of oscillations were consistent with those used for pitch and for roll.

Table 4.1 provides a summary of the frequencies of oscillations and their corresponding reduced frequencies.

Table 4.1. Frequencies of Oscillation and Associated Reduced Frequency

f (Hz)	k_{pitch}	k_{roll}
0.023	0.12	0.05
0.051	0.27	0.10
0.074	040	0.14
0.097	0.52	0.19

CHAPTER V

RESULTS AND DISCUSSIONS: PITCH EXPERIMENTS

Steady State Location of Vortex Breakdown

Steady state pitch experiments have been carried out at several angles of attack ranging from 23° to 40°. The Reynolds number during the testing was 1.7×10^4. The data presented in Figure 5.1 shows the steady state locations of vortex breakdown for variations in angle of attack. The data presented were collected at fixed angles of attack and variations in angle of attack were made in the direction of increasing angle of attack. The flow was allowed a settling time for each test point prior to data collection. Twenty consecutives video frames of data were analysed for each angle of attack. The error bars shown on the graph are estimates of repeatability that have been calculated using the standard deviation. Referring to Figure 5.1, the results show that the location of vortex breakdown remained over the wing surface throughout the entire angle of attack range examined. As the angle of attack increased, the location of vortex breakdown moved toward the apex and, as the angle of attack decreased, the location of vortex breakdown moved aft. A smooth transition in the movement of the location of vortex breakdown with angle of attack was illustrated by the fit of a second ordered curve through the data points using the method of least squares.

It has been previously discussed that many researchers have observed significant

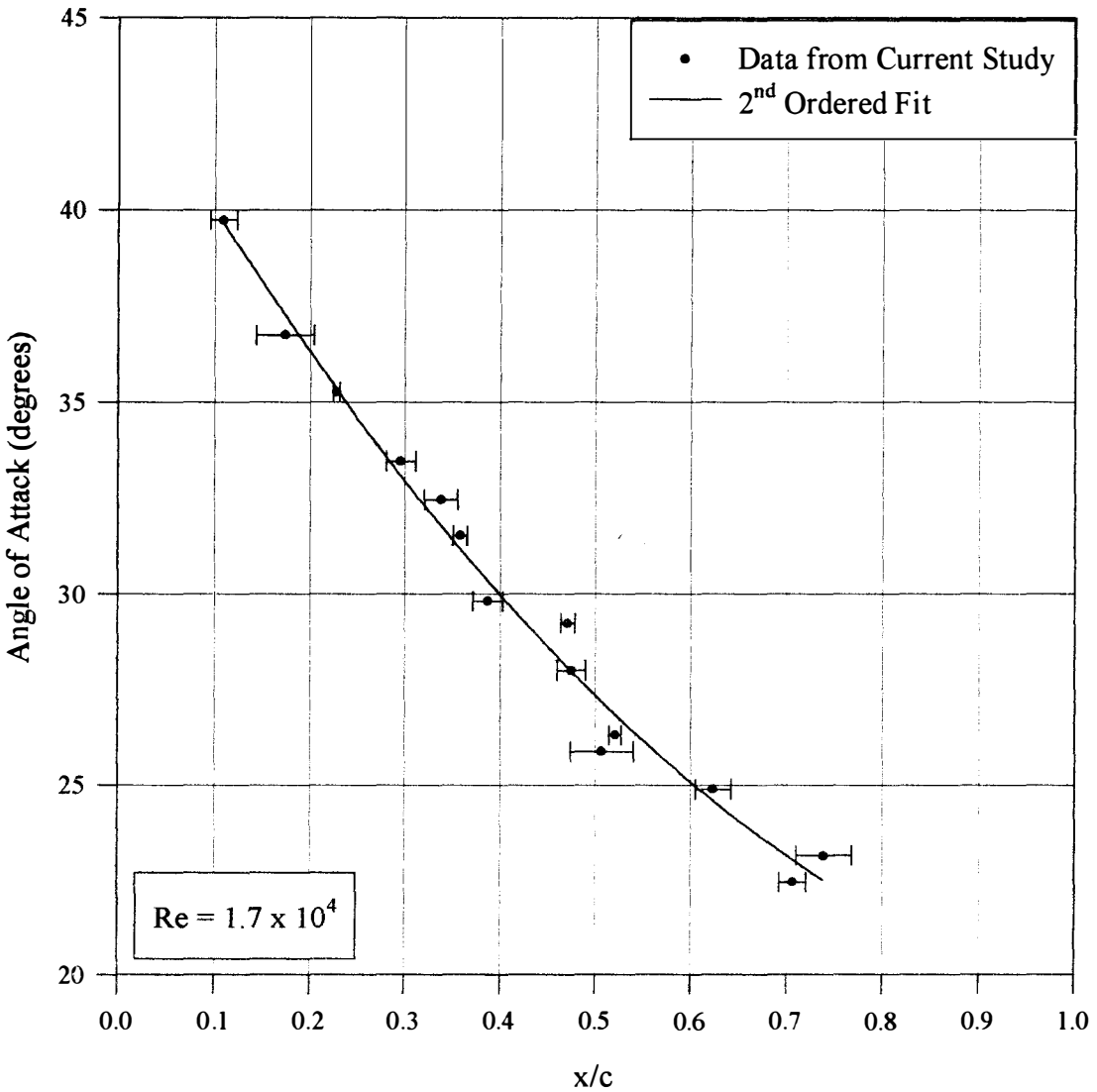

Figure 5.1. Steady State locations of Vortex Breakdown for Variations in Angle of Attack

variations in steady state data presented for similar delta wing designs which were investigated under similar conditions. Thompson[23], for example, reported upon differences in breakdown location of up to 25% for a given angle of attack which he attributed mainly to discrepancies in delta wing geometry between test models and possibly measurement technique. Lowson and Riley[14] also discovered serious anomalies in published data which were attributed to variations in the details of geometry such as thickness to chord ratio and leading edge geometry. Certainly, a comparison of the results of Figure 5.1 with those provided in Figure 2.9 demonstrates the point.

In this study, to ensure the model design and the corresponding experimental results in this study could be validated, the model geometry was based specifically on one of the models used in the studies of Thompson[23]. In addition, the method used to collect the steady state data was also consistent with the methods of Thompson[23]. The data in Figure 5.2 is presented to provide the comparison of Thompson's[23] data with data collected in this study. As a show of data repeatability, a second set of data, which was collected six months apart from the first, is also provided. Referring to Figure 5.2, it can be seen that generally there is good data comparison and that the data was repeatable. It is concluded, therefore that previous published results concerning the location of vortex breakdown have been successfully reproduced using a model of exact geometry used in the previous study. This conclusion is consistent with the conclusion made by Lowson and Riley[14].

Two empirical methods (Equation 6 and 8) have been presented which have been used successfully to predict the location of vortex breakdown over delta wings as a

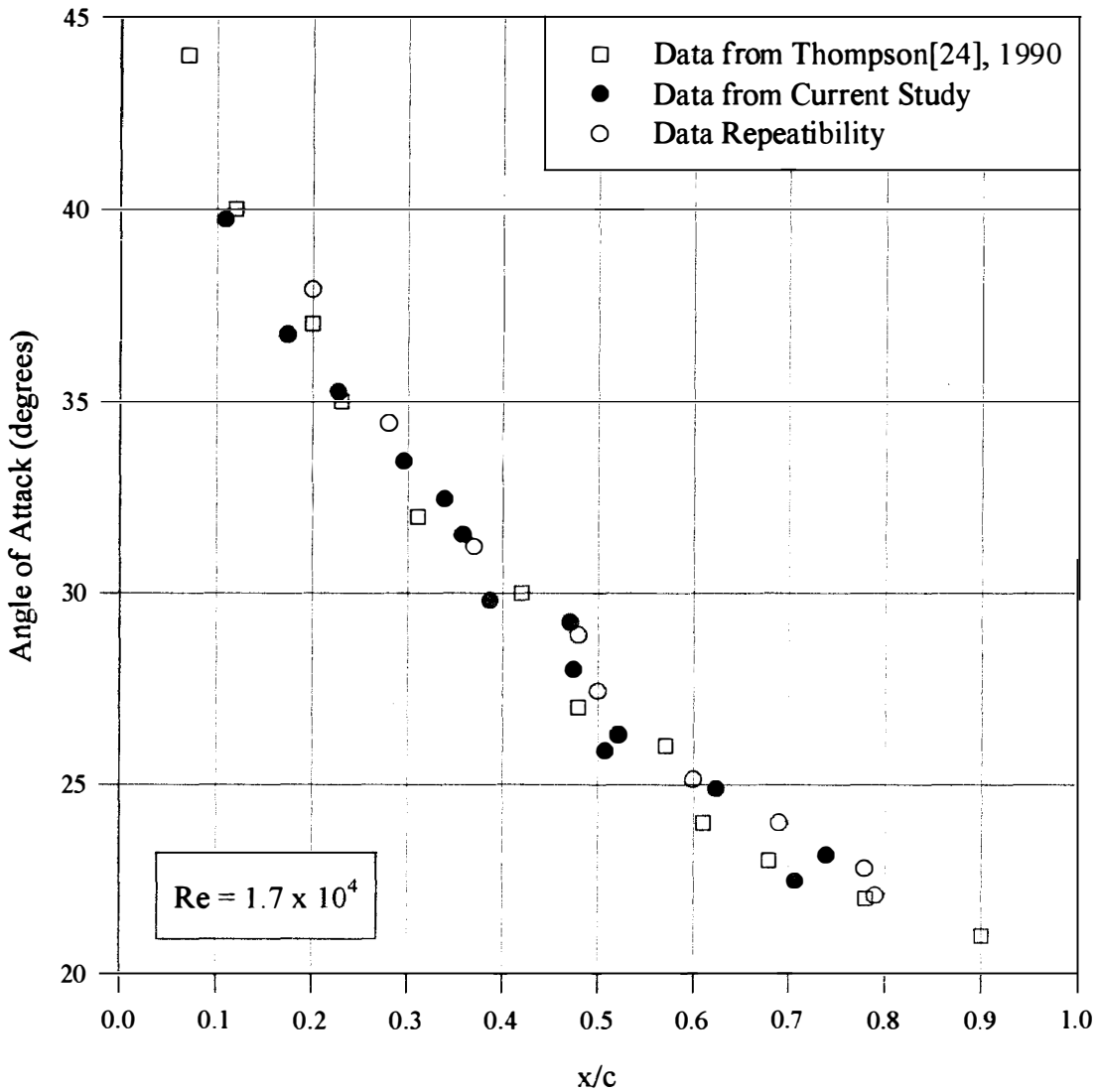

Figure 5.2. Comparison with Thompson[23] of Steady State Vortex Breakdown Locations for Variations in Angle of Attack

function of angle of attack and pitch angle. Equation 6, developed by Huang and Hanff[17], correlates well with published data for variations in angle of attack and for many sweep angles. Equation 8, developed by Huang and Hanff[18] corresponds well to experimental data for variation in roll angle for a 65° delta wing at a fixed pitch angle of 30°. The data in Figure 5.3 is presented to provide a comparison with the experimental data of this study and the results of using the prediction methods. Referring to Figure 5.3, the comparison shows that neither predictions provided by Equation 6 or 8 correspond with the experimental data collected in this study even though the sweep angle of the models were the same. It was observed, however, that the data collected in this study was merely shifted from the two prediction equations. A similar shift in experimental data was analysed by Thompson[23] who attributed such a shift to changes in model thickness and leading edge geometry. Thompson's[23] results showed that a change of the thickness (from a thicker to a thinner wing) resulted in an aft movement of the vortex breakdown location for a given angle of attack. More interestingly, Thompson's[23] results also indicated that a change from a 1 bevel leading edge to a 2 bevel leading edge resulted in an aft movement of the breakdown location for a given angle of attack. His explanation was based on camber. The wing with the single lower surface bevel, as in the case of this study, has a negative camber. The addition of an upper surface bevel that is symmetrical to the lower surface bevel, as in the case of 2 bevel wings, results in the wing having zero camber. The net effect when comparing a single bevel wing to a double bevel wing is an increase in camber from negative to zero. An increase in camber decreases the local effective angle of attack, and, as a result, the location of vortex breakdown is anticipated

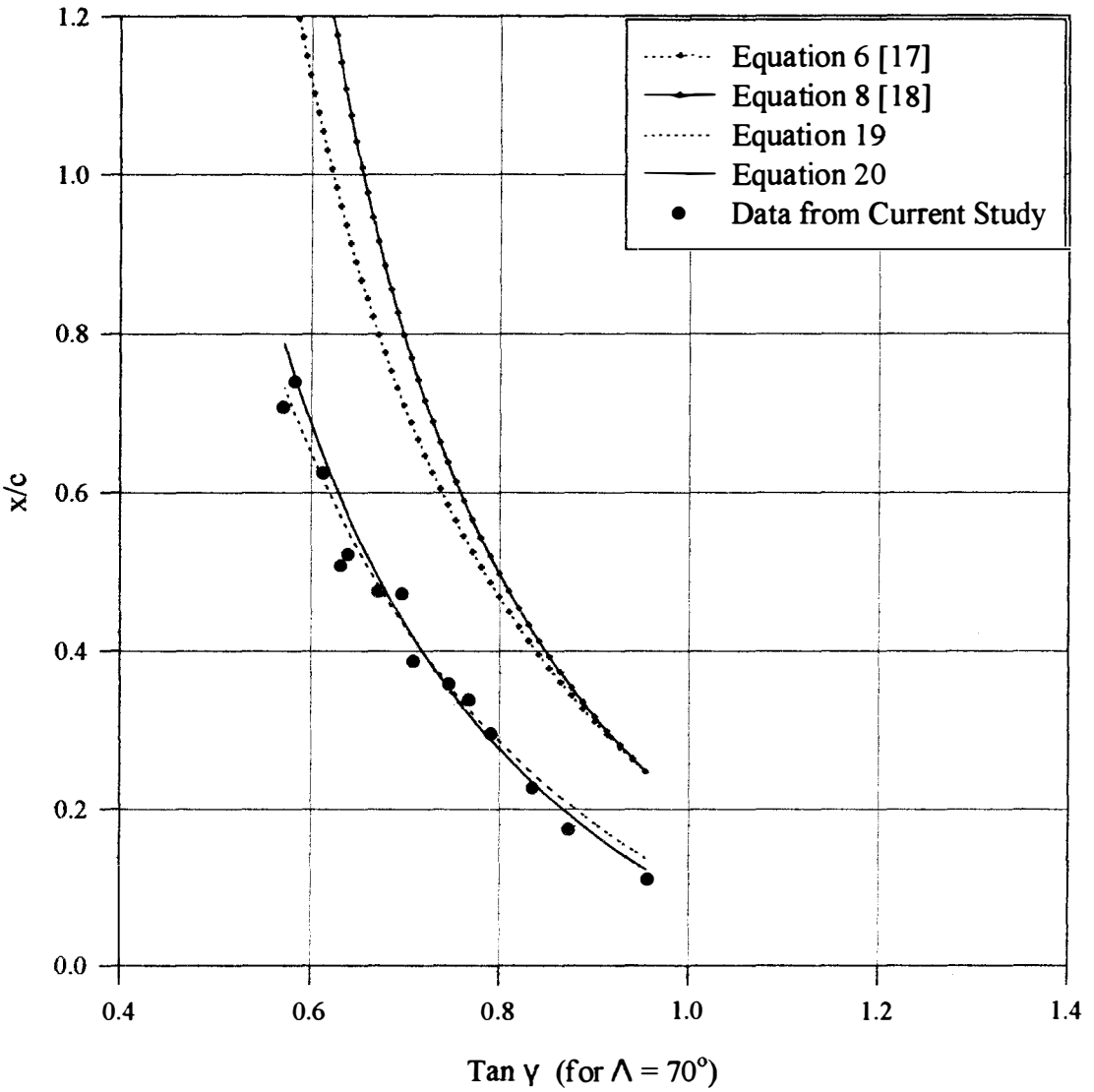

Figure 5.3. Comparison of Steady State Data to Empirical Prediction Equations

to move aft. Thompson[23] argued, though, that the camber effect associated with the two leading edge geometries was probably insufficient to account for the differences in the data.

Equations 6 and 7 were modified to effect a lateral shift (LS) in the predictions. Lowson and Riley[14] reported that an decrease in wing thickness or an increase in leading edge bevel angle will tend to move the location of the vortex breakdown aft and the net effect could be as high as a 5-7° variation in angle of attack for a given vortex breakdown position. It was discussed by Huang and Hanff[17] that the development of the prediction equations were predominately based on the influence of the vortex swirl parameter which can be related to U_ϕ/U_∞ and consequently, tanγ. This is consistent with Lowson and Riley[14] who stated that they believed that the shape of the apex was a key factor in determining the location of vortex breakdown because of its effect on the vorticity shed which forms the centre of the vortex core and that changes in vorticity gradient can have serious effects on the stability of fluids. Therefore, efforts were focussed on effecting a change to the influence of tanγ that would create the desired shift in prediction capability. Accordingly, Equation 6 was modified to the following:

$$\frac{x}{c} = \frac{N}{\tan\gamma - (0.32 - LS)} - A \qquad \textbf{(19)}$$

where:

$$
\begin{aligned}
\gamma &= \cos^{-1}(\cos\alpha(\phi)\ \sin\Lambda(\phi)) \\
N &= 0.4 + 0.1\ \cot\Lambda(\phi) \\
A &= 0.17 + 0.38\cot\Lambda(\phi) + \cot^2\Lambda(\phi) \\
LS &= 0.12 \\
\tan\gamma &\sim U_\phi / U_\infty
\end{aligned}
$$

and Equation 8 was modified as follows:

$$
\frac{x}{c} = \frac{N}{\tan\gamma - B} - A \qquad \textbf{(20)}
$$

where:

$$
\begin{aligned}
\gamma &= \cos^{-1}(\cos\alpha(\phi)\ \sin\Lambda(\phi)) \\
N &= 0.33 + 0.3/\tan^2\Lambda(\phi) \\
A &= 0.20 + 1.6/\tan^2\Lambda(\phi) \\
B &= (0.43 - LS) - 0.1/\tan\Lambda(\phi) \\
LS &= 0.13 \\
\tan\gamma &\sim U_\phi / U_\infty
\end{aligned}
$$

and where (recall Equation 7):

$$
\begin{aligned}
\alpha(\phi) &= \tan^{-1}(\tan\sigma\cos\phi) \\
\Lambda(\phi) &= \Lambda \pm \tan^{-1}(\tan\sigma\sin\phi)
\end{aligned} \qquad \textbf{(7)}
$$

It should be noted that the influence of roll angle on effective angle of attack and effective sweep must be taken into account; however, in the pitch experiments where the roll angle was zero, therefore, the pitch angle was the angle of attack. The difference between

Equations 19 and 20 and Equations 6 and 8 is merely the inclusion of a shift factor. This value was calculated by measuring the average lateral shift between the prediction provided by the empirical method and the experimental data in terms of tanγ. This shift corresponded to reduction in angle of attack of approximately 3-7° which corresponds well with the bevel correction made by Huang and Hanff[18]. Referring to Figure 5.3, this simple change has resulted in a better correlation of experimental data from this study to the predictions provided by Equations 19 and 20.

To further substantiate the modification to Equation 6 and 8, the data in Figure 5.4, which was presented by Thompson[23], is provided to demonstrate the differences associated with a change in model thickness and also a change in leading edge geometry. Figure 5.5 is a presentation of angle of attack versus vortex breakdown location, x/c in a format which is compatible to that presented by Thompson[23]. The comparison of data in the two figures is quite remarkable. For example, the shifts in data between the two graphs in terms of breakdown location for angles of attack between 35° and 40°, are almost identical. The intent of this study, however, was not to develop nor validate an analytical method to predict the location of vortex breakdown. In fact, even though a simple modification has provided for good comparison of results, the limitations of using Equations 19 and 20 and their sensitivity to specific test conditions under which they have been validated are recognized. The applications of Equations 19 and 20 have been restricted to the confines of this study. It is concluded, however, that the leading edge geometry of the delta wing design plays a significant role in affecting the location of the vortex breakdown.

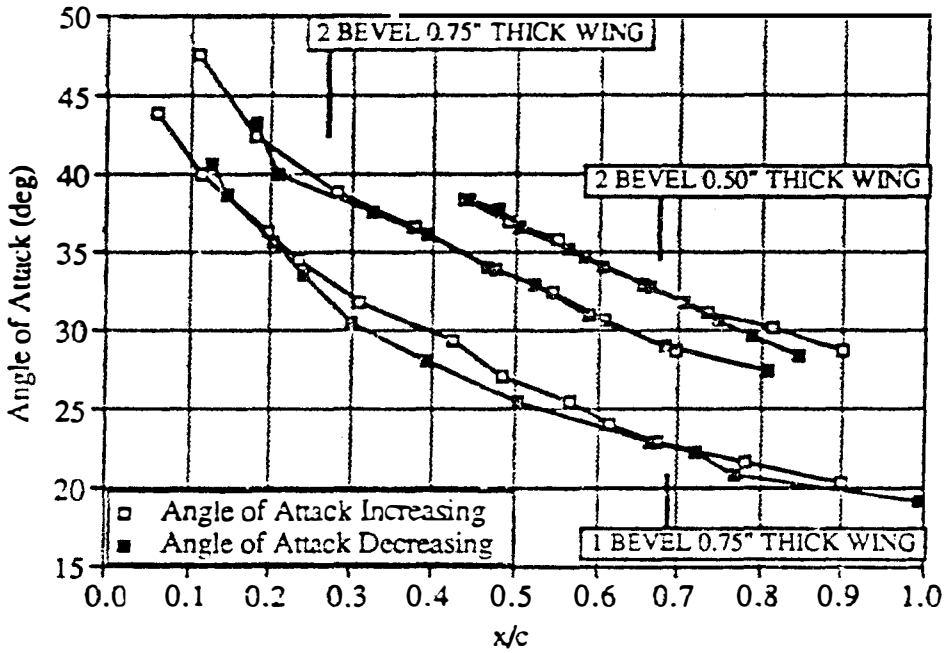

Figure 5.4. Steady Breakdown Location: Thickness and Leading Edge Geometry Effects (Data for 0.50" Wing From LeMay, 1988). [23]

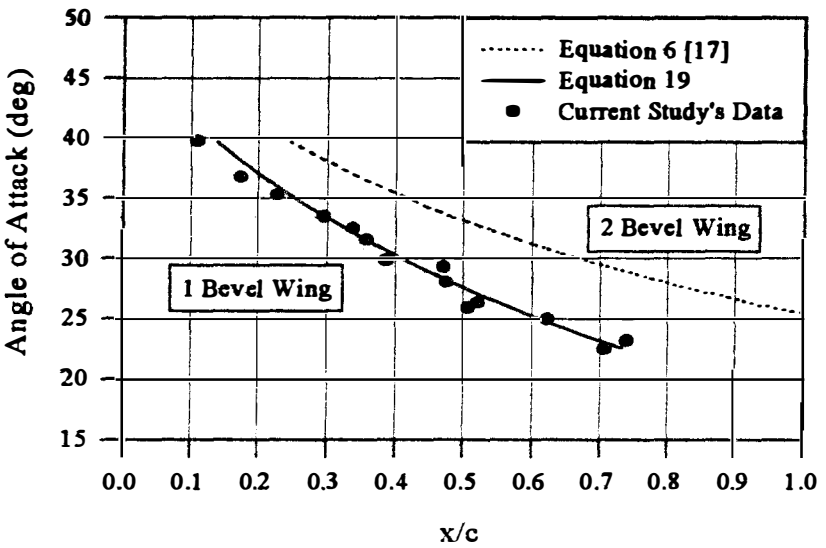

Figure 5.5. Comparison of Single Bevel and Double Bevel Leading Edge Geometry

Vortex Angle Under Steady State Conditions

Often researchers have made observations on other characteristics of vortex flow over delta wings which can also give good indications of sound data validation. For example, Elle[10] observed that the height of vortex above the wing surface increased with increasing angle of attack. As well, Thompson[23] provided data that shows a linear relationship between angle of attack and the angle that the vortex core makes relative to the wing's surface. This angle has been referred to as the vortex angle, θ. The data presented in Figure 5.6 is a comparison of data collected in this study with data collected in Thompson's[23] because of the similarities between the two studies. Note, however, that the vortex angle data collected for each study was collected over two different ranges of angle of attack. Even so, referring to Figure 5.6, there is good correlation of data and a linear approximation can be made which fits through the data from both studies..

It has been observed that other researchers have chosen a different method of investigating the behaviour of the vortex core for variations in angle of attack. Erickson[35], for example, has presented the relationship between angle of attack and the vortex core angle, θ_{CORE}. The vortex core angle is the angle that the vortex core makes relative to the horizon and is related to the vortex angle as follows:

$$\theta_{CORE} = \theta - \alpha \qquad \textbf{(21)}$$

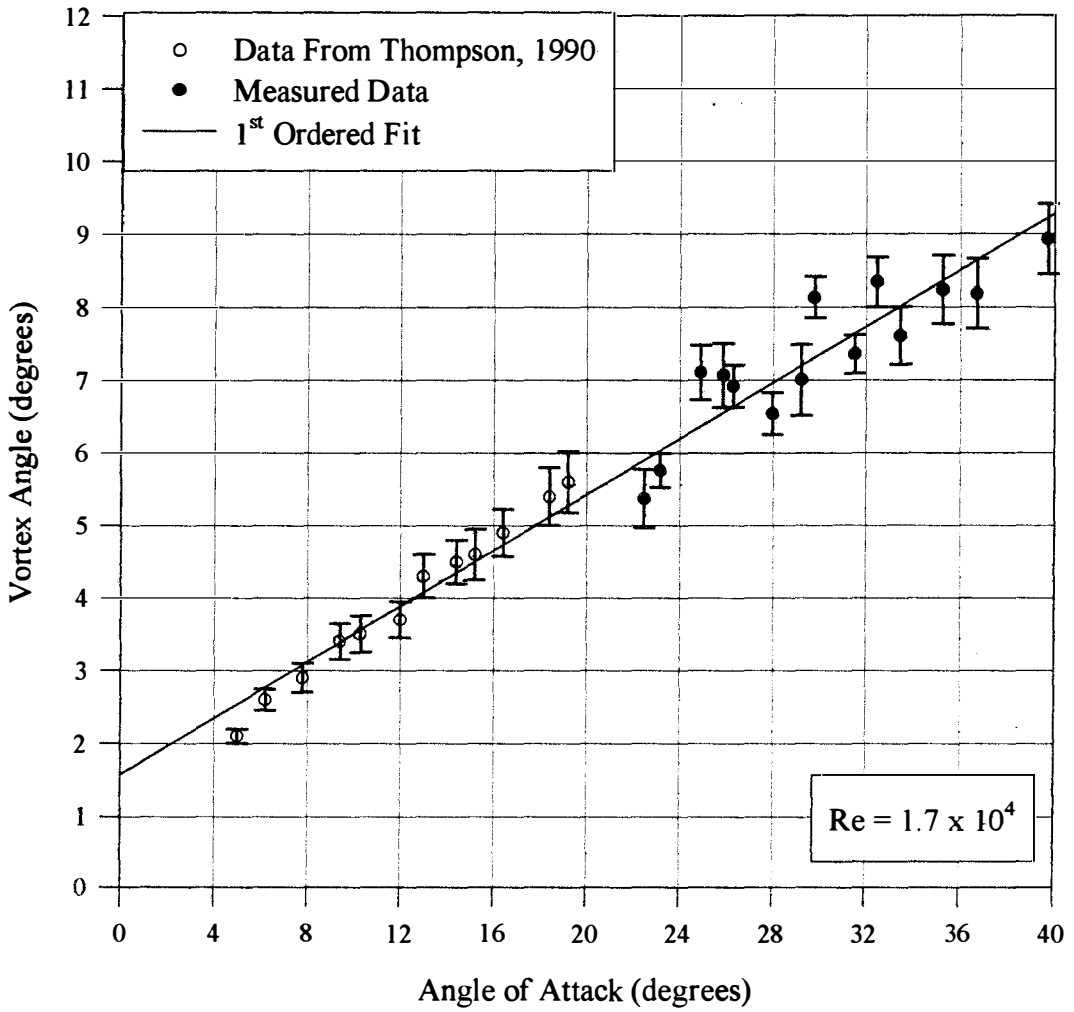

Figure 5.6. Steady State Vortex Core Angle Relative to the Wing Surface for Variations in Angle of Attack

Some example data from Erickson[35] is provided in Figure 5.7. Erickson's[35] experimentation was carried out in a water tunnel; however, he was able to demonstrate good correlation of results with those collected in a wind tunnel. Experimental data from this study in terms of θ_{CORE} is presented in Figure 5.8 for variations in angle of attack. A linear relationship is shown in the resultant data which has been extrapolated to the axes so that comparisons with other data can be made. Referring to Figures 5.7 and 5.8, it can be seen that there is good agreement in results. In fact, Thompson[23] commented on studies carried out by Morris, Ward, Malcolm and Ward[53] who showed a linear change in vortex core angle from 7° to 27° for variations in angle of attack from 10° to 35°. Using these values to compare, the current study has also shown a linear change in vortex core angle from approximately 7° to approximately 27° for variations in angle of attack from 10° to 35° and Erickson[35] showed a linear relationship in vortex core angle from approximately 8° to 25° for variations in angle of attack from 10° to 35°.

It is concluded therefore that the behaviour of the vortex core angle can be a good check of the validity of test results. Because of the cross correlation with tests conducted in a water tunnel as well as a wind tunnel, the format of presenting the vortex core angle versus angle of attack also provides for good data correlation.

Vortex Breakdown During Unsteady Pitching Motion

Experiments involving unsteady pitching motion were carried out in the water tunnel with the delta wing model oscillating about the centre chord location. The

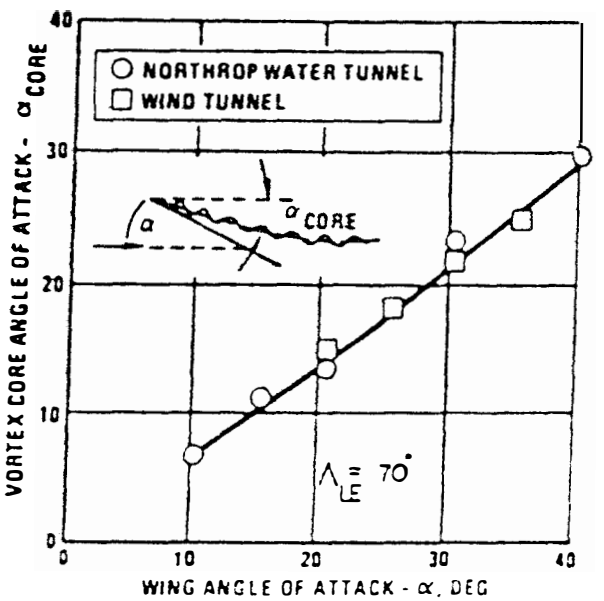

Figure 5.7. Effect of 70° Delta Wing Angle of Attack on Vortex Core Angle of Attack. [35]

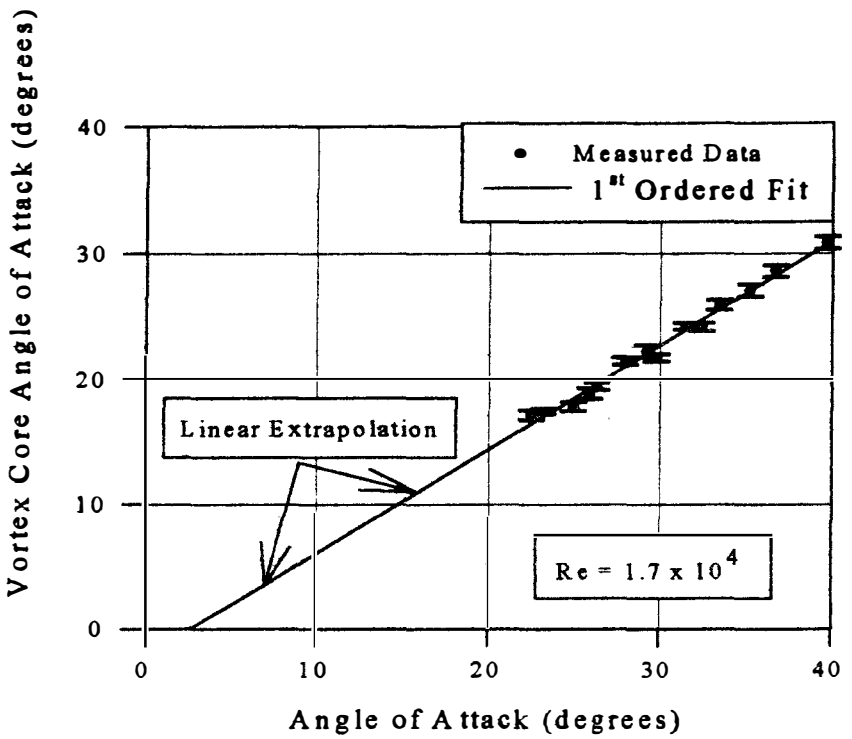

Figure 5.8. Steady State Vortex Core Angle Relative to the Horizon

For Variation in Angle of Attack

Reynolds number of the flow was 1.7×10^4. The input mechanism provided a sinusoidal input which oscillated the model about a mean angle of attack of 30° with an amplitude of ±5°. The range of pitch oscillations was chosen so that the location of vortex breakdown remained over the surface of the delta wing throughout the motion and so that a visible range of movement in the location of vortex breakdown could be seen. In addition, the experiments involving roll motion were conducted at a pitch angle of 30° to allow for comparison with available data and consequently, conducting the unsteady pitch experiments at the same mean angle of attack provided for some continuity of data collection. The unsteady pitch experiments were carried out at four different reduced frequencies. These were $k_{pitch} = 0.12$, $k_{pitch} = 0.27$, $k_{pitch} = 0.40$, and $k_{pitch} = 0.52$ which corresponded to pitch frequencies of 0.023 Hz, 0.051 Hz, 0.074 Hz and 0.097 Hz, respectively. Data was collected for a number of cycles of motion to ensure and to quantify data repeatability. This method was consistent with the methods used by LeMay[25] and Thompson[23]. Figure 5.9 shows an example of the raw data collected for six cycles of motion at each of the reduced frequencies to illustrate the data repeatability. The arrows on the graphs indicate the direction of motion. The arrows pointing up indicate the upstroking portion of the cycle where angle of attack was increasing and the arrows pointing down indicate the downstroking portion of the cycle where the angle of attack was decreasing. The lines drawn on each graph represent a second ordered curve fit of the experimental data. Interestingly enough, these lines compared quite well with the data collected under steady state conditions.

Unfortunately, the amount of data presented on the graphs in Figure 5.9 provides

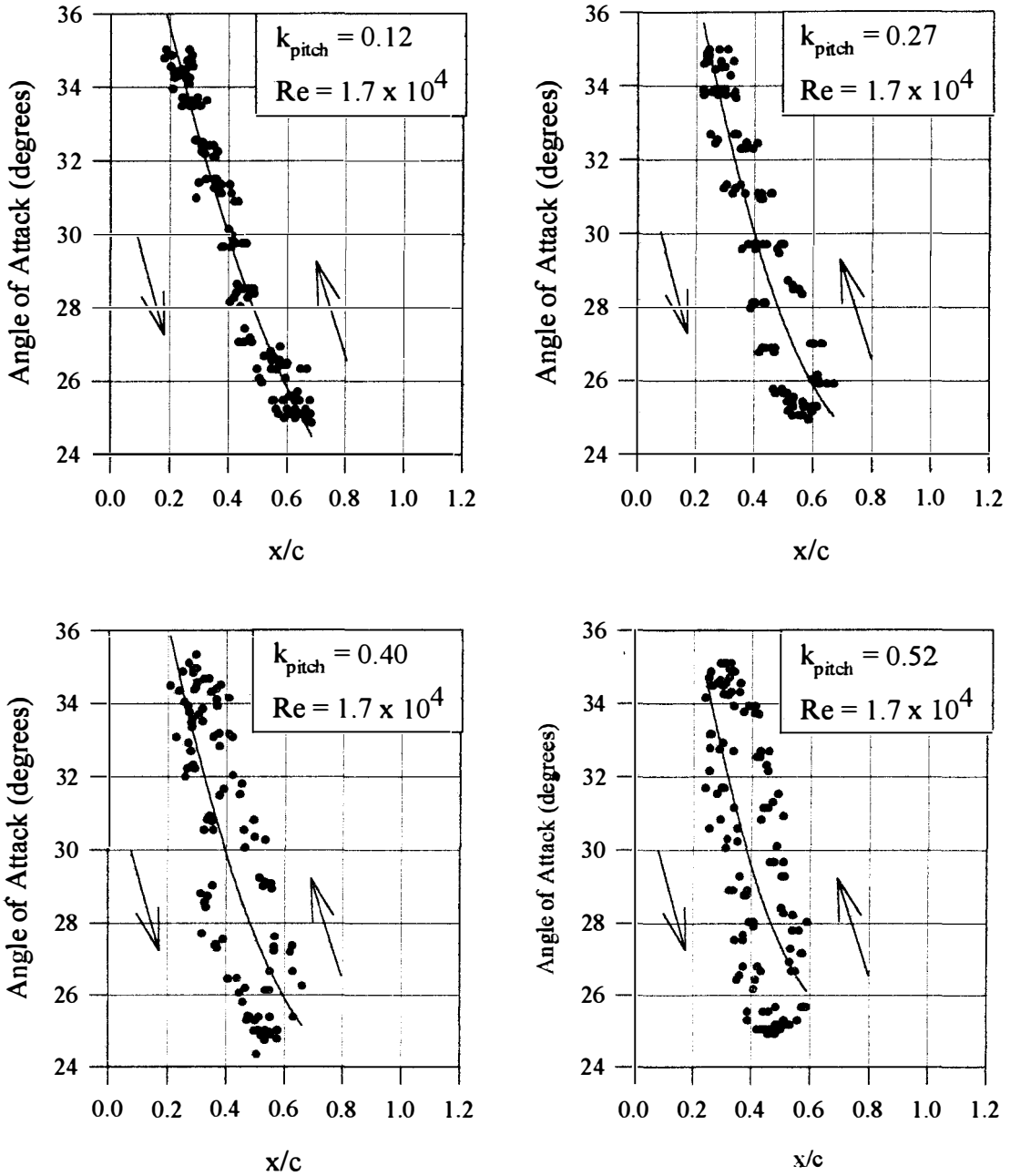

Figure 5.9. Vortex Breakdown Location for Six Cycles of Unsteady Motion

clutter and makes it difficult to conduct a very accurate analysis; although, the trends are still visible. The raw data was averaged over the six cycles to reduce the amount of clutter on the graphs. The results are presented in Figure 5.10 for each of the reduced frequencies tested. The individual data points represent an average of the six cycles analysed and the error bars shown were calculated using the standard deviation. As discussed, the arrows indicate the direction of the wing motion. In addition, the second ordered approximation of the steady state data has been provided so that a direct comparison can be made.

For the lowest reduced frequency tested, $k_{pitch} = 0.12$, the unsteady data compared with the steady data with only slight deviations which were not quite symmetric about the steady data. In fact, the vortex breakdown locations for $k_{pitch} = 0.12$ tended to lag the steady data on the upstroke but was generally comparable to the steady data on the downstroke. As the reduced frequency was increased to $k_{pitch} = 0.27$, the deviations of the unsteady data with the steady data became more symmetric about the steady data and the overall movement of the vortex breakdown decreased. LeMay[25] also made this conclusion regarding symmetry; however, the largest reduced frequency he examined was $k_{pitch} = 0.3$. The experimental results of this study expands the analysis to a reduced frequency of $k_{pitch} = 0.40$ and then $k_{pitch} = 0.52$. The data for all four reduced frequencies examined is provided in Figure 5.11 which shows the location of vortex breakdown for unsteady pitch oscillations as it compares to steady state conditions. Referring to Figure 5.11, it can be seen that, as the reduced frequency was increased above $k_{pitch} = 0.27$, the hysteresis loops continued to expand away from the steady state data but is also rotated

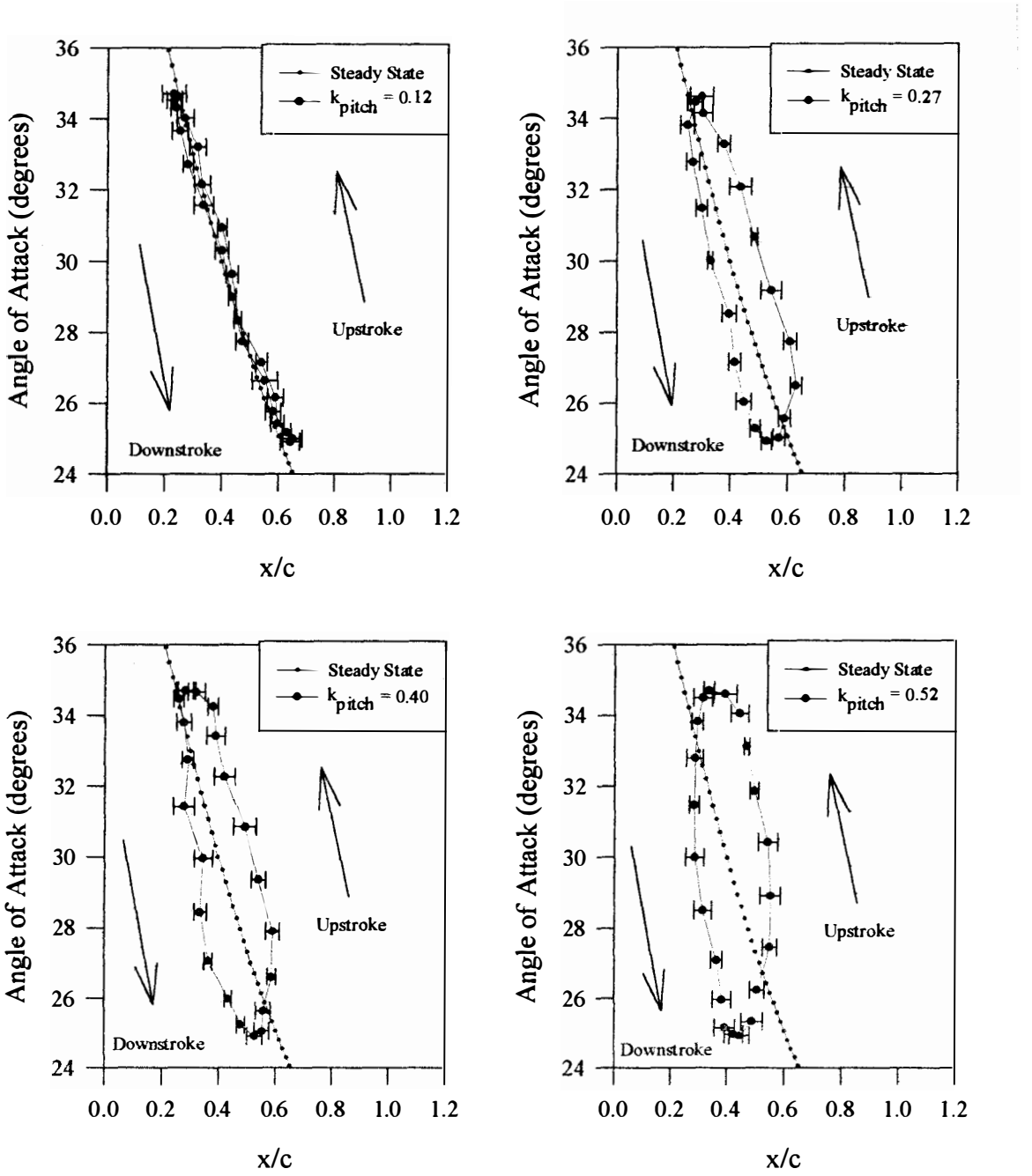

Figure 5.10. Location of Vortex Breakdown for Unsteady Pitch

Oscillations of 30° ± 5°

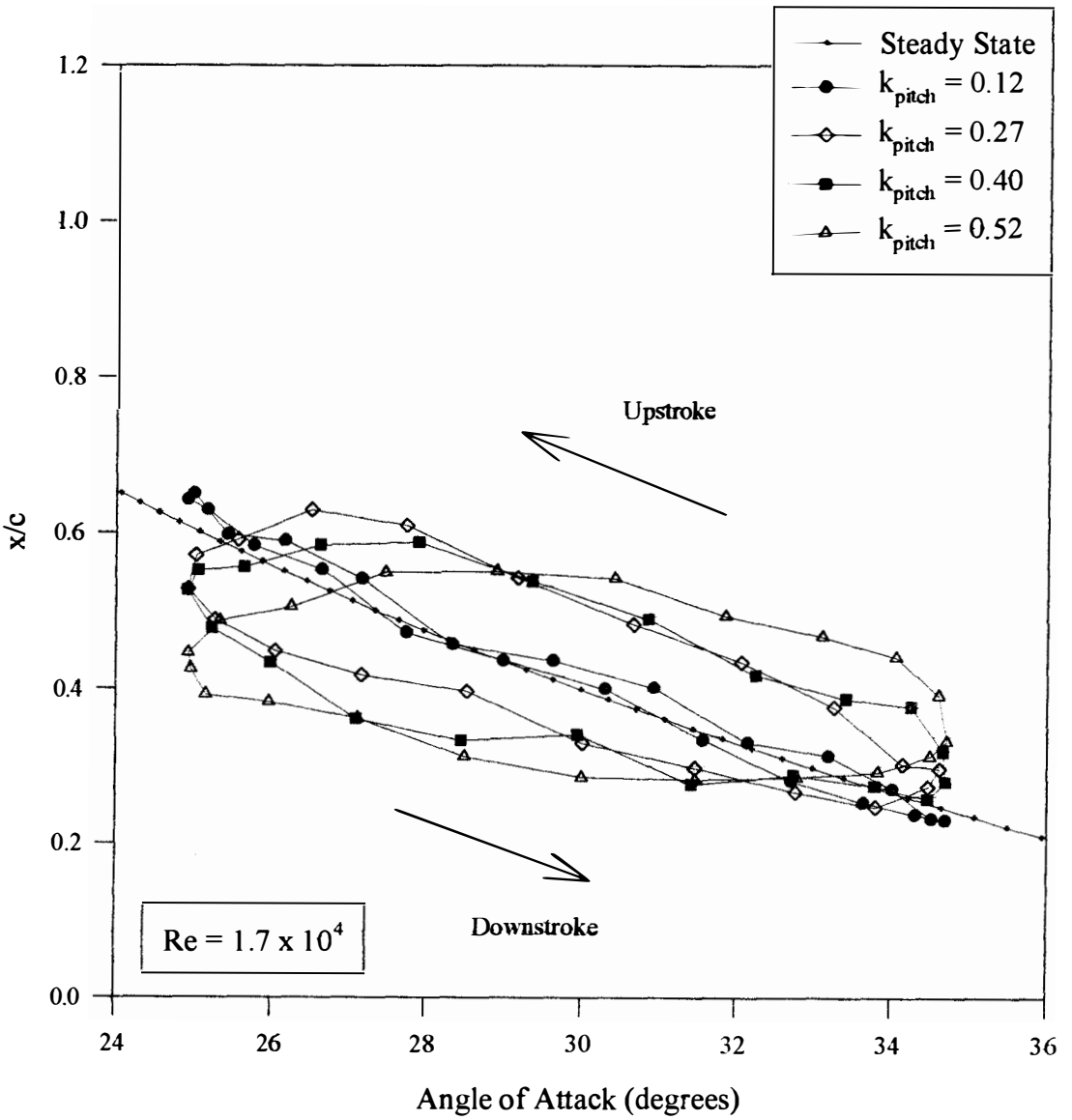

Figure 5.11. Location of Vortex Breakdown for Unsteady Pitch Oscillations of 30° ± 5° as Compared to Steady State Conditions

away from the steady state data. This behaviour was a result an increased hysteresis effect that is shown in a continual restriction of the movement of the location of the vortex breakdown with reduced frequency. Presumably, if the reduced frequency was increased sufficiently high, there would be no movement of the vortex breakdown position at all. In fact, based on the data that is shown in Figure 5.11, the fixed location of vortex breakdown could be that which would exist under steady state conditions.

As discussed, the restriction of the movement of vortex breakdown with reduced frequency is an indication of an increased hysteretic effect which is shown by the reduction in size and by the continual rotation of the hysteresis loops away from the steady state conditions. To illustrate this point, an analysis of the relative locations of the end points has been conducted. The results, provided in Table 5.1, show that, as reduced frequency increased, the end points of the data moved away from the steady state data. These results were consistent with LeMay[25] as shown by Figure 2.13. It was not possible to compare the two studies quantitatively since the model used by LeMay[25] was different (double bevel versus single bevel) and the pitch oscillations were about a mean angle of attack of 34° versus 30°; however, the similarity of trends established in the two studies supports the results of this study.

Vortex Core Angle During Unsteady Pitching Motion

The behaviour of the vortex core angle during unsteady pitching oscillations was examined to determine its relationship with angle of attack as a function of reduced

Table 5.1. Location of Vortex Breakdown at Data End Points Versus Reduced Frequency (Unsteady Pitch)

Location of Vortex Breakdown (x/c)		
Reduced Frequency	Pitch = 25° Roll = 0°	Pitch = 35° Roll = 0°
Steady State	0.60	0.24
$k_{pitch} = 0.12$	0.64	0.23
$k_{pitch} = 0.27$	0.53	0.28
$k_{pitch} = 0.40$	0.53	0.30
$k_{pitch} = 0.52$	0.44	0.33

frequency. The data were collected over six cycles of pitching motion and are presented Figure 5.12 as an average for all four reduced frequencies investigated. In addition, the steady state data and a linear approximation of the steady state data has been included. The data in Figure 5.12 demonstrates that the linear relationship between vortex core angle and angle of attack which existed for steady state conditions continued to exist during unsteady conditions for a given reduced frequency. In fact, all the unsteady data presented in Figure 5.12 correlates well with the steady state data. Interestingly though, Figure 5.12 does show that the data for the lower reduced frequencies tends to be at the top of the data band and the data for the higher reduced frequencies tends to be at the bottom of the data band. For a given angle of attack, this could mean that, as reduced frequency increased, the vortex core angle decreased and consequently the vortex angle increased. The data presented represents not only the average of six cycles of oscillatory motion but also represents the average of the upstroke angle and the downstroke motion. The results, therefore indicate that on the average, the flow during the downstroke portion of the cycle, took longer to adjust to the flow conditions than that during the upstroke portion. This is considered a minor observation since the unsteady data in Figure 5.12 certainly falls within the limits of the steady state data. Therefore, it is concluded that the vortex core angle, θ_{CORE} and consequently the vortex angle, θ, is essentially independent of reduced frequency.

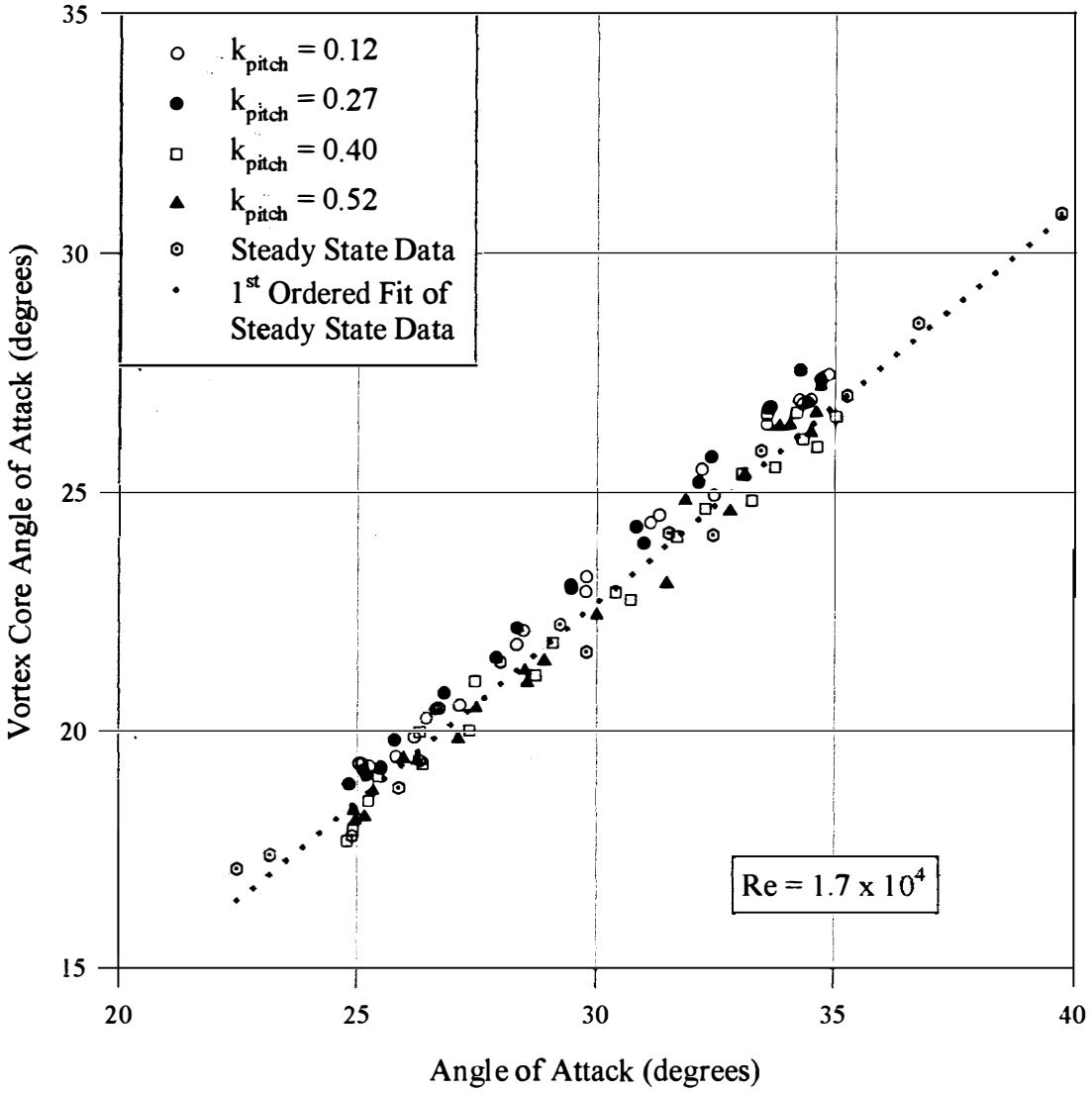

Figure 5.12. Vortex Core Angle Relative to the Horizon Versus Angle of Attack For Unsteady Pitch Oscillations

Phase Lag Due to Unsteady Pitch Oscillations

An investigation into the relationship between the location of vortex breakdown and the instantaneous position of the oscillating delta wing has been carried out. The data presented in Figure 5.13 provides information with respect to the vortex breakdown location as it relates to time. Data from six cycles of oscillations have been analysed to present the average breakdown location over one complete cycle. The error bars shown have been calculated using standard deviation. Data has been presented for all four value of reduced frequency and a difference in symbols has been used to identify the downstroke and the upstroke portion of the delta wing motion. Referring to the data in Figure 5.13, some observations can be made regarding the vortex breakdown location and how it corresponds to the motion of the delta wing. For $k_{pitch} = 0.12$, for example, the location of vortex breakdown moves aft as the delta wing pitches down; however, even after the delta wing has made the transition to the upstroke (as noted by the change in symbol), the location of vortex breakdown continued to move aft until it finally adjusted to the flow. This period of adjustment is considered a phase lag and has been recorded by other researchers. LeMay[25], for example, reported that as reduced frequency increased so did the amount of phase lag. Referring to Figure 5.13, this result has also been shown when examining the amount of time after the wing has transitioned for the location of vortex breakdown to change directions.

It is difficult, however, to compare phase lag for each reduced frequency by analysing the data presented in Figure 5.13. Therefore, the vortex breakdown location

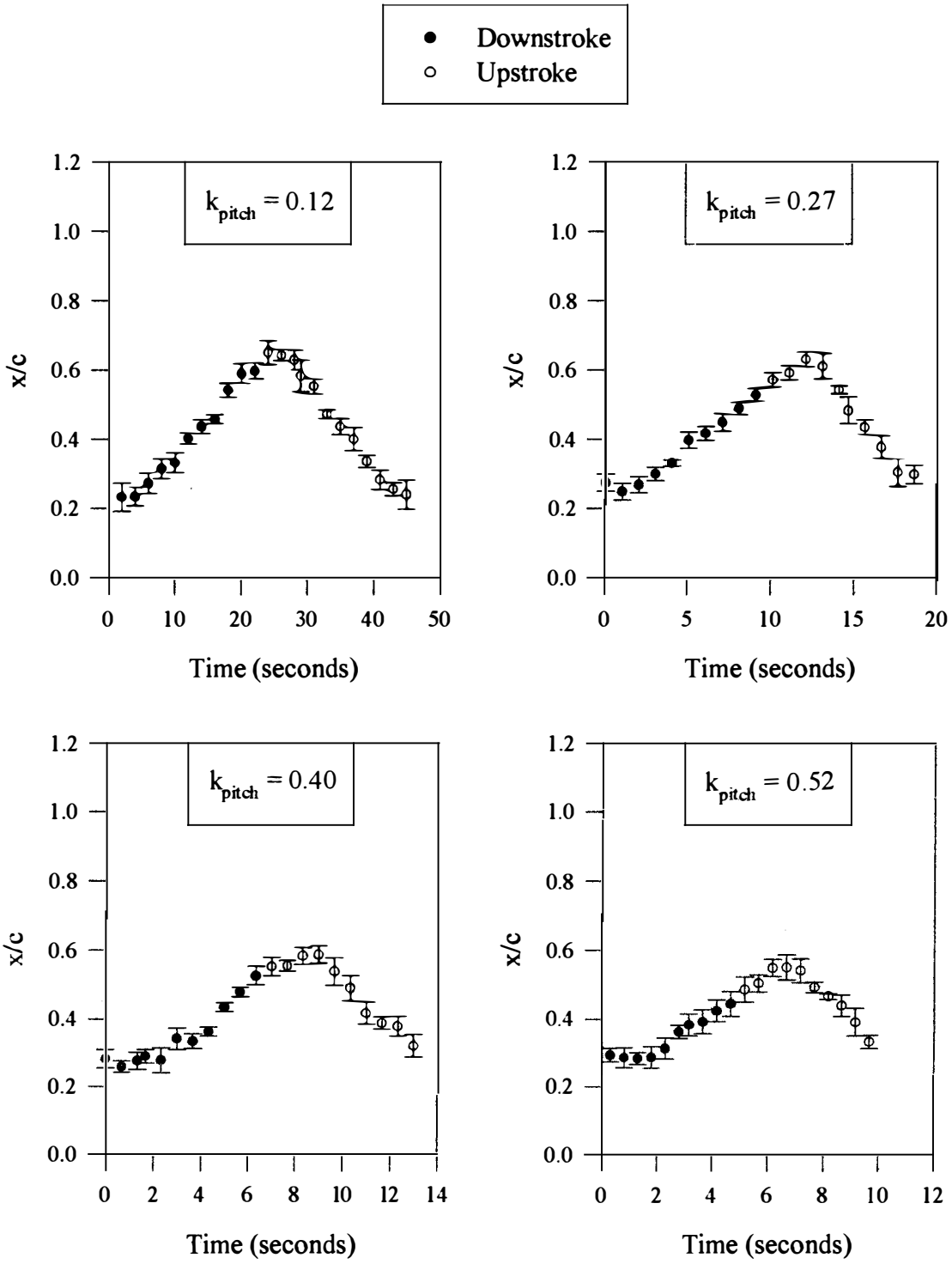

Figure 5.13. Location of Vortex Breakdown vs Time for

Unsteady Pitch Oscillations of $30^{\circ} \pm 5^{\circ}$

was compared directly to the phase angle of the model and the results are presented in Figure 5.14. Referring to Figure 5.14, the phase shift for even the lowest reduced frequency is apparent. At $\omega t = 0^o$, the delta wing motion was in transition from the upstroke to the downstroke and, the point where $\omega t = 180^o$ corresponds with the portion of the delta wing motion which is in transition from downstroke to upstroke. For both transitions, the data from this study showed that the amount of phase lag increased as reduced frequency increased. This result is consistent with the observations made by LeMay[25] as well as Gursul and Yang[21]. Although the tests conducted by LeMay[25] and Gursul and Yang[21] were carried with pitch oscillations about a different mean angle of attack, the amplitude of the oscillations were identical to those used in this study. A comparison of phase lag as a function of reduced frequency which includes some results from LeMay[25] as well as Gursul and Yang[21] is therefore provided in Figure 5.15. The data in terms of location of vortex breakdown versus time was used to identify the points where the movement of vortex breakdown reversed direction. This information in conjunction with the period for each reduced frequency was used to calculated the phase lag. The error incurred in the process was approximately $\pm 8^o$ because only 21-23 data points were used to make up each cycle. This meant that the time between each data point represented approximately 16^o of the overall cycle. Along with the inherent errors in the data and data scatter, it was difficult to pinpoint the exact location of the peaks unless the peak coincided with a data point.

A distinction was observed between the phase lag resulting from the delta wing transitioning from the downstroke to the upstroke (Dn-Up) and from the upstroke to the

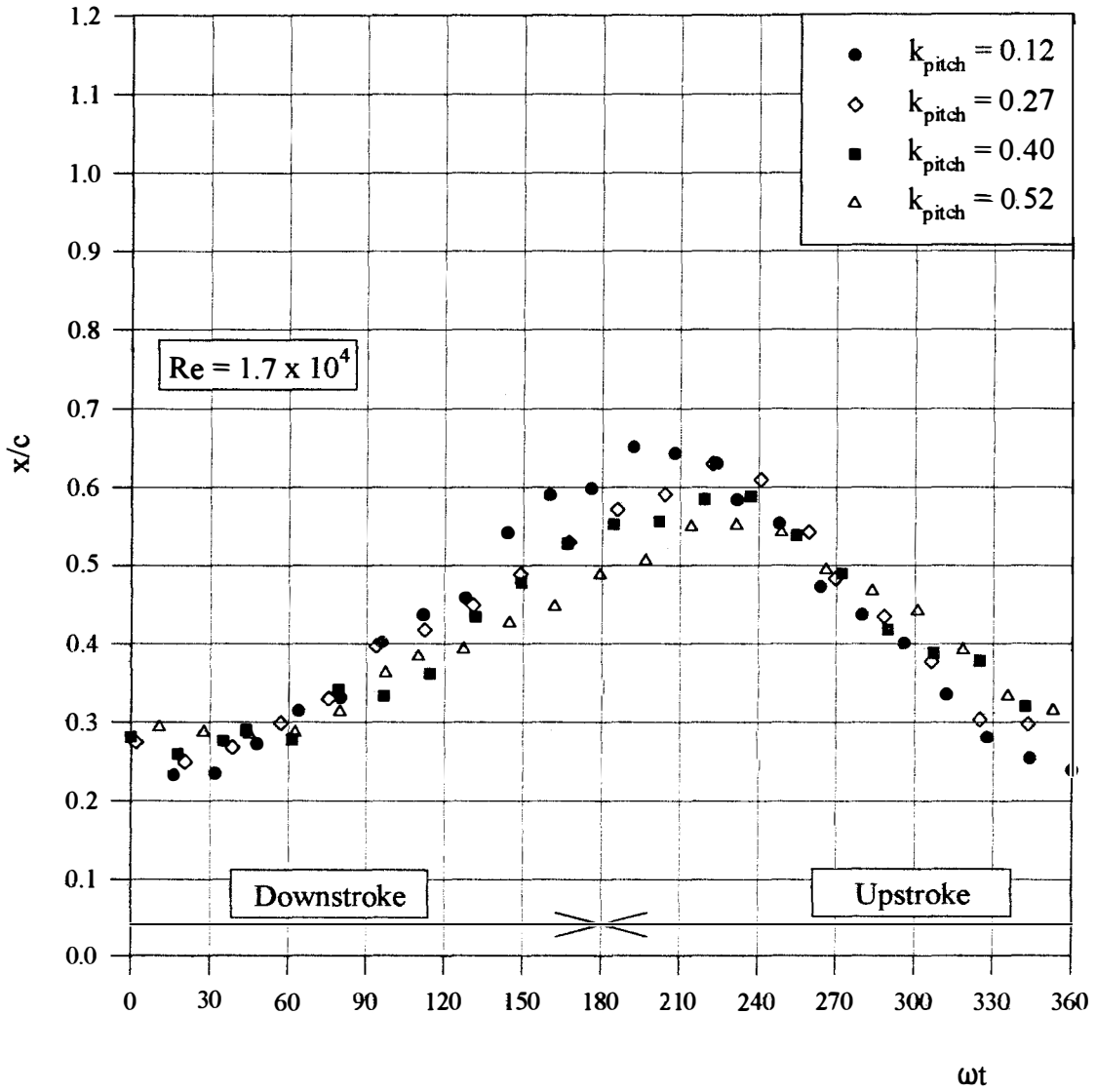

Figure 5.14. Location of Vortex Breakdown vs ωt for

Unsteady Pitch Oscillations of 30° ± 5°

downstroke (Up-Dn). There was a notable increase in phase lag when the delta wing transitioned from the downstroke to the upstroke as compared to the transitioned from the upstroke to the downstroke. Figure 5.15 shows that there is good comparison between the Up-Dn data and published data even though LeMay's[25] test model differed in leading edge geometry and the tests conducted by LeMay[25] and Gursul and Yang[21] were carried out at a different mean angle of attack. It is concluded therefore that a difference existed for phase lag with respect to reduced frequency which depends on the direction of motion of the delta wing.

Summary of Pitch Experiments

Experimentation of a 70° delta wing involving variation of angle of attack under steady state conditions has been carried out for angle of attack variation from 23° to 40°. The resultant steady state data compared well with that presented by Thompson[23]. This comparison provided a verification of results since the model used in this study was an exact replica of the model used by Thompson[23]. The experimental data showed that with an increase in angle of attack, the location of vortex breakdown moved toward the apex and with a decrease in angle of attack, the location of vortex breakdown moved aft. This result was consistent with all published data. In addition, it was observed that, over the range of angle of attack investigated, the transition in the movement of the location of vortex breakdown was smooth. This was illustrated by an approximation of a second ordered curve fit through the data. Comparison with data from Thompson[23] showed

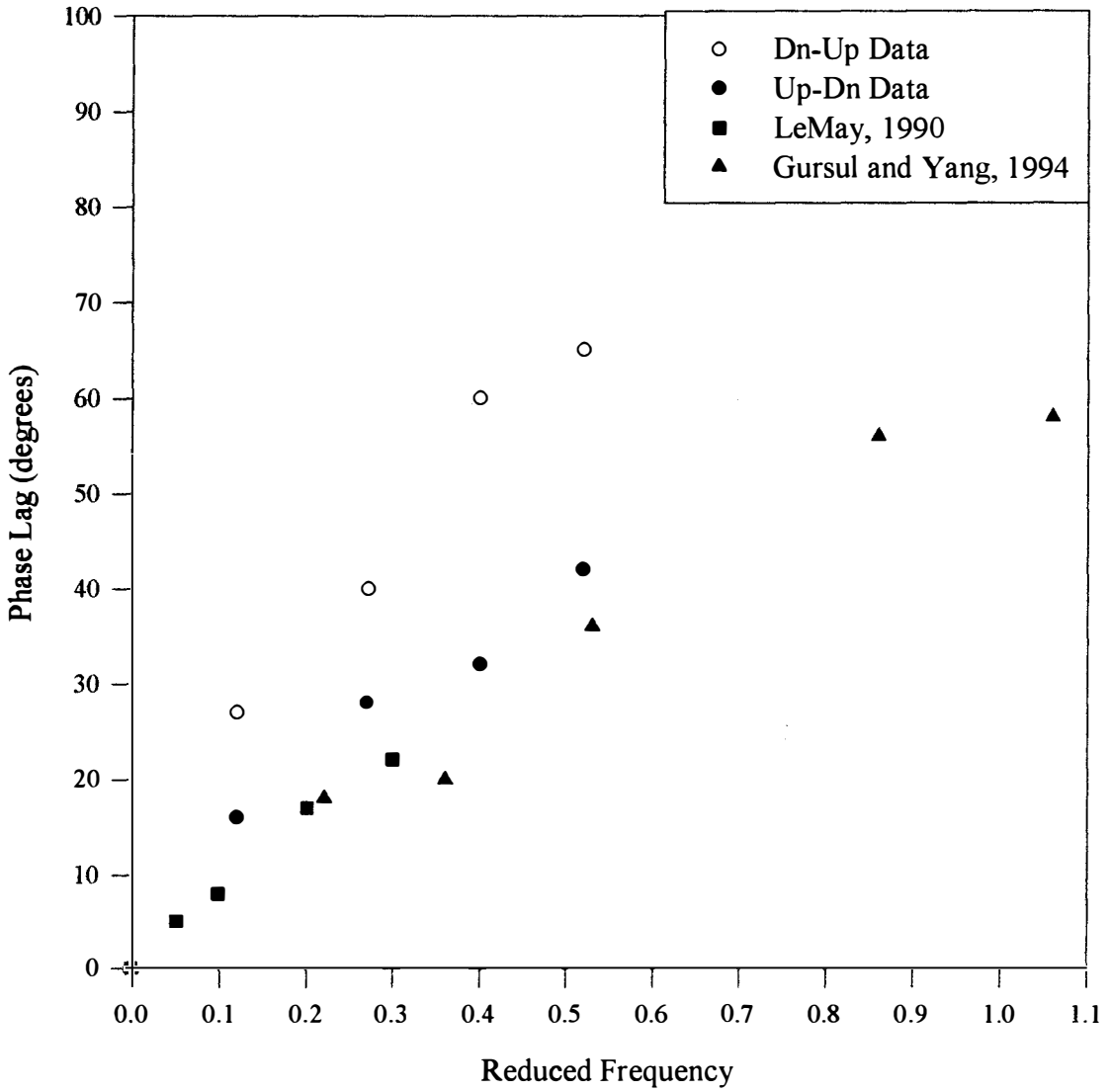

Figure 5.15. Phase Lag as a Function of Reduced Frequency for Unsteady Pitch Oscillations ($30° \pm 5°$)

this result to be consistent; however, comparison with other researchers data showed that the movement in the location of vortex breakdown should have been more pronounced in the 25° -35° range. Based on the review of numerous studies, it was concluded that the discrepancies could have be attributed to differences in geometrical similarity of model geometry. Differences in model geometry have been noted to significantly affect the location of the vortex breakdown and so, it was concluded that duplication of exact model geometry was one of the key factors in enabling data reproduction.

Two empirical prediction equations (Equation 6 & 8) developed by Huang and Hanff[17,18] provided for good correlation with published 70° delta wing data; however, did not provide for correlation with the results of this study. This was expected considering the implications of the model geometry and the corresponding data used to develop the equations. A modification to the prediction equations to accounted for a difference in leading edge geometry was carried out and provided for good correlation of data. Thompson[23] examined a similar shift in data which he attributed to a difference in leading edge geometry between a single bevel leading edge and a double bevel leading edge. When quantitatively comparing the shift reported by Thompson[23] and that effected by the change in the prediction equations, there was good comparison. The intent of this study, however, was not to validate nor to develop an analytical model that would predict the location of vortex breakdown. Caution must be exercised when generalizing the use of empirical methods because of their sensitivity to the test conditions under which they were developed. The modifications to the prediction equations were carried out so that results from this study could be compared to each other. It was concluded,

however, that the leading edge geometry of the delta wing design plays a significant role in affecting the location of the vortex breakdown.

Experimental investigations were carried out with the 70° delta wing oscillating in pitch about the centre chord at a mean angle of attack of 30° with an amplitude of oscillation of ±5°. The study was conducted at four values of reduced frequency ranging from $k_{pitch} = 0.12$ and $k_{pitch} = 0.52$ which corresponded to pitch frequencies ranging from 0.023 Hz to 0.097 Hz. The resultant experimental data was presented so that a comparison with the steady state conditions could be carried out. The results demonstrated that as reduced frequency of the pitch oscillations were increased the amount of hysteresis in the location of the vortex breakdown also increased. This was observed by the restriction in the movement of the location of vortex breakdown as the reduced frequency increased. These results compared well with the results published by LeMay[25]. A direct comparison, however, could not be made because LeMay[25] analysed a different range of motion (34° ± 5°) and the model used in his study had a double bevel leading edge. Still the trends of the results in both studies were similar. It was concluded, therefore, that this study has extended the usable base of data for a 70° delta wing which includes a different range of pitching motion.

An analysis was carried out to determine the behaviour of the vortex angle under steady and unsteady changes in angle of attack. For the steady state conditions, the experimental data showed a linear relationship between vortex angle and angle of attack which compared well with the results from Thompson[23]. In addition, it was observed that the experimental results from this study also compared well with water and wind

tunnel results published by Erickson[35]. A distinction was made between the vortex angle, θ, (which is formed between the vortex core and the wing surface) the vortex core angle, θ_{CORE}, (which is formed between the vortex core and the horizon). It was observed that some researchers had used both, but that both allowed for good comparison of results.

For unsteady pitching conditions, the behaviour of the vortex core angle was investigated to determine its relationship with reduced frequency. The experimental data demonstrated that under conditions of unsteady pitch, there was still a linear relationship between vortex core angle and angle of attack which compared well with the steady state relationship observed. Consequently, it was concluded that the behaviour of vortex core angle as a function of angle of attack was independent of reduced frequency.

It has been observed in this study and in the studies of other researchers that when a delta wing undergoes a pitching motion, there is a phase lag in the corresponding movement in the location of vortex breakdown as the vortex is continually adjusting to the changing flow conditions. Accordingly, an investigation was carried out in this study to examine the relationship between the instantaneous position of the delta wing model and the corresponding location of vortex breakdown as a function of reduced frequency. The results of this study showed that an increase in reduced frequency resulted in an increase in the amount of phase lag. This result was consistent with studies from LeMay[25] and Gursal and Yang[21]. It was observed, however, that there was a distinct difference in the behaviour of vortex breakdown when the wing changed from upstroke to downstroke (Up-Dn) and from downstroke to upstroke (Dn-Up). It was concluded that there was a

notable increase in phase lag when the delta wing transitioned from the downstroke to the upstroke as compared to the phase lag when the wing transitioned from the upstroke to the downstroke.

CHAPTER VI

RESULTS AND DISCUSSIONS: ROLL EXPERIMENTS

Steady State Roll Analysis

This study investigated the behaviour of vortex breakdown over a 70° delta wing for steady state variations in roll angle at a fixed pitch angle. The roll angle was varied from -18° to 18° while the delta wing was fixed at a pitch angle of 30°. The Reynolds number during the testing was 1.7×10^4. The delta wing model used in this study was designed with two dye ports located just beneath and to either side of the apex. Consequently, there were two vortices that were visualized at all times which provided two complete sets of data with which to investigate and make comparisons. As a check of the model setup, initial verification was always carried out to ensure that the locations of vortex breakdown were symmetric for zero roll angle. Data was collected with roll angle increments in the positive direction. The flow was allowed a settling time between roll angles to enable the flow to stabilize. Similar to the steady state pitch analysis, twenty consecutives video frames of data were analysed for each roll angle. The results presented in Figure 6.1 represent the average steady state locations of vortex breakdown for variations in roll angle at a pitch angle of 30°. The error bars shown on the graph are estimates of data repeatability that have been calculated using the standard deviation.

Referring to Figure 6.1, the two sets of data provided relate to the vortex

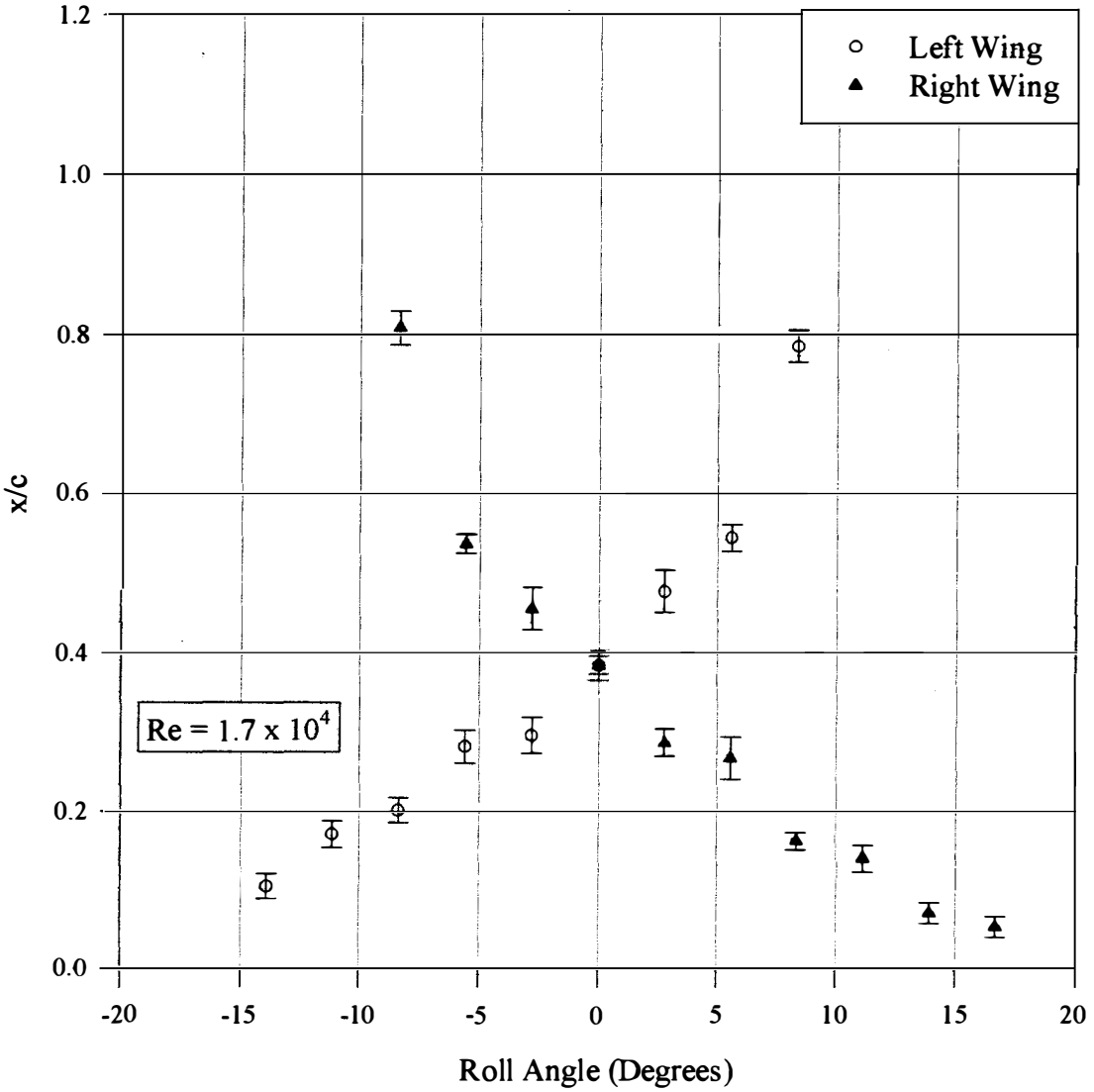

Figure 6.1. Location of Vortex Breakdown for Steady State Variations in Roll

behaviour for the left side of the wing and for the right side of the wing, respectively. For the right wing, for example, the data show that, as the roll angle increased, the location of vortex breakdown moved towards the apex and as the roll angle decreased, the location of vortex breakdown moved aft toward the trailing edge. Physically speaking, this makes sense. For the right wing, an increase in roll angle meant that the right wing rolled down. Because the delta wing was pitched, the right wing was rolled into the flow and therefore experienced an effective decrease in sweep angle (refer to Equation 7). Concurrently, though there was an offsetting decrease in angle of attack which would tend to cause the location of vortex breakdown to move aft. The comparison of the effective changes of sweep and angle of attack have been illustrated using Figure 2.10. The overriding effective change for a wing that rolled into the flow, therefore, was the decrease in sweep angle and a corresponding forward movement in the location of the vortex breakdown. This relationship is consistent with the data published by Huang and Hanff[17].

As the roll angle was decreased, the right wing rolled up and the resultant data showed that the location of the vortex breakdown moved aft toward the trailing edge. Referring to Figure 2.10, it can be seen that, when the right wing rolled up, it experienced an effective increase in sweep angle and an effective decrease in angle of attack. Both factors contributed in the same direction and caused an aft movement in the location of the vortex breakdown.

Referring to Figure 6.1, it can be seen that the behaviour of vortex breakdown over the left wing was the complete opposite to that which occurred over right wing. This is understandable since, when one side of the delta wing rolled up, the other side of the

delta wing rolled down. The fact that the initial conditions were established so that the locations of vortex breakdown for both vortices were symmetric at zero roll angle meant that the resultant data from each side of the delta wing should have been symmetric. The data from the left wing is compared to the data from the right wing in Figure 6.2. So that a direct comparison could be made with the data from the right wing, the data from the left wing was corrected by using a negative roll. Referring to Figure 6.2, it can be seen that the two sets of data compare well which gives a good indication of the symmetric behaviour of the vortex flow over the delta wing.

Referring to Figures 6.2, it would appear that the relationship between the location of vortex breakdown and roll angle is not linear; although, the behaviour over the forward half of the delta wing could be considered linear. This result is consistent with published data. Ericsson[50], for example, presented a discussion on the existence of critical flow states for rolling delta wings. In his report, he presented data that was collected by Jenkins, Myatt and Hanff[53] which showed a linear relationship between the vortex breakdown location and the roll angle for over 80% of the forward portion of a 65° delta wing that was fixed at a pitch angle of 30°. The information Ericsson[50] presented for the left wing is provided in Figure 6.3.

Referring to Figure 6.3, it can be seen that the linear approximation to the data was formed by ignoring one point that was near the trailing edge and out of range for the linear relationship. Ericsson[50] argued that the linear relationship was valid up to a certain critical state of roll angle after which the change in effective sweep would be sufficient to cause the location of vortex breakdown to move aggressively downstream. In

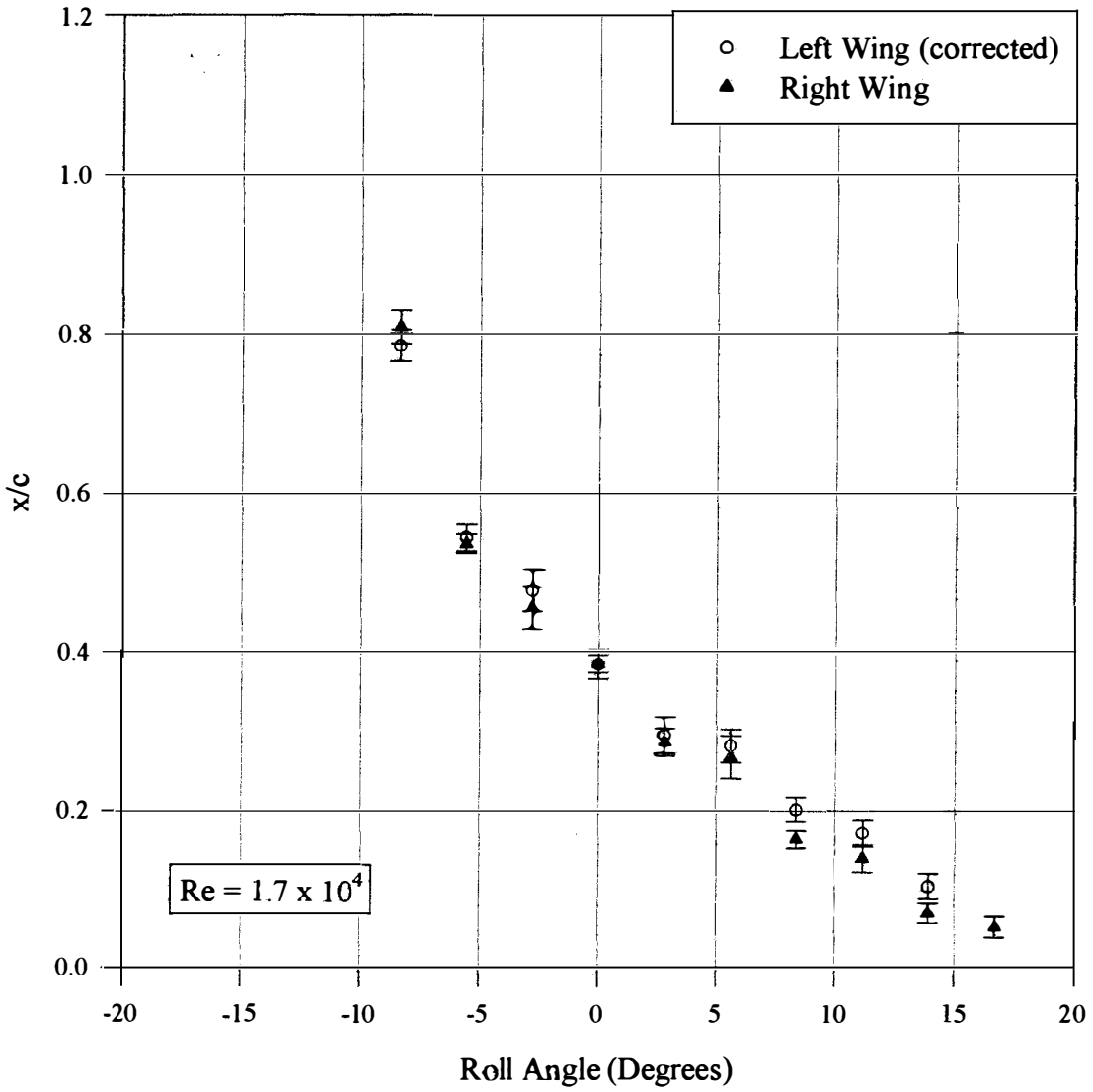

Figure 6.2. Location of Vortex Breakdown for Steady State Variations in Roll

(Left Wing Corrected)

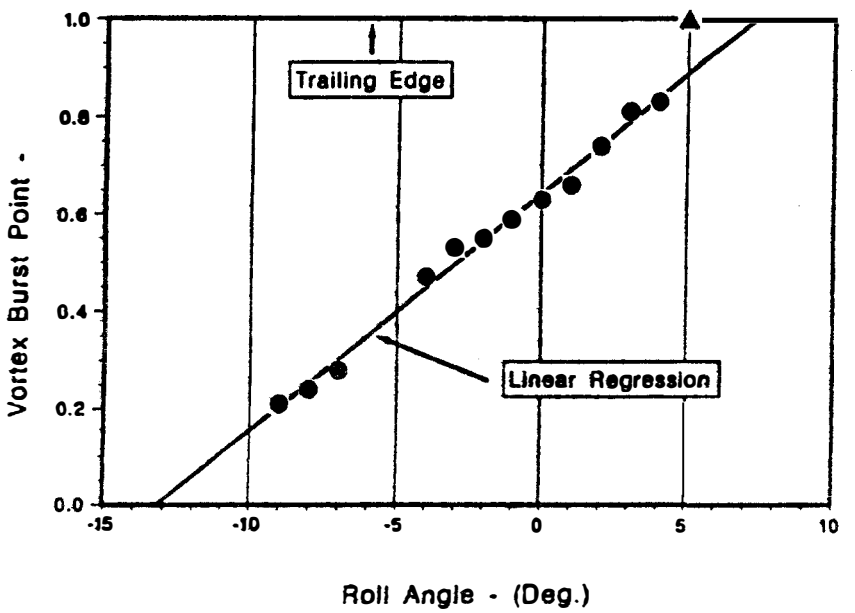

Figure 6.3. Vortex Breakdown Position. [50]

his analysis, Ericsson[50] used the information provided by Wentz and Kohlman[55] to illustrate the effect that sweep angle has on the location of vortex breakdown for a given angle of attack. The graph was provided as Figure 2.9.

Ericsson[50] used the following argument to illustrate his point. He examined a 65° delta wing pitched at 30° for which the effective angle of attack would be slightly below 30° once the wing was rolled. Using the data in Figure 2.9, it can be seen that the location of vortex breakdown would be at the apex for sweep angle of approximately 58°. If the sweep angle were to increase, as in the case when the left wing undergoes a positive roll angle, the location of the vortex breakdown would gradually move aft toward the trailing edge. An increase in sweep angle to 60° would result in the location of the vortex breakdown moving aft to approximately x/c = 0.15. An additional increase in sweep to 65° would result in the location of the vortex breakdown being at approximately x/c = 0.25 and a further increase in sweep to 70° would result in the aft movement of the vortex breakdown to approximately x/c = 0.6. This last significant change would explain the aggressive aft movement of the location of vortex breakdown should the roll angle be sufficient to effect a change in sweep angle close to 70°. Referring to Figure 6.4, which shows the relationship of roll angle on effective leading edge sweep and effective angle of attack for a 65° delta wing, the critical roll angle required to produce an effective sweep angle of 70° is approximately 7°. The data point that was out of limits for the linear regression in Figure 6.3 was collected at a roll angle of 5° which is certainly approaching the critical roll angle. Therefore, the decision to not use the point at the trailing edge in the assessment of the linear relationship was sound and justified.

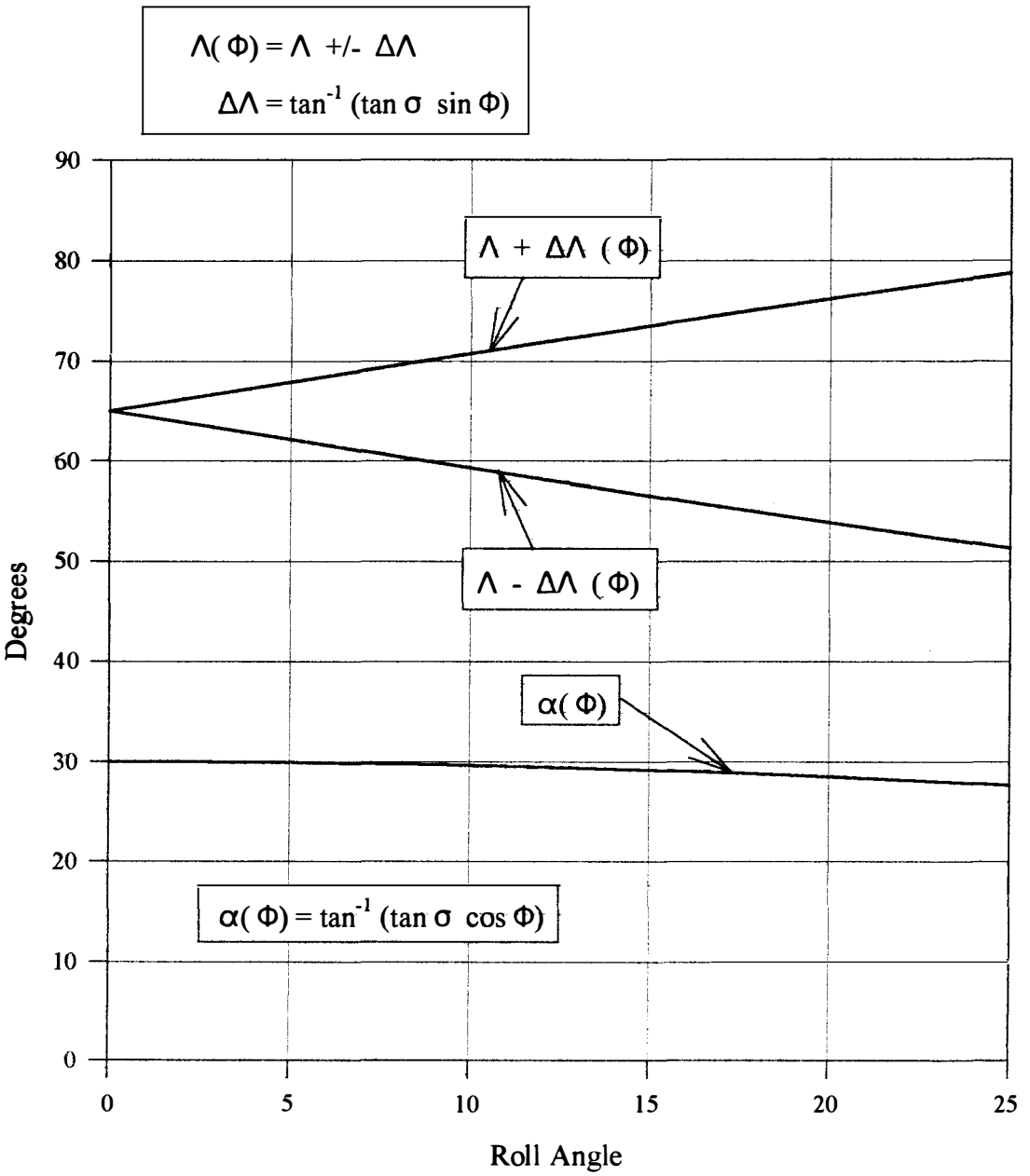

Figure 6.4. Effect of Roll Angle on Effective Leading Edge Sweep and Angle of Attack for a 65° Delta Wing.

In this study, a similar observation was made whereby the data over the aft half of the wing did not correlate linearly or quasi-linearly with the data from the front half of the delta wing. This result is consistent with Ericsson's[50] discussion of critical states. Referring to Figure 6.2, it can be seen that the data points nearest the trailing edge were a result of a negative roll angle with a magnitude of 8.3° (right wing). From Figure 2.10, it can be seen that the effective sweep angle at that roll angle was approximately 75° and the effective angle of attack was slightly less than 30°. For a delta wing with a 75° sweep angle, the data in Figure 2.9 can be used to give a good indication of the behaviour of the location of vortex breakdown at this angle of attack keeping in mind that the data should be corrected for a change in leading edge geometry. Once the 70° delta wing was rolled to provide an effective sweep of 75° at angle of attack of approximately 30°, the location of the vortex breakdown should have been well aft of its initial condition. The complexities of the difference in leading edge geometry, however, make it difficult to predict the precise location.

Disregarding the data points nearest the trailing edge of the wing, the data over the forward half of the wing could be fitted quite accurately with a linear or second ordered approximation as shown in Figure 6.5. Although Ericsson[50] shows his approximation to be linear, Huang and Hanff[17] have shown their's to be quasi-linear.

Referring to Figure 6.5, the linear approximation intersects the roll axis at approximately 18° which means that for a roll angle of approximately 18° the vortex breakdown location should be at the apex. Referring to Figure 2.10, this relates to a sweep angle of approximately 60° and an angles of attack of approximately 29°. In Figure

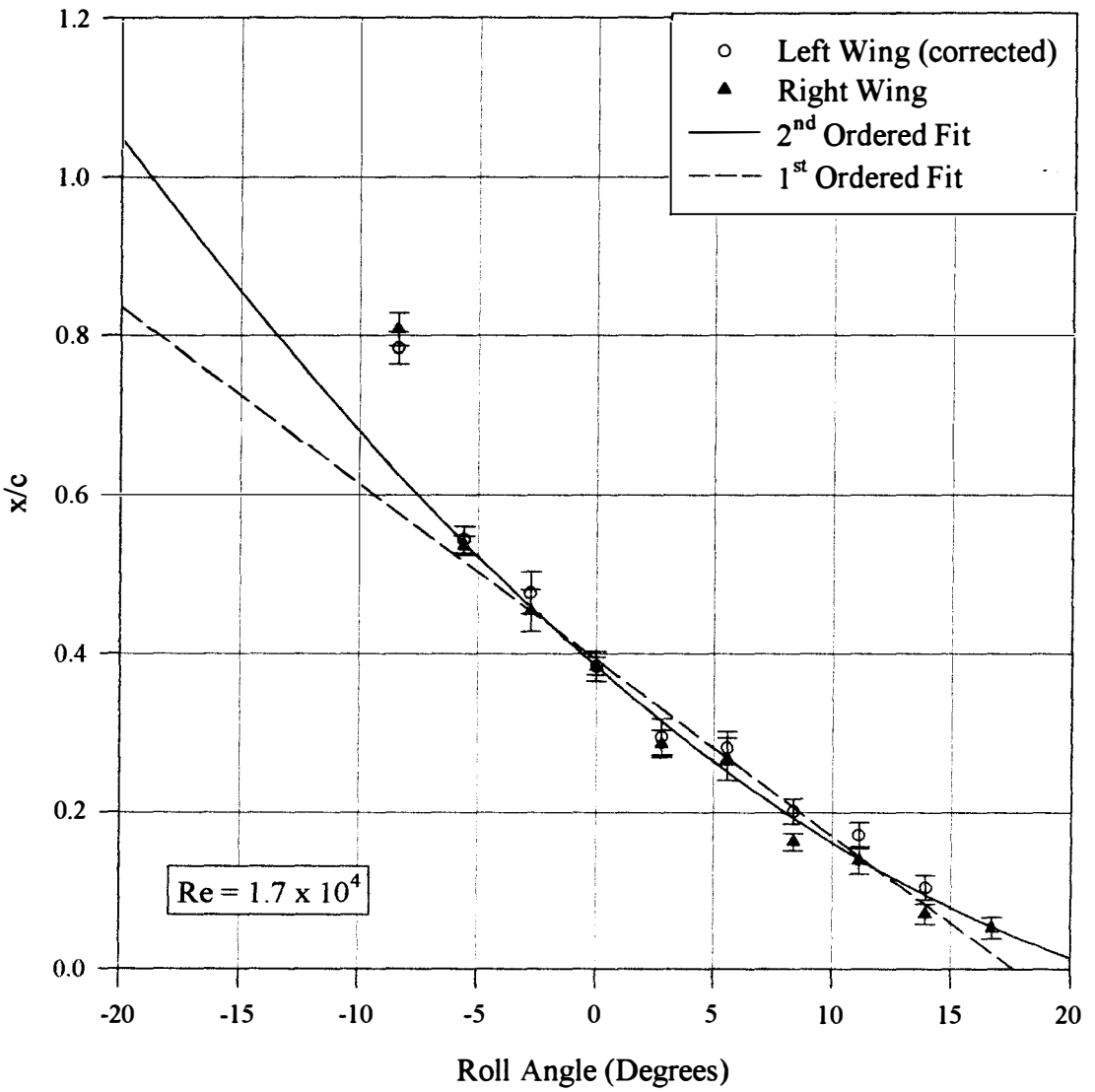

Figure 6.5. First and Second Ordered Approximation of Steady State Locations of Vortex Breakdown for Variations in Roll

6.4, an angle of attack of 29° intersects the 60° delta wing curve at approximately x/c = 0.10 which corresponds well with the amount corrected for the difference in leading edge geometry.

The steady state prediction equations presented in this study (Equation 19 and 20) have shown good correlation to experimental pitch data once modified for what was assumed predominately to be a difference in leading edge geometry. The information presented in Figure 6.6 shows a comparison of prediction versus experimental results for each of the prediction equations under variations in roll. In addition, the first and second ordered approximation have also been included. Referring to Figure 6.6, it can be seen that both equations provide a good estimate of experimental data for the flow over the front half of the delta wing. Neither equation, however, accurately predicts the location of the vortex over the aft portion of the wing. Although Equation 20 does provide an indication of a nonlinear relationship between location of vortex breakdown and roll angle, the nonlinearities in the experimental data collected in this study have not been well predicted by either prediction equation for the aft half of the wing. This conclusion is consistent with that made by Ercisson[47].

Unsteady Roll Analysis

Unsteady roll experiments were carried out with the 70° delta wing at a fixed pitch angle of 30°. The Reynolds number of the flow was 1.7×10^4. Similar to the unsteady pitch experiments, the drive mechanism provided for a sinusoidal input. The maneuvering

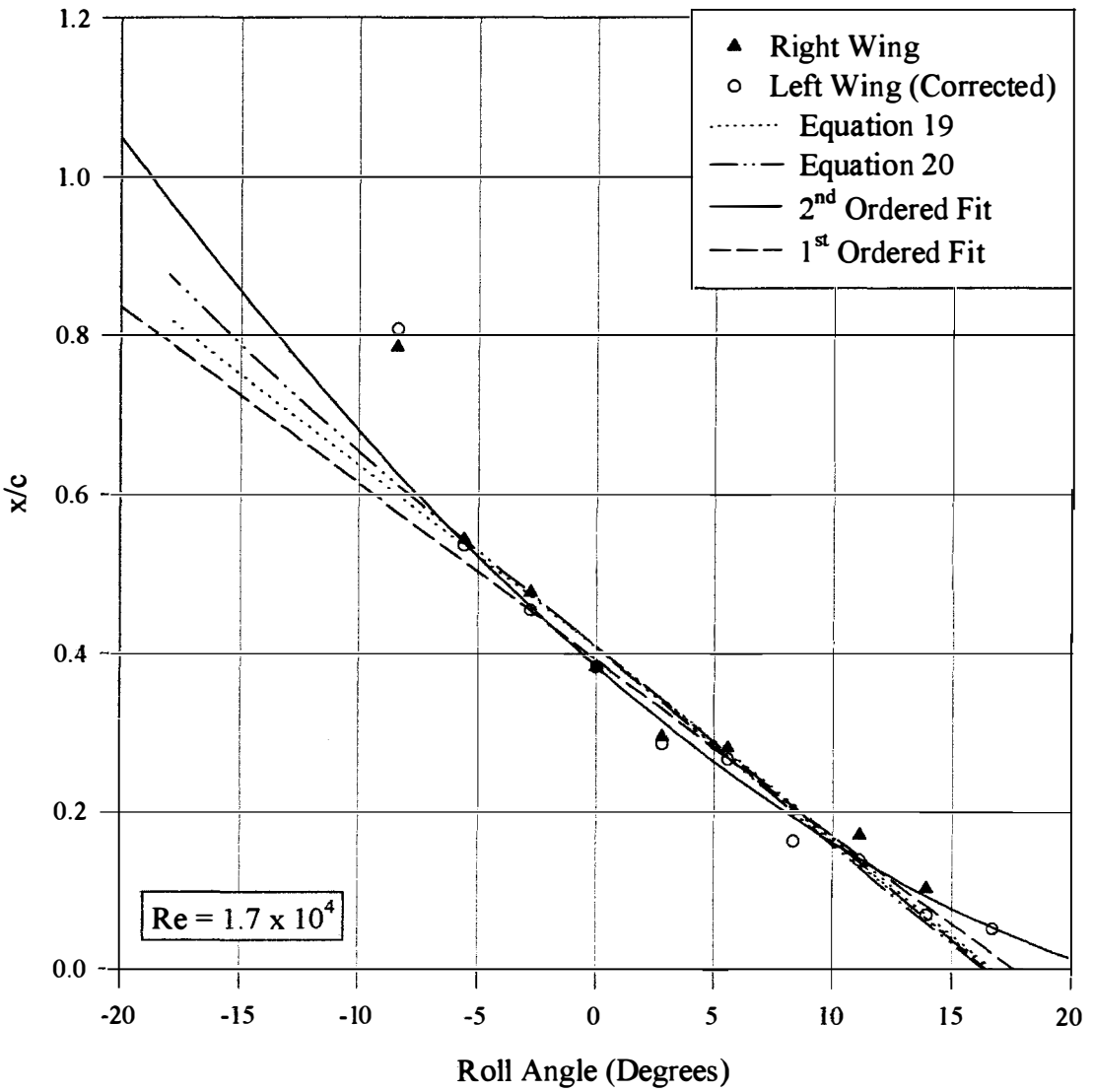

Figure 6.6. Comparison of Experimental Data With Prediction Equations

For Steady State Variations in Roll at a Fixed Pitch Angle of 30°

mechanism was set up to provide oscillations in roll of ±18° about the wing's level position. The limits of roll were chosen within the constraints of the size of the water tunnel test section. The pitch angle at which the model was fixed was selected so that comparison with available data could be made. The unsteady roll experiments were carried out at the same pitch frequencies as for the pitch experiments: 0.023 Hz, 0.051 Hz, 0.074 Hz and 0.097 Hz. Because of the difference in definition of reduced frequency for unsteady roll motion, however, this resulted in the unsteady roll experiments being conducted at four different reduced frequencies. These were $k_{roll} = 0.05$, $k_{roll} = 0.10$, $k_{roll} = 0.14$, and $k_{roll} = 0.19$, respectively. The data were collected over a number of cycles of motion to ensure and to quantify data repeatability as discussed earlier. Because the model design enabled the analysis of both leading edge vortices, the data that is presented is specified whether it was collected from over the left wing or the right wing.

The results presented in Figures 6.7 and 6.8 provide the relationship between the location of vortex breakdown and roll angle for the right and left wing, respectively. Each graph in the figures represents a different reduced frequency as annotated. The individual data points represent an average of the six cycles analysed and the error bars shown were calculated using the standard deviation. In addition, the second ordered approximation of the steady state data has been provided so that a direct comparison can be made with steady state conditions. The arrows on the graphs indicate the direction of motion. The downstroke for the right wing starts at a negative roll angle of -18° and the downstroke for the left wing starts at a positive roll angle of 18°. Conversely, the upstroke for the right wing starts at a positive roll angle of 18° and the upstroke for the left wing starts

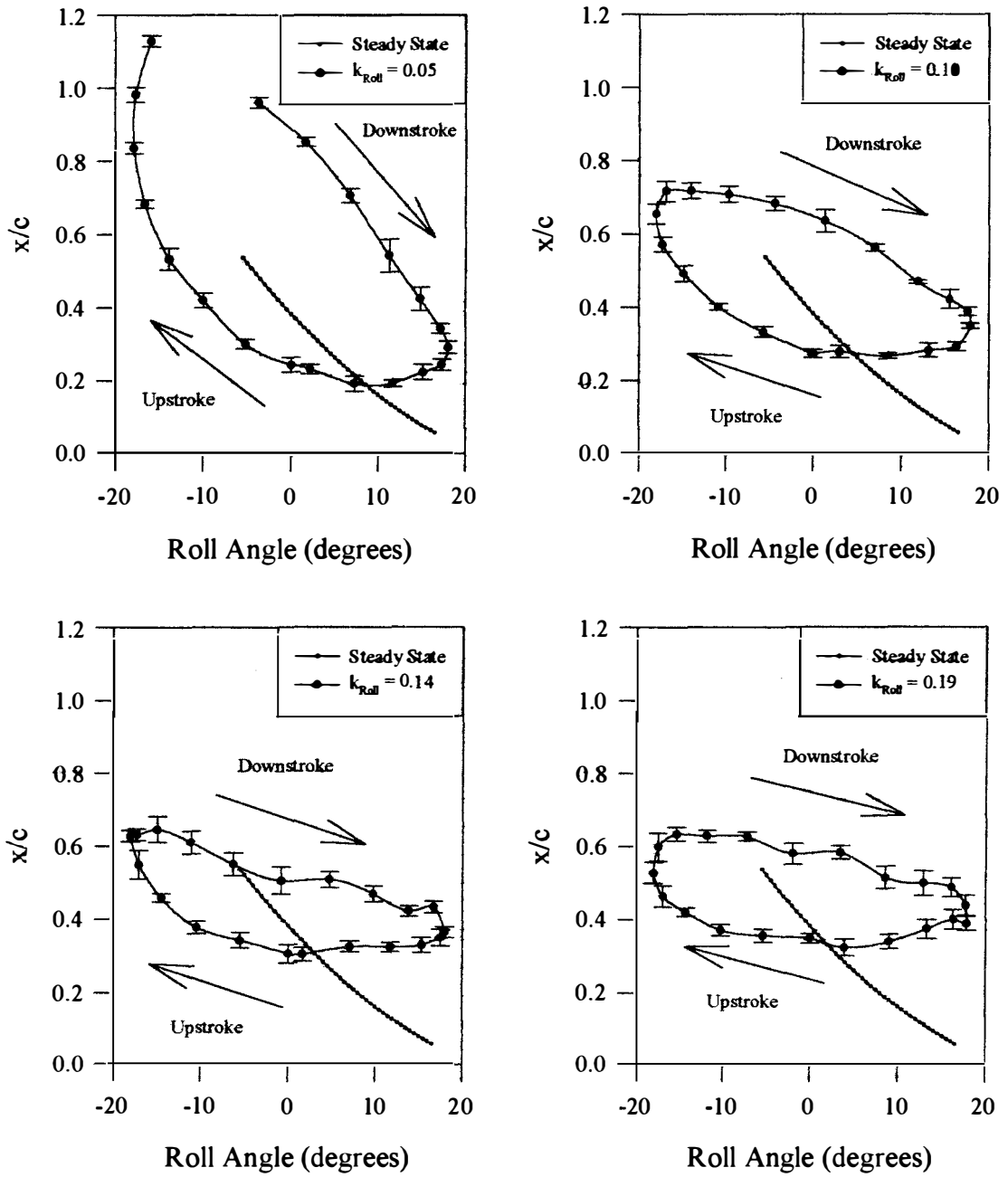

Figure 6.7. Location of Vortex Breakdown During Unsteady Roll Oscillations from ±18°

(Right Wing)

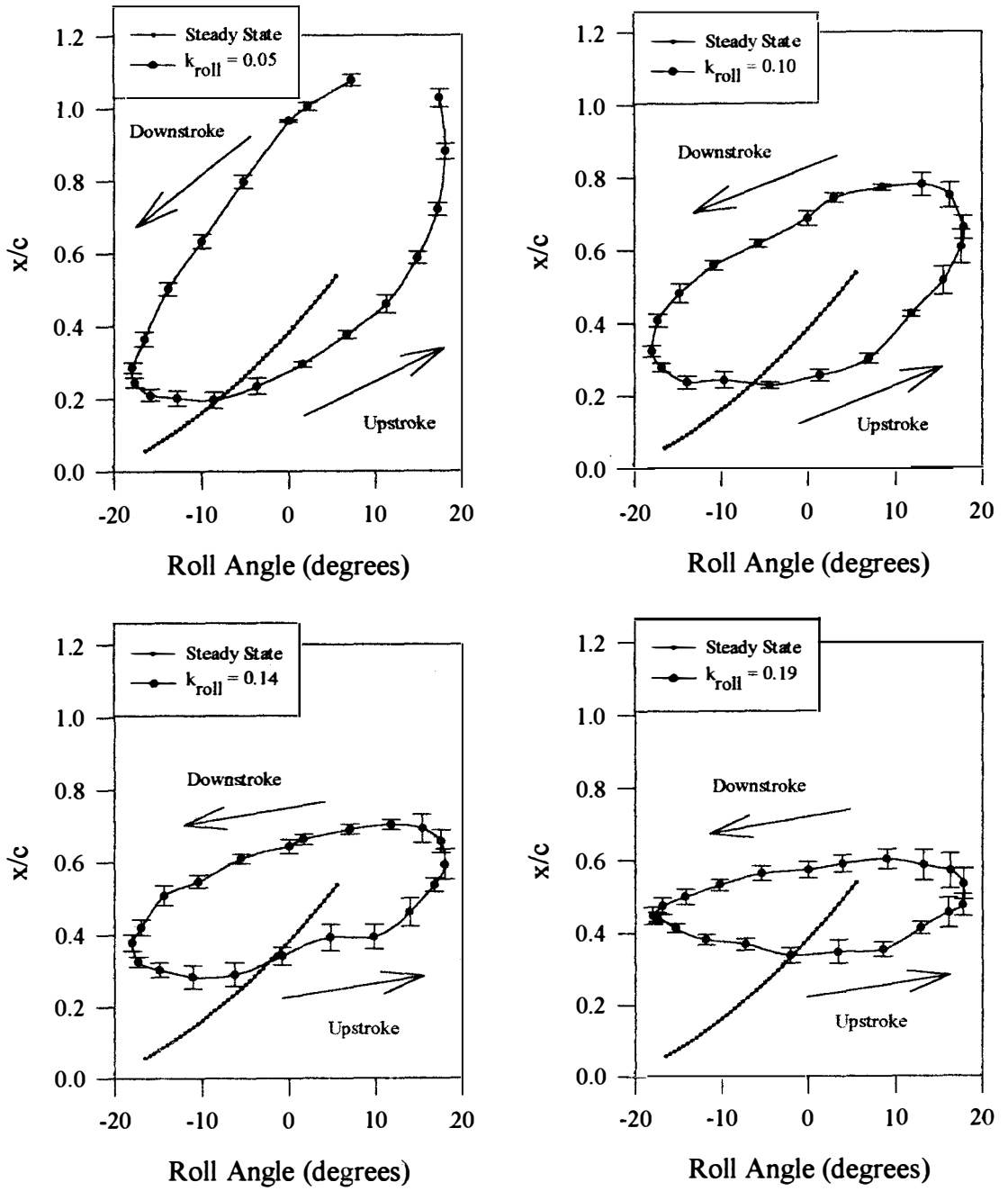

Figure 6.8. Location of Vortex Breakdown During Unsteady Roll Oscillations from ±18°

(Left Wing)

at a negative roll angle of -18°. The curves in the graphs for $k_{roll} = 0.05$ are not closed because of data points that were out of the video frame.

The data in Figures 6.7 and 6.8 demonstrate the deviations from steady state conditions in the behaviour of the vortex breakdown under unsteady conditions. The unsteady motion of the delta wing forced the vortex flow to continually adjust to changing conditions and the result was a hysteresis effect in the behaviour of the location of the vortex breakdown which is shown by the loops created by the unsteady data. It can be seen that, for a given roll angle, the location of the vortex breakdown was consistently further aft during the downstroke than it was during the upstroke. This result was completely opposite to that shown for unsteady pitch motions. The hysteretic effect during unsteady roll motions has been attributed to a time lag inherent with the vortex flow adjusting to changing conditions and, in addition, to the effects of roll rate induced camber. Ericsson[50] provided that the effect of roll rate induced camber was to delay the breakdown on the downstroke and to promote the breakdown on the upstroke (Figure 2.14). The result of this study corresponds to the hysteresis effect demonstrated by Huang and Hanff in their work with a 65° delta wing fixed at a pitch angle of 30° and oscillated about zero roll with roll amplitudes of ±33°.

Although research has been published for 60° and 65° delta wings, this research is the first of its kind for a 70° delta wing at a pitch angle of 30° that was oscillated about zero roll angle with an amplitude of ±18°. By comparing Figure 6.7 with Figure 6.8, it can be seen that the data is quite symmetric. This is a good indication of the setup of experimentation and of data repeatability. To make a comparison of the effects of reduced

frequency, all the data for each wing has been presented together in Figure 6.9 and Figure 6.10 for the right and the left wing, respectively. The data presented in Figures 6.9 and 6.10 show that as reduced frequency was increased the hysteretic effect was also increased. This was demonstrated by the restriction in the movement of the location of vortex breakdown as the reduced frequency was increased. By reviewing the data, it was observed that a restriction in the movement of the location of vortex breakdown was reflected in the rotation of the hysteresis loops away from the steady state conditions for an increased reduced frequency, and therefore, an analysis of the relative locations of the end points has been conducted. The results, provided in Table 6.1, show that the behaviour of the right wing was similar to the behaviour of the flow over the left wing. As the reduced frequency was increased, the location of vortex breakdown moved further away from the steady state condition and a reduction in reduced frequency resulted in the location of vortex breakdown being closer to the steady state condition. This result is consistent with Ericsson[50] who concluded that as the roll rate was reduced (as was the case in this study for a decreased reduced frequency), the roll rate induced camber effects were reduced and so were the deviations of the dynamic from the static conditions.

Phase Lag Due to Unsteady Roll Oscillations

Similar to the investigations for unsteady pitch oscillations, an investigation into the relationship between the location of vortex breakdown and the instantaneous position of the delta wing oscillating in roll has been conducted. The data provided in Figure 6.11

Table 6.1. Location of Vortex Breakdown at Data End Points Versus Reduced Frequency (Unsteady Roll)

Location of Vortex Breakdown (x/c)				
Reduced Frequency	Right Wing		Left Wing	
	Pitch = 30° Roll = -18°	Pitch = 30° Roll = 18°	Pitch = 30° Roll = -18°	Pitch = 30° Roll = 18°
Steady State	>>1	~ 0.04	~ 0.04	>>1
$k_{roll} = 0.05$	0.84	0.29	0.29	0.88
$k_{roll} = 0.10$	0.65	0.33	0.35	0.66
$k_{roll} = 0.14$	0.63	0.38	0.37	0.59
$k_{roll} = 0.19$	0.53	0.45	0.39	0.50

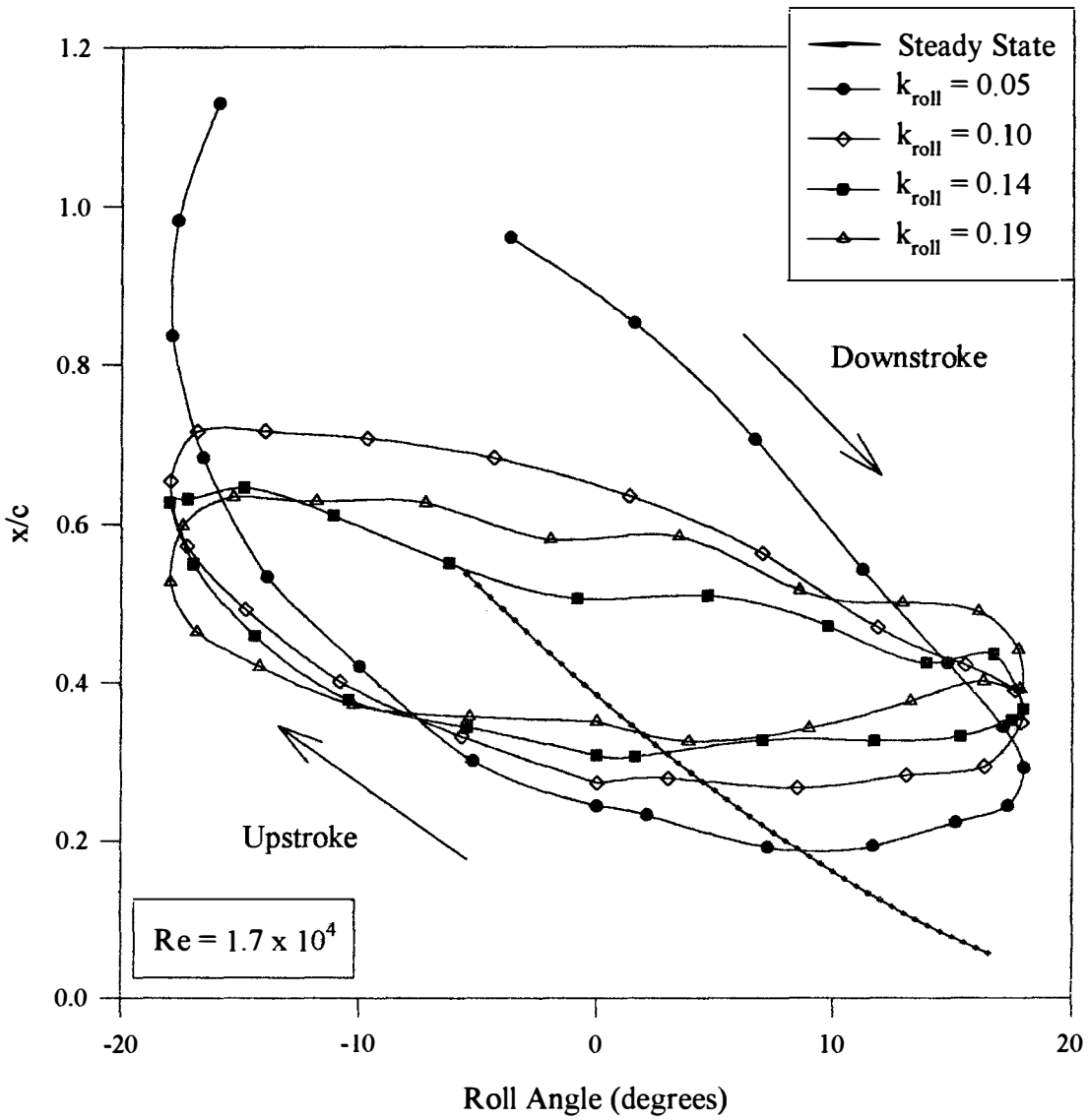

Figure 6.9. Effects of Reduced Frequency During Unsteady Roll Oscillations from ±18°

(Right Wing)

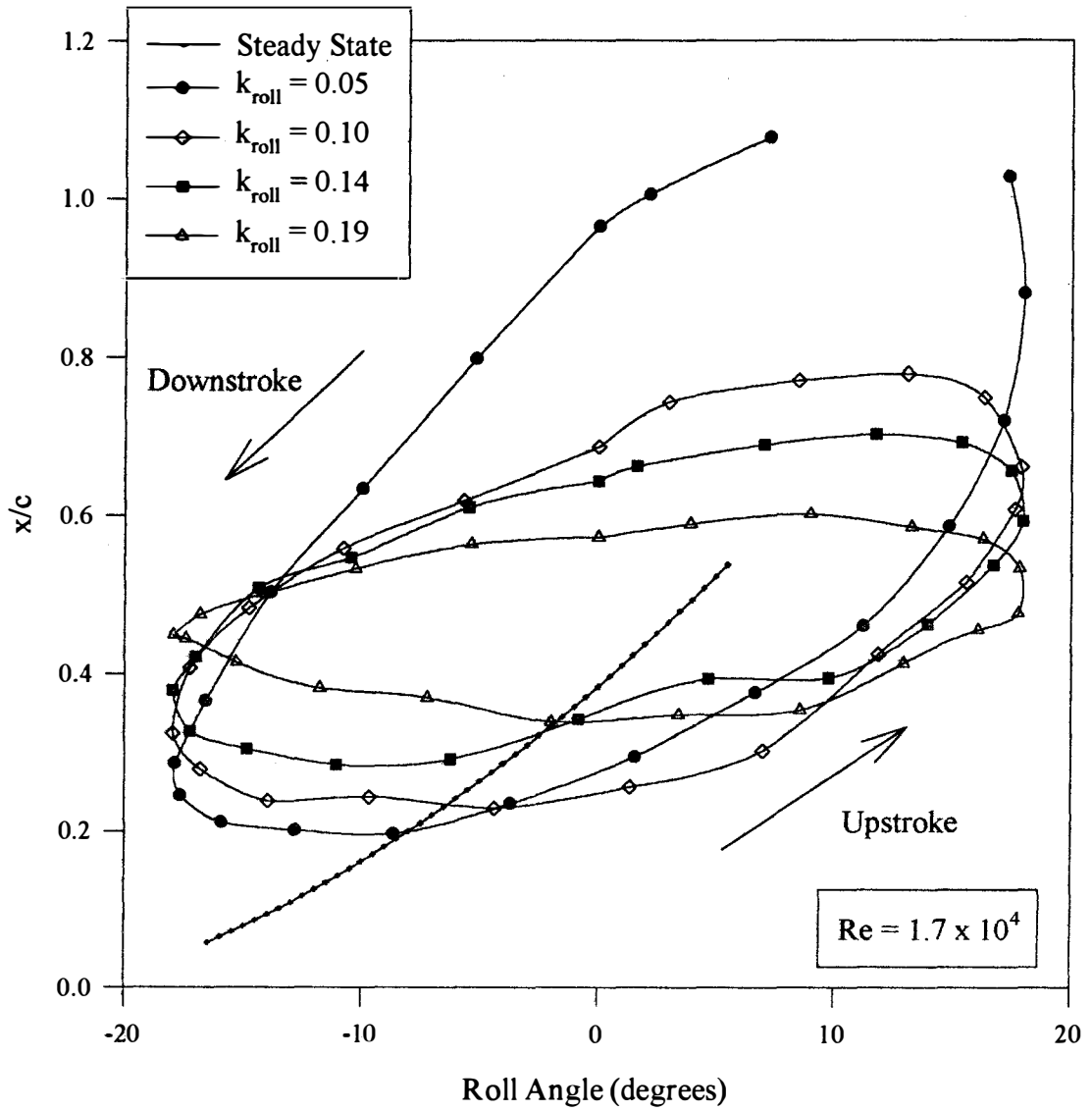

Figure 6.10. Effects of Reduced Frequency During Unsteady Roll Oscillations from ±18°

(Left Wing)

and Figure 6.12 show the location of vortex breakdown as it relates to time for the right wing and left wing respectively. Data from six cycles of oscillations have been analysed to present the average breakdown location over one complete cycle. The error bars shown have been calculated using standard deviation. Data has been presented for all four values of reduced frequency and a different symbols has been used to identify the downstroke and the upstroke portion of the delta wing motion. This way the upstroke and the downstroke of one wing could be compared to that of the other wing directly by matching symbols. It should be noted that the cycle presented started at a roll angle of -18° which meant that the right wing started on the downstroke and as a consequence the left wing started on the upstroke.

As for the analysis of the unsteady pitching motion, the presentation of these graphs makes it difficult to compare data directly as a function of reduced frequency; although, the change in symbol does provide an indication of the transition point between upstroke and downstroke. By noting that the location of vortex breakdown continues to move in its given direction even after the wing has changed directions indicates the presence of a hysteresis effect.

To examine the magnitude of phase lag as a function of reduced frequency, the vortex breakdown location was plotted against the model phase angle for each reduced frequency. The results are presented in Figure 6.13 and Figure 6.14. The point where the $\omega t = 180^{\circ}$ corresponds with the portion of the delta wing motion which is in transition from downstroke to upstroke (for the right wing) and transition from upstroke to downstroke (for the left wing). Referring to these Figures 6.13 and 6.14, the phase lag

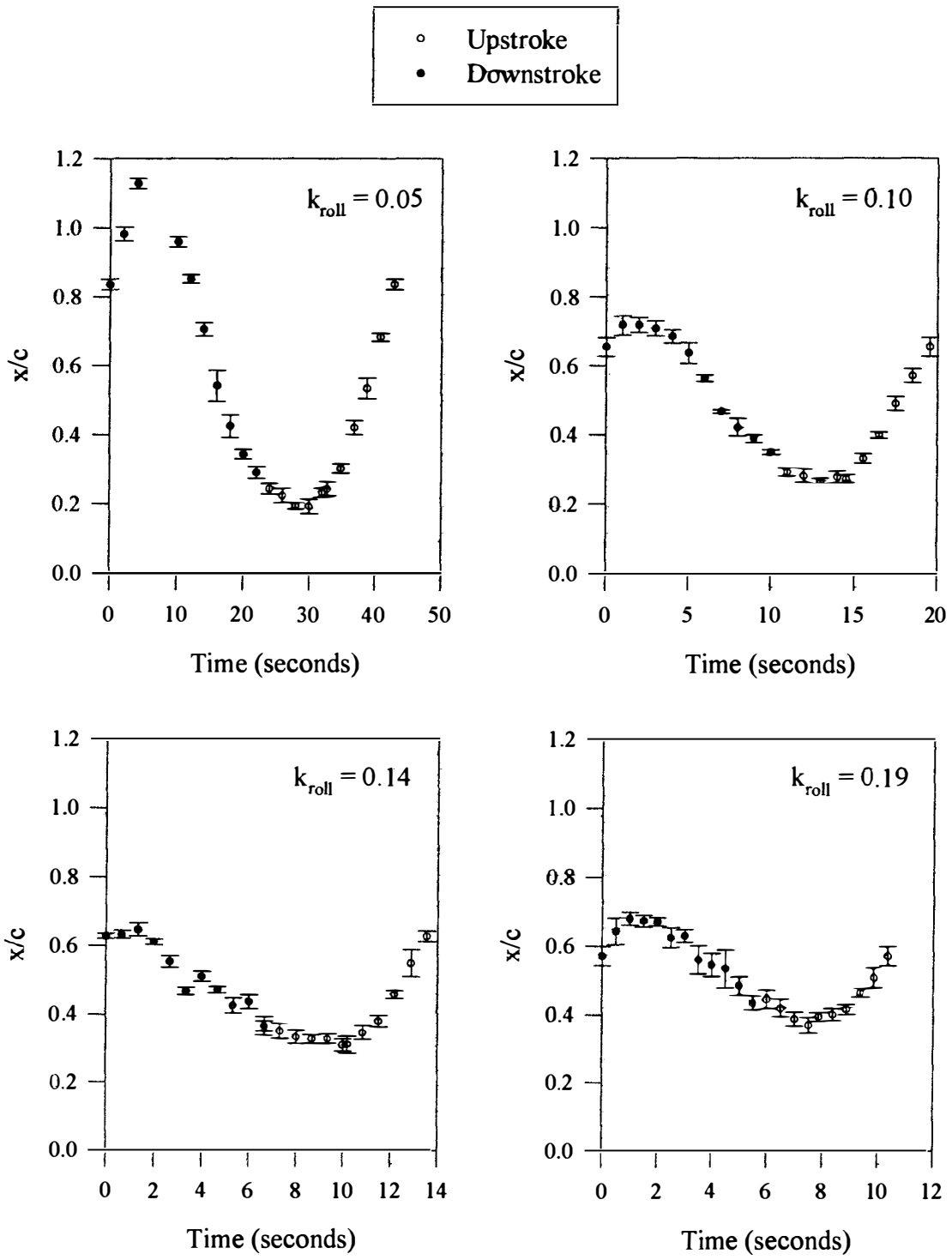

Figure 6.11. Location of Vortex Breakdown vs Time for Unsteady Roll Oscillations of ±18° (Right Wing)

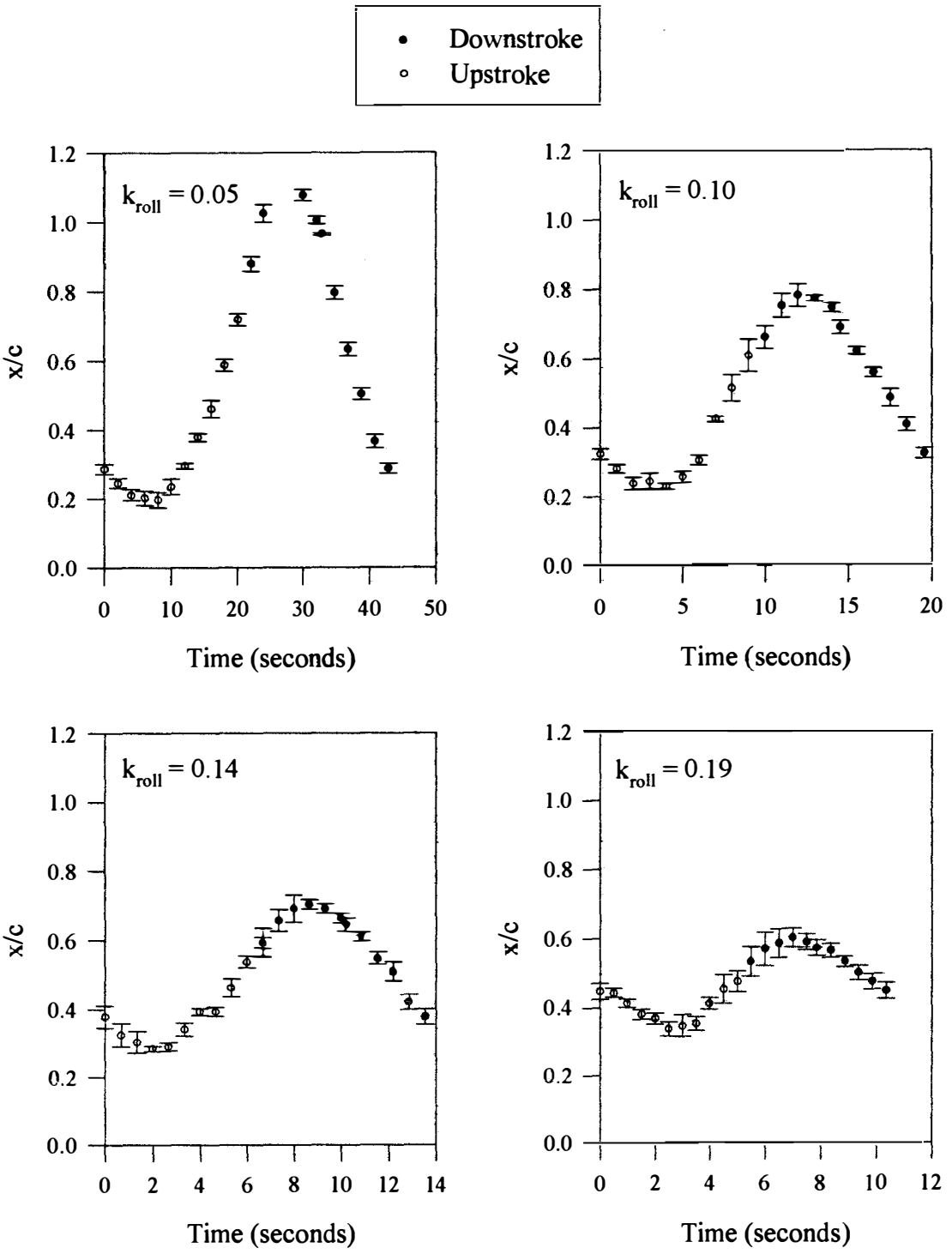

Figure 6.12. Location of Vortex Breakdown vs Time for Unsteady Roll Oscillations of ±18° (Left Wing)

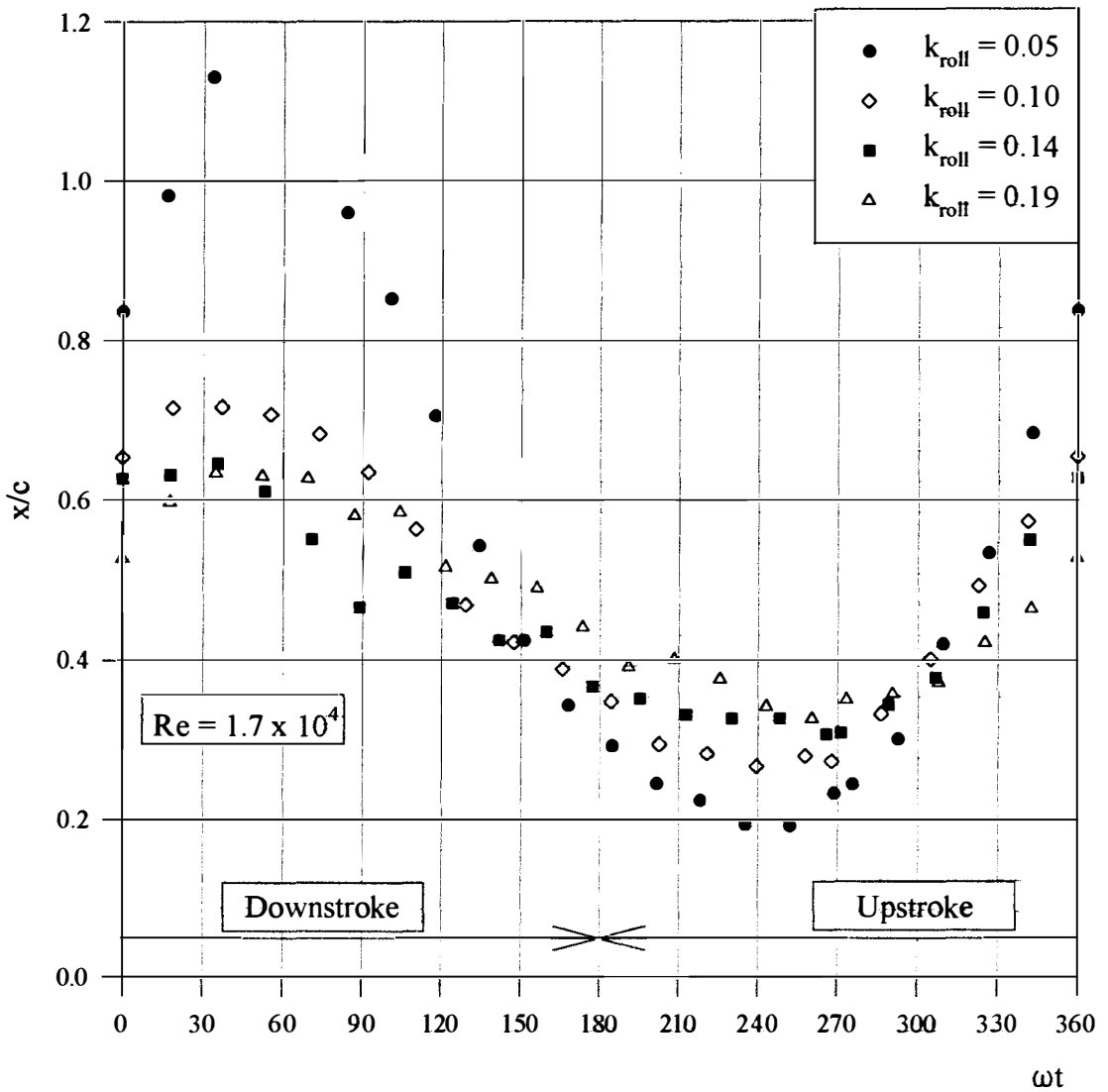

Figure 6.13. Location of Vortex Breakdown vs ωt for Unsteady

Roll Oscillations of ±18° (Right Wing)

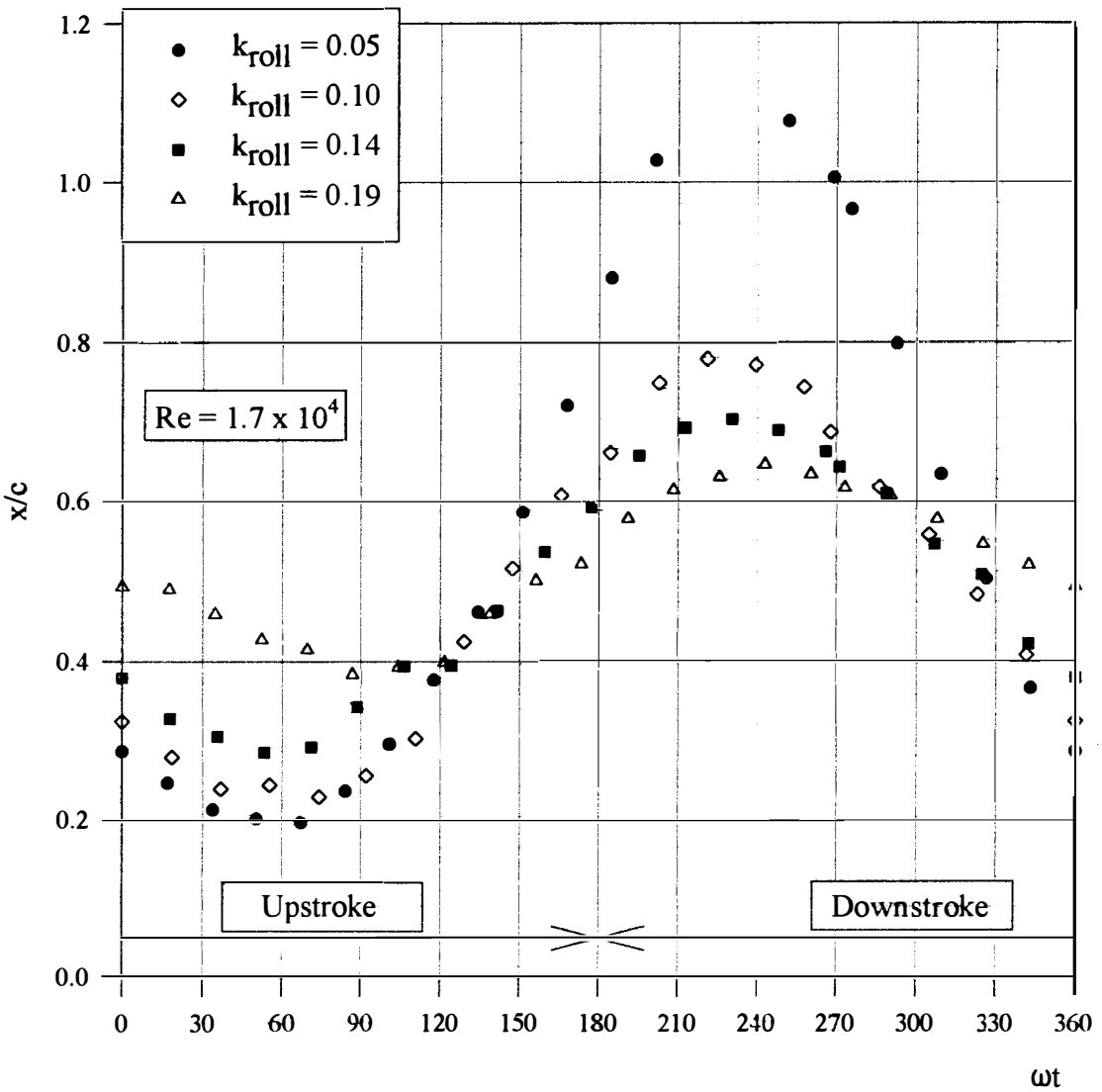

Figure 6.14. Location of Vortex Breakdown vs ωt for Unsteady

Roll Oscillations of ±18° (Left Wing)

due to the hysteresis effect can be seen. For example, for the right wing, when the wing motion transitioned from the downstroke to the upstroke, the location of the vortex breakdown continued to move toward the apex. It was not until some time later after the delta wing had moved through an additional 60° (approximately) that the vortex flow adjusted and the location of the vortex breakdown started to move toward the trailing edge. It can also be seen in Figures 6.13 and 6.14 that, as reduced frequency was increased, the amount of phase lag also increased; although, it would appear that there was an initial jump in phase lag and then the effects became less apparent. This can best be seen by the data for the left wing by examining the transition from the upstroke to the downstroke where it is quite evident that the peaks of the curves are shifted more to the right as reduced frequency increased.

An analysis was carried out to determine quantitatively the relationship between phase lag and reduced frequency. Two distinct relationships were examined: one for the transition from the upstroke to the downstroke and the other for the transition from the downstroke to the upstroke. Because of the symmetric nature of the flow over the delta wing, there were two complete data sets with which to compare and make conclusions.

The data in terms of location of vortex breakdown versus time was used to identify the points where the location of vortex breakdown reversed direction as indicated by the data peaks. This information in conjunction with the period for each reduced frequency was used to calculated the phase lag. The error incurred in the process unfortunately was approximately ±8° because there were only 21-23 data points used to make up each cycle. This meant that the time between each data point represented approximately 16° of the

overall cycle. Along with the inherent errors in the data and data scatter, it was difficult to pinpoint the exact location of the peaks unless the peak coincided with a data point. Still some observations have been made and the results are presented in Figure 6.15.

A difference in the behaviour of the location of vortex breakdown has been noticed for the transition from the upstroke to the downstroke and the downstroke to the upstroke. The data demonstrated that the phase lag was consistently less when the wing transitioned from the upstoke to the downstroke than when it transitioned from the downstroke to the upstroke. This behaviour was consistent with the behaviour shown for unsteady pitching motions. Referring to Figure 6.15, it can be seen, however, that the relationship between phase lag and reduced frequency is quite different for a rolling delta wing than for a pitching delta wing within the limits of the reduced frequencies examined. For the unsteady rolling motion, for example, even low values of reduced frequency result in a large phase lag. This is understandable considering the roll oscillations had a larger amplitude of oscillation than that of the pitch oscillations.

Summary of Roll Experiments

The research carried out in this study furthered the understanding of the behaviour of vortex breakdown over delta wings under conditions of steady and unsteady roll to include the analysis of a 70° delta wing. The fact that there were two distinct sources of data (from the left wing and the right wing) which provided similar results also gave good verification of test results.

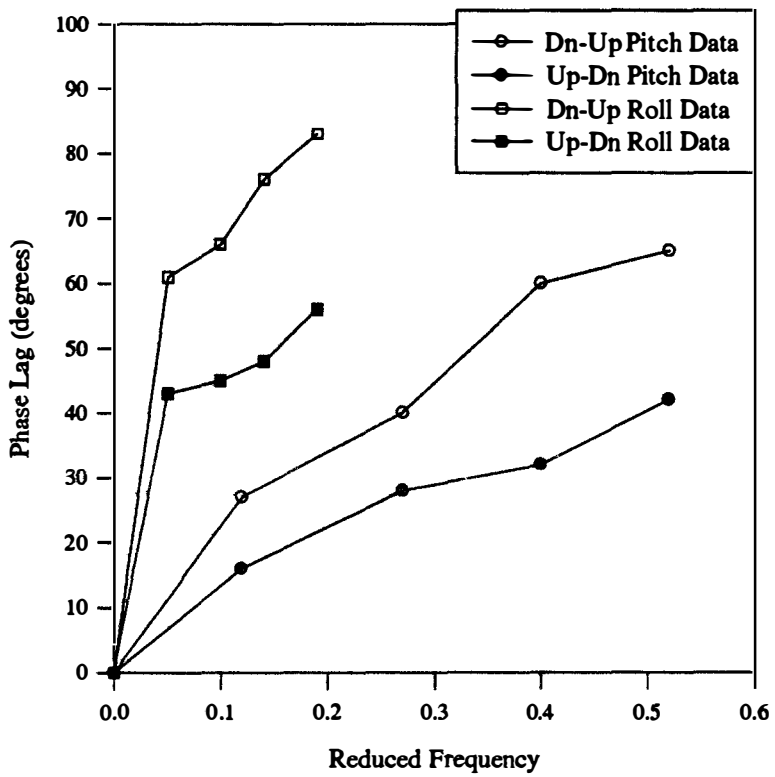

Figure 6.15. Phase Lag as a Function of Reduced Frequency for Unsteady Roll Motion as Compared to Unsteady Pitching Motion

A study was conducted to investigate the behaviour of vortex breakdown over a 70° delta for steady state variations in roll angle. Experimentation was carried out a roll angles varying from -18° to 18° with the delta wing fixed at a pitch angle of 30°. The pitch angle was chosen to be consistent with other studies. Two complete sets of data were analysed: one for the right side of the delta wing and the other for the left. It was observed that the vortex behaviour over the right wing was completely opposite to the vortex behaviour over the left wing. The resultant data showed that, for the right wing, as the roll angle increased, the location of the vortex breakdown moved toward the apex and, as the roll angle decreased, the location of the vortex breakdown moved aft. This result was consistent with the observations made by Huang and Hanff[18]

The exact opposite behaviour was observed for the left wing. By correcting for the roll angle, the data from the left wing was compared to the data from the right wing and the results showed that the behaviour of vortex breakdown was symmetric. In addition, the resultant data showed that the behaviour of the movement of the location of vortex breakdown with roll angle as the location of vortex breakdown travelled over the front half of the delta wing could be considered linear. As the location of the vortex breakdown travelled further back on the wing, however, the relationship between location of vortex breakdown and roll angle became nonlinear. This conclusion was similar to that obtained by Ericsson[50] whose discussion on critical states provided great insight into this phenomenon.

The steady state prediction equations provided by Huang and Hanff[17][18], which were modified to reflect a change of leading edge geometry, and which appeared to

provide good results for the pitch experiments, were tested against the steady state experimental roll data. The results showed that both prediction equations were successful in predicting the location of the vortex breakdown over the front half of the wing; however, neither accurately predicted the location of the vortex breakdown over the aft portion of the wing. This is consistent with the conclusion made by Ericsson[50] especially considering the existence of critical states and the nonlinear effects they impose on the behaviour of vortex breakdown.

Unsteady roll experiments were carried out with the 70° delta wing fixed at a pitch angle of 30° with roll oscillations of ±18° about the wings level position. The unsteady roll experiments were conducted at the same pitch frequencies as for the unsteady pitch analysis which ranged from 0.023 Hz to 0.097 Hz. Because of the difference in definition in reduced frequency between pitch and roll, however, this meant that the unsteady roll experiments were carried out at reduced frequencies that varied from $k_{roll} = 0.05$ to $k_{roll} = 0.19$. The resultant unsteady vortex breakdown data was compared with the steady state data. The results indicated that when the delta wing was oscillated in roll there was a hysteresis effect in the behaviour of the location of the vortex breakdown. The data collected from both sides of wing showed that the behaviour was symmetric in terms of upstroke and downstroke. The upstroke for the right wing was defined by the wing rolling from a positive angle of attack and the upstroke for the left wing was defined by a negative angle of attack. The hysteretic behaviour was demonstrated by the location of the vortex breakdown being consistently further aft on the downstroke than it was on the upstroke. This effect was attributed to a time lag associated with the vortex flow

adjusting to continually changing conditions and to the effect of roll rate induced camber that were presented by Ericsson[50]. An analysis of the effects of reduced frequency on the location of vortex breakdown was conducted. The experimental data showed that, as reduced frequency was increased, the amount of hysteresis also increased. This was seen by an increase with reduced frequency of the restriction of the movement of the location of vortex breakdown.

An investigation of the phase lag associated with the location of the vortex breakdown as it related to the instantaneous position of the delta wing was carried out. A distinct relationship was observed for the transition of movement from the upstroke to the downstroke and from the downstroke to the upstroke which was repeatable for the right side and the left side of the wing. The experimental data showed that the phase lag was consistently less when the wing transitioned from the upstroke to the downstroke than when it transitioned from the downstroke to the upstroke. In addition, the unsteady roll oscillations resulted in a larger phase lag than did the unsteady pitch oscillations. This was understandable, however, considering the unsteady roll amplitude was $\pm 18^{o}$ whereas the unsteady pitch amplitude was $\pm 5^{o}$.

CHAPTER VII

RESULTS AND DISCUSSIONS: MANEUVERING EXPERIMENTS

Steady State Variations Simultaneously in Pitch and Roll

This study investigated the behaviour of vortex breakdown over a 70° delta wing for simultaneous steady state variations in pitch and roll angles (termed maneuvering). The Reynolds number during the testing was 1.7×10^4. The model placement was consistently verified so that the locations of vortex breakdown were symmetric for zero roll angle. The steady state experiments were carried out with the maneuvering apparatus setup to provide changes in pitch that were accompanied by corresponding changes in roll so that the pitch angle varied bewteen 25° and 35° while the roll angle varied between -18° and 18°; therefore, each data point analysed represented a unique value of pitch and roll angle. A positive movement in pitch corresponded to a positive movement in roll and vice versa. The data was collected for increments in pitch and roll that were made in the positive direction similar to the other steady state experiments in this study. The flow was allowed a settling time between increments to enable the flow to stabilize. Twenty consecutives video frames of data were analysed for each pitch-roll angle combination. The results represent the average locations of vortex breakdown for steady state variations in pitch and roll angle and are presented in Figure 7.1. The error bars have been calculated using the standard deviation.

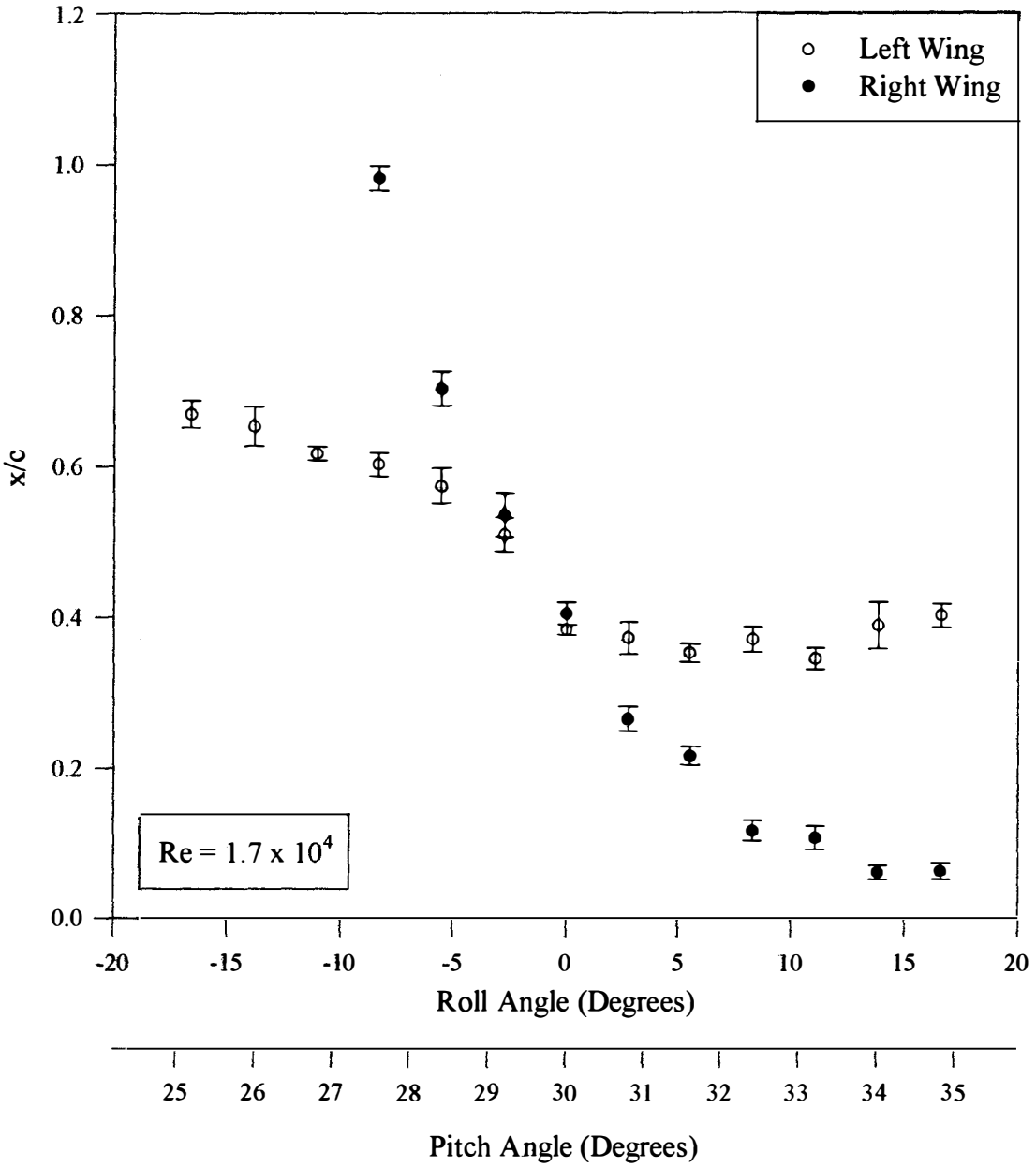

Figure 7.1. Location of Vortex Breakdown for Simultaneous Steady State Variations in Pitch and Roll

Because of the two dye ports, a separate set of data was collected for the right wing and another for the left wing. Unlike the roll experiments, these two data sets represented two distinctly different relative motions for the maneuvering experiments. For variations in pitch, for example, an increase in pitch angle defined the upstroke. For variations in roll; however, the upstroke was defined as the wing that physically moved up. This meant that for a positve increase in roll angle, the left wing experienced an upstroke while the right wing experienced a downstroke. Therefore, for variations in pitch and roll in the same direction, as the delta wing increased in pitch, the right wing moved down and the left wing moved up. Consequently, the two sets of data collected represented relative movements of pitch that were accompanied with movements in roll that were in phase (left wing) and with movements in roll that were 180° out of phase (right wing).

Referring to Figure 7.1, the results of the steady state analysis are provided. The experimental data show that, for the right wing, a decrease in pitch with roll angle resulted in the aft movement of the location of vortex breakdown. Conversely, an increase in pitch with roll angle resulted in the the location of vortex breakdown moving toward the apex. For the left wing, a similar behaviour in movement of location of vortex breakdown was observed; however, the movement of the location of vortex breakdown was more restricted for the left wing as compared to the right wing. In fact, for the larger pitch and roll angles tested, the location of vortex breakdown over the left wing began to move aft again. This can explained by analysing the beahviour of vortex breakdown under steady state pitch conditions and steady state roll conditions. Referring to Figures 5.1 and 6.1, it can be seen that the effect of a change in pitch angle was the same for the right wing as for

the left wing. An increase in pitch angle caused the location of vortex breakdown to move toward the apex and a decrease in pitch angle caused the location of vortex breakdown to move aft. For a change in roll angle, however, the effect was completely opposite for the right wing compared to the left wing. For the right wing, an increase in roll angle caused the location of vortex breakdown to move toward the apex and a decrease in roll angle caused the location of vortex breakdown to move aft. For the left wing, an increase in roll angle caused the location of vortex breakdown to move aft and a decrease in roll angle caused the location of vortex breakdown to move forward toward the apex.

For the right wing, the effects of pitch and roll work in the same direction. Therefore, an increase in the pitch angle with the roll angle should result in a forward movement of the location of vortex breakdown for the right wing. This is the result that was reflected in the experimental data. Similarly, an decrease in the pitch angle and the roll angle should result in an aft placement of the location of vortex breakdown for the right wing. The experimental data also demonstrated this result.

For the left wing, the effects of pitch and roll work in opposite directions. From the data, however, it would appear that the dominant effect was the change in pitch because the net effect was for the location of the vortex breakdown to follow the pitch trend. This result was seen up to a certain value of roll angle when the effects of roll seemed to dominate and the location of the vortex breakdown moved aft again. For example, the results in Figures 5.1 and 6.1 show that, for a decrease pitch angle and roll angle, the effects of pitch caused the location of vortex breakdown to move aft and the effects of roll caused it to move forward. The experimental data in Figure 7.1 shows that

the net effect for a decrease pitch and roll angle was for the location of vortex breakdown to move aft. Although, the movement aft was dampened by the effects of roll, the data showed that the effects of pitch tended to dominated.

For an increasing pitch angle and roll angle, Figures 5.1 and 6.1 show that the effects of pitch caused the location of vortex breakdown to move forward whereas the effects of roll cause it to move aft. The experimental data in Figure 7.1 show that the net effect was for the location of vortex breakdown to move forward initially and then begin to move back. Therefore, initially the dominant effect was the influence of pitch and then the dominant effect became the roll. This results corresponds well with Ericsson's[50] discussion of critical states. The dominating effect was the pitch until such a critical roll angle when aggressive behaviour in the movement of the location of vortex breakdown took over. Such behaviour was seen in the results of the steady roll experiments where, for an essentially constant angle of attack, the effect of the change in roll angle increased the amount of sweep of the delta wing. Once a critical roll angle had been reached to effect a critical change in the delta wing sweep angle, the location of vortex breakdown moved aft aggressively. In the case where not only the roll angle is change but so is the pitch angle, the effective change of the increased roll angle on the left wing is "softened" by the increased pitch angle and corresponding increase in angle of attack.

It is not possible to compare directly all the steady state data in one graph for each type variation because the steady state pitch data was collected at one roll angle (0^{o}) and the steady state roll data was collected at one pitch angle (30^{o}). Except for one condition during the maneuvering tests (where pitch angle was 30^{o} and roll angle was 0^{o}), any

variations in one variable changed the other variable. To make a direct comparison of experimental steady state data, further experimentation must be carried out for a variation in roll angle at different angles of attack or variations in pitch angle at different roll angles.

An analysis of the steady state prediction equations was carried out. Figure 7.2 has been presented which compares the experimental data to the predictions made by Equations 19 and 23. Referring to Figure 7.2, it can be seen that, although there are good trends in the predictions, neither prediction equation accurately predicts the location of vortex breakdown for simultaneous steady state variations in pitch and roll even in the region where, previously, good agreement had been shown. As previously discussed in the analysis of steady state variations in roll, it is reasonable to believe that the nonlinear effects of critical states makes it difficult to predict the location of vortex breakdown using emperical models.

Unsteady Maneuvering

Unsteady maneuvering experiments were carried out with the 70° delta wing oscillating in pitch while undergoing corresponding roll oscillations. The Reynolds number of the flow was 1.7×10^4. The drive mechanism provided for a sinusoidal input to the maneuvering apparatus so that the model oscillated in pitch about a mean pitch angle of 30° and an amplitude of ±5° while oscillating in roll about 0° with an amplitude of ±18°. These test conditions were selected so that comparison to the unsteady pitch and unsteady roll experiments could be carried out. The unsteady maneuvering experiments

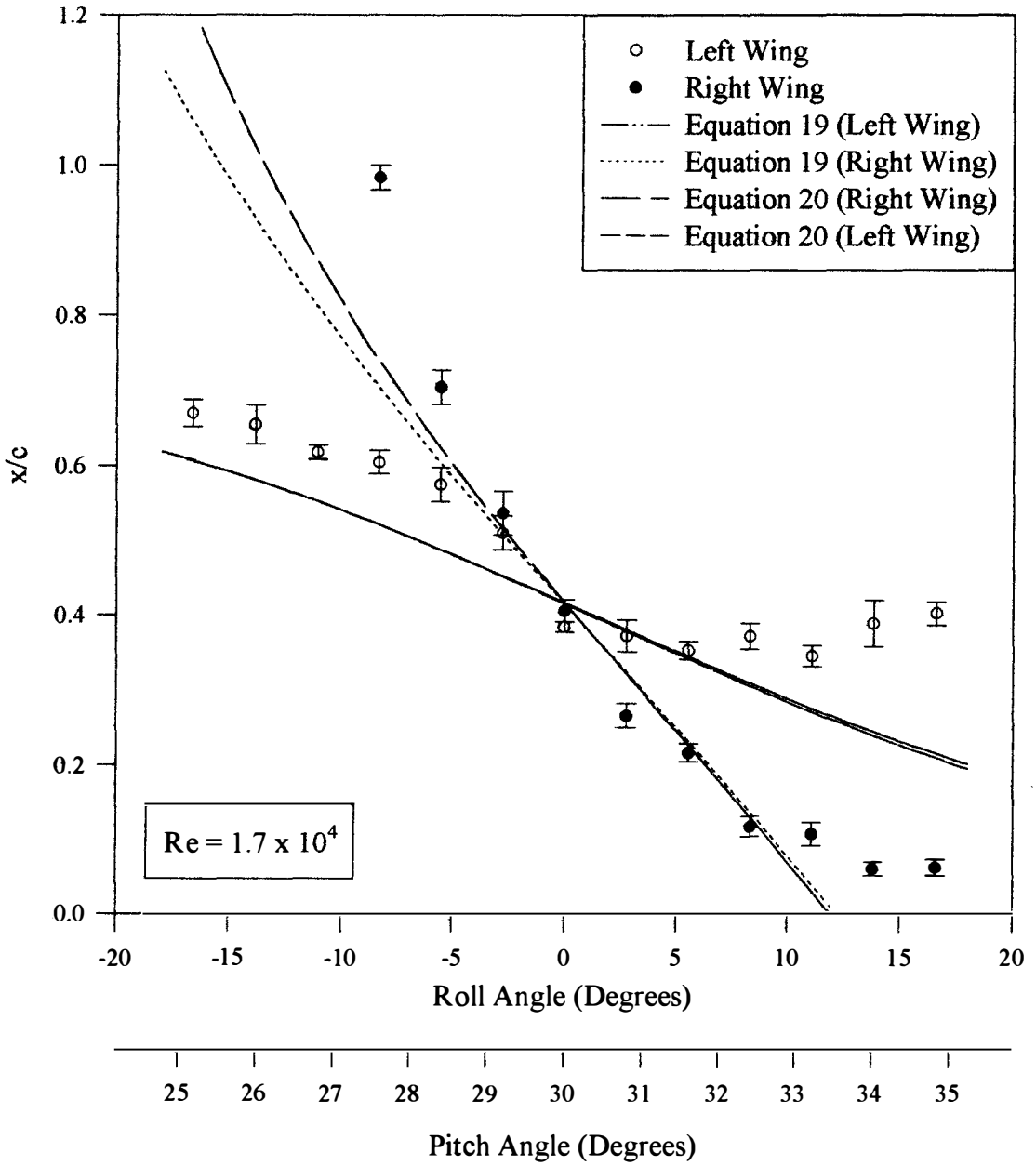

Figure 7.2. Comparison of Experimental Data With Data from Prediction Equations For Simultaneous Steady State Variations in Pitch and Roll

were carried out at the same pitch frequencies as in previous experiments: 0.023 Hz, 0.051 Hz, 0.074 Hz and 0.097 Hz. Because of the difference in definition of reduced frequency for unsteady pitch motion and unsteady roll motion, however, this resulted in two values of reduced frequency for each of the four pitch frequencies tested. The tests were conducted in order that the reduced frequencies tested were the same as in previously experiments during this study. The data was collected over a number of cycles of motion to ensure and to quantify data repeatability in terms of error bars. As discussed for the steady state analysis, the flow over the left wing and the flow over the right wing provided two sets of data; however, because of the definition of the upstroke and the downstroke, each data set represented a combination of pitch and roll motion that were in phase (left wing) and 180° out of phase (right wing). The presentation of the data is provided which annotates which data was collected from the right wing and the left wing. As well, arrows have been provided where appropriate which show the direction of motion. The direction has been based on the direction of the pitching motion only. When interpreting the data, it should be kept in mind that the left wing was in phase with the pitching motion and that the right wing was out of phase with the pitching motion. The results presented in Figures 7.3 and 7.4 provide the unsteady relationship between the location of vortex breakdown and combinations of pitch and roll roll angles for the right and left wing, respectively. Each graph in the figures represents a different reduced frequency as annotaed and the steady state data has been included for comparison.

The data in Figures 7.3 and 7.4 demonstrate a hysteresis effect that was similarly shown for unsteady pitching motions as well as unsteady rolling motions indicating that

the behaviour of the location of vortex breakdown is dramatically affected by the unsteady motion of the wing. The hysteresis effect is illustrated by the loops around the steady state data created by the unsteady data. Because each side of the wing has undergone a unique motion during one cycle of motion, however, the data from the right wing is distinctly different from the data from the left wing.

For the right wing, Figure 7.3 shows that, for a given combination of pitch and roll angles, the location of the vortex breakdown was consistently further aft during the upstroke than it was during the downstroke. Considering the term upstroke refers to the pitch up motion and for a pitch up motion the right wing actually pitched down, this result is consistent with the result shown for unsteady pitch as well as unsteady roll.

Figure 7.3 illustrates, however, that for the right wing, the coupling effect of unsteady maneuvering was a reduction in the overall hysteresis in the location of vortex breakdown. This was more noticeable for the higher reduced frequencies, but can be seen by comparing the relative size of the hysteresis loops for oscillations in pure roll with the hysteresis loops in Figure 7.3. When adding the effects of pitch, for example, to the unsteady rolling motion, a comparison of Figures 6.7 and Figure 7.3, demonstrates a relaxation in the restriction of the movement of vortex breakdown through the entire motion cycle. This is consistent with the summation of the individual behaviours of vortex breakdown as related to the influences of unsteady pitch and unsteady roll which can be seen in Figures 5.11 and 6.7 respectively. For the right wing, for example, an upstroke of pitching motion caused a delay in the movement of the location of vortex breakdown. Because pitch and roll were out of phase, the right wing was undergoing a downstroke

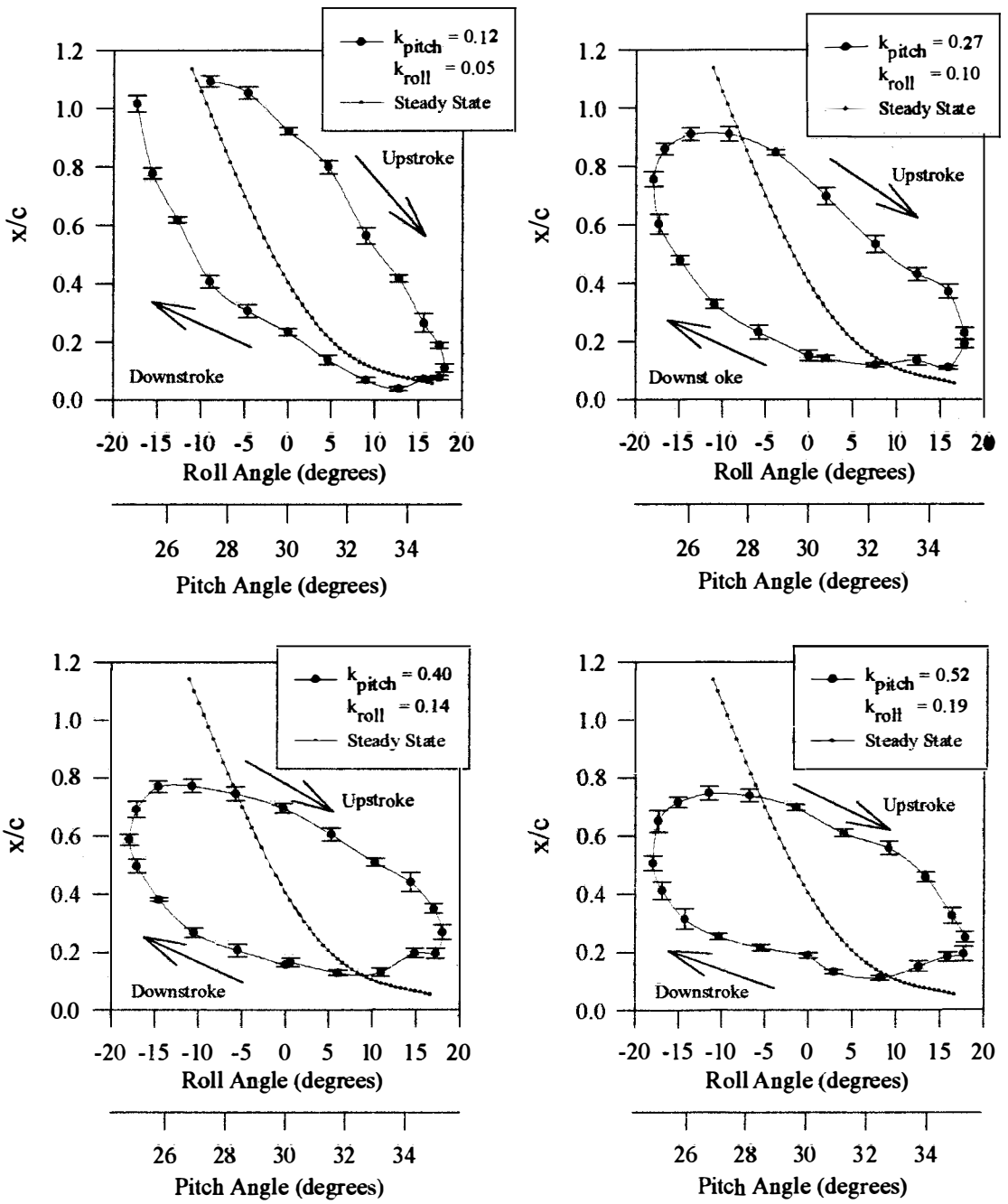

Figure 7.3. Location of Vortex Breakdown for Unsteady Maneuvering in Pitch While Rolling (Right Wing)

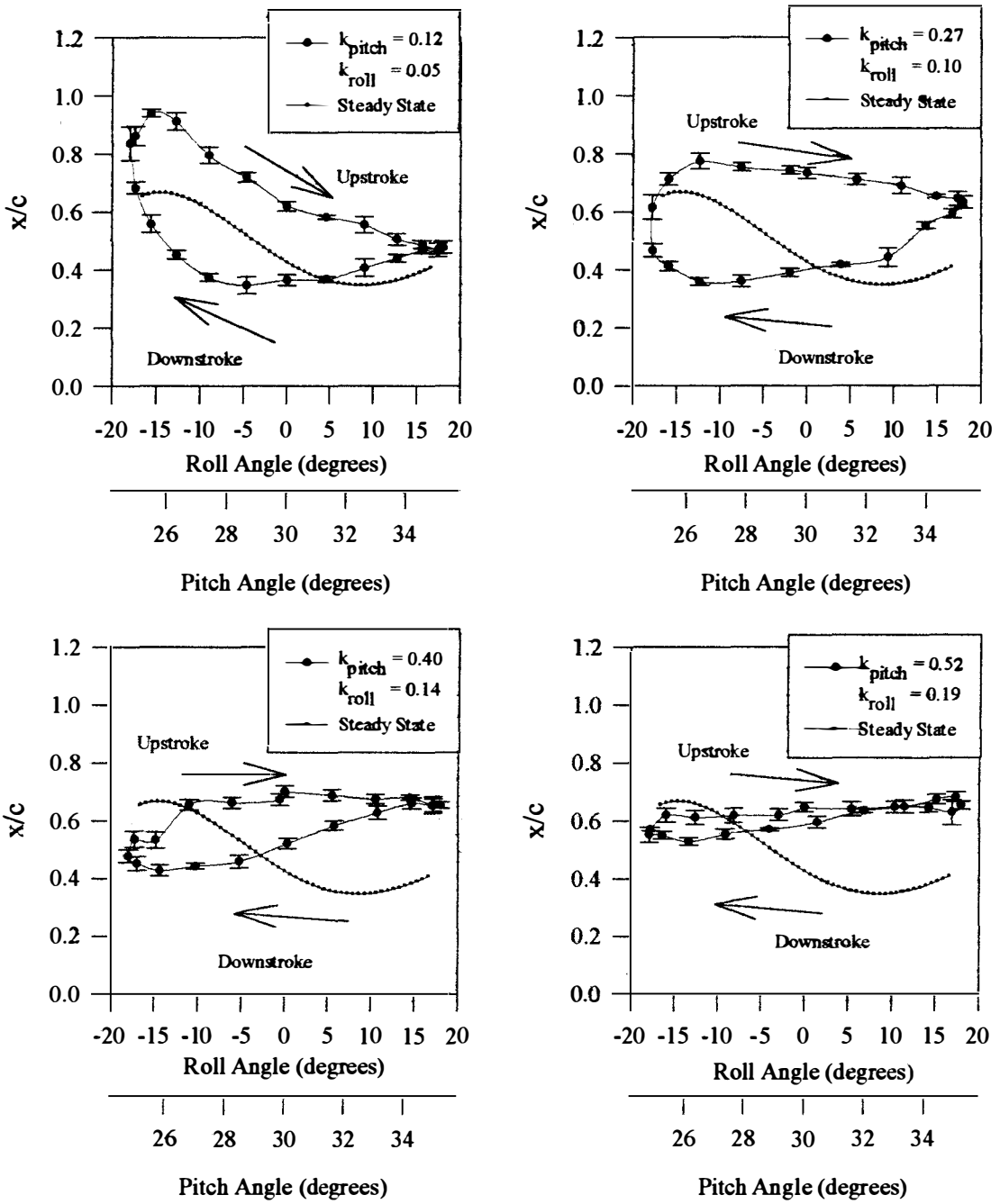

Figure 7.4. Location of Vortex Breakdown for Unsteady Maneuvering in Pitch While Rolling (Left Wing)

and a downstroke of rolling motion also caused a delay in the movement of the location of the vortex breakdown. Although the individual motions were 180° out of phase, the individual influences were in phase and the hysteretic effects were relaxed accordingly.

For the left wing, the information provided in Figure 7.4 also shows that, for a given combination of pitch and roll angles, the location of the vortex breakdown was consistently further aft during the upstroke than it was during the downstroke. Although this result is also consistent with the results from the analysis of unsteady pitch and unsteady roll, the results for the left wing are quite different from the results from the right wing. Figure 7.4 shows that, for the left wing, the coupling effect of the unsteady maneuvering motion was an increase in the hysteresis effect. This can be seen by comparing Figure 6.8 and 7.4 where the data shows that the addition of pitch to the rolling motion results in the further restriction of the movement of the location of vortex breakdown throughout the entire motion cycle. This is also consistent with the summation of the individual behaviours of vortex breakdown as related to the influences of unsteady pitch and unsteady roll which can be seen in Figures 5.11 and 6.8 respectively. For the left wing, an upstroke of pitching motion caused a delay in the movement of the location of vortex breakdown; but, because pitch and roll were in phase, the left wing also experienced an upstroke of rolling motion which caused an advancement in the movement of the location of the vortex breakdown. Therefore, although the individual motions were in phase, the individual influences were 180° out of phase and countered each other. The hysteretic effects were increased accordingly.

To analyse the effects of reduced frequency, all the data for each wing has been

presented together in Figure 7.5 and Figure 7.6 for the right and the left wing, respectively. The data presented in Figures 7.5 and 7.6 show that, as the reduced frequency was increased, there was also an increase in the hysteresis effect which is illustrated by the restriction in the movement of the position of vortex breakdown. By reviewing the data, it was observed that a restriction in the movement of the location of vortex breakdown was reflected in the rotation of the hysteresis loops away from the steady state conditions for an increased redeuced frequency, and therefore, an analysis of the relative locations of the end points has been conducted. The results are provided in Table 7.1. For the right wing, the data in Table 7.1 shows that as the reduced frequency was increased, the location of vortex breakdown moved further away from the steady state condition and a reduction in reduced frequency resulted in the location of vortex breakdown being closer to the steady state condition. This result is consistent with the results for the study of unsteady pitch and unsteady roll motion. For the left wing, the behaviour of the location of vortex breakdown was similar for negative roll and a lower pitch angle; however, for a positive roll angle at an elevated pitch angle, the location of the vortex breakdown became fixed for the higher reduced frequencies.

Phase Lag Due to Unsteady Maneuvering

Similar to previous unsteady investigations, an investigation was carried out into the relationship between the location of vortex breakdown and the instantaneous position of the delta wing as it maneuvered in pitch and roll. The data provided in Figure 7.7 and

Table 7.1. Location of Vortex Breakdown at Data End Points Versus Reduced Frequency (Unsteady Maneuvering)

Location of Vortex Breakdown (x/c)				
Reduced Frequency	Right Wing		Left Wing	
	Pitch = 25° Roll = -18°	Pitch = 35° Roll = 18°	Pitch = 25° Roll = -18°	Pitch = 35° Roll = 18°
k = 0 Steady State	>>1	~ 0.05	0.66	0.41
$k_{pitch} = 0.12$ $k_{roll} = 0.05$	1.02	0.11	0.84	0.48
$k_{pitch} = 0.27$ $k_{roll} = 0.10$	0.75	0.19	0.62	0.63
$k_{pitch} = 0.40$ $k_{roll} = 0.14$	0.59	0.27	0.48	0.66
$k_{pitch} = 0.52$ $k_{roll} = 0.19$	0.50	0.26	0.55	0.66

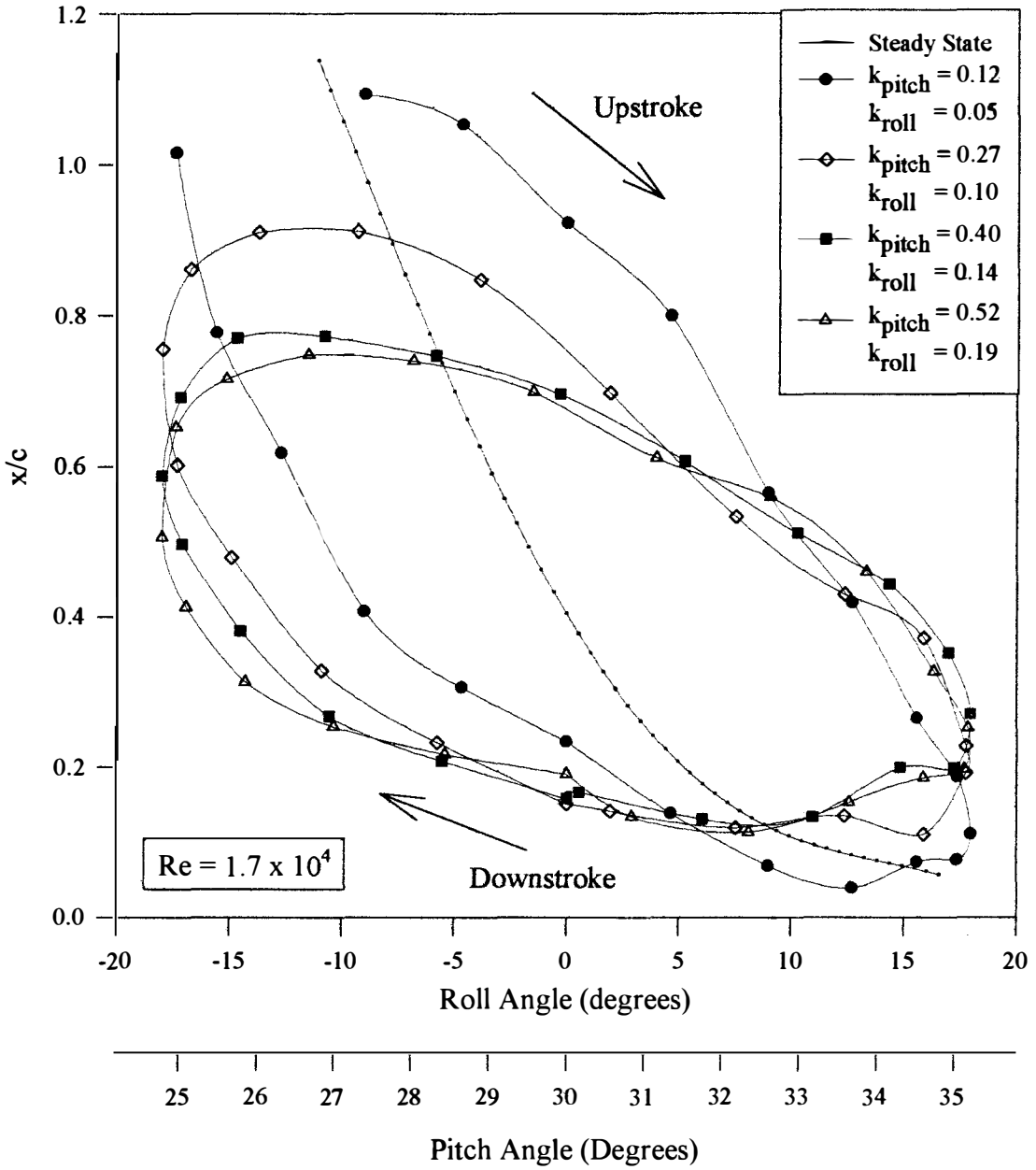

Figure 7.5. Effects of Reduced Frequency for Unsteady Maneuvering in Pitch While Rolling (Right Wing)

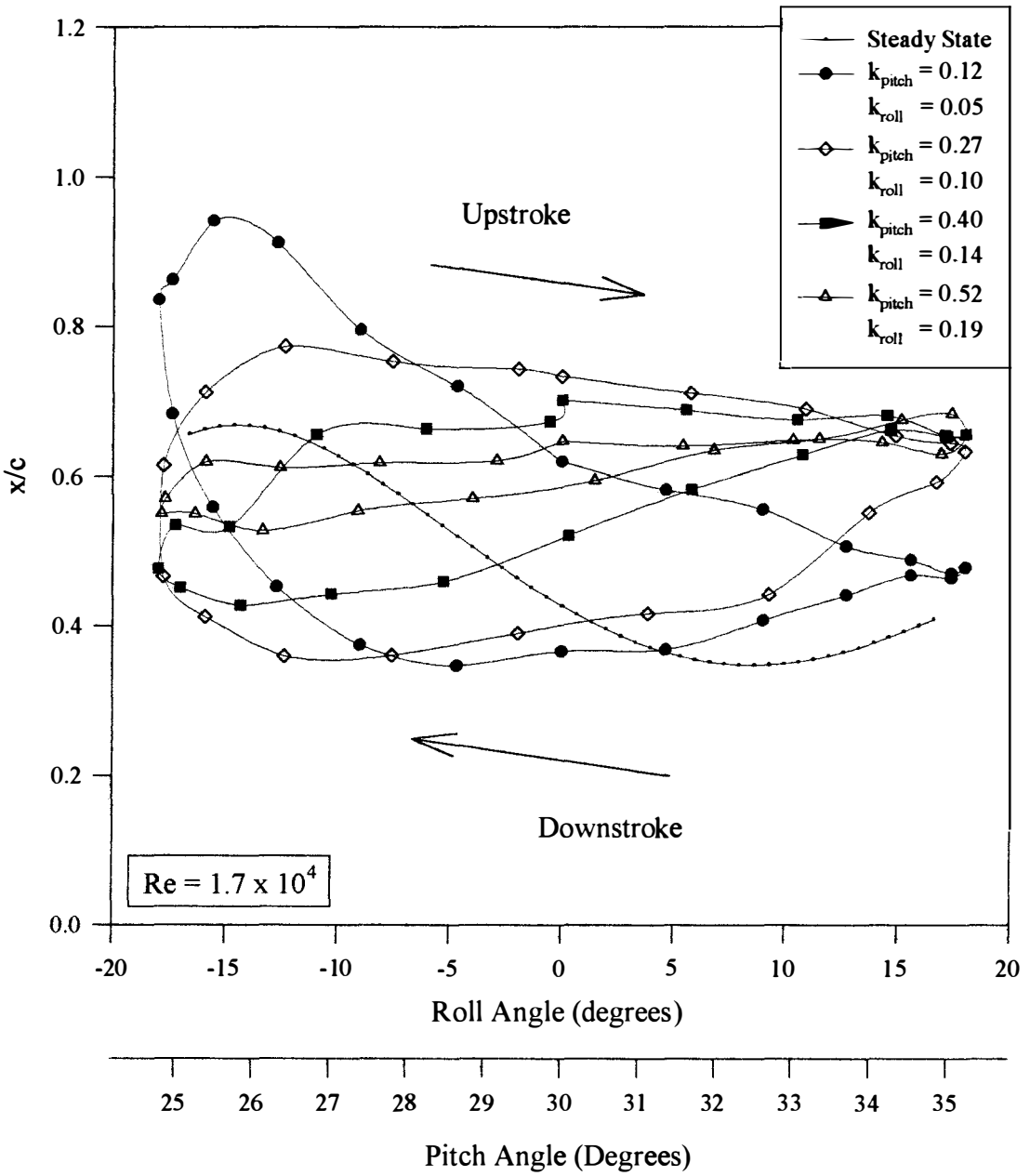

Figure 7.6. Effects of Reduced Frequency for Unsteady Maneuvering in Pitch While Rolling (Left Wing)

Figure 7.8 show the location of vortex breakdown as it relates to time for the right wing and left wing respectively. Data from six cycles of oscillations have been analysed to present the average breakdown location over one complete cycle. The error bars shown have been calculated using standard deviation. Data has been presented for all four values of reduced frequency and a different symbols has been used to identify the downstroke and the upstroke portion of the delta wing motion.

To examine the magnitude of phase lag as a function of reduced frequency, the vortex breakdown location was plotted against the model phase angle for each reduced frequency. The results are presented in Figure 7.9 and Figure 7.10. For the maneuvering experimentation, the relationship between the relative movement of the right and the left wing in terms of upstroke and downstroke is important. To be consistent, the upstroke for these tests has been defined as a positve increase in pitch angle. The upstroke and the downstroke have been identified on the graphs.

Referring to Figures 7.9 and 7.10, the phase lag in the vortex breakdown motion can be seen. For both wings, it can be seen that, as reduced frequency was increased, the amount of phase lag also increased. This result is similar to the results of the tests involving unsteady pitch and unsteady roll motion. In quantifying the relationship between phase lag and reduced frequency, the same uncertainty existed in the maneuvering data as for the other unsteady analyses. The error was approximately $\pm 8^{o}$ because of the low number of data points used to reproduce the cycle and because it was sometimes difficult to pinpoint the exact location of the peaks unless the peak coincided with a data point. However, some interesting trends were noted. For the right wing, for example, there was

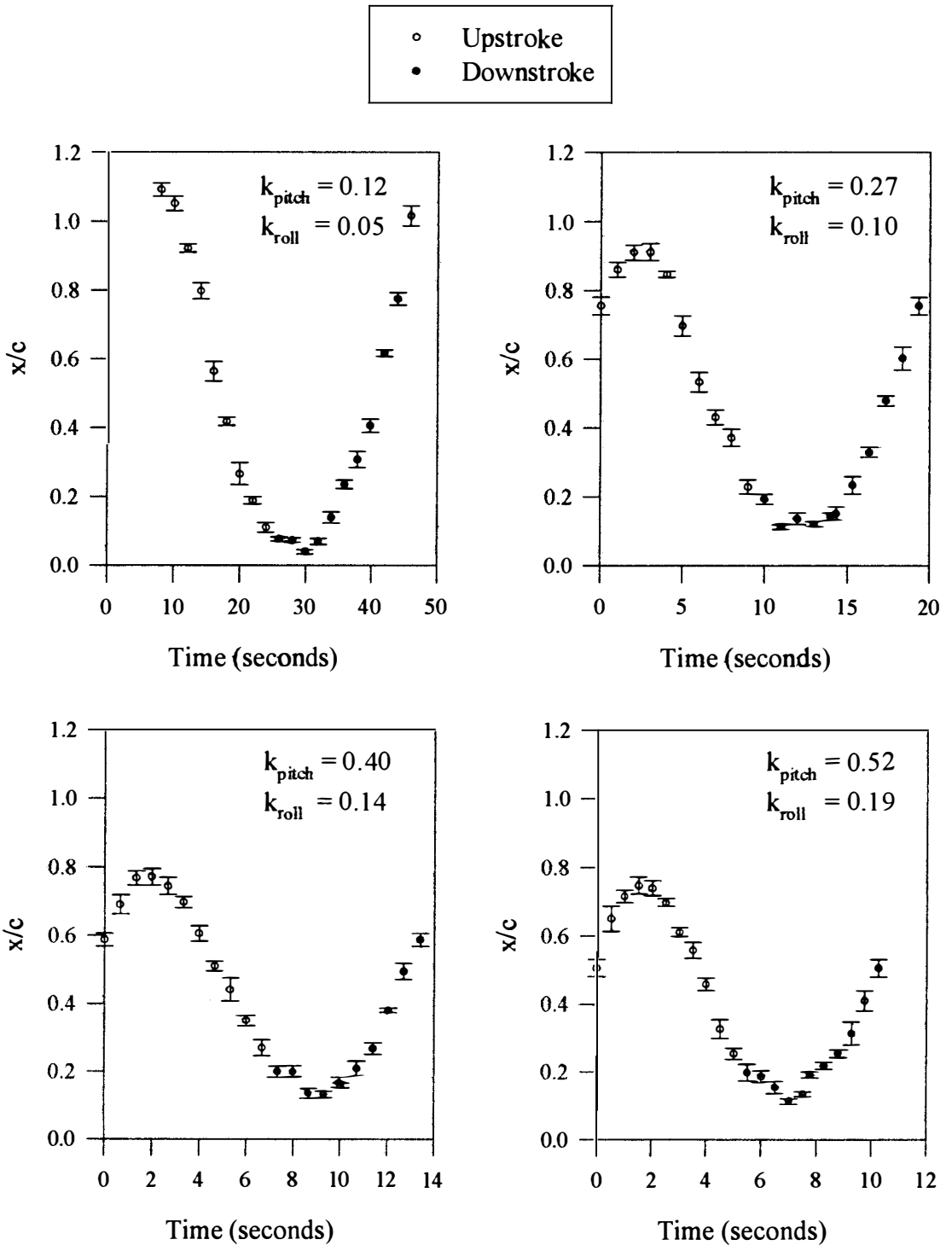

Figure 7.7. Location of Vortex Breakdown vs Time for Unsteady Maneuvering in Pitch While Rolling (Right Wing)

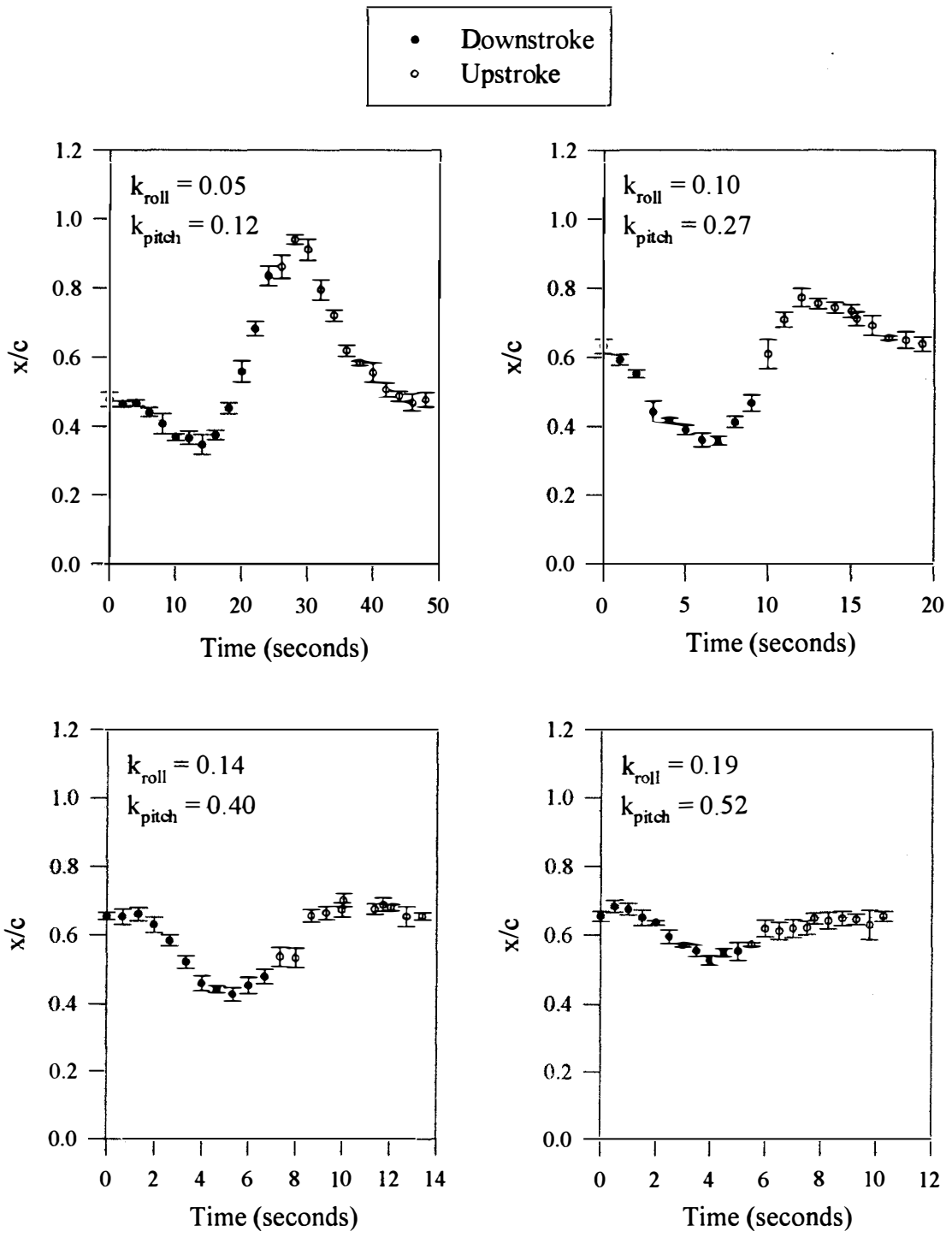

Figure 7.8. Location of Vortex Breakdown vs Time for Unsteady Maneuvering in Pitch While Rolling (Left Wing)

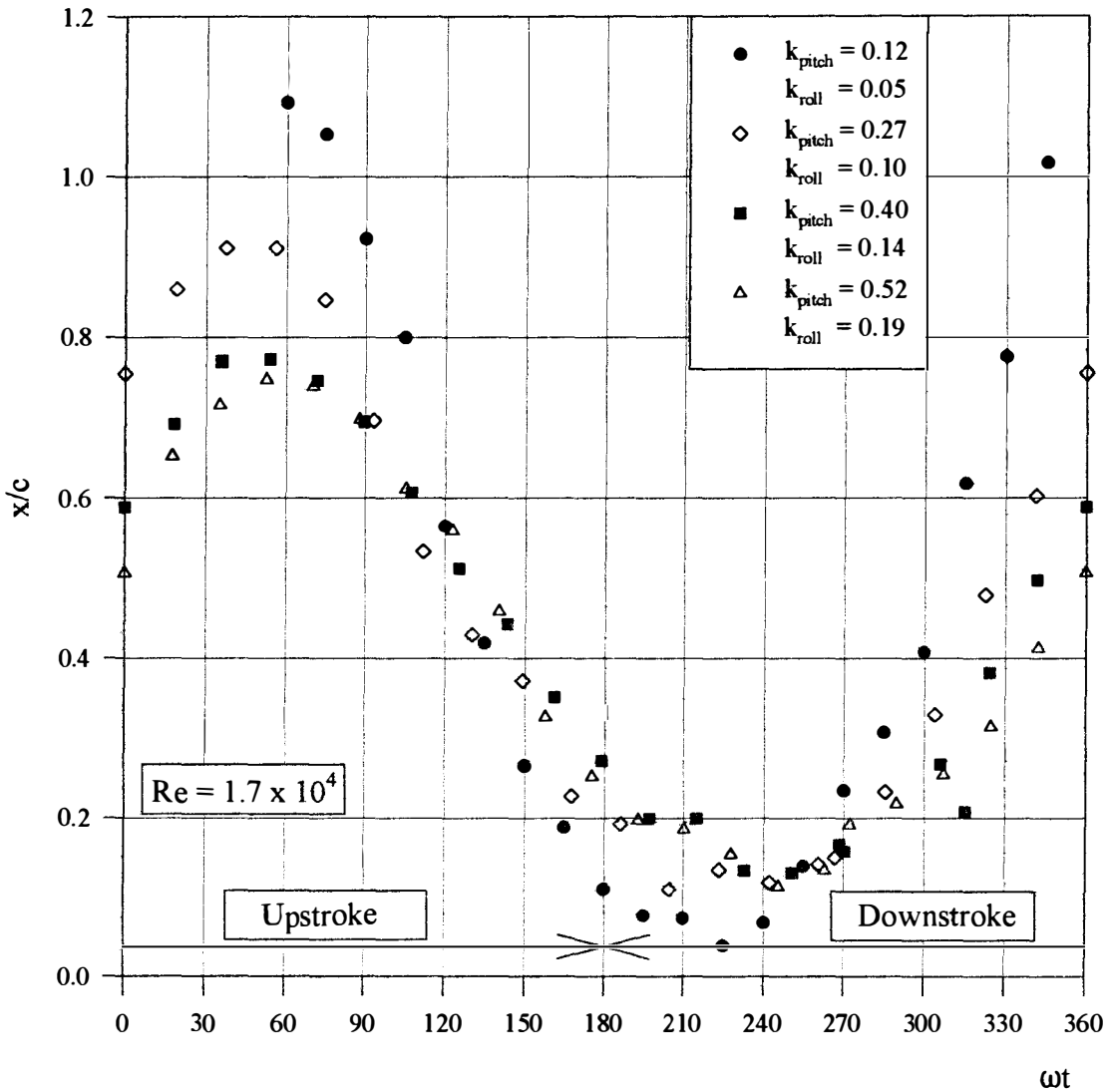

Figure 7.9. Location of Vortex Breakdown vs ωt for Unsteady Maneuvering in Pitch While Rolling (Right Wing)

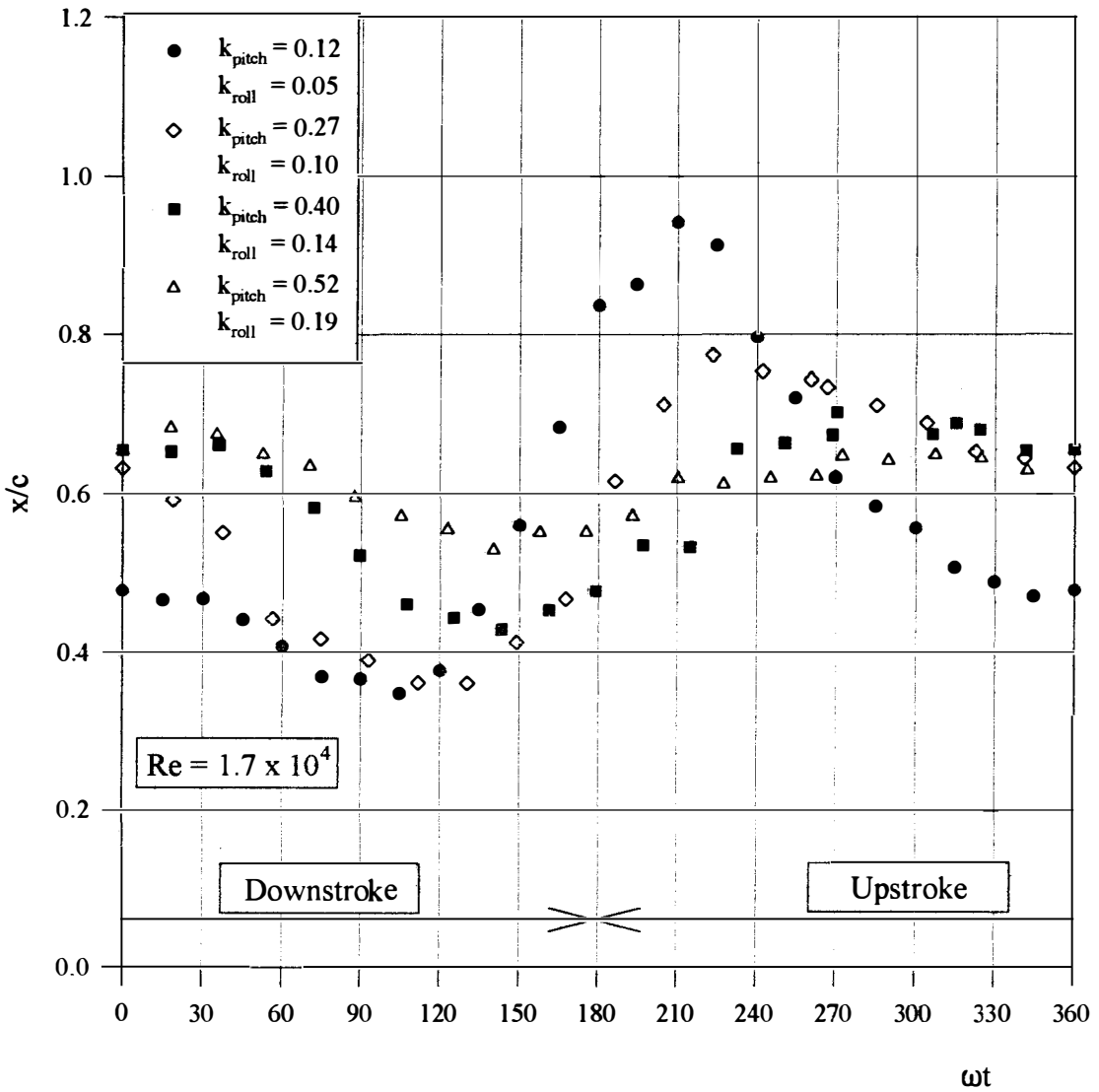

Figure 7.10. Location of Vortex Breakdown vs ωt for Unsteady Maneuvering in Pitch While Rolling (Left Wing)

an equal phase shift when transitioning from the upstroke to the downstroke as for transitioning from the downstroke to the upstroke. For the left wing; however, a big difference was noted between the two transitions. The phase shift was larger for the left wing when it transitioned from the upstroke to the downstroke than for the downstroke to the upstroke.

A comparison of the results was made with those from the unsteady analyses of pure pitch and pure roll. Because of the definition of reduced frequency for pitch and roll, however, the data was viewed two different ways. For example, the delta wing could be either viewed as oscillating in pitch at a given reduced frequency while undergoing roll oscillations or oscillating in roll at a given reduced frequency while undergoing pitch oscillations. Accordingly, the two comparisons are presented in Figure 7.11 and Figure 7.12. Figure 7.11 is a comparison of maneuvering data with unsteady pitch data and Figure 7.12 is a comparison of maneuvering data with unsteady roll data. A distinction has been made for the right and the left wings.

The results in Figure 7.11 show that for the right wing that is transitioning from the upstroke to the downstroke during pitch oscillations, any oscillations in roll tend to increase the phase lag. This result is even more pronounced for the left wing. For the transition from the downstroke to the upstroke, the result of the added roll oscillation had little effect on either side of the wing until the larger reduced frequency and then the effect was very pronounced on the left wing. The results in Figure 7.12 show that the addition of a pitch oscillations to a wing undergoing roll oscillations had little effect on the right side of the wing but had a dramatic effect on the left side of the wing.

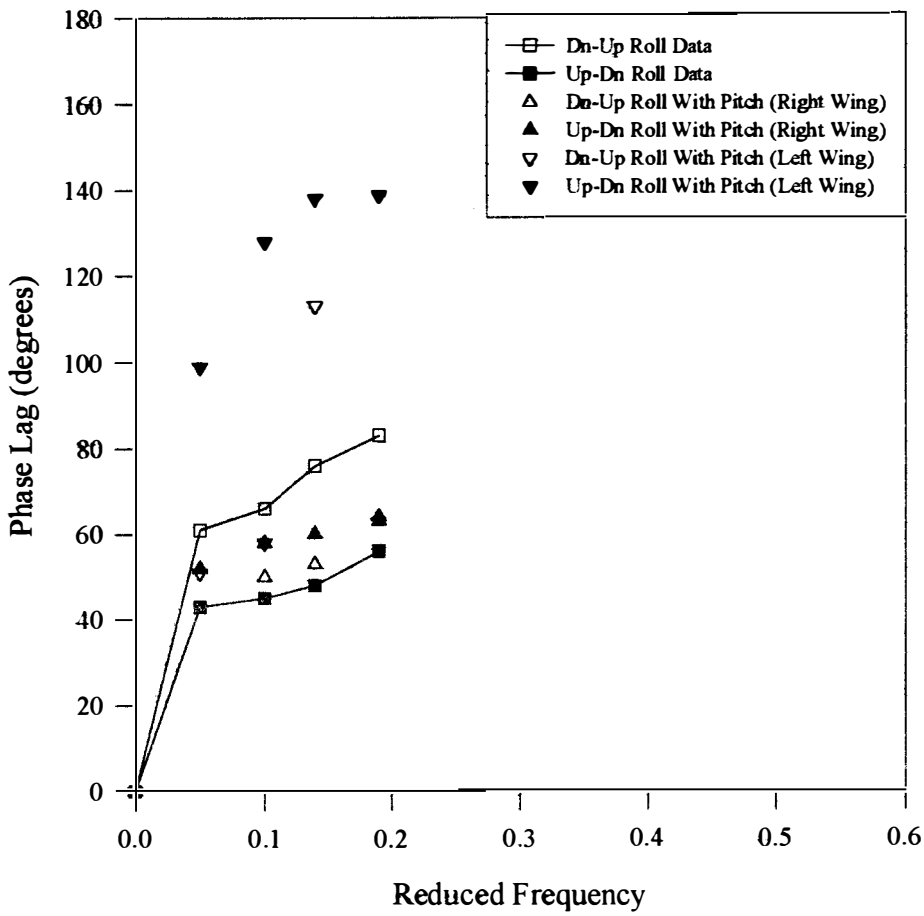

Figure 7.11. Phase Lag as a Function of Reduced Frequency for Unsteady Maneuvering as Compared to Unsteady Pitch Motion

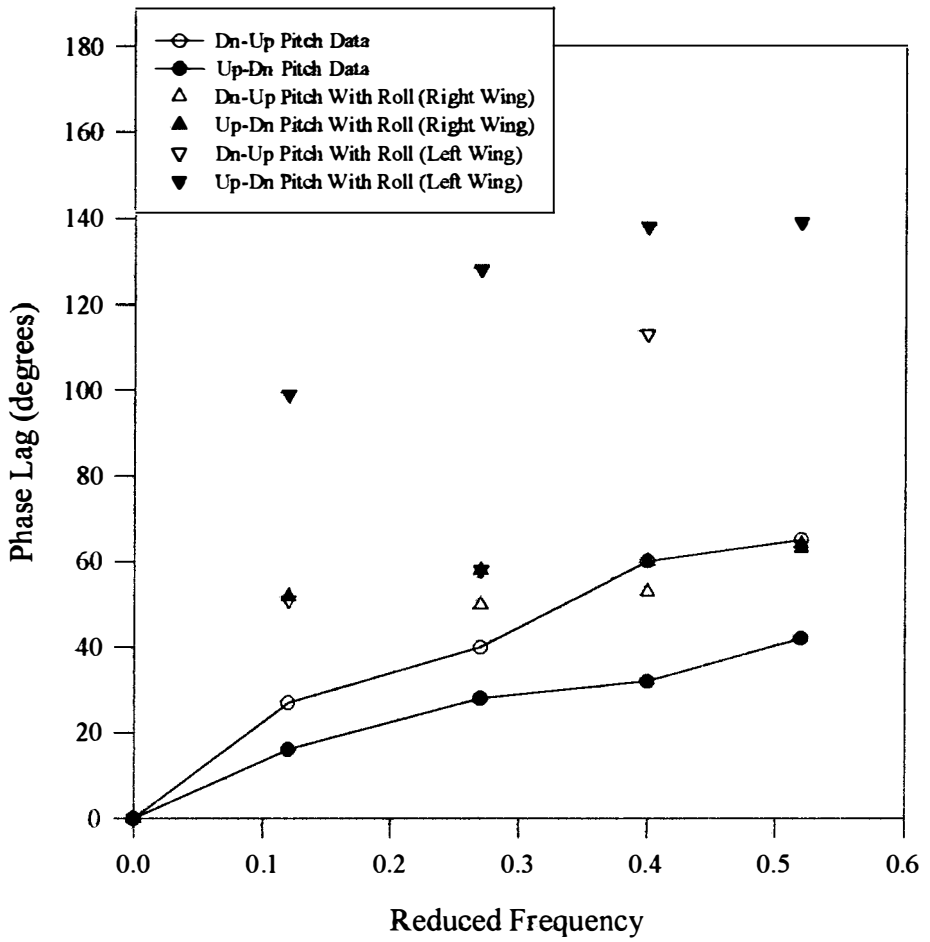

Figure 7.12. Phase Lag as a Function of Reduced Frequency for Unsteady Maneuvering as Compared to Unsteady Roll Motion

Summary of Maneuvering Experiments

The research conducted in this study was the first of it kind to examine the coupling effects on the location of vortex breakdown as the 70° delta wing was maneuvered in steady and unsteady conditions with variations in pitch and simultaneous variations in roll. For simplicity, this motion was termed maneuvering throughout the study. For all the tests, the maneuvering apparatus was set up so that a positive movement in pitch corresponded to a positive movement in roll. The resultant effect on the movement of the model was that as the model pitched up, the left wing pitched up and the right wing pitched down. The left wing, therefore, was considered to be in phase for movements in pitch and roll and the right wing was considered 180° out of phase. Accordingly, because of the symmetry of results shown with the roll experiments, two unique relative movements were analysed with the production of the two data sets.

For steady state maneuvering, variations in pitch and roll from 24° - 35° and -18° to 18° respectively were analysed to coincide with the experimentation carried out for pure steady state pitch and pure steady state roll. For the right wing, the experimental data showed that a decrease in pitch and roll angle resulted in the aft movement of the location of the vortex breakdown and an increase in pitch and roll angle resulted in the forward movement of the location of vortex breakdown. By comparing the effects of pure pitch and pure roll, it was concluded that the coupling effect on the right wing was a summation of the individual effects of pitch and roll. For the left wing, the location of the vortex breakdown also moved forward for an increase in pitch and roll angle and moved back for

a decrease in pitch and roll angle; however, the movement of the location of the vortex breakdown was more restricted for the left wing. This behaviour was also analysed by examining the individual effects of pitch and roll and it was concluded that the coupling effects for the left wing was also a summation of the individual affects of pitch and roll, but the dominating effect appeared to be the pitch up to a certain point where the nonlinearities observed for the roll movement took over.

Unsteady maneuvering experiments were carried out with the 70° delta wing oscillating in pitch while undergoing a corresponding roll oscillation. In pitch, the model oscillated about a mean angle of attack of 30° with an amplitude of ±5° and, in roll, the model oscillated about the centerline with an amplitude of ±18°. The unsteady maneuvering experiments were conducted at the same pitch frequencies for the other unsteady experiments and the reduced frequencies were kept consistent with those tested in the other unsteady investigations. The direction of the wing motion was defined by the pitch motion keeping in mind that the right wing was 180° out of phase and that the left wing was in phase with the pitch motion. The resultant data showed that a hysteresis effect existed for the right wing as well as the left wing which was seen by the deviations in the unsteady data from the steady state data.

For the right wing, the unsteady results showed a delay in breakdown location for the upstroke and an advancement in the location of the vortex breakdown for the downstroke as compared to the steady state data. This result was reasonable because the pitch and roll motion were actually out of phase and the right wing was actually on the upstroke. In comparison of the unsteady maneuvering data to the unsteady pitch and

unsteady roll data for the right wing, the results showed that the coupling effect of pitch and roll was a reduction in the overall hysteresis effect. This result was illustrated by the widening of the hysteresis loops indicating that there was less of a restriction in the movement of the location of the vortex breakdown.

For the left wing, the unsteady results also showed a delay in breakdown location for the upstroke and an advancement in the location of the vortex breakdown for the downstroke as compared to the steady state data; however, the movement in the location of vortex breakdown was more restricted. This result was reasonable because the pitch and roll motion were in phase and the effects of the roll motion dampened the effects of the pitch motion. In comparison of the unsteady maneuvering data to the unsteady pitch and unsteady roll data for the left wing, the results showed that the coupling effect of pitch and roll was an increase in the overall hysteresis effect as indicated by the restriction in the movement of the location of the vortex breakdown. In addition, the results of this investigation showed that an increase in reduced frequency increased the hysteresis effects which was shown by the restriction in movement of the location of vortex breakdown with increased reduced frequency.

An investigation was carried out to determine the relationship between phase lag and reduced frequency. The results of the investigation showed that for both wings, there was an increase in phase lag with an increase of reduced frequency. However, it was observed that there was a distinct difference in the phase lag for the right and the left wing. The right wing for example experienced an equal phase shift for a transition from the upstroke to the downstroke as for the transition from the downstroke to the upstroke.

The left wing, however, demonstrated a noticeable difference between the transition from the upstroke to the downstroke and the transition from the downstroke to the upstroke.

Because of the difference in definition of reduced frequency for the pitch and the roll motion, it was not possible to compare all the unsteady data together since the maneuvering data represented a unique combination of reduced frequencies for pitch and roll. Therefore an comparison of the maneuvering data was made separately with the unsteady pitch data and the unsteady roll data. The motion was described as either an oscillation in pitch at a given reduced frequency while undergoing roll oscillations or an oscillation in roll at a given reduced frequency while undergoing oscillations in pitch. In comparison with the pitch data, the results showed that for the right wing transitioning from the upstroke to the downstroke, any oscillations in roll tended to increase the phase lag. This result is even more pronounced for the left wing. For the transition from the downstroke to the upstroke, the result of the added roll oscillation had little effect on either side of the wing until the larger reduced frequency and then the effect was very pronounced on the left wing. In comparison with the roll data, the results showed that the addition of a pitch oscillation had little effect on the right side of the delta wing but had a dramatic effect on the left side of the delta wing.

CHAPTER VIII

CONCLUSIONS

An experimental investigation of a 70° delta wing under steady state and unsteady conditions has been successfully carried out in the RMC water tunnel. The test program included quantitative and qualitative studies using dye injection as a means of flow visualization to examine the behaviour of vortex breakdown under variations of pitch, roll and combinations of pitch and roll, termed maneuvering. The investigations carried out in this study was the first of their kind to analyse the coupling effect of pitch and roll on the behaviour of vortex breakdown under steady state and unsteady conditions. In addition, the results provided for an increased understanding of the flow over a 70° delta wing in terms of variations in pure pitch and pure roll angle.

The experimental investigation of the 70° delta wing involving steady state variations in pitch angle was carried out for angle of attack variations from 23° to 40°. The results were consistent with published data. In addition, two steady state empirical prediction equations were examined successfully under modification for leading edge geometry. Unsteady experiments were carried out with the 70° delta wing oscillating in pitch about the centre chord at a mean angle of attack of 30° with an amplitude of oscillation of ±5°. Four values of reduced frequency were tested ranging from $k_{pitch} = 0.12$ and $k_{pitch} = 0.52$ which corresponded to pitch frequencies ranging from 0.023 Hz to 0.097 Hz. The unsteady results demonstrated that as reduced frequency increased the amount of

hysteresis in the location of the vortex breakdown also increased. As well, the unsteady results showed that an increase in reduced frequency resulted in an increase in the amount of phase lag and that there was a distinct increase in phase lag when the delta wing transitioned from the downstroke to the upstroke (Dn-Up) as compared to the phase lag when the wing transitioned from the upstroke to the downstroke (Up-Dn).

An analysis was carried out to determine the behaviour of the vortex angle under steady and unsteady changes in angle of attack. For the steady state conditions, the experimental data showed a linear relationship between vortex angle core and angle of attack which compared well with published data. For unsteady pitching conditions, it was shown that the behaviour of vortex core angle as a function of angle of attack was independent of reduced frequency.

Investigation of the behaviour of vortex breakdown over a 70° delta for steady state variations in roll angle was conducted for roll angles varying from -18° to 18° with the delta wing fixed at a pitch angle of 30°. It was observed that the vortex behaviour over the right wing was symmetrically opposite to the vortex behaviour over the left wing. For the right wing, as the roll angle increased, the location of the vortex breakdown moved toward the apex and, as the roll angle decreased, the location of the vortex breakdown moved aft. The resultant data showed that the relationship between roll angle and the location of vortex breakdown over the front half of the delta wing could be considered linear. After a certain critical value of roll angle, however, the relationship between location of vortex breakdown and roll angle was nonlinear. The prediction equations which were modified to reflect a change of leading edge geometry were

successful in predicting the steady state location of the vortex breakdown over the front half of the wing; however, neither accurately predicted the location of the vortex breakdown over the aft portion of the wing.

Unsteady roll experiments were carried out with the 70° delta wing fixed at a pitch angle of 30° with roll oscillations of ±18° about the wings level position. The same frequencies of oscillation as for the unsteady pitch analysis were used but because of the difference in definition in reduced frequency between pitch and roll, this meant that the unsteady roll experiments were carried out at reduced roll frequencies that varied from k_{roll} = 0.05 to k_{roll} = 0.19. The unsteady results showed a hysteresis effect in the behaviour of the location of the vortex breakdown. The data collected from both sides of wing indicated that the behaviour was symmetric in terms of upstroke and downstroke. The unsteady results also showed that, as reduced frequency increased, the amount of hysteresis also increased. The same result was shown in terms of the amount of phase lag. In addition, the phase lag was consistently less when the wing transitioned from the upstroke to the downstroke (Up-Dn) than when it transitioned from the downstroke to the upstroke (Dn-Up).

The research conducted in this study was the first of it kind to examine the coupling effects of pitch and roll on the location of vortex breakdown as the 70° delta wing was maneuvered under steady and unsteady conditions. The maneuvering apparatus was set up so that a positive movement in pitch corresponded to a positive movement in roll which meant that as the model pitched up, the left wing pitched up and the right wing pitched down. The left wing, therefore, was considered to be in phase for movements in

pitch and roll and the right wing was considered 180° out of phase.

For steady state maneuvering, variations in pitch and roll from 25° to 35° and -18° to 18° respectively were analysed to coincide with the experimentation carried out for pure steady state pitch and pure steady state roll. For the right wing, the results showed that a decrease in pitch and roll angle resulted in the aft movement of the location of the vortex breakdown and an increase in pitch and roll angle resulted in the forward movement of the location of vortex breakdown. By comparing the effects of pure pitch and pure roll, it was concluded that the coupling effect on the right wing was an apparent superposition of the individual effects. For the left wing, the location of the vortex breakdown also moved forward for an increase in pitch and roll angle and moved back for a decrease in pitch and roll angle; however, the movement of the location of the vortex breakdown was more restricted for the left wing. By examining the individual effects of pitch and roll, it was concluded that the coupling effects for the left wing was also an apparent superposition of the individual effects. For the left wing, the dominating effect appeared to be the pitch until a critical value of roll angle was reached where the roll effect took over.

Unsteady maneuvering experiments were carried out with the 70° delta wing oscillating in pitch while undergoing a simultaneous roll oscillation. In pitch, the model oscillated about a mean angle of attack of 30° with an amplitude of ±5° and, in roll, the model oscillated about the centerline with an amplitude of ±18°. The unsteady maneuvering experiments were conducted at the same frequencies of oscillation as already tested and the reduced frequencies were kept consistent with those already tested. The unsteady data showed that a hysteresis effect existed for both the right wing and the left

wing. For the right wing, the unsteady results showed that the coupling effect of pitch and roll was a reduction in the overall hysteresis effect. For the left wing, the unsteady results showed that the coupling effect of pitch and roll was an increase in the overall hysteresis effect. In addition, the results of this investigation showed that an increase in reduced frequency increased the hysteresis effects for both wings. The results of the investigation also showed that for both wings, there was an increase in phase lag with an increase of reduced frequency. However, it was observed that there was a distinct difference in the phase lag for the right and the left wing. The right wing experienced an equal phase shift for a transition from the upstroke to the downstroke (Up-Dn) as for the transition from the downstroke to the upstroke (Dn-Up). The left wing, however, demonstrated a noticeable diffence between the transition from the upstroke to the downstroke (Up-Dn) and the transition from the downstroke to the upstroke (Dn-Up).

In comparison with the pitch data, the unsteady results showed that the addition of a roll oscillation increased the phase lag for both sides of the wing. In comparison with the roll data, the results showed that the addition of a pitch oscillation had little effect on the right side of the delta wing but had a dramatic effect on the left side of the delta wing.

CHAPTER IX

RECOMMENDATIONS

This section provides recommendations which have been divided into two separate categories. The first involves some lessons that were learned in the process of conducting the experimentation in this research program which could be beneficial to future studies of the same nature. The second pertains to critical areas of research required to further the investigation started in this study and to others areas of that may be of interest.

In termed of lessons learned, the primary observation presented is related to the data acquisition and analysis process. Modern technology has allowed for the use of relatively low cost data acquisition equipment which can provide for very accurate results. The trade-off is the amount of time required to process the results. The method of using SuperVHS video technology to record the data, for example, proved to be quite successful; however, the process involved in reducing the data was very time consuming and prone to human error. If a more automated method could be found for tracking the location of vortex breakdown from the video recorded source, a more in-depth analysis of the behaviour of the vortex breakdown phenomenon based on time increments, that were much closer together, could carried out. This was one of the critical factors in being able to analyse the phase lag relationship of the behaviour of the vortex breakdown with respect to the position of the test model. Another observation in terms of the data acquisition and analysis process is the absolute requirement for optimum resolution of the

digitized video frames being analysed. The higher the resolution, the more storage space necessary for the data; however, the advent of Zip discs have made this very economical. In addition, it is recommended that the method used to digitize the video data makes use of current software programs that allow for the digization of a number of successive frames of video.

One of the most critical factors in carrying out this experimentation to a high degree of accuracy and repeatability was the initial setup of the delta wing model in the test section of the water tunnel. A good check on the model orientation proved to be a verification that the delta wing produced symmetric results in terms of location of the vortex breakdown for each side of the delta wing when the roll angle was zero.

In terms of uncertainty, the steady pitch angle was very simple to measure and the method used for measurements provided for very accurate results. The roll angle, however, was not easily measured and had to be calculated and the accuracy of the results suffered. The magnitude of the roll angle was equally important as the magnitude of the pitch angle. For future studies involving roll, it would be very beneficial to invest in an apparatus that could provide accurate and instantaneous roll angle measurements.

Finally, it was determined that exact model geometry was paramount in being able to reproduce existing test data. Close attention must be placed on the design of the delta wing in terms of geometric similarity which must include leading edge geometry and thickness to chord ratio.

As discussed, the experimentation carried out in this study was the first of its kind to analyse the coupling effect of pitch and roll on the behaviour of vortex breakdown

under steady state and unsteady conditions. As a result, there is much more research that could take place that would expand the data base of information available related to the maneuvering of a delta wing and which could provide more incite into the coupling effects and the complex flow characteristics of vortex breakdown.

In this study, only one type of input motion was analysed. It would be beneficial to examine the behaviour of the location of vortex breakdown in terms of time history for a transient input motion. This would enable the analysis of the time for the vortex flow to adjust to the new steady state conditions and, some have argued, may provide a more practical representation of aircraft maneuvres.

It was commented upon in this study that leading edge geometry is a critical factor to be considered for reproducing available data. In fact, this comment has been made by many researchers based on experimental data from pitch studies. To further this analysis, therefore, a study could be carried out to investigate the effect of leading edge geometry to include variation in roll as well as the coupling effects of pitch and roll.

One of the limitations in the experimentation portion of this research was the maneuvering apparatus design so that the movements in pitch and roll were driven from the same source. This was a simple method of effecting a maneuver in pitch and roll; however, it imposed a restriction in terms the flexibility of changing the parameters in the test program. It would be beneficial, for example, to oscillate the model in pitch and roll at the same reduced frequency and it would be equally beneficial to oscillate the model in pitch and roll with the same amplitudes of oscillation. It is recommended, therefore, that a study be conducted with variety of combinations of pitch and roll as well as reduced

frequencies to further the understanding of the vortex breakdown phenomenon for a maneuvering delta wing.

In this study, the steady and unsteady roll experiments were conducted at a specific angle of attack to coincide with other researchers. It is recommended that this base of information be expanded to include the behaviour of vortex breakdown in conditions of steady and unsteady roll at different pitch angles. In addition, it would be beneficial to extend this approach to include a study of the behaviour of vortex breakdown under conditions of steady and unsteady pitch for other than zero roll angles.

Finally, an extension of the research conducted in this study could be geared toward investigating methods of flow control and their relationship on the location of vortex breakdown over delta wing geometries that maneuever in steady state and unsteady conditions.

LIST OF REFERENCES

LIST OF REFERENCES

1. Wu, J.M., "Unsteady Flow Phenomenon," Unsteady Flow Phenomenon Short Course Lecture Notes held at UTSI, February 1989.

2. Polhamus, E. C., "Vortex Lift Research: Early Contributions And Some Current Challenges," NASA Langley Research Center, Hampton, Virginia.

3. Polhamus, E.C., "A Concept of The Vortex Lift of Sharp-Edge Delta Wings Based on a Leading-Edge-Suction Analogy," NASA TN D-3767, 1966.

4. Hemsch, Michael.J., and Luckring, James.M., "Connection Between Leading Edge Sweep, Vortex Lift and Vortex Strength For Delta Wings", Journal of Aircraft, Vol 27, No. 5, May 1990, pp. 473-475.

5. Peake, D.J., "On Issues Concerning Flow Separation And Vortical Flows In Three Dimensions", Paper No. 1, AGARD-CP-342, April 1983.

6. Wedemeyer, E., "Vortex Breakdown," Paper No. 9, AGARD-LS-121, December 1982.

7. Lee, M. and Ho, C., "Vortex Dynamics of Delta Wings," Department of Aerospace Engineering, University of Southern California, Los Angeles, California, Lecture Notes in Engineering No. 46, Springer-Verlag, 1989.

8. Gad-el-Hak, M., and Blackwelder, R.F., "The Discrete Vortices From a Delta Wing," AIAA Journal, Vol. 23, June 1985, pp. 961-962.

9. Peckham,D.H., and Atkinson, S.A., "Preliminary Results of Low Speed Wind Tunnel Tests on a Gothic Wing of Aspect Ratio 1.0," Aeronautical Research Council Current Papers, No. 508, April 1957.

10. Elle, B.J., "An Investigation at Low Speed of the Flow Near The Apex of The Delta Wings With Sharp Leading Edges," Aeronautical Research Council Reports and Memoranda, No. 3176, 1961.

11. Lambourne, N.C., and Bryer, D.W., "Some Measurements in Vortex Flow Generated by Sharp Leading Edge Having 65 Degree Sweep," British Aeronautical Research Council, London, ARC CP 477, 1960.

12. Van Dyke, M., "An Album Of Fluid Motion," The Parabolic Press, Stanford, California, 1982.

13. Liebovich, S., "Vortex Stability and Breakdown," AIAA J, Vol. 22, No. 9, September 1984, pp 1192-1206.

14. Lowson, M.V., and Riley, A.J., "Vortex Breakdown Control by Delta Wing Geometry," AIAA Journal of Aircraft, Vol. 32, No. 4, July-August 1995, pp. 832-838.

15. Wentz, W.H., and Kohlman, D.L., "Vortex Breakdown on Slender Sharp-Edged Wings," Journal of Aircraft, Vol. 8, No. 3, 1971, pp 156-161.

16. Lee, M., and Ho, C.M., "Lift Force of Delta Wings," Applied Mechanics Review, Vol. 43, No. 9, 1990.

17. Huang, X.Z, and Hanff, E.S., "Prediction of Leading Edge Vortex Breakdown on a Delta Wing Oscillating in Roll," AIAA Paper 92-2677, June 1992.

18. Huang, X.Z, and Hanff, E.S., "Prediction of Normal Force on a Delta Wing Rolling at High Incidence," AIAA Paper 93-3686, August 1993.

19. Erickson, Gary, E., "Water Tunnel Studies of Leading-Edge Vortices," Journal of Aircraft, Vol. 19, No. 6, 1982, pp. 442-448.

20. Jarrah, Mohammand-Ameen M., "Low-Speed Wind-Tunnel Investigation of Flow About Delta Wings, Oscillating in Pitch to Very High Angles of Attack," AIAA Paper 89-0295, January 1989.

21. Gursul, I., and Yang, H., "Vortex Breakdown Over a Pitching Delta Wing," AIAA Paper 94-0536, January 1994.

22. Atta, R., and Rockwell, D., "Hysteresis of Vortex Development And Breakdown on an Oscillating Delta Wing," AIAA Journal, Vol. 25, No. 11, November 1987, pp 1512-1513.

23. Thompson, Scott, A., "The Unsteady Aerodynamics of a Delta Wing Undergoing Large Amplitude Pitching Motions," PhD Dissertation, University of Notre Dame, 1992.

24. Ashley, H., Jarrah, M.A.M., Katz, J., and Vaneck, T., "Unsteady Aerodynamic Loading of Delta Wings For Low And High Angles of Attack," June 1990

25. LeMay, S.P., Batill, S.M., and Nelson, R.C., "Vortex Dynamics on a Pitching Delta Wing," AIAA Journal of Aircraft, Vol. 27, February 1990, pp. 131-138.

26. Gad-el-Hak, M., and Ho., C.M., "The Pitching Delta Wing," AIAA Journal, Vol. 23, November 1985, pp. 1660-1665.

27. Reynolds, G.A., and Abtahi, A.A., "Instabilities in Leading Edge Vortex Development," AIAA Paper 87-2424, August 1987.

28. Magness, C., Robinson, O., and Rockwell, D., "Control of Leading-Edge Vortices on a Delta Wing," AIAA Paper 89-0999, March 1989.

29. Wolffelt, K.W., "Investigation of The Movement of Vortex Burst Position With Dynamically Changing Angle of Attack For a Schematic Delta Wing in a Water Tunnel With Correlation to Similar Studies in Wind Tunnel," AGARD Paper CPP-413, October 1986.

30. Brandon, Jay M., and Shah, Gautam, H., "Effect of Large Amplitude Pitch Motions on The Unsteady Aerodynamic Characteristics of Flat Plate Wings," AIAA Paper 88-4331, August 1988.

31. Laidlaw, W.R., "Theoretical and Experimental Pressure Distributions on Low Aspect Ratio Wings Oscillating in an Incompressible Flow," MIT Aeroelastic and Structures Research Laboratory Technical Report 51-2, September 1954.

32. Woodgate, L., "Measurements of the Pitching-Moment Derivatives on a Sharp Edged Delta Wing in Incompressible Flow," Aeronautic research Council Reports and Memoranda, No. 3379, October 1963.

33. Lambourne, N.C., and Bryer, D.W., "The Bursting of Leading Edge Vortices - Some Observations and Discussion of The Phenomenon," British Aeronautical Research Council, London, ARC R&M 3282, 1962.

34. Lowson, M.V., "Some Experiments With Vortex Breakdown," Journal of the Royal Aeronautical Society, Vol. 68, 1964, pp. 343-346.

35. Erickson, Gary, E., "Water Tunnel Studies of Leading-Edge Vortices," Journal of Aircraft, Vol. 19, No. 6, 1982, pp. 442-448.

36. Atta, R., and Rockwell, D., "Leading-Edge Vortices Due to Low Reynolds Number Flow Past a Pitching Delta Wing," AIAA Journal, Vol. 28, No. 6., June 1990, pp 995-1004.

37. Brandon, Jay M., and Shah, Gautam, H., "Unsteady Aerodynamic Characteristics of a Fighter Model Undergoing Large Amplitude Pitching at High Angles of

Attack," AIAA Paper 90-0309, January 1990.

38. Jarrah, M.A.M., "Visualization of the Flow About a Delta Wing Maneuvering in Pitch to Very High Angles of Attack," International Symposium on Nonsteady Fluid Dynamics, June 1990.

39. Jarrah, M.A.M., "Visualization of the Flow About a Delta Wing Maneuvering in Pitch to Very High Angles of Attack," International Symposium on Nonsteady Fluid Dynamics, June 1990.

40. Hebbar, S.K, Platzer, M.F., "Vortex Breakdown Studies of a Canard-configured X-31A-like Fighter Aircraft Model," Journal of Aircraft, Vol. 30, No. 3, May - June 1993, pp 405-408.

41. Rediniotis, O.K., Stapountzis, H., Telionis, D.P., "Periodic Vortex Shedding Over Delta Wings," AIAA Journal, Vol. 31, No. 9, 1993, pp. 1555-1562.

42. Rediniotis, O.K., Klute, S.M., Hoang, N.T., and Telionis, D.P., "Dynamic Pitch-up of a Delta Wing," AIAA Journal, Vol. 32, No. 4, 1994, pp. 716- 725.

43. Lin, J.C., and Rockwell, D., "Transient Structure of Vortex Breakdown on a Delta Wing," AIAA Journal, Vol. 33, No. 1, 1995, pp. 6- 12.

44. Hanff, E.S., and Jenkins, S.B., "Large-Amplitude High Rate Roll Experiments on a Delta and Double Delta Wing," AIAA Paper 90-0224, January 1990.

45. Ericsson, L.E., and Hanff, E.S., "Unique High-Alpha Roll Dynamics of a Sharp-Edged 65 Deg Delta Wing," Journal of Aircraft, Vol. 31, No. 3, 1994, pp. 520-525.

46. Ericsson, L.E., and Hanff, E.S., "Further Analysis of High-Rate Rolling Experiments of a 65-Deg Delta Wing," Journal of Aircraft, Vol. 31, No. 6, November-December 1994, pp. 1350-1357.

47. Ericsson, L.E., "Difficulties in Predicting Vortex Breakdown Effects on a Rolling Delta Wing," Journal of Aircraft, Vol. 33, No. 3, May-June 1996, pp. 477-484.

48. Chaderjian, N. M., and Schiff, L.b., "Navier Stokes Prediction of Large-Amplitude Forced and Free-to-Roll Delta Wing Oscillations," AIAA Paper 94-1884, June 1994.

49. Hanff, E.S., and Ericsson, L.E., "Multiple Roll Attractors of a Delta Wing at High Incidence," Paper 31, AGARD-CP-494, July 1991.

50. Ericsson, L.E., "Flow Physics of Critical States for Rolling Delta Wings," Journal of Aircraft, Vol. 32, No. 3, May-June 1995, pp. 603-610.

51. Randall, J., and, Waugh, J., "Analysis of the Flow Properties in the Royal Military College of Canada (RMC) Water Tunnel," Final Written Report Mechanical

52. Manor, D., Miller, L., and Wentz, W.H., Jr, "Static and Dynamic Water Tunnel Tests of Slender Wings and Wing-Body Configurations at Extreme Angles of Attack," AIAA Paper 90-3021, 1990.

53. Morris, S.L., Ward, D.T., Malcolm, G.N., and Ward, D.T., "Nonintrusive Measurements of Vortex Flow on Delta Wings in a Water Tunnel," AIAA Paper 88-2595-CP, June 1988.

54. Jenkins, J.E., Myatt, J.H., and Hanff, E.S., "Body-Axis Rolling Motion Critical States of a 65-Deg Delta Wing," AIAA Paper 93-0621, January 1993.

55. Wentz, W.H., and Kohlman, D.L., "Vortex Breakdown on Slender Sharp-Edged Wings," Journal of Aircraft, Vol. 8, No. 3, 1971, pp 156-161.

BIBLIOGRAPHY

BIBLIOGRAPHY

Atta, R., and Rockwell, D., "Hysteresis of Vortex Development And Breakdown on an Oscillating Delta Wing," AIAA Journal, Vol. 25, No. 11, November 1987, pp 1512-1513.

Atta, R., and Rockwell, D., "Leading-Edge Vortices Due to Low Reynolds Number Flow Past a Pitching Delta Wing," AIAA Journal, Vol. 28, No. 6., June 1990, pp 995-1004.

Ashley, H., Jarrah, M.A.M., Katz, J., and Vaneck, T., "Usteady Aerodynamic Loading of Delta Wings For Low And High Angles of Attack," International Symposium on Nonsteady Fluid Dynamics, June 1990.

Berry, F.C., "High Alpha," Air Force Magazine, October 1990.

Bragg, M.B., and Soltani, M.R., "An Experimental Study of The Effect of Asymmetrical Vortex Bursting on a Pitching Delta Wing," AIAA Paper 88-4334, August 1988.

Brandon, Jay M., and Shah, Gautam, H., "Effect of Large Amplitude Pitch Motions on The Unsteady Aerodynamic Characteristics of Flat-Plate Wings," AIAA Paper 88-4331, August 1988.

Brandon, Jay M., and Shah, Gautam, H., "Unsteady Aerodynamic Characteristics of a Fighter Model Undergoing Large Amplitude Pitching at High Angles of Attack," AIAA Paper 90-0309, January 1990.

Cavazos, Odilon V., Jr., "A Flow Visualization Study of LEX Generated Vortices on a Scale Model of a F/A-18 Fighter Aircraft at High Angles of Attack," Master's Thesis, Naval Post Graduate School, Monterey, California, June 1990.

Crowe, J.A., Robertson, C.T., "Engineering Fluid Mechanics," Houghton Mifflin Company, Boston, 1975.

Chaderjian, N. M., and Schiff, L.b., "Navier Stokes Prediction of Large-Amplitude Forced and Free-to-Roll Delta Wing Oscillations," AIAA Paper 94-1884, June 1994.

Cunningham, Atlee M. Jr., and Bushlow, Todd, "Steady and Unsteady Force Testing of Fighter Model in a Water Tunnel," AIAA Paper 90-2815, August 1990.

Elle, B.J., "An Investigation at Low Speed of the Flow Near The Apex of The Delta

Wings With Sharp Leading Edges," Aeronautical Research Council Reports and Memoranda, No. 3176, 1961.

Erickson, Gary, E., "Effects of Non-Planar Strake-Wing on the Vortex Lift Characteristics of a Twin-Jet Fighter Configuration," AIAA Paper 80-0329, January 1980.

Erickson, Gary, E., "Flow Studies of Slender Wing Vortices," AIAA Paper 80-1423, July 1980.

Erickson, Gary, E., "Water Tunnel Studies of Leading-Edge Vortices," Journal of Aircraft, Vol. 19, No. 6, 1982, pp. 442-448.

Ericsson, L.E., and Hanff, E.S., "Unique High-Alpha Roll Dynamics of a Sharp-Edged 65 Deg Delta Wing," Journal of Aircraft, Vol. 31, No. 3, 1994, pp. 520-525.

Ericsson, L.E., and Hanff, E.S., "Further Analysis of High-Rate Rolling Experiments of a 65-Deg Delta Wing," Journal of Aircraft, Vol. 31, No. 6, November-December 1994, pp. 1350-1357.

Ericsson, L.E., "Difficulties in Predicting Vortex Breakdown Effects on a Rolling Delta Wing," Journal of Aircraft, Vol. 33, No. 3, May-June 1996, pp. 477-484.

Ericsson, L.E., "Flow Physics of Critical States for Rolling Delta Wings," Journal of Aircraft, Vol. 32, No. 3, May-June 1995, pp. 603-610.

Gad-el-Hak, M., and Blackwelder, R.F., "The Discrete Vortices From a Delta Wing," AIAA Journal, Vol. 23, June 1985, pp. 961-962.

Gad-el-Hak, M., and Ho., C.M., "The Pitching Delta Wing," AIAA Journal, Vol. 23, November 1985, pp. 1660-1665.

Gad-el-Hak, M., "Visualization Techniques for Unsteady Flows: An Overview," Journal Of Fluids Engineering Vol 110, pp. 231-243, September 1988.

Ghia, U., Zuo, L., Ghia, K., "Analysis & Control of Unsteady Separated Flows," AIAA Paper 89-1018, March 1989.

Greenwell, D.I., and Wood, N.J., "Determination of Vortex Burst Location on Delta Wings From Surface Pressure Measurements," AIAA Journal, Vol. 30, No 11, November 1992, pp 2736-2739.

Gursul, I., and Yang, H., "Vortex Breakdown Over a Pitching Delta Wing," AIAA Paper 94-0536, January 1994.

Gursul, I., Srinivas, S., and Batta, G., "Active Control of Vortex Breakdown Over a Delta Wing," AIAA Journal, Vol. 33, No. 9, June 1995.

Hanff, E.S., and Jenkins, S.B., "Large-Amplitude High Rate Roll Experiments on a Delta and Double Delta Wing," AIAA Paper 90-0224, January 1990.

Hanff, E.S., and Ericsson, L.E., "Multiple Roll Attractors of a Delta Wing at High Incidence," Paper 31, AGARD-CP-494, July 1991.

Hebbar, S.K, Platzer, M.F., "Vortex Breakdown Studies of a Canard-configured X-31A-like Fighter Aircraft Model," Journal of Aircraft, Vol. 30, No. 3, May - June 1993, pp 405-408.

Hemsch, Michael.J., and Luckring, James.M., "Connection Between Leading Edge Sweep, Vortex Lift and Vortex Strength For Delta Wings", Journal of Aircraft, Vol 27, No. 5, May 1990, pp. 473-475.

Herlt, S., "High Angle of Attack and the Eagle," McAir Production Support Digest Vol 37, N0. 31990.

Huang, X.Z, and Hanff, E.S., "Prediction of Leading Edge Vortex Breakdown on a Delta Wing Oscillating in Roll," AIAA Paper 92-2677, June 1992.

Huang, X.Z, and Hanff, E.S., "Prediction of Normal Force on a Delta Wing Rolling at High Incidence," AIAA Paper 93-3686, August 1993.

Jarrah, Mohammand-Ameen M., "Unsteady Aerodynamics of Delta Wings Performing Maneuvers to High Angle of Attack," PhD Dissertation, Stanford University, December 1988.

Jarrah, Mohammand-Ameen M., "Low-Speed Wind-Tunnel Investigation of Flow About Delta Wings, Oscillating in Pitch to Very High Angles of Attack," AIAA Paper 89-0295, January 1989.

Jarrah, M.A.M., "Visualization of the Flow About a Delta Wing Maneuvering in Pitch to Very High Angles of Attack," International Symposium on Nonsteady Fluid Dynamics, June 1990.

Jenkins, J.E., Myatt, J.H., and Hanff, E.S., "Body-Axis Rolling Motion Critical States of a 65-Deg Delta Wing," AIAA Paper 93-0621, January 1993.

Katz, J., and Levin, D., "Static Measurements of Slender Delta Wing Rolling Moment Hysteresis," Journal of Aircraft, Vol. 28, No. 4, April 1991, pp 282-283.

Laidlaw, W.R., "Theoretical and Experimental Pressure Distributions on Low Aspect Ratio Wings Oscillating in an Incompressible Flow," MIT Aeroelastic and Structures Research Laboratory Technical Report 51-2, September 1954.

Lamar, J.E., "Nonlinear Lift Control at High Speed and High Angle of Attack," Paper No. 4, AGARD-R-740, February 1986.

Lambourne, N.C., and Bryer, D.W., "Some Measurements in Vortex Flow Generated by Sharp Leading Edge Having 65 Degree Sweep," British Aeronautical Research Council, London, ARC CP 477, 1960.

Lambourne, N.C., and Bryer, D.W., "The Bursting of Leading Edge Vortices - Some Observations and Discussion of The Phenomenon," British Aeronautical Research Council, London, ARC R&M 3282, 1962.

Lee, M. and Ho, C., "Vortex Dynamics of Delta Wings," Department of Aerospace Engineering, University of Southern California, Los Angeles, California, Lecture Notes in Engineering No. 46, Springer-Verlag, 1989.

Lee, M., and Ho, C.M., "Lift Force of Delta Wings," Applied Mechanics Review, Vol. 43, No. 9, 1990.

LeMay, S.P., Batill, S.M., and Nelson, R.C., "Vortex Dynamics on a Pitching Delta Wing," AIAA Journal of Aircraft, Vol. 27, February 1990, pp. 131-138.

Liebovich, S., "Vortex Stability and Breakdown," AIAA Journal, Vol. 22, No. 9, September 1984, pp. 1192-1206.

Limin, S., Yanhau, Q., "An Investigation of Improving High Angle of Attack Performance and Flap Effectiveness of a Configuration with Delta Wing by Spanwise Blowing," China Aerodynamic Research and Development Center, Sichuan, China.

Lin, J.C., and Rockwell, D., "Transient Structure of Vortex Breakdown on a Delta Wing," AIAA Journal, Vol. 33, No. 1, 1995, pp. 6- 12.

Lowson, M.V., "Some Experiments With Vortex Breakdown," Journal of the Royal Aeronautical Society, Vol. 68, 1964, pp. 343-346.

Little, H.S., and Eaton, J.K., "Unsteady Flowfield Behind a Vortex Generator Rapidly Pitched to an Angle of Attack," AIAA Journal, Vol. 29, No. 4, April 1991, pp 577-584.

Lowson, M.V., and Riley, A.J., "Vortex Breakdown Control by Delta Wing Geometry,"

AIAA Journal of Aircraft, Vol. 32, No. 4, July-August 1995, pp. 832-838.

Magness, C., Robinson, O., and Rockwell, D., "Control of Leading-Edge Vortices on a Delta Wing," AIAA Paper 89-0999, March 1989.

Manor, D., Miller, L., and Wentz, W.H., Jr, "Static and Dynamic Water Tunnel Tests of Slender Wings and Wing-Body Configurations at Extreme Angles of Attack," AIAA Paper 90-3021, 1990.

Morris, S.L., Ward, D.T., Malcolm, G.N., and Ward, D.T., "Nonintrusive Measurements of Vortex Flow on Delta Wings in a Water Tunnel," AIAA Paper 88-2595-CP, June 1988.

Nelson, R.C. "Visualization Techniques for Studying High Angle of Attack Separated Vortical," AIAA Paper 88-2025, AIAA Journal pp. 234-241, 1988.

Panton, R.L., "Effects of a Contoured Apex on Vortex Breakdown," Journal of Aircraft, Vol. 27, No. 3, March 1990, pp 285-288.

Peake, D.J., "On Issues Concerning Flow Separation And Vortical Flows In Three Dimensions", Paper No. 1, AGARD-CP-342, April 1983.

Peckham,D.H., and Atkinson, S.A., "Preliminary Results of Low Speed Wind Tunnel Tests on a Gothic Wing of Aspect Ratio 1.0," Aeronautical Research Council Current Papers, No. 508, April 1957.

Polhamus, E.C., "A Concept of The Vortex Lift of Sharp-Edge Delta Wings Based on a Leading-Edge-Suction Analogy," NASA TN D-3767, 1966.

Polhamus, E.C., "Predictions of Vortex Lift Characteristics by a Leading Edge Suction Analogy," AIAA Journal of Aircraft, Vol. 8, April 1971, pp. 193-199.

Polhamus, E. C., "Vortex Lift Research: Early Contributions And Some Current Challenges," NASA Langley Research Center, Hampton, Virginia.

Randall, J., and, Waugh, J., "Analysis of the Flow Properties in the Royal Military College of Canada (RMC) Water Tunnel," Final Written Report Mechanical Engineering, March 1996.

Rao, D.M., "Vortical Flow Management for Improved Configuration Aerodynamics - Recent Experiences," Paper No. 30, AGARD-CP-342, April 1983.

Rao, D.M., Campbell J.F., "Vortical Flow Management Techniques," Aerospace Sci.

Vol. 24, pp. 173-224, 1987.

Rediniotis, O.K., Stapountzis, H., Telionis, D.P., "Vortex Shedding Over Delta Wings," AIAA Journal, Vol. 28, No. 5, 1990 pp. 944-946.

Rediniotis, O.K., Stapountzis, H., Telionis, D.P., "Periodic Vortex Shedding Over Delta Wings," AIAA Journal, Vol. 31, No. 9, 1993 pp. 1555-1562.

Rediniotis, O.K., Klute, S.M., Hoang, N.T., and Telionis, D.P., "Dynamic Pitch-up of a Delta Wing," AIAA Journal, Vol. 32, No. 4, 1994, pp. 716- 725.

Reynolds, G.A., and Abtahi, A.A., "Instabilities in Leading Edge Vortex Development," AIAA Paper 87-2424, August 1987.

Rockwell, D., Atta, R., Kuo, CH., Hefele, C., Magness, C., and Utsch, T., "On Unsteady Flow Structure From Swept Edges Subjected to Controlled Motion."

Sawyer, R., and Sullivan, J., "Lift Development on Delta Wings Undergoing Constant Acceleration From Rest," AIAA Paper 90-0310, January 1990.

Seginer, A., Salomon, M., "Augmentation of Fighter Aircraft Performance by Spanwise Blowing Over the Wing Leading Edge," Paper No. 33, AGARD-CP-342, April 1983.

Settles, G.S., "Modern Developments in Flow Visualization," AIAA Paper 84-1599, Vol. 24, No. 8, August 1986.

Schlicting, H., "boundary-Layer Theory," McGraw-Hill Book Company, New York.

Srinivas. S., Gursul, I., and Batta, G., "Active Control of Vortex Breakdown Over Delta Wings," AIAA Paper 94-2215, June 1994

Sweetman, B., "Fighter Agility," International Defence Review, Vol 23, 4/1990.

Thompson, D.H., "Water Tunnel Flow Visualization of Vortex Breakdown Over The F/A-18," Australian Defence Science and Technology Organization, Report No. ALL-FLIGHT-MUCH-R-179, December 1990.

Thompson, SA., Batill, S.M., and Nelson R.C., "The Separated Flow Field on a Slender Delta Wing Undergoing Transient Pitching Motions," AIAA Paper 89-0194, January 1989.

Thompson, SA., Batill, S.M., and Nelson R.C., "Delta Wing Surface Pressures For High

Angle of Attack Maneuvers," AIAA Paper 90-2813, August 1990.

Thompson, Scott, A., "The Unsteady Aerodynamics of a Delta Wing Undergoing Large Amplitude Pitching Motions," PhD Dissertation, University of Notre Dame, 1992.

Vakili, A.D., "Review of Vortical Flow Utilization," AIAA Paper 90-1429, UTSI, AIAA 16th Aerodynamic Ground Testing Conference, Seattle, WA, June 1990.

Vakili, A.D., "Flow Visualization and Measurement Techniques," Unsteady Flow Phenomenon Short Course Lecture Notes held at UTSI, February 1989.

Van Dyke, M., "An Album Of Fluid Motion," The Parabolic Press, Stanford, California, 1982.

Wedemeyer, E., "Vortex Breakdown," Paper No. 9, AGARD-LS-121, December 1982.

Wentz, W.H., and Kohlman, D.L., "Vortex Breakdown on Slender Sharp-Edged Wings," Journal of Aircraft, Vol. 8, No. 3, 1971, pp 156-161.

Wolffelt, K.W., "Investigation of The Movement of Vortex Burst Position With Dynamically Changing Angle of Attack For a Schematic Delta Wing in a Water Tunnel With Correlation to Similar Studies in Wind Tunnel," AGARD Paper CPP-413, October 1986.

Woodgate, L., "Measurements of the Pitching-Moment Derivatives on a Sharp Edged Delta Wing in Incompressible Flow," Aeronautic research Council Reports and Memoranda, No. 3379, October 1963.

Wu, J.M., "Unsteady Flow Phenomenon," Unsteady Flow Phenomenon Short Course Lecture Notes held at UTSI, February 1989.

APPENDIXES

APPENDIX A

EVALUATION OF ROLL ANGLES

Because of the nature of the experimental setup, it was not possible to directly measure the steady state roll angle. However, the steady state roll angle could be evaluated using information obtained with regards to the travel distance of the C-Beams. For example, Figure A.1 provides a side view of the model in the water tunnel which highlights the pitch rotation of the model.

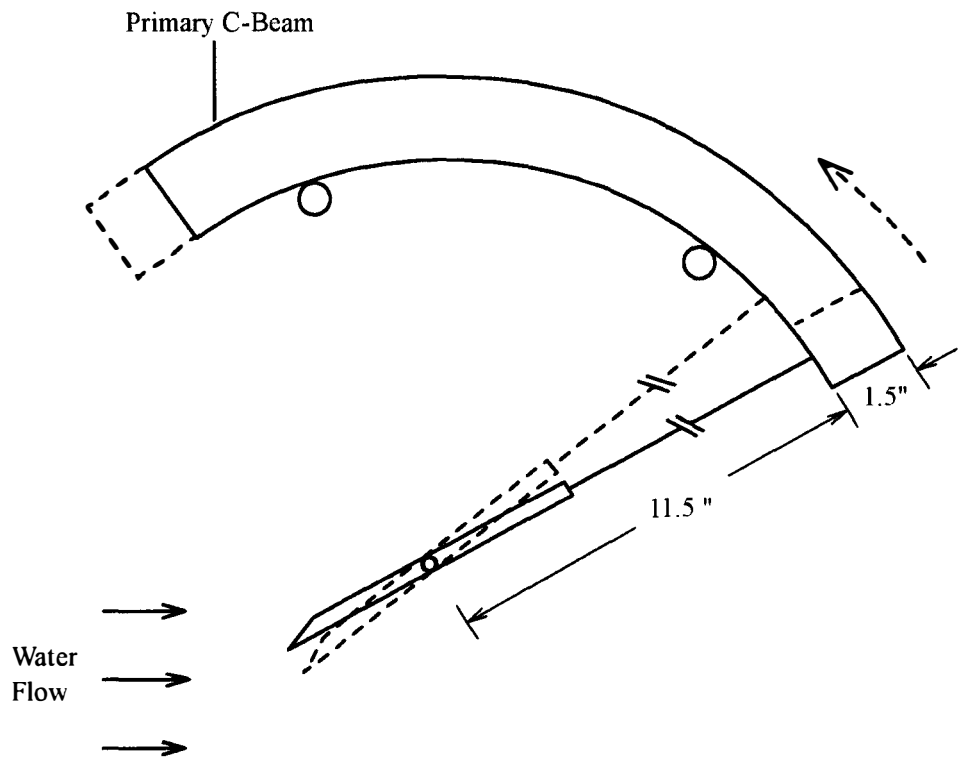

Figure A.1. Delta Wing Model Undergoing Pitch Rotation

As previously discussed, this was achieved by disconnecting the Secondary Drive Cam and the Connecting Rod. The Primary C-Beam was driven alone by the Primary Drive Cam which received its input from the drive mechanism. With the aid of processed data from the video equipment, measurements of the pitch angle were easily carried out. The Drive Mechanism was setup to provide pitch oscillations that varied about a mean pitch angle with an amplitude of $\pm 5^{\circ}$. Using simple trigonometric relationships, the horizontal travel of the top of the Primary C-Beam could be determined as follows:

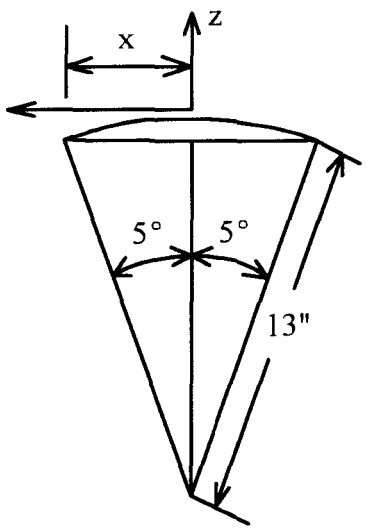

$$x = r\sin\sigma$$
$$= 13.0\sin\pm 5$$
$$\therefore x = \pm 1.133 \textit{ inches}$$

Since the two C-Beams were the same radius, the Secondary C-Beam would travel the same distance when the Secondary Drive Cam was connected. To allow the model to roll, the Primary Drive Cam was disconnected and fixed at a pitch angle of 30°. The Connecting Rod was connected to the end of the sting and to the Secondary C-Beam.

When the Secondary Drive Cam was moved by the Drive Mechanism at an offset distance from the Primary C-Beam, the connecting rod translated a rolling motion onto the sting and consequently the model. The distance between the Primary and the Secondary C-Beams was measured with a micrometer as being 3.49 ±0.005 inches and so the amplitude of the roll oscillations could be determined as follows:

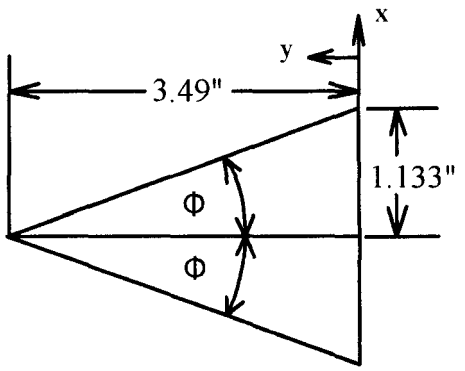

View From Top of Both C-Beams

$$\tan\phi = \frac{x}{y} = \frac{\pm 1.133}{3.49}$$
$$\therefore \phi = \pm 18.0^\circ$$

Referring to Figure 3.5, this meant that the total horizontal movement of the horizontal linking rod of the Drive Mechanism represented a roll movement on the model of ±18°. This linear distance was measured and marked off in equal increments. Each increment represented 2.77° of roll. The ruler used to identify the increments was accurate to 1/32 of an inch. Accordingly, the uncertainty associated with the roll angle was ±0.346°. This uncertainty must be added to the uncertainty that already exists in the evaluation of the oscillation amplitude. The uncertainty associated with the calculated roll amplitude of ±18° was based on the uncertainty associated with the measurement of the

pitch angle (repeatable to within 0.5%) plus the uncertainty associated with measuring the distance between C-Beams (0.1%). The total uncertainty associated with the calculation of the roll amplitude was within 0.6% for a maximum uncertainty of 0.1°. Therefore, the uncertainty associated with the evaluation of the steady state roll angle was ±0.446°.

For test conditions involving unsteady roll motion, the magnitude of the roll could be determined at any time knowing the frequency of oscillation and the amplitude of oscillation as long as an initial condition could be identified. The zero roll condition was used as the starting point and was identified by lining up the lines on the model with the reference line drawn on the bottom of the tunnel. Since the data could be analysed frame by frame, the deviations from zero roll angle were accounted for in terms of time and then calculated in terms of roll angle. The uncertainty associated with the calculated roll angles for the unsteady motion was made up of the uncertainty associated with the measurement of the pitch angle (repeatable to within 0.5%) plus the uncertainty associated with measuring the distance between C-Beams (0.1%). Therefore, the calculation of roll angle for unsteady motion was performed with an uncertainty within 0.6%.

APPENDIX B

ANALYSIS OF THE ROLL CORRECTION FACTOR

When the experiments conducted involved any amount of roll, it became necessary to view the model from a different angle. A mirror was set up at a 45° angle beneath the tunnel which allowed the camera to be focussed on the top surface of the model as it was viewed through the bottom of the test section. This provided a mirror image view of the model. A schematic diagram of the side view and top view of the delta wing model that has undergone a negative roll angle is provided in Figure B.1. For clarity, only the root chord line has been drawn on the side view. To determine the non-dimensional distance x/c, an analytical approach was developed so that the analysis of only one view was necessary. Because the top view of the model provided the best flow visualization of both vortices and because there were some case where the side view was impractical to use, the approach was based on using the top view only.

Referring to Figure B.1, some variables could be easily measured from a digitization of the top view of the delta wing using the technique with the software program Sigma Scan as described earlier in this report. These were:

d_p, the project distance from the location of vortex breakdown to the apex;

ψ, the angle the vortex core makes with the projected root chord line;

θ', the vortex core angle for zero roll angle; and

c_p, the projected root chord length where $c_p = c \cos\sigma$.

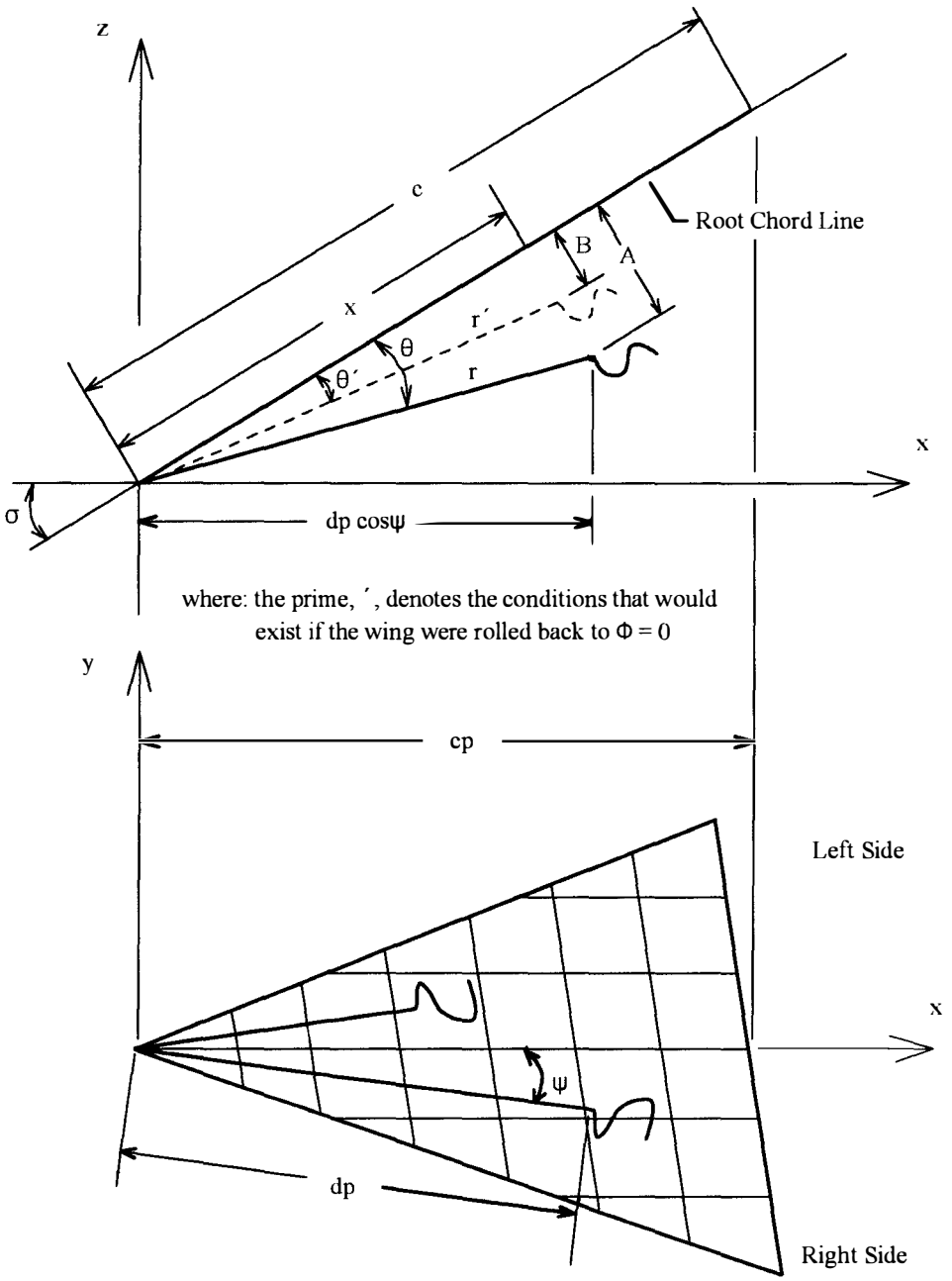

Note: Delta Wing View is a Mirror Image Through Bottom Of Test Section

Figure B.1. Schematic Diagram of Side and Top View of Delta Wing

In addition, the instantaneous model pitch angle, σ, and roll angle, ϕ, were known. Under steady state conditions, pitch and roll were measured and under dynamic conditions, pitch and roll were determined as a function of time. It was then assumed that the vortex angle, θ, remained constant for a given pitch angle when the delta wing was rolled. This result was proven by Huang and Hanff[18] who showed the following:

$$\frac{z}{s} = m$$

where: z is the height of the vortex breakdown location above the wing surface;

s is the local wing semi-span; and

m is a constant.

To relate this to the vortex angle, the local distance, x, can be expressed in terms of s. The local distance, x, is the distance from the apex of the delta wing to the location of the vortex breakdown along the root chord line. For a 70° swept delta wing:

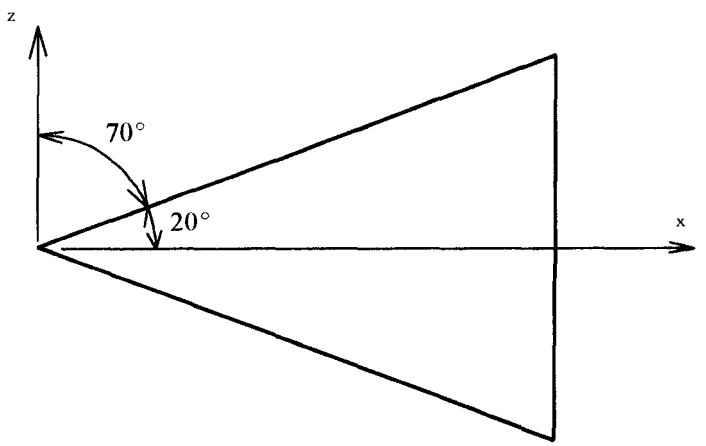

$$\frac{s}{x} = \tan 20$$

or

$$s = x\tan 20$$

From the above equation, it can be seen that:

$$z = (x\tan 20)m$$

It is now possible to express θ in terms of x and z as follows:

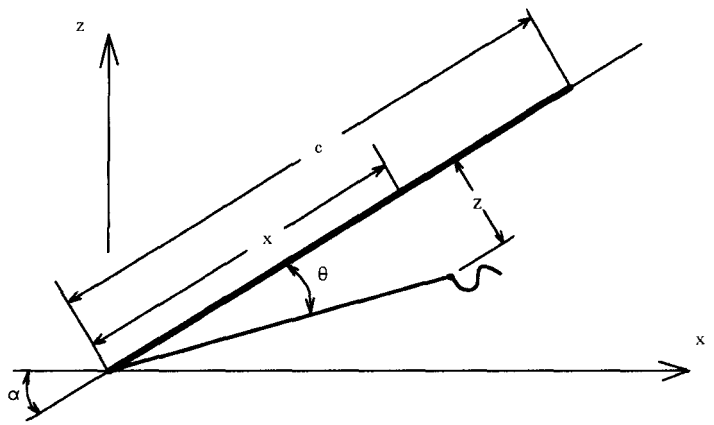

$$\tan\theta = \frac{z}{x}$$

$$= \frac{(x\tan 20)m}{x}$$

$$\therefore \tan\theta = m\tan 20$$

And so, since m is constant for a given pitch angle, therefore, θ is constant for a given pitch angle, σ.

Knowing that the vortex angle remained constant for a given pitch angle, allowed the roll angle to be taken into accounted. Referring to Figure B.1, the dotted line on the side view schematic of the delta wing represents the vortex as it would be seen if the wing were rolled back to wings level (zero roll angle). This is the only condition where the vortex angle could be viewed as the true vortex angle. With the delta wing rolled, the vortex angle seen is a projected vortex angle. From Figure B.1, the following equations, based on simple geometry, can be found:

$$x = r\cos\theta \tag{B1}$$

$$x = r'\cos\theta' \tag{B2}$$

$$d_p\cos\psi = r\cos(\sigma - \theta) \tag{B3}$$

$$c_p = c\cos\sigma \tag{B4}$$

Presently, there are only four equations, but there are five unknowns; however, a co-ordinate transformation can be carried out to provide the necessary information that is missing. Figure B.2 represent a view of the delta wing as seen when looking from the trailing edge toward the apex. The point, P, represents the location of the vortex

breakdown. A co-ordinate axis system has been placed so that any variation in roll angle is represented as a two-dimensional rotation of the co-ordinate axes about the z-axis.

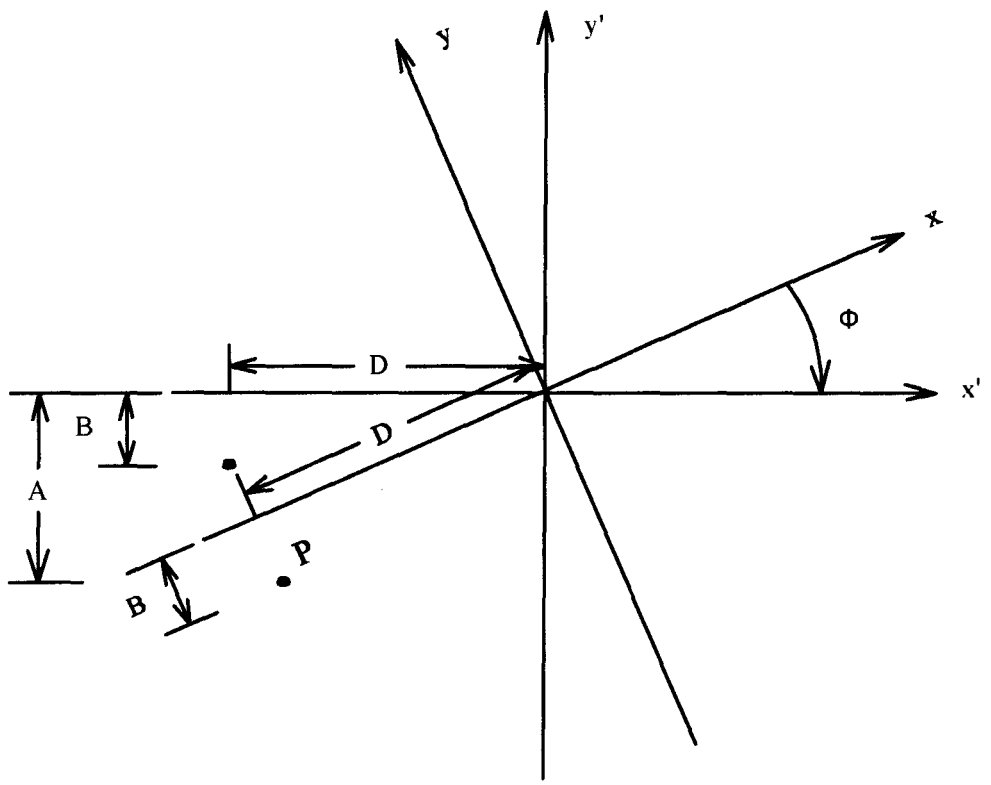

Note: This represents a negative roll angle with respect to the model; however, a positive co-ordinate transformation is required to bring the model back to wings level

Figure B.2. Two Dimensional Co-ordinate Transformation

The following equations apply:

$$x = x'\cos\phi - y'\sin\phi$$
$$y = y'\cos\phi - x'\sin\phi$$

The first case examined is the case of a negative roll angle which, when corrected, must be rolled back in the positive direction. Referring to Figure B.2, the following information can be found:

$$P(x,y) = (-D,-B)$$
$$P(x',y') = (-d\sin\psi,-A)$$

Applying the second co-ordinate transform equation:

$$y = y'\cos\phi - x'\sin\phi$$
$$-B = -A\cos\phi + (-D\sin\psi)\sin\phi$$
$$A\cos\phi = B - d\sin\psi\sin\phi$$

or

$$A = \frac{B - d\sin\psi\sin\phi}{\cos\phi} \qquad \textbf{(B5)}$$

Two other unknowns have been introduced; however, Figure B.1 shows that:

$$A = r\sin\theta \tag{B6}$$

$$B = r'\sin\theta' \tag{B7}$$

And so, there are now seven equations with seven unknowns which can be solved to find:

$$\frac{x}{c} = \frac{d_p \cos\psi}{\cos\sigma + \sin\sigma\left[\dfrac{\dfrac{\tan\theta'}{\cos\phi} - \cos\sigma\tan\psi\tan\phi}{1 + \sin\sigma\tan\psi\tan\phi}\right]} \cdot \frac{\cos\sigma}{c_p}$$

The same equation can be used for roll angles in the other direction but merely using a roll angle of the opposite sign.

VITA

Harry James Kowal was born 8 May 1962 in Zwiebrucken, West Germany. He grew up in Petawawa, Ontario, Canada. His parents, Maurice and Jessie, recently retired in Sydney, Cape Breton Island, Nova Scotia, Canada after spending 27 years in Petawawa. Harry graduated from Champlain High School, Pembroke, Ontario, Canada in 1980 after which he entered in the Canadian Armed Forces under the Regular Officer Training Plan.

Harry attended university at The Royal Military College of Canada, Kingston, Ontario. He graduated in 1984 with a Bachelor Degree in Mechanical Engineering and was commissioned as an Officer with the rank of Second-Lieutenant. Harry then proceeded to the Canadian Forces School of Aerospace Engineering in Borden, Ontario where he completed his training as an Aerospace Engineer. He was promoted to the rank of Lieutenant shortly there after.

In his first tour of duty, Harry worked for National Defence Headquarters, Ottawa, Ontario serving in the Directorate General of Aerospace Engineering and Maintenance as the Life Cycle Material Manager for helicopter engines. During this time, Harry was promoted to the rank of Captain. Harry also successfully became a Licensed Professional Engineer under the Association for Professional Engineers of Ontario.

In 1988, Harry was accepted by the Canadian Forces for sponsored graduate studies. He entered The University of Tennessee Space Institute (UTSI) in August 1988 and graduated in August 1990 with a Master of Science Degree in Aerospace Engineering. During his two years at UTSI, Harry fulfilled the requirements for two separate degree

programs completing a thesis, a written exam for the second degree, and 19 courses (some of which were at the doctorate level). On the advise of Dr Ahmad Vakili and Dr Roger Crawford, Harry entered a PhD program in the spring of 1990.

Harry then travelled to Cold Lake, Alberta where he worked in Flight Dynamics as an Aerodynamics Specialist for the Aerospace Engineering Test Establishment. After four years of flight test experience and with the accumulation of over 100 flights in ten different type aircraft, Harry was granted the qualification as a Qualified Flight Test Engineer. Harry is the only Canadian to achieve the military qualification without having had formal training at a Test Pilot School.

In 1994, Harry was posted to The Royal Military College of Canada where he joined the teaching staff as a Lecturer in the Mechanical Engineering Department. Shortly after his arrival, he was appointed to the position of Squadron Commander, a duty in addition to his teaching responsibilities. In May 1995, Harry was promoted to his current rank of Major and was appointed a Division Commander responsible for four squadrons. He maintained his faculty position in the Mechanical Engineering Department and, in September 1995, was promoted to Assistant Professor.

Harry James Kowal has a remarkable wife, Cheryl Anne, without whom most of the above would not have been possible. Cheryl is a Registered Nurse and a wonderful mother. Harry and Cheryl have been blessed with two beautiful children, Sarah Elizabeth and Stephanie Lynne who possess an entire list of talents of their own.